ISSN (1230-0322)
2021, Vol. 71, No. 4

Food

Polish Journal of Food and Nutrition Sciences

formerly Acta Alimentaria Polonica

Published
by Institute of Animal Reproduction and Food Research of the Polish Academy of Sciences, Olsztyn

Published since 1957 as
Roczniki Chemii i Technologii Żywności and Acta Alimentaria Polonica (1975–1991)

EDITOR-IN-CHIEF
Dr. Magdalena Karamać, Department of Chemical and Physical Properties of Food, Institute of Animal Reproduction and Food Research of the Polish Academy of Sciences, Olsztyn, Poland

SECTION EDITORS
Food Technology Section
Prof. Adriano Gomes da Cruz, Department of Food, Federal Institute of Education, Science and Technology of Rio de Janeiro (IFRJ), Rio de Janeiro, Brazil
Dr. Zeb Pietrasik, Meat, Food and Bio Processing Branch, Alberta Agriculture and Forestry, Leduc, Canada
Prof. Alberto Schiraldi, DISTAM, University of Milan, Italy

Food Chemistry Section
Prof. Ryszard Amarowicz, Department of Chemical and Physical Properties of Food, Institute of Animal Reproduction and Food Research of the Polish Academy of Sciences, Olsztyn, Poland
Dr. Agnieszka Kosińska-Cagnazzo, Independent Researcher, Sion, Switzerland

Food Quality and Functionality Section
Prof. Vural Gökmen, Department of Food Engineering, Hacettepe University, Ankara, Turkey
Prof. Piotr Minkiewicz, Department of Food Biochemistry, University of Warmia and Mazury in Olsztyn, Poland

Nutritional Research Section
Prof. Jerzy Juśkiewicz, Department of Biological Function of Food,
Institute of Animal Reproduction and Food Research of the Polish Academy of Sciences, Olsztyn, Poland
Prof. Andre Mazur, INRA, Clermont, France
Dr. Luisa Pozzo, The Institute of Agricultural Biology and Biotechnology, CNR, Pisa, Italy

LANGUAGE EDITOR
Prof. Ron Pegg, University of Georgia, Athens, USA

STATISTICAL EDITOR
Dr. Magdalena Karamać, Institute of Animal Reproduction and Food Research of the Polish Academy of Sciences, Olsztyn, Poland

EXECUTIVE EDITOR, NEWS AND MISCELLANEA SECTION
Joanna Molga, Institute of Animal Reproduction and Food Research of the Polish Academy of Sciences, Olsztyn, Poland;
E-mail: pjfns@pan.olsztyn.pl

SCOPE: The Journal covers fundamental and applied research in food area and nutrition sciences with a stress on interdisciplinary studies in the areas of food, nutrition and related subjects.

POLICY: Editors select submitted manuscripts in relation to their relevance to the scope. Referees are selected from the Advisory Board and from Polish and international scientific centres. Identity of referees is kept confidential.

AUTHORSHIP FORMS referring to Authorship Responsibility, Conflict of Interest and Financial Disclosure, Copyright Transfer and Acknowledgement, and Ethical Approval of Studies are required for all authors.

FREQUENCY: Quarterly – one volume in four issues (March, June, September, December).

COVERED by Web of Science, Current Contents/Agriculture, Biology & Environmental Sciences, Journal Citation Reports and Science Citation Index Expanded, BIOSIS (Biological Abstracts), SCOPUS, FSTA (formerly: Food Science and Technology Abstracts), CAS (Chemical Abstracts), AGRICOLA, AGRO-LIBREX data base, EBSCO, FOODLINE, Leatherhead FOOD RA data base FROSTI, AGRIS and Index Copernicus data bases, Polish Scientific Journals Contents (PSJC) Life Science data base available at http://psjc.icm.edu.pl and any www browser; ProQuest: The Summon, Bacteriology Abstracts, Immunology Abstracts.

EDITORIAL AND BUSINESS CORRESPONDENCE: Submit contributions (see Instructions to Authors) and address all communications regarding subscriptions, changes of address, etc. to:

CORRESPONDENCE TO: Ms. Joanna Molga
Polish Journal of Food and Nutrition Sciences
Institute of Animal Reproduction and Food Research
of Polish Academy of Sciences
ul. Tuwima 10, 10-747 Olsztyn, Poland
e-mail: pjfns@pan.olsztyn.pl; http://journal.pan.olsztyn.pl

ISSN (1230–0322)
2 0 2 1 , Vol. 71, No. 4

Polish Journal of Food and Nutrition Sciences

formerly Acta Alimentaria Polonica

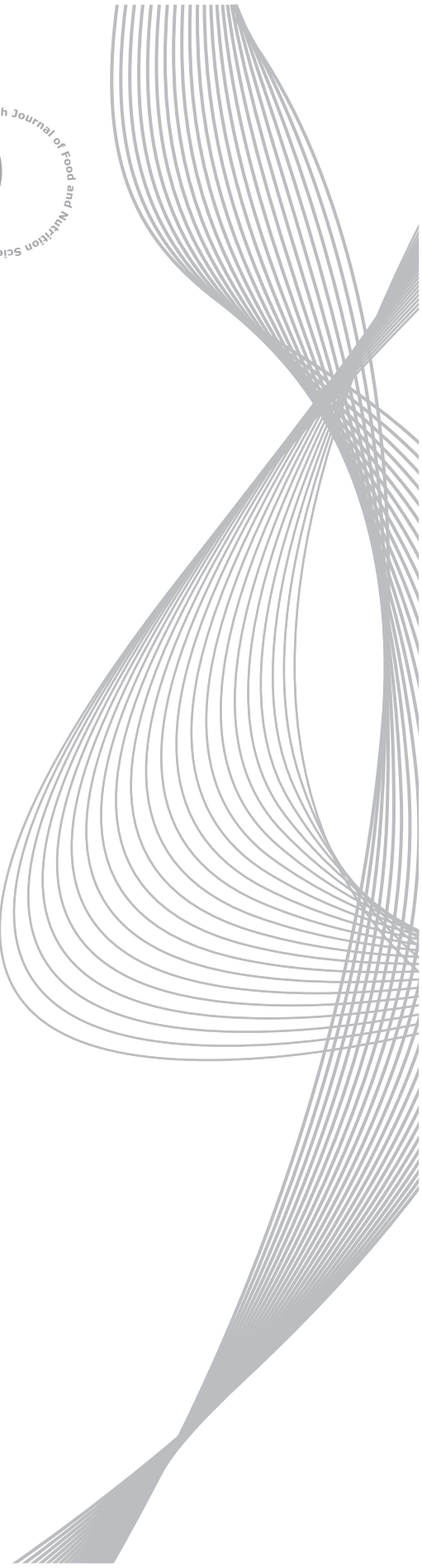

Published

by Institute of Animal Reproduction and Food Research of the Polish Academy of Sciences, Olsztyn

Advisory Board of PJFNS 2019–2022

Marek Adamczak
University of Warmia and Mazury in Olsztyn, Poland
Huda Al-Kateb
Birmingham City University, Birmingham, UK
Wilfried Andlauer
University of Applied Sciences and Arts Western Switzerland Valais, Sion, Switzerland
Anna Brzozowska
Warsaw University of Life Sciences, Poland
Zuzana Ciesarova
VUP Food Research Institute, Bratislava, Slovak Republic
Maria Dolores Del Castillo
CSIC-UAM, Madrid, Spain
Juana Frias
Institute of Food Science, Technology and Nutrition (ICTAN), Madrid, Spain
Liwei Gu
University of Florida, Gainesville, USA
Henryk Jeleń
Poznań University of Life Sciences, Poland
Georgios Koutsidis
Northumbria University, Newcastle-upon-Tyne, UK
Andrzej Lenart
Warsaw University of Life Sciences, Poland
John Lodge
Northumbria University, Newcastle-upon-Tyne, UK
Adolfo J. Martinez-Rodriguez
CSIC-UAM, Madrid, Spain
Francisco J. Morales
CSIC, Madrid, Spain
Zhongli Pan
University of California, Davis, USA;
World Food Center, China
Ron B. Pegg
University of Georgia, Athens, USA
Mariusz K. Piskuła
Institute of Animal Reproduction and Food Research of the Polish Academy of Sciences in Olsztyn, Poland
Da-Wen Sun
National University of Ireland, Dublin, Ireland
Lida Wądołowska
Warmia and Mazury University, Olsztyn, Poland
Zenon Zduńczyk
Institute of Animal Reproduction and Food Research of the Polish Academy of Sciences in Olsztyn, Poland
Henryk Zieliński
Institute of Animal Reproduction and Food Research of the Polish Academy of Sciences in Olsztyn, Poland

Pol. J. Food Nutr. Sci. 2021, Vol. 71, No. 4

POLISH JOURNAL OF FOOD AND NUTRITION SCIENCES
covered by CURRENT CONTENTS/AGRICULTURE, BIOLOGY & ENVIRONMENTAL SCIENCES, JOURNAL CITATION REPORTS AND SCIENCE CITATION INDEX EXPANDED, SCOPUS, DOAJ, EBSCO, BIOSIS, IFIS Publishing and CAS abstracts, and AGRO-Librex, FROSTI, and AGRIS data bases
2021, VOL. 71, NO. 4

REVIEW PAPER

ORIGINAL PAPERS

© Copyright by Institute of Animal Reproduction and Food Research
of Polish Academy of Sciences, Olsztyn, Poland
www.pan.olsztyn.pl

Subscription

2021 – One volume, four issues per volume. Annual subscription rates are: Poland 150 PLN, all other countries 80 EUR. Prices are subject to exchange rate fluctuation. Subscription payments should be made by direct bank transfer to Bank Gospodarki Żywnościowej, Olsztyn, Poland, account No 17203000451110000000452110 SWIFT code: GOPZPLWOLA with corresponding banks preferably. Subscription and advertising offices at the Institute of Animal Reproduction and Food Research of Polish Academy of Sciences, ul. J. Tuwima 10, 10-747 Olsztyn, Poland, tel./fax (48 89) 5234670, fax (48 89) 5240124, e-mail: pjfns@pan.olsztyn.pl; http://journal.pan.olsztyn.pl

Zamówienia prenumeraty: Joanna Molga (e-mail: pjfns@pan.olsztyn.pl)

Wersja pierwotna (referencyjna) kwartalnika PJFNS: wersja papierowa (ISSN 1230–0322)
Nakład: 70 egz.; Ark. wyd. 19,2; Ark. druk. 19,2
Skład i druk: Mercurius, www.mercurius.com.pl

Pol. J. Food Nutr. Sci., 2021, Vol. 71, No. 4, pp. 353–381
On-line ISSN: 2083-6007
Print ISSN: 1230-0322
DOI: 10.31883/pjfns/143164
http://journal.pan.olsztyn.pl

Review article
Section: Nutrition

Diet-Induced Adipocyte Browning

Oskar Wojciech Wiśniewski[1], Aleksander Rajczewski[1], Agnieszka Szumigała[1], Magdalena Gibas-Dorna[2]*

[1]Students' Scientific Society, Faculty of Medicine, Poznan University of Medical Sciences, 10 Fredry Street, 61–701 Poznan, Poland
[2]Department of Applied and Clinical Physiology, Collegium Medicum, University of Zielona Gora, 28 Zyty Street, 65–046 Zielona Gora, Poland

Key words: adipocyte browning, beige adipose tissue, brite adipose tissue, diet, diet therapy, obesity

The adipocyte browning process is a phenomenon that consists in the molecular and morphological remodeling of preadipocytes or mature white adipocytes into multilocular beige fat cells expressing thermogenesis-associated genes. Adipocyte browning may occur physiologically, mainly upon cold or exercise stimulation. However, it can also be induced by exogenous compounds, such as drugs or dietary components. Since adipocyte browning is followed by increased energy expenditure, weight loss, and improved metabolic health, it emerges as a novel therapeutic target in the treatment of obesity and obesity-related diseases. In addition, it contributes to the lowering of both systemic and adipose tissue inflammation, which are promoted in obese states. Thus, the role of adipocyte browning should be emphasized in the context of a dramatically increasing population of obese individuals. In this paper, we focus on dietary components and general dietary modifications, which may affect adipocyte browning by its stimulation or inhibition. We discuss browning properties of amino acids, carbohydrates, fatty acids, and retinoids, as well as present adipocyte browning potential of the wide range of non-nutrients, including glucosinolates, alkaloids, terpenes and terpenoids, flavonoids and other phenolic compounds. We also demonstrate the influence of edible plant extracts and food ingredients of animal origin on adipose tissue browning. Finally, we analyze browning effects of caloric restriction, intermittent fasting and various dietary macronutrient compositions, as well as the significance of microbiota in adipocyte browning process.

ABBREVIATIONS

AMPK: 5'-AMP-activated protein kinase; β_3-AR: β_3-adrenergic receptor; BAT: brown adipose tissue; C/EBPα: CCAAT/enhancer-binding protein α; CIDEA: cell death activator CIDE-A; CITED1: Cbp/p300-interacting transactivator 1; COX7A1: cytochrome c oxidase subunit 7A1, mitochondrial; COX8B: cytochrome c oxidase subunit 8B, mitochondrial; CPT1A: carnitine *O*-palmitoyltransferase 1, liver isoform; CPT1B: carnitine *O*-palmitoyltransferase 1, muscle isoform; Cyt C: cytochrome c; DHA: docosahexaenoic acid; DIO2: type II iodothyronine deiodinase; ELOVL3: elongation of very long chain fatty acids protein 3; EPA: eicosapentaenoic acid; eWAT: epididymal white adipose tissue; FGF21: fibroblast growth factor 21; GPRs: G protein-coupled receptors; HDL-C: high-density lipoprotein cholesterol; IL-6: interleukin 6; iWAT: inguinal white adipose tissue; LDL-C: low-density lipoprotein cholesterol; NRF1: nuclear respiratory factor 1; NRF2: nuclear respiratory factor 2; PGC1α: peroxisome proliferator-activated receptor γ coactivator 1-α; PPARα: peroxisome proliferator-activated receptor α; PPARγ: peroxisome proliferator-activated receptor γ; PRDM16: PR domain-containing protein 16; rWAT: retroperitoneal white adipose tissue; sWAT: subcutaneous WAT; TBX1: T-box transcription factor TBX1; TFAM: transcription factor A, mitochondrial; TMEM26: transmembrane protein 26; TNF-α: tumor necrosis factor α; UCP1: uncoupling protein 1; WAT: white adipose tissue.

INTRODUCTION

Over the last decades, the understanding of adipose tissue has changed unquestionably. Gradually, it came out that it is not only the storage site of lipids but also an active endocrine organ, which modulates the functioning of the whole organism [Luo & Liu, 2016]. In addition, recent years of preclinical trials have proven that white adipose tissue (WAT) has a transformative potential, as it can differentiate into beige adipose tissue upon definite stimulation in the process called adipocyte browning (also known as beiging or britening) [Rosenwald *et al.*, 2013].

More precisely, the adipocyte browning process is a phenomenon, which involves not only already existing white

* Corresponding Author:
E-mail: wisniewski.oskar@outlook.com (O.W. Wiśniewski)

Submitted: 8 July 2021
Accepted: 18 October 2021
Published on-line: 15 November 2021

© Copyright by Institute of Animal Reproduction and Food Research of the Polish Academy of Sciences
© 2021 Author(s). This is an open access article licensed under the Creative Commons Attribution-NonCommercial-NoDerivs License (http://creativecommons.org/licenses/by-nc-nd/4.0/).

adipocytes, but also preadipocytes, which can differentiate into both white or beige fat cells [Harms & Seale, 2013]. During the adipocyte browning, the clusters of stimulated cells undergo histological, cytological, and molecular changes, finally acquiring the beige adipose tissue phenotype [Wu *et al.*, 2012].

Beige adipose tissue (also called brite adipose tissue, brown-like adipose tissue, inducible-brown adipose tissue) is a subtype of brown adipose tissue (BAT), which contains adipocytes that share features of both white and "classical" brown fat cells [Lidell *et al.*, 2013]. Their unique gene expression pattern includes genetic hallmarks specific for beige adipocytes as well as genes expressed in both "classical" brown and beige fat cells (Table 1) [Wu *et al.*, 2012]. In contrast to white adipocytes, beige cells are abundant with uncoupling protein 1 (UCP1)-positive mitochondria, which enables the process called non-shivering thermogenesis [Shabalina *et al.*, 2013]. Heat generation and distribution as a key function of beige cells, is associated with their high degree of sympathetic innervation and vascularization [Kajimura *et al.*, 2015]. As compared with WAT cells, beige adipocytes contain more, but smaller in size, lipid droplets, which results in multilocular morphology of beige adipose tissue (in contrast to unilocular WAT) [Harms & Seale, 2013]. These lipid droplets are rich in triglycerides that supply an energy for thermogenesis.

Taken together, the adipocyte browning process that occurs when body's demands for heat generation and dissipation are greatly elevated, involves induction of mitochondrial biogenesis, UCP1 expression, triggered β-oxidation, angiogenesis and enhanced sympathetic innervation [Harms & Seale, 2013].

The assessment of gene expression alterations is essential to confirm adipocyte browning, therefore detailed knowledge about genes involved in this process is necessary to interpret the scientific results (Table 1). *Cd137, Tbx1,* and *Tmem26* seem to be specific markers for beige adipocytes, while the expression of other genes differs a lot when most prevalent WAT depots are considered: epididymal, inguinal and retroperitoneal WAT (eWAT, iWAT, and rWAT, respectively) [de Jong *et al.*, 2015].

There is a wide range of browning activators including endogenous (hormones, growth factors, or cytokines) and exogenous (mostly dietary components or pharmacological agents) factors, whereas browning inhibitors are relatively rare [Wisniewski *et al.*, 2018]. The most studied and presumably the most potent browning-positive effect is associated with increased sympathetic nervous system activity and β_3-adrenergic signaling pathway in response to cold [Contreras *et al.*, 2014]. Importantly, adipocyte browning is reversible, and so-called whitening of beige adipocytes may occur, depending on environmental conditions [Rosenwald *et al.*, 2013].

The clinical significance of adipocyte browning is associated with an improvement of metabolic health [Wisniewski *et al.*, 2018; Wisniewski, 2019]. Induction of beige fat thermogenesis results in increased lipolysis and energy expenditure, followed by reduced adiposity and weight loss [Yoneshiro *et al.*, 2013]. Furthermore, adipocyte browning decreases low-grade systemic inflammation by diminishing proinflammatory cytokine concentrations and enhancing anti-inflammatory adipokines production [Min *et al.*, 2016; Zhuang *et al.*, 2019], as well as improves glucose tolerance [Chondronikola *et al.*, 2014]. Hence, adipocyte browning emerges as a novel therapeutic approach to obesity and obesity-related complications, such as type 2 diabetes, hypertension, dyslipidemia, or non-alcoholic steatohepatitis [Wisniewski *et al.*, 2018].

In order to summarize the knowledge and inspire further research, we aimed to present a comprehensive review of the current literature about dietary components and dietary interventions that may elicit adipocyte browning.

AMINO ACIDS

Betaine

Betaine (trimethylglycine) is a common natural amino acid mostly found in wheat, spinach, beetroots, and shellfish [Ross *et al.*, 2014]. In humans, it is well known as an intermediate product of choline degradation, although it exhibits multiple positive metabolic effects by itself [Ueland, 2011]. Apart from improving insulin sensitivity, blood lipid profile, and anti-inflammatory activity, betaine affects adipogenesis and promotes adipocyte browning [Du *et al.*, 2018]. Du *et al.* [2018] proved that betaine suppresses proliferation and differentiation of 3T3-L1 preadipocytes by cell cycle blockage between G1/S phases and downregulation of C/EBPα and PPARγ. Furthermore, betaine upregulates *Ucp1*, *Pparg*, *Ppargc1a*, *Cidea,* and *Cd137*, as well as stimulates mitochondrial biogenesis, in Kunming mice after 13-week administration of a high-fat diet and 1% betaine in water, which, in turn, results in reduced body fat, lowered lipid accumulation and increased β-oxidation in myocytes mass [Du *et al.*, 2018].

Leucine

Leucine is an essential branched-chain amino acid with the highest content in proteins of soybeans, meat, eggs, and nuts [Rondanelli *et al.*, 2021]. Unlike another essential amino acid – methionine, there are many significant inconsistencies in the role of leucine in the adipocyte browning process.

Two studies confirm the browning properties of leucine supplementation [Binder *et al.*, 2014; Jiao *et al.*, 2016]. The first one revealed that 21-week supplementation of C57BL/6J mice with 1.5% L-leucine resulted in increased *Ucp1, Ucp3,* and *Cpt1* mRNAs in eWAT, albeit these changes were not associated with elevated energy expenditure and weight loss [Binder *et al.*, 2014]. The other research evidenced reduced body weight and enhanced expression of browning-related proteins, such as UCP1, PGC1α, β_3-AR, and FGF21, in eWAT and BAT of C57BL/6J mice after 24 weeks of dietary intervention with both 1.5% or 3.0% L-leucine [Jiao *et al.*, 2016]. Furthermore, decreased adipocyte size, lowered concentrations of lipogenic enzymes (acetyl-CoA carboxylase and fatty acid synthase) as well as encouraging lipolysis by increasing adipose triglyceride lipase and phosphorylated hormone-sensitive lipase at the protein level were found upon diet supplementation with both 1.5% or 3.0% L-leucine. Thus, the signs of adipocyte browning, raised thermogenesis, and adipose tissue remodeling were reported [Jiao *et al.*, 2016].

TABLE 1. Genes used in adipocyte browning research (based on UniProt database).

Gene names *HUMAN (Murine)*	Encoded protein	Abbreviation
Genes highly expressed in both beige and "classical" brown adipocytes		
ADRB3 (Adrb3)	β_3-adrenergic receptor	β_3-AR
CIDEA (Cidea)	Cell death activator CIDE-A	CIDEA
DIO2 (Dio2)	Type II iodothyronine deiodinase	DIO2
EBF2 (Ebf2)	Early B-cell factor 2	EBF2
ELOVL3 (Elovl3)	Elongation of very long chain fatty acids protein 3	ELOVL3
PPARA (Ppara)	Peroxisome proliferator-activated receptor α	PPARα
PPARG (Pparg)	Peroxisome proliferator-activated receptor γ	PPARγ
PPARGC1A (Ppargc1a)	Peroxisome proliferator-activated receptor γ coactivator 1-α	PGC1α
PRDM16 (Prdm16)	PR domain-containing protein 16	PRDM16
UCP1 (Ucp1)	Uncoupling protein 1	UCP1
Genes specific for beige adipocytes		
CD137 (Cd137)	CD137	CD137
CITED1 (Cited1)	Cbp/p300-interacting transactivator 1	CITED1
FGF21 (Fgf21)	Fibroblast growth factor 21	FGF21
HOXC9 (Hoxc9)	Homeobox protein Hox-C9	HOXC9
TBX1 (Tbx1)	T-box transcription factor TBX1	TBX1
TMEM26 (Tmem26)	Transmembrane protein 26	TMEM26
Genes specific for "classical" brown adipocytes		
EVA1 (Eva1)	Protein eva-1	EVA1
LHX8 (Lhx8)	LIM/homeobox protein Lhx8	LHX8
ZIC1 (Zic1)	Zinc finger protein ZIC 1	ZIC1
Genes strongly associated with mitochondrial biogenesis		
NRF1 (Nrf1)	Nuclear respiratory factor 1	NRF1
NRF2 (Nrf2)	Nuclear respiratory factor 2	NRF2
TFAM (Tfam)	Transcription factor A, mitochondrial	TFAM
Genes strongly associated with β-oxidation and mitochondrial activity		
ACADM (Acadm)	Medium-chain specific acyl-CoA dehydrogenase, mitochondrial	MCAD
COX7A1 (Cox7a1)	Cytochrome c oxidase subunit 7A1, mitochondrial	COX7A1
(Cox8b)	Cytochrome c oxidase subunit 8B, mitochondrial	COX8B
CPT1A (Cpt1a)	Carnitine *O*-palmitoyltransferase 1, liver isoform	CPT1A
CPT1B (Cpt1b)	Carnitine *O*-palmitoyltransferase 1, muscle isoform	CPT1B
CYCS (Cycs)	Cytochrome c	Cyt C
Genes highly expressed in white adipocytes		
ALDH1A1 (Aldh1a1)	Retinal dehydrogenase 1	ALDH1
CEBPA (Cebpa)	CCAAT/enhancer-binding protein α	C/EBPα
FABP4 (Fabp4)	Fatty acid-binding protein type 4	FABP4
LPIN1 (Lpin1)	Phosphatidate phosphatase LPIN1	LIPIN1
PSAT1 (Psat1)	Phosphoserine aminotransferase	PSAT1
RETN (Retn)	Resistin	
SREBP1 (Srebp1)	Sterol regulatory element-binding protein 1	SREBP1
(Zfp423)	Zinc finger protein 423	ZFP423

However, another two study groups have indicated that adipocyte browning is induced by leucine restriction rather than by supplementation [Cheng *et al.*, 2010; Wanders *et al.*, 2015]. Two papers described elevated expression of UCP1 at both protein and mRNA levels as well as upregulated *Ppargc1a, Pparg,* and *Adrb3* in BAT of C57BL/6J mice after 1-week of total leucine restriction [Cheng *et al.*, 2010, 2011]. Moreover, the same alterations of the abovementioned lipogenic and lipolytic enzymes, as well as weight loss and diminished adipocyte size, were observed. In addition, a significant increase in UCP1 at both mRNA and protein levels in iWAT and BAT of C57BL/6J mice as well as a raised transcription of *Cidea, Cox7a,* and *Cox8b* in iWAT were detected upon 8 weeks of leucine restriction by 85% [Wanders *et al.*, 2015]. Similarly, a low-leucine diet resulted in broadened deposits of multilocular adipocytes, nevertheless heightened acetyl-CoA carboxylase and fatty acid synthase mRNAs were noted in eWAT and iWAT contrarily [Wanders *et al.*, 2015]. Taken together, based on the presented data, the impact of leucine on adipocyte browning remains not fully recognized.

Similarly as for methionine restriction, FGF21 overexpression and sympathetic nervous system activation were suggested as the possible mechanisms of the adipocyte browning in the case of leucine deprivation [Cheng *et al.*, 2010, 2011; Wanders *et al.*, 2015], while no mechanisms supporting the browning on leucine-rich diet were presented [Binder *et al.*, 2014; Jiao *et al.*, 2016].

Positive effects resulting from leucine administration or restriction beneficially influence metabolic outcomes. Upon prolonged leucine supplementation, decreased production of proinflammatory cytokines, diminished circulating leptin and leptin resistance were reported [Binder *et al.*, 2014; Jiao *et al.*, 2016]. Nevertheless, there are discrepancies, whether higher or lower leucine intake contributes to improved glucose metabolism [Binder *et al.*, 2014; Cheng *et al.*, 2011; Jiao *et al.*, 2016].

Methionine

Eggs, meat, grain, and dairy products are the predominant source of dietary methionine, an essential amino acid which profoundly modulates human metabolism [Górska-Warsewicz *et al.*, 2018]. However, recent data suggest that methionine restriction may also be beneficial in obesity and obesity-related diseases due to adipocyte browning stimulation [Jiang *et al.*, 2015; Stone *et al.*, 2015; Wanders *et al.*, 2017]. Over a 5-fold reduction in dietary methionine intake significantly elevated *Ucp1*, *Ppargc1a*, *Cidea, Cox7a1, Cox8b,* and *Adrb3* mRNAs in murine iWAT *in vivo* [Stone *et al.*, 2015; Wanders *et al.*, 2017]. Furthermore, the upregulation of *Ucp1, Cidea,* and *Elovl3* was also present in BAT. In addition, methionine restriction activates sympathetic drive and leads to the liver overexpression of FGF21 [Stone *et al.*, 2015; Wanders *et al.*, 2017], which is recognized as an independent activator in browning processes [Fisher *et al.*, 2012]. As a result of the adipocyte browning and pleiotropic functions of FGF21 itself, improved insulin sensitivity, weight loss, and a reduction in plasma and hepatic triglycerides were also reported [Stone *et al.*, 2015; Wanders *et al.*, 2017]. Similar browning and metabolic effects (↑ UCP1 and FGF21; ↓ body mass, glucose, and hepatic triglycerides) were also evidenced in mice with impaired intestinal and renal methionine absorption due to methionine transporter knockdown [Jiang *et al.*, 2015].

Taurine

Seafood is the primary source of exogenous taurine, one of the most common amino acids in the human body composition [Laidlaw *et al.*, 1990]. Guo *et al.* [2019] studied the impact of taurine on adipocyte browning and reported that intraperitoneal taurine administration resulted in the upregulation of *Ucp1*, *Ppargc1a*, *Tfam*, and *Cpt1b* expression in iWAT, eWAT, and BAT of C57BL6 mice. The same alterations of browning-specific genes were observed in C3H10T1/2 cells upon taurine supplementation [Guo *et al.*, 2019]. Consequently, dietary taurine promoted mitochondrial biogenesis, increased β-oxidation, and raised energy expenditure, leading to higher free fatty acids utilization, reduced adiposity, and weight loss with improved glucose tolerance and insulin sensitivity. Mechanistically, taurine stimulates AMPK phosphorylation, thus activating the AMPK/PGC1α pathway [Guo *et al.*, 2019].

CARBOHYDRATES

L-Rhamnose

L-Rhamnose is a monosaccharide that is a component of plant cell walls and bacteria [Jiang *et al.*, 2021]. It is used as a sweetener that is able to reduce both cholesterogenesis and triacylglycerol synthesis [Bai *et al.*, 2015]. In addition, 3T3-L1 preadipocyte supplementation with L-rhamnose resulted in an elevated concentration of browning-related proteins such as UCP1, PRDM16, and PGC1α as well as *Cd137*, *Cited1*, *Prdm16*, *Tbx1,* and *Tmem26* mRNAs [Choi *et al.*, 2018]. Several different signaling pathways, including β_3-AR, SIRT1, PKA, and p-38, take part in this process. L-Rhamnose administration was associated with activation of the AMPK and acetyl-CoA carboxylase proteins, increased acyl-coenzyme A oxidase, carnitine *O*-palmitoyltransferase 1, and phosphorylated hormone sensitive lipase levels. What is more, L-rhamnose activated HIB1B brown adipocytes by increasing expression of brown-fat markers (UCP1, PRDM16, and PGC1α) and changing morphology of fat cells [Choi *et al.*, 2018].

Trehalose

Trehalose is an anti-inflammatory disaccharide [Arai *et al.*, 2019] present in honey, fungi and yeast [Oku & Nakamura, 2000] that exhibits the ability to reduce insulin secretion and improve glucose tolerance [Arai *et al.*, 2019]. A 16 weeks of drinking water with trehalose resulted in WAT browning in experimental mice, which was confirmed by increased expression of *Cidea* and *Ucp1* mRNAs in iWAT [Arai *et al.*, 2019]. Similar but not significant tendency was observed in the mesenteric adipose tissue. Trehalose-induced WAT browning was accompanied with reduced serum glucose and elevated core temperature as a consequence of thermogenesis intensification. Moreover, trehalose caused the expansion of multilocular UCP1-positive adipocytes in both iWAT

and mesenteric WAT. Also, possible fibroblast growth factor 21 (FGF21) involvement in trehalose-induced adipocyte browning was investigated, though its concentration did not increase during the experiment, suggesting a different underlying mechanism [Arai *et al.*, 2019].

Inulin

Over 30,000 plant species (*e.g.*, *Cichorium intybus, Asparagus* sp., *Allium* sp.) are sources of inulin, a non-digestible carbohydrate known especially as a prebiotic and dietary sugar replacer in diabetics [Shoaib *et al.*, 2016]. A recent study by Weitkunat *et al.* [2017] evidenced browning properties of inulin, mainly attributed to short-chain fatty acids production. The 30-week inulin supplementation significantly raised *Ucp1*, *Ppargc1a* and *Cidea* mRNA levels in sWAT of C57BL/6JRj mice. Moreover, inulin ameliorated high-fat diet induced adipocyte hyperplasia and altered fecal microbiota composition, preferring overgrowth of *Bifidobacterium* [Weitkunat *et al.*, 2017].

FATTY ACIDS

α-Linolenic, γ-linolenic and pinolenic acids

Primary subcutaneous adipocytes of C57BL/6 mice were reported to upregulate the expression of *Ucp1* upon *in vitro* α-linolenic acid, γ-linolenic acid or pinolenic acid administration, which are different octadecatrienoic acid isomers, found mainly in the wide range of seeds [Shin & Ajuwon, 2018a]. Moreover, an insignificant increase in *Ppargc1a* mRNA was noted. However, only the pinolenic acid potentiated the browning effect of norepinephrine associated with sympathetic nervous system stimulation, while γ-linolenic acid additionally decreased *Cidea* transcription [Shin & Ajuwon, 2018a]. Furthermore, γ-linolenic acid slightly but insignificantly elevated *Ucp1* in both 3T3-L1 and 10T1/2 adipocytes [Shin & Ajuwon, 2018a].

Linoleic and conjugated linoleic acids

Conjugated linoleic acid is a mixture of linoleic acid isomers, mostly *cis*-9, *trans*-11 and *trans*-10, *cis*-12, derived from sunflower oil, ruminant meats, or dairy products [Shen & McIntosh, 2016]. Results obtained in murine trials proved that conjugated linoleic acid is an adipocyte browning inductor since it increased mRNAs of *Ucp1*, *Ppargc1a*, and *Cpt1b* in epididymal WAT as well as energy expenditure [Wendel *et al.*, 2009]. The possible mechanism of browning initiation might be connected with β_3-adrenergic activity but the effect is rather short lasting and not maintained over a few weeks of conjugated linoleic acid supplementation [Wendel *et al.*, 2009]. Therefore, the other pathways play a significant role in conjugated linoleic acid-driven browning process. In addition, results of conjugated linoleic acid administration may be partially mediated by a group of G protein-coupled receptors (GPRs) [Sauer *et al.*, 2004]. The conjugated linoleic acid browning properties were indirectly observed in several clinical trials reporting significant weight loss in conjugated linoleic acid subjects [Blankson *et al.*, 2000; Smedman & Vessby, 2001; Watras *et al.*, 2007]. Apart from the adipocyte browning promotion, conjugated linoleic acid elevated lipolysis, β-oxidation, white adipocyte apoptosis, and decreased adipogenesis [Hargrave *et al.*, 2002; LaRosa *et al.*, 2006]. Interestingly, a few research disclosed raised inflammatory markers, such as C-reactive protein, upon dietary interventions with conjugated linoleic acid [Steck *et al.*, 2007].

Contrary to conjugated linoleic acid, the linoleic acid supplementation evoked accumulation of fat and increased body mass as well as diminished thermogenesis and oxygen consumption in the C57BL/6 mice model [Shin & Ajuwon, 2018b]. Furthermore, no signs of browning-specific gene upregulation were noted. Nevertheless, linoleic acid addition to murine primary subcutaneous adipocytes *in vitro* resulted in *Ucp1* overexpression and insignificant *Ppargc1a* mRNA elevation [Shin & Ajuwon, 2018a]. Thus, the discrepancy between conjugated linoleic acid and linoleic acid browning properties *in vivo* may be attributed to the fact that high-fat diet itself leads to adipocyte browning inhibition, and linoleic acid is not capable of attenuating high-fat diet-induced alterations [Shin & Ajuwon, 2018b].

10-Oxo-12(*Z*)-octadecenoic acid

10-Oxo-12(*Z*)-octadecenoic acid is a product of saturation metabolism of linoleic acid by gut microbiota, especially *Lactobacillus* spp. [Kishino *et al.*, 2013]. Upon its administration, a significant increase in expression of *Ucp1, Prdm16, Ppargc1a, Tbx1, Cpt1b,* and *Adrb3* in iWAT, as well as BAT, of C57BL/6 mice was observed [M. Kim *et al.*, 2017]. 10-Oxo-12(*Z*)-octadecenoic acid induced adipocyte browning and weight loss *via* gastrointestinal TRPV1 receptors, which activated β_3-adrenergic signaling, a potent browning stimulator. Furthermore, its supplementation reduced blood glucose and triglycerides [M. Kim *et al.*, 2017].

Oleic acid

Olive oil is the most common source of oleic acid, a monounsaturated *n*-9 fatty acid, and a crucial element of the Mediterranean diet [Marcelino *et al.*, 2019]. Regarding adipocyte browning, oleic acid administration resulted in marginally augmented *Ucp1* expression in 3T3-L1 adipocytes, while no effect of oleic acid was observed in 10T1/2 cells or murine primary subcutaneous adipocytes *in vitro* [Shin & Ajuwon, 2018a]. Surprisingly, oleic acid did not show a potent browning-inducing effect, in contrast to the outcomes of olive oil supplementation (see: *Olive oil* section) [Shin & Ajuwon, 2018b].

Stearic acid

Animal fats, as well as cocoa and shea butter, are products abundant in stearic acid, which acts as a potent adipocyte browning inhibitor [Shin & Ajuwon, 2018b]. Stearic acid-rich diet based on high shea butter intake resulted in diminished *Ucp1, Ppargc1a,* and *Adrb3* expression in eWAT and also lowered the *Ucp1* mRNA level in sWAT of C57BL/6 mice [Shin & Ajuwon, 2018b]. Interestingly, shea butter diet significantly upregulated *Prdm16* in eWAT and *Tfam* in sWAT, although increased content of WAT and total body weight were noticed. Moreover, no alterations of browning-specific genes were observed in murine primary subcutaneous adipocytes as

well as 3T3-L1 and 10T1/2 cell lines *in vitro*, except for *Cidea* downregulation in primary subcutaneous adipocytes [Shin & Ajuwon, 2018a]. In addition, stearic acid supplementation led to elevated triglycerides accumulation in the liver as well as raised blood glucose and insulin [Shin & Ajuwon, 2018b].

Arachidonic acid

Arachidonic acid is a product of linoleic acid metabolism, which serves as a substrate for prostaglandins production [Sonnweber *et al.*, 2018]. Common dietary sources of arachidonic acid are eggs, fishes, meat and poultry [Taber *et al.*, 1998]. Recent research revealed that intake of arachidonic acid may inhibit adipocyte browning in human multipotent adipose-derived stem cells, which was manifested by decreased UCP1 at both mRNA and protein levels [Pisani *et al.*, 2014]. In addition, a significant decline in mitochondrial activity, as well as impaired browning upon β_3-AR agonist, was observed. Since elevated expression of both isoforms of cyclooxygenase (COX-1 and COX-2) and increased concentrations of prostaglandins E2 and F2α were noted in adipocytes, a prostaglandins-dependent pathway was suggested as the mechanism of browning suppression [Pisani *et al.*, 2014]. However, the same prostaglandin E2 was previously considered as a browning activator in both human and murine models [García-Alonso *et al.*, 2013, 2016]. This discrepancy might be attributed to the stimulation of different receptors for prostaglandin E2. High affinity EP4 receptor activity was recognized to promote cAMP signaling and stimulate browning, while low affinity EP1 receptor working through calcium signaling pathway evoked the opposite effect [Pisani *et al.*, 2014].

Moreover, the suppressive effect of arachidonic acid on the adipocyte browning was also reported in interscapular WAT of C57BL/6J mice (↓ UCP1, PRDM16, PGC1α, C/EBPβ), while in gonadal WAT molecular signs of browning (↑ UCP1, PRDM16, PGC1α, C/EBPβ, CIDEA) were found [Zhuang *et al.*, 2017]. Interestingly, arachidonic acid supplementation showed gender-specific effects on metabolic outcomes and inflammation. Arachidonic acid beneficially modulated insulin sensitivity and adipose tissue inflammation in female mice, and did the opposite in males [Zhuang *et al.*, 2017]. Possibly this is due to altered composition of gut microbiota in female mice (reduced Firmicutes/Bacteroidetes ratio), as a result of gender-dependent arachidonic acid interaction [Zhuang *et al.*, 2017].

Docosahexaenoic and eicosapentaenoic acids

n-3 Long-chain polyunsaturated fatty acids, such as docosahexaenoic and eicosapentaenoic acids (DHA and EPA, respectively), are well-known metabolism regulators found mainly in fish oil [Kris-Etherton *et al.*, 2009]. Recent research has suggested that positive metabolic effects of DHA and EPA might be associated with stimulation of the adipocyte browning [Bargut *et al.*, 2019; Laiglesia *et al.*, 2016; Zhao & Chen, 2014].

Both DHA and EPA, as well as a mixture of DHA with EPA, reduced adipocyte size and significantly increased expression of browning-specific genes, such as *Ucp1, Cd137, Ppargc1a, Nrf1, Tfam, Ppara, Pparg*, in iWAT of C57BL/6 mice [Bargut *et al.*, 2019]. Interestingly, the most potent effect was exerted by EPA itself, while DHA+EPA supplementation resulted mostly in significantly smaller gene upregulation than single EPA or DHA. Similarly, the above-mentioned genes were also overexpressed in BAT in response to both DHA and EPA as well as its mixture, except for insignificant *Ppargc1a* alteration upon DHA+EPA [Bargut *et al.*, 2019]. Furthermore, both DHA and EPA raised *Prdm16, Cidea, Cpt1b,* and *Cox8b* in iWAT of C57BL/6 mice; however, only the DHA-treated group showed a decreased fat mass and adipocyte volume as well as upregulation of *Cebpb* and bone morphogenetic protein 7 [Zhuang *et al.*, 2019]. Moreover, both DHA and EPA were responsible for the elevated expression of *Ucp1, Ppargc1a, Pparg, Cidea, Cpt1b,* and *Cox8b* in 3T3-L1 adipocytes [Zhuang *et al.*, 2019]. Nevertheless, DHA supplementation increased the expression of those genes to a greater extent than EPA and initiated the adipocyte browning a few days earlier [Zhuang *et al.*, 2019], suggesting DHA to be a more potent browning activator than EPA, on the contrary to the previously described paper [Bargut *et al.*, 2019].

Signs of adipocyte browning were also reported in human differentiated subcutaneous adipocytes upon EPA administration *in vitro* [Laiglesia *et al.*, 2016]. The addition of EPA to the medium was associated with an enhanced expression of *UCP1, PRDM16, CIDEA, CD137, TBX1, NRF1, TFAM,* and *CPT1A,* which is in line with the results obtained on murine model [Zhao & Chen, 2014].

However, one of the *in vivo* studies completely denied EPA-induced adipocyte browning presenting no effect of EPA in upregulating *Ucp1, Prdm16, Ppargc1a, Pparg, Cidea*, *Elovl3,* and *Fgf21* genes in murine iWAT, while showing that all of them were significantly enhanced in BAT [Pahlavani *et al.*, 2017].

There are also inconsistencies regarding the role of DHA and EPA in lipolysis and lipogenesis. Two of the studies report significant elevation in hormone-sensitive lipase expression [Bargut *et al.*, 2019], with concomitant increase in the lipolytic rate and inhibition of lipogenic enzymes, including fatty acid synthase [Laiglesia *et al.*, 2016]. On the other hand, another study showed inhibition of hormone-sensitive lipase and adipose triglyceride lipase, indicating lipolysis suppression, as well as overexpression of glycerol-3-phosphate acyltransferase 1 and 3 involved in lipogenesis [Zhao & Chen, 2014].

Furthermore, DHA, and EPA elevated serum adiponectin and decreased leptin [Bargut *et al.*, 2016; Zhuang *et al.*, 2019]. Interestingly, DHA also reduced the level of low-grade systemic inflammation, diminishing tumor necrosis factor α (TNF-α) and interleukin 6 (IL-6) concentrations, and increasing anti-inflammatory IL-10 [Zhuang *et al.*, 2019]. Moreover, EPA enhanced glucose transporter type 4 and lipoprotein lipase mRNAs, which might contribute to lowered blood glucose, low-density lipoprotein cholesterol (LDL-C), and total cholesterol [Bargut *et al.*, 2019; Zhao & Chen, 2014].

Several mechanisms of DHA and EPA-induced adipocyte browning have been proposed so far. First of them is the activation of the sympathetic nervous system, which might be a result of β_3-AR or TRPV1 receptors stimulation or FGF21 action [Bargut *et al.*, 2016; Kim *et al.*, 2015]. Another possible

TABLE 2. Summary of *in vivo* studies of docosahexaenoic acid (DHA) and eicosapentaenoic acid (EPA) regarding adipocyte browning stimulation.

Substance	Dose (g/kg/day)	Duration (week)	Research material	Adipose tissue deposit	Genes/mRNAs alterations	Reference
DHA	8.47	5	C57BL/6 mice	iWAT and BAT	↑↑ *Ucp1, Cd137, Ppargc1a, Nrf1, Tfam, Ppara, Pparg* ↑ *Fndc5, Hsl*	Bargut *et al.* [2019]
DHA	10	15	C57BL/6J mice	iWAT	↑ *Prdm16, Cidea, Cpt1b, Cox8b*	Zhuang *et al.* [2019]
EPA	8.47	5	C57BL/6 mice	iWAT and BAT	↑↑↑ *Ucp1, Cd137, Ppargc1a, Nrf1, Tfam, Ppara, Pparg* ↑ *Fndc5, Hsl*	Bargut *et al.* [2019]
EPA	10	15	C57BL/6J mice	iWAT	↑ *Prdm16, Cidea, Cpt1b, Cox8b*	Zhuang *et al.* [2019]
EPA	36	11	C57BL/6J mice	iWAT	↔ *Ucp1, Prdm16, Ppargc1a, Pparg, Cidea*, *Elovl3, Fgf21* ↔ *Fndc5*	Pahlavani *et al.* [2017]
EPA	36	11	C57BL/6J mice	BAT	↑ *Ucp1, Prdm16, Ppargc1a, Pparg, Cidea*, *Elovl3, Fgf21* ↔ *Fndc5*	Pahlavani *et al.* [2017]
DHA + EPA	4.235 + 4.235	5	C57BL/6 mice	iWAT	↑ *Ucp1, Cd137, Ppargc1a, Nrf1, Tfam, Ppara, Pparg* ↑ *Fndc5,* ↓ *Hsl*	Bargut *et al.* [2019]
DHA + EPA	4.235 + 4.235	5	C57BL/6 mice	BAT	↑ *Ucp1, Cd137, Nrf1, Tfam, Ppara, Pparg*	Bargut *et al.* [2019]

BAT: brown adipose tissue; *Cidea*: cell death activator CIDE-A; *Cox8b*: cytochrome c oxidase subunit 8B, mitochondrial; *Cpt1b*: carnitine *O*-palmitoyltransferase 1, muscle isoform; *Elovl3*: elongation of very long chain fatty acids protein 3; *Fgf21*: fibroblast growth factor 21; *Fndc5*: fibronectin type III domain-containing protein 5; *Hsl*: hormone-sensitive lipase; iWAT: inguinal white adipose tissue; *Nrf1*: nuclear respiratory factor 1; *Ppara*: peroxisome proliferator-activated receptor α; *Pparg*: peroxisome proliferator-activated receptor γ; *Ppargc1a*: peroxisome proliferator-activated receptor γ coactivator 1-α; *Prdm16*: PR domain-containing protein 16; *Tfam*: transcription factor A, mitochondrial; *Ucp1*: uncoupling protein 1.

mechanism involves AMPK/PGC1α or SIRT1/PGC1α pathways, which play role in mitochondrial biogenesis [Laiglesia *et al.*, 2016; Zhao & Chen, 2014]. Interestingly, AMPK/PGC1α signaling may be partially induced by apelin, which secretion might be augmented in response to fish oil consumption [Yuzbashian *et al.*, 2018]. Moreover, the action of DHA and EPA is associated with the GPR120 receptor, which promotes microRNAs miR-30b and miR-378 to modulate gene expression as well as may be linked with FGF21 activity and attenuation of inflammation-related browning inhibition [Kim *et al.*, 2016; Lund *et al.*, 2018; Quesada-López *et al.*, 2016].

In addition, both DHA and EPA, as well as DHA+EPA, were found to elevate fibronectin type III domain-containing protein 5 expression in murine iWAT, a precursor of irisin, which is capable of adipocyte browning stimulation itself [Bargut *et al.*, 2019]. However, other studies failed to detect changes in irisin concentrations in iWAT and BAT upon EPA supplementation [Pahlavani *et al.*, 2017].

The summary of the above-mentioned *in vivo* and *in vitro* studies concerning DHA and EPA browning potential is presented in Table 2 and Table 3, respectively.

Palmitoyl lactic acid

Palmitoyl lactic acid is often used as an emulsifying agent of food [Unno *et al.*, 2018]. Using the 3T3-L1 preadipocytes model, Unno *et al.* [2018] revealed that palmitoyl lactic acid as a substantial component of krill *Euphausia superba* oil fraction had adipocyte browning properties. Through unknown mechanism, palmitoyl lactic acid increased UCP1, PRDM16, PPARγ, and PGC1α at both mRNA as well as protein levels and upregulated expression of *Cidea*, *Cited1, Cox7a1*, *Fgf21,* and *Tmem26* after 7 days of administration. Moreover, it stimulated adipogenesis, inducing perilipin and fatty acid-binding protein 4, as well as elevated accumulation of lipids in small droplets. Interestingly, palmitoyl lactic acid is the only fatty acid so far that boosted adipogenesis in the presence of dexamethasone [Unno *et al.*, 2018].

Short-chain fatty acids

Short-chain fatty acids originate from dietary fibers during intestinal fermentation, and are an essential source of energy for colonocytes [Wong *et al.*, 2006]. Acetic, propionic, and butyric acids are the most prevalent short-chain fatty acids [Tazoe *et al.*, 2008]. Recently, Lu *et al.* [2016] proved that short-chain fatty acids also participated in adipocyte browning, leading to enhanced expression of *Ppargc1a*, *Tbx1*, *Tmem26*, *Cd137*, *Nrf1*, *Tfam,* as well as increased β-oxidation and mitochondrial biogenesis, in eWAT of C57BL/6J male mice. Moreover, Hu *et al.* [2016] confirmed that acetic acid administration resulted in elevated UCP1 and PGC1α, both at mRNA and protein level in immortalized brown adipocytes, while Weitkunat *et al.* [2017] reported upregulation of *Ppargc1a* mRNA and cytochrome c oxidase activity in sWAT of C57BL/6JRj mice. Interestingly, short-chain fatty acids reversed high-fat diet-induced adipocyte hyperplasia and altered microbiota composition, preferring overgrowth of *Bifidobacterium* [Weitkunat *et al.*, 2017] and reducing Firmicutes/Bacteroidetes ratio [Lu *et al.*, 2016]. Furthermore, propionic acid was found to increase transcription of neuregulin 4 [Weitkunat *et al.*, 2017], a batokine considered as an inhibitor of hepatic lipogenesis [Villarroya *et al.*, 2017]; however, only acetic acid supplementation resulted in the suppression of lipogenesis in the liver [Weitkunat *et al.*, 2017]. In addition,

TABLE 3. Summary of *in vitro* studies of docosahexaenoic acid (DHA) and eicosapentaenoic acid (EPA) regarding adipocyte browning stimulation.

Substance	Concentration (μM)	Duration (day)	Research material	Genes/mRNAs alterations	Protein alterations	Reference
DHA	100	8	3T3-L1 cells	↑↑↑ *Ucp1, Ppargc1a, Pparg, Cidea, Cpt1b, Cox8b*	Not studied	Zhuang *et al.* [2019]
EPA	100	8	3T3-L1 cells	↑ *Ucp1, Ppargc1a, Pparg, Cidea, Cpt1b, Cox8b*	Not studied	Zhuang *et al.* [2019]
EPA	200	8	iWAT-derived SVC	↑ *Ucp1, Prdm16, Ppargc1a, Cidea, Cd137, Nrf1, Tfam, Tbx1, Cpt1a* ↓ *Hsl, Atgl*	Not studied	Zhao & Chen [2014]
EPA	100	1	overweight female-derived sWAT	↑ *UCP1, PRDM16, CIDEA, CD137, TBX1, NRF1, TFAM, TMEM26, CPT1A*	Not studied	Laiglesia *et al.* [2016]

Atgl: adipose triglyceride lipase; *Cidea*: cell death activator CIDE-A; *Cox8b*: cytochrome c oxidase subunit 8B, mitochondrial; *Cpt1a*: carnitine *O*-palmitoyltransferase 1, liver isoform; *Cpt1b*: carnitine *O*-palmitoyltransferase 1, muscle isoform; *Hsl*: hormone-sensitive lipase; iWAT: inguinal white adipose tissue; *Nrf1*: nuclear respiratory factor 1; *Ppara*: peroxisome proliferator-activated receptor α; *Pparg*: peroxisome proliferator-activated receptor γ; *Ppargc1a*: peroxisome proliferator-activated receptor γ coactivator 1-α; *Prdm16*: PR domain-containing protein 16; SVC: stromal vascular cells; sWAT: subcutaneous white adipose tissue; *Tbx1*: T-box transcription factor TBX1; *Tfam*: transcription factor A, mitochondrial; *Tmem26*: transmembrane protein 26; *Ucp1*: uncoupling protein 1.

short-chain fatty acids improved carbohydrate and lipid metabolism as well as reduced the concentration of proinflammatory cytokines [Lu *et al.*, 2016; Weitkunat *et al.*, 2017].

All effects of short-chain fatty acids are likely mediated by GPR43, which promotes phosphorylation of extracellular signal-regulated kinases 1/2 and cAMP response element--binding protein [Hu *et al.*, 2016], while the role of GPR41 remains unclear [Hu *et al.*, 2016; Lu *et al.*, 2016]. Taken together, short-chain fatty acids attenuated weight gain in high-fat diet mice [Lu *et al.*, 2016; Weitkunat *et al.*, 2017], and acetic acid was found to have the highest impact [Lu *et al.*, 2016].

RETINOIDS

All-*trans* retinoic acid is a bioactive form of vitamin A, the latter found primarily in vegetables, fruits, dairy products, eggs, and meat in the form of retinol and its esters, or provitamin A [Dawson, 2000]. While the role of all-*trans* retinoic acid in the treatment of acute promyelocytic leukemia and acne is well known [Bershad *et al.*, 1999; Meng-er *et al.*, 1988], recent studies revealed its involvement in adipocyte browning activation [Guo *et al.*, 2016; Murholm *et al.*, 2013; Tourniaire *et al.*, 2015; Wang *et al.*, 2017].

Administration of all-*trans* retinoic acid significantly upregulated expression of *Ucp1, Prdm16, Pparg, Cidea, Elovl3,* and *Cox7a1* in iWAT of C57BL6 mice *in vivo* and iWAT-derived stromal vascular cells *in vitro* [Wang *et al.*, 2017]. Furthermore, a similar increase of BAT markers, including *Ucp1, Ppargc1a, Ppara,* and *Cd137,* was observed in eWAT and rWAT of Naval Medical Research Institute mice [Mercader *et al.*, 2006; Tourniaire *et al.*, 2015]; however no molecular signs of the adipocyte browning were reported in human multipotent adipose-derived stem cells or human preadipocytes upon all-*trans* retinoic acid supplementation [Murholm *et al.*, 2013]. In addition, all-*trans* retinoic acid induced mitochondrial biogenesis, β-oxidation, and oxidative phosphorylation capacity in murine *in vivo* and *in vitro* models [Tourniaire *et al.*, 2015]. Finally, all-*trans* retinoic acid altered adipocyte morphology to multilocular and elevated angiogenesis by upregulation of vascular endothelial growth factor A and its receptors [Mercader *et al.*, 2006; Wang *et al.*, 2017]. All actions of all--*trans* retinoic acid resulted in decreased adiposity, weight loss, reduced plasma glucose and triglycerides, as well as improved insulin sensitivity [Berry & Noy, 2009; Wang *et al.*, 2017].

The main mechanism of all-*trans* retinoic acid is associated with direct stimulation of retinoic acid response elements by binding to retinoic acid receptors, which form complexes with retinoid X receptors in promoter/enhancer regions of all-*trans* retinoic acid-dependent genes [Murholm *et al.*, 2013]. Thus, the downstream mechanism of all-*trans* retinoic acid-induced adipocyte browning at least partially refers to the activation of retinoic acid response elements on *Ucp1, Prdm16,* vascular endothelial growth factor A, and lipocalin 2 genes [Guo *et al.*, 2016; Murholm *et al.*, 2013; Wang *et al.*, 2017].

GLUCOSINOLATES AND OTHER SULFUR--CONTAINING PLANT SECONDARY METABOLITES

Glucoraphanin and sulforaphane

Broccoli and cauliflower are the sources of glucosinolates, including glucoraphanin, which is a precursor of biologically active sulforaphane – an activator of *Nrf2* [Houghton *et al.*, 2016]. Bioavailability of glucoraphanin ranges from 10% to 40% [Fahey *et al.*, 2015], the latter achieved upon plant myrosinase addition, which enhances glucoraphanin conversion to sulforaphane [Shapiro *et al.*, 2001]. Nagata *et al.* [2017] tested glucoraphanin supplementation in wild-type and *Nrf2* knockout ($Nrf2^{-/-}$) mice. They found that the glucoraphanin-rich diet mitigated decreased UCP1 levels in eWAT and iWAT of high-fat diet wild-type mice through the NRF2--related pathway. The browning-positive effect of glucoraphanin was confirmed with enhanced expression of *Nqo1* (target gene of NRF2) and browning-specific genes, such as *Ucp1, Prdm16, Cidea,* and *Elovl3,* after sulforaphane administration. Interestingly, BAT in wild-type mice was not affected by glucoraphanin supplementation since no differences were noticed in mRNA levels of *Ucp1* and *Ppargc1a* [Nagata *et al.*, 2017]. Furthermore, *in vitro* studies on 3T3-L1 adipocytes evidenced

that sulforaphane upregulated expression of UCP1, SIRT1, PGC1α, NRF1, and NRF2 proteins, suggesting the activation of Sirt1/PGC1α pathway and NRF-mediated mitochondrial biogenesis as a primary mechanism of sulforaphane-induced adipocyte browning [H. Q. Zhang *et al.*, 2016].

Allicin

Allicin is a substance found in garlic and known for its antimicrobial properties since decades [Cavallito & Bailey, 1944]. The bioavailability of allicin is the highest when garlic is consumed raw (80%), and diminishes significantly when it is roasted (30%), pickled (19%) or boiled (16%) [Lawson & Hunsaker, 2018]. Recent studies show that allicin may affect the adipocyte browning, increasing *Ucp1, Prdm16,* and *Ppargc1a* mRNAs as well as mitochondria mass in differentiated 3T3-L1 adipocytes [Lee *et al.*, 2019]. In addition, its browning-positive effect was evidenced in iWAT of C57BL/6J mice. Upon 8-week supplementation with allicin, multilocular morphology of the adipocytes, elevated expression of *Ucp1, Prdm16,* and *Ppargc1a*, and attenuated weight gain were observed [Lee *et al.*, 2019].

Overexpression of the KLF15 transcription factor and its enhanced binding to the *Ucp1* promoter at the Sp1ER site was suggested as a part of the allicin-induced adipocyte browning mechanism [Lee *et al.*, 2019]. Moreover, allicin activated the extracellular signal-regulated kinases 1/2 pathway, which additionally intensified the expression of browning activators, including KLF15.

Interestingly, allicin reduced serum triglycerides and free fatty acids concentrations, not only preventing obesity but also improving metabolic health [Lee *et al.*, 2019].

VOLATILE ORGANIC COMPOUNDS

D-Limonene

D-Limonene is the major constituent of citrus oils, found in orange, mandarin, lemon, grapefruit and lime [Sun, 2007]. After oral administration, 43% of ingested D-limonene is bioavailable, according to a rat study [Chen *et al.*, 1998]. An *in vitro* study on 3T3-L1 adipocytes showed that limonene stimulates transcription of *Ucp1*, *Prdm16, Pparg*, *Cited1*, *Cidea*, *Fgf21* as well as translation of UCP1, PRDM16, PGC1α, and C/EBPβ, all indicative of adipocyte browning [Lone & Yun, 2016]. Mechanistically, the activation of β_3-AR signaling and mitogen-activated protein kinase/extracellular signal-regulated kinases pathway was suggested in D-limonene's browning-positive effects. In addition, limonene supplementation elevated phosphorylation of AMPK and acetyl-CoA carboxylase, which stimulated lipolysis and provided a supply of fatty acids as a source of energy for thermogenesis [Lone & Yun, 2016].

Menthol

Menthol, an agonist of the TRPM8 receptor, is derived from *i.a.* peppermint, or corn mint [Peier *et al.*, 2002]. After ingestion, the mean recovery of menthol as glucuronide ranged from 45.6% (menthol capsule) to 56.6% (mint candy/tea) [Gelal *et al.*, 1999]. Jiang *et al.* [2017] examined whether WAT adipocytes could be deluded by menthol mimicking cold exposure *via* TRPM8-related cooling sensation and induce adipocyte browning. Results of their *in vitro* study on murine white adipocytes revealed that menthol stimulation increased mRNAs of *Ucp1* and *Pgc1α* unless TRPM8 was blocked, supporting the role of TRPM8 in adipocyte browning. Mechanistically, TRPM8 activation resulted in higher cytoplasmic content of calcium, which energized PKA in an unknown pathway [Jiang *et al.*, 2017]. Interestingly, the contribution of TRPA1 in mediating menthol-induced adipocyte browning is also under consideration [Farco & Grundmann, 2013]. Menthol's browning-positive effect was also corroborated *in vivo* since its supplementation enhanced expression of *Ppargc1a, Ucp1, Prdm16, Trpm8,* and *Adrb3* in both eWAT and sWAT of high-fat diet mice, while transcription of *Pparg* remained unchanged [Jiang *et al.*, 2017]. Additionally, menthol counteracted adipocyte hypertrophy, leading to a reduced diameter of fat cells. Of note, there is also evidence of menthol-mediated browning in human adipocytes *in vitro* [Rossato *et al.*, 2014].

Phytol

Phytol, a branched-chain fatty alcohol present in chlorophyll molecules, improves glucose tolerance, expression of β-oxidation enzymes, and reduces serum fatty acid concentrations [Zhang *et al.*, 2018]. Rat studies revealed that bioavailability of phytol given orally varies between 30–66% [Mize *et al.*, 1966]. Its derivative is phytanic acid, known for WAT browning and increasing the expression of the UCP1 in HIB1B cells [Schluter *et al.*, 2002]. Major food sources of phytanic acid are dairy lipids and ruminant meat [Verhoeven & Jakobs, 2001].

Reduction of adipocyte diameter and formation of multilocular adipocytes, as well as increased expression of UCP1, PRDM16, PGC1α, Cyt C, and pyruvate dehydrogenase, also suggest the participation of phytol in the browning process in both iWAT of C57BL/6J mice and 3T3-L1 cells [Zhang *et al.*, 2018]. Additionally, overexpression of *Cidea*, *Elovl3*, *Cd137* and *Tmem26* mRNAs was observed in 3T3-L1 preadipocytes. Furthermore, the administration of phytol also multiplied mitochondrial content and O_2 consumption, resulting in better weight cont. Activation of the AMPKα pathway is considered as an underlying mechanism of phytol-induced adipocyte browning [Zhang *et al.*, 2018].

Thymol

Thymol is a phenolic monoterpene component obtained from the *Thymus* species, which is used as a food additive or aroma [Choi *et al.*, 2017]. Its bioavailability after oral administration is at least 16% [Kohlert *et al.*, 2002]. It acts as a pleiotropic agent, exerting neuroprotective, anti-inflammatory, antibacterial, and anti-diabetic effects. Recent studies reported, it may also lead to the browning of WAT [Choi *et al.*, 2017].

Upon 6- to 8-day thymol administration, the expression of BAT-specific genes, such as *Ucp1*, *Prdm16*, *Ppargc1a*, *Tbx1, Tmem26*, *Cidea*, *Cited1,* and *Fgf21*, significantly increased in 3T3-L1 adipocytes [Choi *et al.*, 2017]. Elevated concentrations of UCP1, PRDM16, PGC1α, PPARγ, and C/EBPβ proteins were also observed. In addition, a substantial rise

in mitochondrial biogenesis occurred due to the upregulation of the *Tfam* and *Nrf1* genes.

The activation of β_3-AR, resulting in the activation of PKA and p38 mitogen-activated protein kinase, as well as enhanced phosphorylation of AMPK, was suggested as a possible mechanistic explanation of thymol-induced adipocyte browning [Choi *et al.*, 2017].

By raising the level of carnitine *O*-palmitoyltransferase 1 and acyl-coenzyme A oxidase thymol intensified β-oxidation [Choi *et al.*, 2017]. A reduction in triglycerides and lipoprotein lipase levels and an increment in hormone sensitive lipase and perilipin were also noted.

trans-Anethole

trans-Anethole is a compound of essential oils derived from *i.a.*: anise, star anise, and fennel [Bartoňková & Dvořák, 2018], characterized with very high bioavailability of 95% when administered orally [Bounds & Caldwell, 1996]. Kang *et al.* [2018] provided evidence of its browning properties in the C57BL/6 mice model and 3T3-L1 adipocytes. *trans*-Anethole increased BAT marker protein levels PGC1α, UCP1, PRDM16, and upregulated beige adipose tissue-selective genes (*Cd137*, *Cited1*, *Tbx1*, *Tmem26)* by activation of β_3-AR and SIRT1 pathways. In addition, *trans*-anethole not only induced browning and elevated BAT mass, but also activated brown cells and decreased WAT depots and body weight [Kang *et al.*, 2018].

PHENOLIC COMPOUNDS

Phenolic acids

Ellagic acid is an anti-oxidative phenolic compound of nuts, raspberries, and other plants or fruits [Vattem & Shetty, 2005]. However its bioavailability from the diet is low, only 10% [Doyle & Griffiths, 1980]. Its adipocyte browning potential was studied in male rats in the timespan of 24 weeks [L. Wang *et al.*, 2019]. Results revealed that administration of ellagic acid evoked browning of iWAT in high-fat diet animals, which was proved by increased expression of PGC1α, UCP1, *Ppara, Prdm16, Cidea, Tmem26,* and *Cd137,* whereas C/EBPβ, PPARγ, and C/EBPα were decreased. This phenomenon could be explained by lowered levels of zinc finger protein 423 and retinal dehydrogenase 1 mRNAs since both are responsible for preserving the white adipocyte phenotype [L. Wang *et al.*, 2019]. Hence, suppression of these molecules by ellagic acid is considered as the principal mechanism of ellagic acid-related browning. In addition, ellagic acid promoted activation of BAT and improved metabolism, leading to reduced weight, insulin resistance as well as lowered accumulation of lipids in the liver [L. Wang *et al.*, 2019]. Interestingly, ellagic acid supplementation altered adipokines profile, decreasing plasma concentration of "white" adipogenic marker – resistin, without changing adiponectin which might possibly prevent effects of resistin on liver steatosis [L. Wang *et al.*, 2019]. Notably, gut microbiota transforms ellagic acid into urolithin A [Bialonska *et al.*, 2009], characterized with higher bioavailability than the ellagic acid [Landete, 2011]. Thus, it needs to be elucidated if the latter contributes to the browning and metabolic effects of ellagic acid.

Flavonoids

Flowers, honeycombs, and mushrooms are the sources of the chrysin, which carries numerous health benefits, including anti-cancer, anti-inflammatory, anti-diabetic, hypolipidemic, and hypocholesterolemic effects [Choi & Yun, 2016]. At the same time, the bioavailability of chrysin in humans is very low (0.003–0.02%) [Walle *et al.*, 2001]. Studies on 3T3-L1 cells showed that it is also engaged in adipocyte browning by increasing the expression of BAT-specific proteins (UCP1, PRDM16, PGC1α, PPARγ, C/EBPβ) and genes (*Ucp1*, *Ppargc1a*, *Prdm16*, *Cidea*, *Cited1*, *Fgf21*, *Tbx1*, *Tmem26*) [Choi & Yun, 2016]. Chrysin stimulated this process by activating the AMPK pathway. The expansion of multilocular adipocytes was also reported. Moreover, an increment in hormone-sensitive lipase, perilipin, lipoprotein lipase, carnitine *O*-palmitoyltransferase 1 and acyl-coenzyme A oxidase levels was observed, as well as acetyl-CoA carboxylase phosphorylation, which indicates its influence on lipid metabolism [Choi & Yun, 2016].

Cacao and tea are the rich sources of (–)-epicatechin [Bártíková *et al.*, 2017; Ramiro-Puig & Castell, 2009]. The bioavailability of this flavan-3-ol was described by urinary recovery ranging from 24.1 to 29.8%, 24 h after ingestion of cacao or chocolate, respectively, while the majority of (–)-epicatechin metabolites (80%) are eliminated in just 8 h [Baba *et al.*, 2000]. (–)-Epicatechin was tested on human adipocytes (isolated from sWAT during surgery) and adipocytes from obese C57BL/6 mice [Varela *et al.*, 2017]. (–)-Epicatechin provoked adipocyte browning in both groups, which was demonstrated with higher levels of BAT hallmarks, such as UCP1, PRDM16, and DIO2. There are a few possible mechanisms of (–)-epicatechin-induced adipocyte browning: raised phosphorylation of AMPK and acetyl-CoA carboxylase, lower acetylation of PPARγ and PGC1α, as well as the promotion of mitochondrial biogenesis [Varela *et al.*, 2017]. Moreover, (–)-epicatechin multiplies mitochondrial activity and intensifies fatty acid oxidation. Interestingly, (–)-epicatechin reduced TNF-α and IL-6 plasma concentrations, additionally providing an anti-inflammatory effect [Varela *et al.*, 2017].

Genistein belongs to isoflavones, phytoestrogens derived from *Fabaceae, e.g.*, *Soiae semen* [Jaiswal *et al.*, 2019]. Its absolute bioavailability in mice was found to be 89%; however, only 9.4% maintained the biologically active aglycone form [Andrade *et al.*, 2010]. After genistein administration under both, control and peroxidative stress conditions, Grossini *et al.* [2018] reported a dose-dependent increase in UCP1 expression in human preadipocytes isolated from visceral WAT. The same effect was also observed in differentiated brown adipocytes, but to a greater extent, determining genistein as a potent adipocyte browning inductor even in the case of oxidative stress [Grossini *et al.*, 2018]. At the molecular level, browning properties of genistein were associated with activation of Akt and AMPKα/β and subsequent elevation of mitofusin-2. In addition, the browning potential of genistein was also studied *in vivo* on female Wistar rats after ovariectomy [Shen *et al.*, 2019]. Genistein was found to increase translation of UCP1, PRDM16, PGC1α, CIDEA, NRF1, and TFAM, as well as a transcription of *Ppargc1a, Ucp1,* and *Tbx1* in iWAT after 4-week therapy. The promotion

of adipocyte browning resulted in upregulation of both nuclear estrogen receptor-α (ERα) and plasma irisin [Shen *et al.*, 2019], a browning-inducing myokine [Boström *et al.*, 2012]. Moreover, genistein exerted an anti-inflammatory effect, improved insulin sensitivity, mitigated lipogenesis in the liver, and facilitated weight reduction [Shen *et al.*, 2019]. Thus, genistein appeared to be beneficial particularly in postmenopausal conditions.

Hesperidin, a citrus flavanone, regulates metabolic processes, prevents obesity, sensitizes cells to insulin, and acts as an antioxidant [Mosqueda-Solís *et al.*, 2018]. Its bioavailability is variable and depends, to a great extent, on the composition of the intestinal flora [Mas-Capdevila *et al.*, 2020]. According to recent research, hesperidin lessened adipocyte size in both rWAT and iWAT of Wistar rats after 8-week supplementation [Mosqueda-Solís *et al.*, 2018]. Besides, multilocular cells exhibiting positive staining for UCP1 and CIDEA were detected in the latter. However, hesperidin caused no difference in the expression of *Ucp1*, *Ppargc1a*, *Prdm16,* and *Cidea* mRNAs in iWAT. CIDEA protein concentrations did not significantly increase in rWAT, while in iWAT there was a substantial rise after administration of hesperidin. In BAT, total UCP1 protein level was higher compared to the control group. It is also worth noting that after hesperidin supplementation rats did not demonstrate a reduction in body fat percentage [Mosqueda-Solís *et al.*, 2018].

Licochalcone A is found in *Glycyrrhiza uralensis*. This chalcone is known for its anti-oxidative and immunomodulatory effects [Jia *et al.*, 2017], despite its poor bioavailability of 3.3% after oral administration [Weng *et al.*, 2019]. It was also reported to enhance expression of UCP1 in 3T3-L1 adipocytes after 4 days of exposure [Lee *et al.*, 2018]. Its browning potential was confirmed by histological and immunochemical signs of browning in iWAT after 19 days of its peritoneal administration to C57BL/6 mice. PRDM16 and PGC1α levels were increased as well, which may partly explain the mechanism of browning. Another mechanistic evidence might be attributed to the downregulation of PPARγ, C/EBPα, and sterol regulatory element-binding protein 1c, which was reported in 3T3-L1 adipocytes by Quan *et al.* [2012]. Interestingly, licochalcone A was also found to multiply the browning effects of two browning activators: triiodothyronine and rosiglitazone [Lee *et al.*, 2018]. Moreover, it may exert beneficial effects on metabolic health, leading to the weight loss, improvement of dyslipidemia and insulin resistance.

Luteolin is a flavone found in plants such as peppermint, broccoli, celery, and oregano [Hostetler *et al.*, 2017]. When administered orally at the dosage of 50 mg/kg per rat body weight, only low bioavailability of 4.10% was achieved [Sarawek *et al.*, 2008]. X. Zhang *et al.* [2016] proved that luteolin enhanced expression of *Ucp1, Ppargc1a, Ppara, Cidea, Elovl3, Tmem26, Cd137, Cited1,* and *Sirt1* in sWAT, but not in eWAT, of C57BL/6 mice fed a high-fat diet. They also demonstrated a significant increase in UCP1 and a change in sWAT adipocyte phenotype (multilocular morphology). Moreover, luteolin was found to enhance the thermogenic activity of BAT by upregulating *Ucp1, Ppargc1a, Ppara, Cidea,* and *Sirt1,* though *Elovl3* and *Prdm16* were not affected. Interestingly, the browning-positive effect of luteolin was also evidenced in mice administered a low-fat diet [X. Zhang *et al.*, 2016]. The action of luteolin is tightly connected with AMPK phosphorylation, which results in the induction of PGC1α and promotes thermogenesis [X. Zhang *et al.*, 2016]. Of note, the effect of luteolin on *Prdm16* mRNA needs to be elucidated since its elevation was noticed only *in vitro* [X. Zhang *et al.*, 2016].

Nobiletin and naringenin are citrus flavonoids that positively influence glucose and lipid metabolism, as well as reduce oxidative stress [Gandhi *et al.*, 2020]. According to rat studies, they are characterized with similar bioavailability of 20–30% after oral administration [Felgines *et al.*, 2000; Zhang *et al.*, 2020]. The browning potential of nobiletin was demonstrated in 3T3-L1 adipocytes *in vitro* [Lone *et al.*, 2018]. By activating PKA and p-AMPK pathways, it enhanced mitochondrial biogenesis and elevated expression of transcriptional factors involved in browning: C/EBPβ, PPAR , PPARα. Furthermore, upon nobiletin supply, *Cd137, Cidea,* and *Tmem26* mRNAs, as well as PGC1α, PRDM16, UCP1, and FGF21 concentrations, increased. Additionally, nobiletin activated HIB1B brown adipocytes, upregulating expression of PRDM16, UCP1, and PGC1α [Lone *et al.*, 2018]. However, a study on Ldlr-/- mice *in vivo* questions its browning effect since no significant browning-specific features were found [Burke *et al.*, 2018]. Thus, the exact impact of nobiletin on adipocyte browning remains inconsistent and requires further studies. Similarly, there is a discrepancy concerning the browning characteristics of naringenin. A study on C57BL6/J mice *in vivo* disclosed increased *Ucp1* levels in epididymal WAT [Assini *et al.*, 2015], which was not confirmed in the *in vivo* study performed on Ldlr-/- mice [Burke *et al.*, 2018]. Nevertheless, beneficial metabolic effects of both nobiletin and naringenin were observed by Burke *et al.* [2018], despite the lack of adipocyte browning evidence at the molecular level. Reduced insulin resistance, improved lipid profile, ameliorated lipid accumulation in the liver and weight loss were reported.

Quercetin is a flavonol present in onion peel, apples, berries, and leafy vegetables [Silvester *et al.*, 2019] with antioxidant, anti-inflammatory [Lee *et al.*, 2017], and insulin resistance-reducing properties that can affect adipocyte browning [Forney *et al.*, 2018]. Its bioavailability is influenced by various factors, such as the content of lipids or indigestible fiber in the diet [Kaşıkcı & Bağdatlıoğlu, 2016]. The absolute bioavailability of quercetin in rats is estimated at 16.0–27.5%, depending on the solvent [Khaled *et al.*, 2003]. According to a 9-week study on C57BL/6J mice, the supply of quercetin resulted in iWAT and eWAT decrement, as well as the expansion of multilocular cells, increased number and diminished size of adipocytes in iWAT and eWAT [Forney *et al.*, 2018]. What is more, quercetin supplementation led to an attenuated expression of pro-inflammatory genes, such as *Cd11b*, *Cd68* in iWAT, while in eWAT there was a depletion in monocyte chemoattractant protein 1 and *Cd68* levels. Additionally, quercetin administration contributed to a decline in the serum leptin concentration [Forney *et al.*, 2018].

Pentamethylquercetin is the cardioprotective flavonoid found in the sea buckthorn [Mao *et al.*, 2009]. Due to the presence of additional methyl groups, its bioavailability is higher than that of quercetin [Chen *et al.*, 2011].

Pentamethylquercetin is known as an anti-diabetic [Wang *et al.*, 2011] and anti-obesity agent that reduces serum glucose, triglycerides, total cholesterol and LDL-C concentrations [Han *et al.*, 2017]. It was also found to reduce intracellular triglyceride concentration without enhancing lipolysis in 3T3-L1 adipocytes [Han *et al.*, 2017]. Administration of pentamethylquercetin was associated with elevated levels of *Cebpa* and *Pparg* mRNAs, and PPARγ protein, therefore, it was revealed that it did not lower the triglyceride levels by inhibiting their expression. It was also shown to upregulate *Ucp1*, *Ppargc1a*, *Cidea*, *Prdm16,* and increase the size and density of eWAT adipocytes in C57BL/6 mice, which was indicative of adipocyte browning [Han *et al.*, 2017]. Consequently, the number of cells showing multilocular morphology was multiplied due to pentamethylquercetin supplementation. Besides, an increment in interscapular BAT with simultaneous decline in eWAT mass was noted, compared to the control administered a high-fat diet [Han *et al.*, 2017].

Other phenolic compounds

Curcumin (diferuloylmethane) is an anti-inflammatory, anticancerous [Lone *et al.*, 2016], antidiabetic, and antiobesity turmeric-derived curcuminoid [Silvester *et al.*, 2019; Shan Wang *et al.*, 2015], known for its ability to inhibit adipogenesis and adipocyte differentiation [Lone *et al.*, 2016]. Unfortunately, its bioavailability in both humans and rats is poor, though may be enhanced by concomitant piperine administration [Shoba *et al.*, 1998]. Curcumin is often used as an ingredient in dietary supplements and flavor/color-enhancers for foods, such as curry powders, mustards, butters, cheeses [Lone *et al.*, 2016]. Recent studies revealed that its supply resulted in overexpression of the *Ucp1*, *Ppargc1a*, *Prdm16,* and *Cidea* genes in C57BL/6 mice iWAT [Shan Wang *et al.*, 2015], as well as 3T3-L1 cells and primary white adipocytes from iWAT of rats [Lone *et al.*, 2016]. Intensified mitochondrial biogenesis was also demonstrated, indicated by accretion in PGC1α amount [Lone *et al.*, 2016; Shan Wang *et al.*, 2015]. In C57BL/6 mice, curcumin supplementation was also found to increase the expression of thermogenic genes regulating adaptive thermogenesis and to beneficially influence weight and fat mass. These effects were observed in iWAT [Shan Wang *et al.*, 2015]. In cultured white 3T3-L1 adipocytes and in primary white adipocytes isolated from iWAT of rats, curcumin administration enhanced the expression of genes and increased contents of protein markers specific for BAT. Higher expression of *Pparg*, *Tmem26, Fgf21,* and *Cidea* genes and significant rise of UCP1, PGC1α, PRDM16, and C/EBPβ was noted [Lone *et al.*, 2016]. Furthermore, the addition of curcumin resulted in a substantial rise in levels of carnitine *O*-palmitoyltransferase 1, Cyt C, hormone sensitive lipase, and phospho-acetyl-CoA carboxylase, which suggests an intensified mitochondrial oxidation, as well as reinforced lipolysis and reduced fatty acid synthesis [Lone *et al.*, 2016]. Two different mechanisms leading to the occurrence of the above effects are considered. The first one indicates the activation of the AMPK pathway [Lone *et al.*, 2016], while the second suggests the influence of an elevated noradrenaline level on β_3-AR [Okla *et al.*, 2017; Shan Wang *et al.*, 2015].

Raspberry ketone is a food additive used in beverages and sweets which is sourced from *Rubus idaeus* [Leu *et al.*, 2018]. According to the murine study, its bioavailability is very high and its metabolism is rapid [Zhao *et al.*, 2019]. The effect of its administration on the browning of 3T3-L1 adipocytes was investigated by Leu *et al*. [2018], who demonstrated elevated levels of browning-specific proteins: UCP1, PGC1α, PRDM16, and C/EBPβ. What is more, raspberry ketone suppressed adipocyte autophagy, which normally is involved in WAT adipocyte differentiation and adipogenesis, and, in turn, increased the activity of BAT. Similarly, a substantial rise of PRDM16 and PGC1α was observed in iWAT of Wistar rats with ovariectomy-induced obesity [Leu *et al.*, 2018].

Red wine and grapes skin are rich in a natural phenolic compound named resveratrol, which belongs to stilbenoids [S. Wang *et al.*, 2015; Zou *et al.*, 2017; Zu *et al.*, 2018]. Despite over 70% absorption, bioavailability of oral resveratrol is very low, but it has been shown to accumulate in the cells of the gastrointestinal tract [Walle *et al.*, 2004]. Resveratrol has a beneficial influence on metabolism, preventing obesity and inhibiting adipogenesis [Rayalam *et al.*, 2008]. Studies revealed that its properties result mostly from involvement in WAT browning activation [Andrade *et al.*, 2019; S. Wang *et al.*, 2015; Zou *et al.*, 2017]. In CD1 mice, a 4-week supplementation with resveratrol attenuated weight gain, and lowered insulin and triglyceride serum levels [S. Wang *et al.*, 2015]. Additionally, its administration contributed to the expansion of smaller, multilocular adipocytes in iWAT, which are typically found in BAT. Besides, increased UCP1, PRDM16, and Cyt C contents with overexpression of phosphorylated AMPKα were observed, without affecting PPARγ and fatty acid-binding protein 4 concentrations. Resveratrol-supplemented mice consumed significantly more oxygen, with the level of CO_2 excreted being the same as in the control group, suggesting that fatty acid oxidation was the main source of energy [S. Wang *et al.*, 2015]. Thus, the average heat production was intensified. Furthermore, iWAT-derived stromal vascular cell analysis evidenced that resveratrol inhibited the expression of adipogenic markers, such as *Pparg* and fatty acid-binding protein 4, and prevented lipid accumulation, but only when used in higher concentrations (20 μM or 40 μM) [S. Wang *et al.*, 2015]. Resveratrol enhanced the expression of BAT hallmarks (*Ucp1*, *Prdm16*, *Cidea*, *Elovl3*) as well as *Ppargc1a*, which is crucial for mitochondrial biogenesis and intense oxidative phosphorylation. Beige fat markers, such as *Cd137*, *Tbx1*, and *Tmem26*, were also elevated and UCP1, PRDM16, Cyt C, and pyruvate dehydrogenase protein levels were raised. Finally, it augmented oxygen consumption. The effects of resveratrol on metabolic health are due to multiple mechanisms, including activation of AMPK pathway [S. Wang *et al.*, 2015]. Interestingly, pregnant mice supplementation with resveratrol induced browning and increased BAT metabolic activity in their offspring [Zou *et al.*, 2017]. This effect contributed to enhanced expression of UCP1 protein and *Ucp1, Ppargc1a, Prdm16, Cidea, Elovl3* mRNAs in BAT, iWAT, and eWAT of their offspring. Upregulation of *Cox7a1* was also observed in BAT, while an accretion of Cyt C, *Cd137*, *Tbx1,* and *Tmem*26 was demonstrated in both iWAT and eWAT where fatty

TABLE 4. Summary of *in vivo* studies of resveratrol regarding adipocyte browning stimulation.

Dose	Duration (week)	Research material	Adipose tissue deposit	Genes/mRNAs alterations	Protein alterations	Reference
100 (mg/kg/day)	4	CD1 mice	iWAT	Not studied	↑ UCP1, PRDM16, Cyt C ↔ PPARγ, FABP4	S. Wang *et al.* [2015]
200 (mg/kg/day)	3	C57BL/6J mice (pregnant)	iWAT and eWAT	↑ *Ucp1, Ppargc1a, Prdm16, Cidea, Elovl3, Cyt C, Cd137, Tbx1, Tmem26* ↔ *Fabp4, Pparg*	↑ UCP1, Cyt C ↔ PPARγ, FABP4	Zou *et al.* [2017]
			BAT	↑ *Ucp1, Ppargc1a, Prdm16, Cidea, Elovl3, Cox7a1*	↑ UCP1	
			sWAT	↑ *Ucp1, Prdm16, Sirt1, Fndc5* ↔ *Ppargc1a*	Not studied	
400 (mg/kg/day)	8	FVB/N mice	vWAT	↑ *Prdm16, Sirt1* ↔ *Ucp1, Ppargc1a, Fndc5*	Not studied	Andrade *et al.* [2019]
			BAT	↑ *Ucp1, Prdm16, Sirt1* ↔ *Ppargc1a, Fndc5*	Not studied	
500 (mg/day)	4	human	sWAT	↑ *UCP1, PRDM16, FNDC5, SIRT1* ↔ *PPARGC1A*	Not studied	Andrade *et al.* [2019]

BAT: brown adipose tissue; *Cidea*: cell death activator CIDE-A; *Cyt C*: cytochrome c; *Elovl3*: elongation of very long chain fatty acids protein 3; eWAT: epididymal white adipose tissue; *Fabp4*: Fatty acid-binding protein type 4; *Fndc5*: fibronectin type III domain-containing protein 5; iWAT: inguinal white adipose tissue; *Pparg*: peroxisome proliferator-activated receptor γ; *Ppargc1a*: peroxisome proliferator-activated receptor γ coactivator 1-α; *Prdm16*: PR domain-containing protein 16; *Sirt1*: sirtuin 1; sWAT: subcutaneous white adipose tissue; *Tbx1*: T-box transcription factor TBX1; *Tmem26*: transmembrane protein 26; *Ucp1*: uncoupling protein 1; vWAT: visceral white adipose tissue.

acid-binding protein 4, *Pparg* mRNAs and their protein levels were not affected by resveratrol. What is more, resveratrol administration reversed high-fat diet-induced attenuation of AMPKα phosphorylation in BAT, iWAT, and eWAT, and also decreased serum triglyceride and insulin, but not glucose [Zou *et al.*, 2017]. Most of the above-described alterations, except for those present in eWAT, were also demonstrated in 3-month-old adult descendants, which implies a significant long-term effect of resveratrol supplementation in pregnant mice on the metabolic processes of the offspring [Zou *et al.*, 2017]. It is worth noting that there are forms of resveratrol characterized by greater bioavailability, stability, and solubility than the free resveratrol – resveratrol encapsulated lipid nanocarriers and resveratrol encapsulated liposomes [Zu *et al.*, 2018]. Both of them dose-dependently stimulated expression of *Ucp1* mRNA and other browning markers, although resveratrol encapsulated liposomes exhibited greater biological activity. These compounds may be degraded in the digestive system, therefore to evoke a full browning effect they should be administered intravenously, which is invasive, carries a risk of complications and generates higher costs [Zu *et al.*, 2018]. An 8-week resveratrol supplementation was also assessed in Friend Virus B NIH mice [Andrade *et al.*, 2019], and was found to cause a substantial reduction in body adiposity and an increment of BAT mass. Moreover, upregulation of *Ucp1, Prdm16,* and *Sirt1* mRNAs in BAT and sWAT, as well as elevation of adiponectin concentration and decline in glucose and insulin levels were demonstrated in the resveratrol-supplemented high-fat diet group. Furthermore, the enhancement of *Prdm16* and *Sirt1* expression was observed in visceral WAT in the mice administered the resveratrol-supplemented high-fat diet [Andrade *et al.*, 2019]. In the human study, 4-week administration of resveratrol to obese study participants demonstrated overexpression of *UCP1*, *PRDM16*, *SIRT1*, and fibronectin type III domain-containing protein 5, and no change in *PPARGC1A*, regardless of resveratrol intake [Andrade *et al.*, 2019]. Overall, the researchers concluded that the effects of resveratrol are likely related to the activation of thermogenesis genes and fibronectin type III domain-containing protein 5 [Andrade *et al.*, 2019]. Crucial data on resveratrol-induced adipocyte browning are summarized in Table 4 (*in vivo* studies) and Table 5 (*in vitro* studies).

ALKALOIDS

Caffeine

As a component of coffee and some beverages, caffeine seems to be a common adipocyte browning stimulant characterized by more than 99% bioavailability upon oral administration [Bonati *et al.*, 1982]. Velickovic *et al.* [2019] demonstrated that drinking 65 mg of caffeine (the equivalent of a cup of coffee) resulted in a significantly higher temperature of the supraclavicular region (the vital BAT location) in young adults with BMI within the normal limits, assessed after 30 min. Furthermore, when testing the effect of caffeine *in vitro,* using mouse mesenchymal stem cells and human bone marrow-derived stem cells, they found an increase in UCP1 levels confirming caffeine as a browning inductor. Mechanistically, caffeine exerted its browning-positive effect by upregulation of PGC1α, *Pparg*, *Prdm16,* and *Adrb3*, as well as downregulation of *Adra2* and *Trpv2* [Velickovic *et al.*, 2019]. In addition, enhanced expression of β_3-AR and diminished of α_2-AR, acting antagonistically to β_3-AR [Lafontan *et al.*, 1997], may potentiate adipocyte browning in response to β-adrenergic stimulation, *e.g.*, during cold exposure [Velickovic *et al.*, 2019]. Nevertheless, it needs to be highlighted that elevated temperature of the skin could be evoked by an increase in blood flow rather than BAT activity, although Velickovic *et al.* [2019] undermined this possibility.

TABLE 5. Summary of *in vitro* studies of resveratrol regarding adipocyte browning stimulation.

Substance	Concentration (μM)	Duration (day)	Research material	Genes/mRNAs alterations	Protein alterations	Reference
Resveratrol	10	7	iWAT-derived SVC	↑ *Ucp1, Prdm16, Cidea, Elovl3, Ppargc1a, Cd137, Tbx1, Tmem26* ↔ *Fabp4, Pparg*	↑ UCP1, PRDM16, Cyt C	S. Wang *et al.* [2015]
Resveratrol	20 or 40	7	iWAT-derived SVC	↑ *Ucp1, Prdm16, Cidea, Elovl3, Ppargc1a, Cd137, Tbx1, Tmem26* ↓ *Fabp4, Pparg*	↑ UCP1, PRDM16, Cyt C	S. Wang *et al.* [2015]
Resveratrol Resveratrol (nanocarriers) Resveratrol (liposomes)	5 or 10 or 20	7	3T3-L1 cells	↑ *Prdm16* ↔ *Ucp1, Pparg, Ppargc1a, Cd137, Tmem26, Tfam*	Not studied	Zu *et al.* [2018]

Cidea: cell death activator CIDE-A; *Cyt C*: cytochrome c; *Elovl3*: elongation of very long chain fatty acids protein 3; *Fabp4*: Fatty acid-binding protein type 4; iWAT: inguinal white adipose tissue; *Pparg*: peroxisome proliferator-activated receptor γ; *Ppargc1a*: peroxisome proliferator-activated receptor γ coactivator 1-α; *Prdm16*: PR domain-containing protein 16; SVC: stromal vascular cells; *Tbx1*: T-box transcription factor TBX1; *Tmem26*: transmembrane protein 26; *Ucp1*: uncoupling protein 1.

Capsaicin

Capsaicin, a TRPV1 agonist, is an ingredient present in chili peppers [Baboota *et al.*, 2014] with anti-inflammatory, antioxidant, antiobesity, and antidiabetic properties [Mosqueda-Solís *et al.*, 2018]. Regarding bioavailability, nearly 94% of the oral capsaicin dosage was rapidly absorbed from the gastrointestinal tract of Wistar rats and just as fast metabolized in the liver, reaching 24.4% of maximum tissue distribution an 1 h after the administration [Suresh & Srinivasan, 2010]. Capsaicin exhibits a dose-dependent effect on lipid accumulation in 3T3-L1 preadipocytes – low concentrations suppress, whereas higher intensify that process [Baboota *et al.*, 2014]. Both small and large quantities increase the expression of *Pparg*, but *Ucp1*, *Ppargc1a*, *Prdm16*, *Dio2* and *Ppara,* are raised only at a low dose of capsaicin. Surprisingly, its low dose caused the enhanced expression of *Ucp1* negative regulator – vitamin D receptor, as well as the increment of anti-adipogenic genes, while the addition of its high dose caused a significant decrement. Browning-positive effects of capsaicin were associated with TRPV1 overexpression on adipocytes [Baboota *et al.*, 2014].

The influence of capsaicin on sWAT was also investigated, and it was shown that a 3-month consumption resulted in augmented expression of the BAT genes – *Ucp1*, *Ppargc1a*, *Cidea*, prostaglandin-endoperoxide synthase 2, and brain-derived neurotrophic factor in Laboratory Animal Centre A-strain (LACA) mice [Baboota *et al.*, 2014].

MIXTURES OF COMPOUNDS

A few studies investigated the mutual effects of well-established adipocyte browning activators (Table 6). Simultaneous administration of resveratrol and quercetin were evidenced to synergistically induce adipocyte browning, leading to more expressed features of beige adipose tissue and better metabolic outcomes than each of the substances separately [Arias *et al.*, 2017]. On the other hand, combination of hesperidin and capsaicin restricted their browning activities, compared to both isolated hesperidin and capsaicin [Mosqueda-Solís *et al.*, 2018]. Thus, before implementation of any treatment with a mixture of compounds, the interactions between browning activators should be studied, since the cumulative effect may appear far less significant than expected.

EDIBLE PLANT EXTRACTS/PARTS

Cinnamon extract

Cinnamon is a spice obtained from the bark of the cinnamon tree with anti-cancer, antibacterial, and anti-inflammatory properties [Gruenwald *et al.*, 2010]. It turns out that it also affects the process of browning adipocytes [Kwan *et al.*, 2017]. According to the study by Helal *et al.* [2014], the bioavailability of the constituents of the cinnamon extract was 53%, 22%, 47%, 90%, and 64% for quercetin 3-rhamnoside, syringic and coumaric acids, kaempferol and cinnamaldehyde, respectively.

Multilocular morphology of adipocytes was observed 24 h after cinnamon extract was added to 3T3-L1 cells [Kwan *et al.*, 2017]. Bioactive compounds identified in the cinnamon extract were protocatechuic acid, (+)-catechin, chlorogenic acid, esculetin, quercetin, and icariin. Cinnamon extract increased the expression of *Ucp1* mRNA and UCP1 protein as well as specific for BAT genes including *Prdm16*, *Ppargc1a, Pparg*, *Cidea,* and *Cpt1*. Enhanced mitochondrial protein production was also observed. Furthermore, cinnamon extract augmented the promoter activity of the UCP1 gene in HEK293 cells and 3T3-L1 adipocytes [Kwan *et al.*, 2017]. Mechanistically, β_3-adrenergic stimulation was involved. In mature subcutaneous adipocytes obtained from C57BLKS db/db mice, there was an increase in UCP1 protein, *Prdm16,* and *Cidea* expression after 24 h cinnamon extract supplementation, which was not observed in eWAT [Kwan *et al.*, 2017]. In addition, in diet-induced obese mice, cinnamon extract enhanced UCP1 protein level as well as *Ucp1*, *Prdm16,* and *Cidea* mRNAs in sWAT, but not eWAT or perirenal adipocytes [Kwan *et al.*, 2017]. Oral administration of cinnamon extract for 15 days resulted in weight loss without reducing organ weight or food intake.

TABLE 6. Summary of the selected mixtures of components influencing adipocyte browning.

Substance	Dose	Test subjects	Duration (week)	Results of mixture therapy (*vs*. each substance separately)	Reference
Resveratrol + quercetin	15 mg resveratrol/kg/day 30 mg quercetin/kg/day	Rats	6	Attenuation of weight gain Reduction of subcutaneous WAT and abdominal WAT depots Increase in multilocular adipocytes	Arias *et al.* [2017]
Hesperidin + capsaicin	100 mg hesperidin/kg/day 4 mg capsaicin/kg/day	Wistar rats	8	Lesser adipocyte size Weaker browning-inducing properties	Mosqueda-Solís *et al.* [2018]

WAT: white adipose tissue.

Germinated soy germ extract

Germinated soy germ extract (rich in nutrients and bioactive compounds, such as linoleic and linolenic acids, isoflavones, tocopherols, and free amino acids, including γ-aminobutyric acid) [Kim *et al.*, 2013] was tested *in vitro* and *in vivo* on 3T3-L1 preadipocytes and high-fat diet fed mice, showing its ability to promote UCP1 expression and adipocyte browning [Kim *et al.*, 2019]. Moreover, it upregulated β-oxidation and lipolysis in beige adipocytes [Kim *et al.*, 2019]. In addition, germinated soy germ extract affected transcription and translation of endocannabinoid system genes encoding cannabinoid receptor type 2, *N*-acyl-phosphatidylethanolamine-hydrolyzing phospholipase D, diacylglycerol lipase-α, and fatty-acid amide hydrolase 1 proteins [Kim *et al.*, 2019], which are likely to mediate germinated soy germ extract browning properties since cannabinoids could induce adipocyte browning itself [Rossi *et al.*, 2018].

Ginger rhizome

Ginger is a widely used spice obtained from the rhizome of *Zingiber officinale Rosco*, that may have beneficial effects in reducing obesity [J. Wang *et al.*, 2017]. It appears to have the ability to induce WAT browning and improve BAT function by increasing brown and beige key proteins and genes, including UCP1, PRDM16, as well as *Cidea*, *Tmem26,* and *Cited1*, in both BAT and WAT of ginger-supplemented C57BL/6J mice [J. Wang *et al.*, 2019]. The underlying mechanism was the AMPK activation. Moreover, 16-week ginger supplementation upregulated *Tfam* and *Nrf1* genes, as well as *Ppargc1a* mRNA, involved in mitochondrial biogenesis and oxidative phosphorylation [J. Wang *et al.*, 2019]. As a result, not only decreased levels of serum glucose, triglycerides, total cholesterol and high-density lipoprotein cholesterol (HDL-C) but also attenuated body weight gain and intensified energy expenditure were observed.

***Glycyrrhiza uralensis* extract**

A methyl dichloride fraction of *Glycyrrhiza uralensis* containing licochalcone A, isoliquiritigenin, and liquiritigenin was tested alongside licochalcone A in the abovementioned study by Lee *et al.* [2018]. The same results as for licochalcone A were obtained, providing evidence that the *Glycyrrhiza uralensis* extract has the ability to induce adipocyte browning. Upregulation of PRDM16 and PGC1α, as well as browning-specific adipose tissue remodeling were followed by weight loss and improvement in glucose and lipid metabolism [Lee *et al.*, 2018].

Grape extracts

An extract from grape pomace contains many flavonoids and phenolic caids, of which (–)-epicatechin, quercetin, (+)-catechin, and syringic acid are the most abundant [Rodriguez Lanzi *et al.*, 2016]. The research on spontaneously hypertensive rats, characterized by increased sympathetic nervous system drive, and normotensive Wistar–Kyoto rats, showed browning of eWAT in the spontaneously hypertensive group after 10 weeks of grape pomace extract supplementation to high-fat diet [Rodriguez Lanzi *et al.*, 2018]. The browning was evidenced with augmented levels of BAT marker proteins: UCP1, PRDM16, PGC1α, and PPARγ. On the contrary, rats of the Wistar–Kyoto fed with the same diet as spontaneously hypertensive rats displayed an elevated concentration of PPARγ and only a slight increase in UCP1. Nevertheless, they also (as well as spontaneously hypertensive rats) profited from the grape pomace extract administration, achieving healthier eWAT expansion – favoring adipocyte hyperplasia over hypertrophy, which lessened WAT inflammation. In addition, grape pomace extract effects on browning and the activation of β-adrenergic receptors were studied on 3T3-L1 adipocytes [Rodriguez Lanzi *et al.*, 2018]. The results disclosed elevated expression of UCP1 following an increase in p38 and extracellular signal-regulated kinases 1/2 activity. Thus, the mechanism of grape pomace extract-mediated adipocyte browning is tightly connected with β-adrenergic stimulation and its downstream cascade.

On the other hand, a similar *in vivo* study describing the influence of grape seed proanthocyanidin extract on rats revealed no browning effects in retroperitoneal WAT [Pascual-Serrano *et al.*, 2018]. Nevertheless, grape seed proanthocyanidin extract altered adipogenesis, promoting adipocytes hyperplasia rather than hypertrophy, which is considered to be protective in the context of metabolic complications related to obesity [Blüher, 2013]. Considering the abovementioned studies, it seems that some components of grape pomace, but not grape seeds, are associated with adipocyte browning.

Green tea extract

Flavan-3-ols are major constituents of green tea extract [Chen *et al.*, 2001]. The bioavailability of compounds of this flavonoid class is rather low. Chen *et al.* [1997] reported that

only 13.7% of (–)-epigallocatechin, 31.2% of (–)-epicatechin, and 0.1% of (–)-epigallocatechin-3-gallate administrated to rats within portion of 200 mg/kg of decaffeinated green tea were bioavailable. Nevertheless, green tea extract was found to stimulate adipocyte browning in male C57BL/6J mice, which was confirmed with an elevated transcription of *Ppargc1a, Prdm16,* and *Cited1,* as well as increased UCP1 concentration, in subcutaneous WAT of the green tea extract-supplemented mice [Neyrinck *et al.*, 2017]. Moreover, the addition of green tea extract to high-fat diet was able to reverse adipocyte whitening in iBAT by increasing *Ppargc1a* and inhibiting fatty acid-binding protein 4 expression [Neyrinck *et al.*, 2017]. Interestingly, tea polyphenols increased the amount of *Akkermansia muciniphila* in the gut microbiota of high-fat diet mice [Liu *et al.*, 2017], which is believed to be positively correlated with the browning of WAT [Gao *et al.*, 2018]. On the contrary, C57BL/6J mice, treated with decaffeinated green tea extract (a mixture of (–)-epigallocatechin, (–)-epicatechin-3-gallate, (–)-epigallocatechin-3-gallate, and (–)-epicatechin), did not present higher levels of *Ucp1* under similar conditions [Sae-Tan *et al.*, 2015]. In this study, caffeine was likely to interfere with tea flavan-3-ols by increasing sympathetic drive and browning effects. Further research is, however, needed to study the browning properties of tea polyphenols in details.

Immature *Citrus reticulata* fruit extract

Synephrine (16 mg/g), hesperidin (9.14 mg/g), narirutin (4.52 mg/g), nobiletin (2.54 mg/g), and tangeretin (1.67 mg/g) were the predominant phenolic compounds of immature *Citrus reticulata* fruit water extract [Chou *et al.*, 2018]. Interestingly, the content of synephrine, nobiletin and tangeretin in the immature *Citrus reticulata* fruit extract was significantly higher than in other *Citrus* species [Sun *et al.*, 2013]. Chou *et al.* [2018] proved the browning effects of the immature *Citrus reticulata* extract-rich diet on murine (C57BL/6) iWAT. After 11 weeks of immature *Citrus reticulata* extract supplementation, adipocytes became multilocular, and concentrations of PGC1α and UCP1 proteins increased. In addition, immature *Citrus reticulata* extract supplementation was responsible for the upregulation of thermogenic genes and beige adipose tissue hallmarks, such as *Cidea*, *Tmem26, Prdm16,* and *Cd137*. The mechanism of browning is most likely linked with *p*-synephrine, almost selective ligand to β_3-AR [Chou *et al.*, 2018]. Furthermore, other components of immature *Citrus reticulata* extract, naringin and hesperidin, were reported to strengthen the thermogenic effect of *p*-synephrine [Stohs *et al.*, 2011]. Besides adipocyte browning, immature *Citrus reticulata* extract can improve metabolic health by reducing dyslipidemia, insulin resistance, obesity, and lipid accumulation in the liver [Chou *et al.*, 2018].

Olive oil

Olive oil, composed of tri-, di-, and monoacylglycerols build up with mainly oleic, linoleic, palmitic, and stearic acids, as well as containing a wide range of sterols, tocopherols, and phenolic compounds, including hydroxytyrosol and oleuropein, is one of the fundamental and highly bioavailable constituents of the Mediterranean diet [Boskou *et al.*, 2006; Vissers *et al.*, 2004]. Its consumption reduces inflammation and prevents from civilization diseases, such as cardiovascular and neurodegenerative ones [Angeloni *et al.*, 2017; Marcelino *et al.*, 2019]. In addition, recent research reported that dietary supplementation with olive oil in C57BL/6 mice reduced weight gain and adipose tissue expansion, which coexisted with increased thermogenesis and oxygen consumption [Shin & Ajuwon, 2018b]. Nevertheless, these changes were not supported with overexpression of browning-specific genes, such as *Ucp1, Prdm16,* and *Ppargc1a,* in sWAT and BAT, while *Ppargc1a, Tfam, Adrb3,* and *Cpt1a* were upregulated in eWAT. However, a significant surge in *Ucp1* mRNA, but not protein, was found in BAT of Wistar rats upon 4-week olive oil supplementation [Rodríguez *et al.*, 2002]. Finally, olive oil administration slightly attenuated high-fat diet-induced increase in blood glucose and insulin [Shin & Ajuwon, 2018b].

Onion peel extracts

Flavonols (quercetin and isoquercetin) and anthocyanins are major constituents of onion peel extract [Krithika *et al.*, 2020; Wijerathne *et al.*, 2019]. A study on C57BL/6 mice showed no change in body mass, the weight of eWAT and rWAT, after 8-week supplementation with onion peel extract compared to the high-fat control diet [Lee *et al.*, 2017]. Nevertheless, it revealed the influence of the onion peel extract on gene expression, which included *Ucp1*, *Prdm16*, *Cidea,* and *Ppargc1a* increment in rWAT, while in sWAT there was no change in *Prdm16* and *Ppargc1a* levels, but *Ucp1* and *Cidea* were raised. Furthermore, elevated *Ucp1, Ppargc1a, Tbx1*, and *Cpt1a* expression was reported in 3T3-L1 preadipocytes upon onion peel extract administration [Lee *et al.*, 2017].

In addition, fractions of onion peel extract were also investigated by Lee *et al.* [2017] on 3T3-L1 cells. Onion peel ethyl acetate fraction, containing quercetin and isoquercetin, increased *Tbx1*, *Cpt1a*, and *Ppargc1a* transcription, as well as inhibited fatty acid synthase and acetyl-CoA carboxylase. On the contrary, onion peel water fraction, consisting of isoquercetin only, did not induce such changes. Nevertheless, both onion peel water and ethyl acetate fractions were capable of dose-dependent enhancement of *Ucp1* expression [Lee *et al.*, 2017].

Taken together, it seems that quercetin was the component of onion peel extracts, which played the pivotal role in adipocyte browning stimulation. Therefore, activation of the AMPK pathway is presumably the browning mechanism of the presented onion extracts [Lee *et al.*, 2017].

Raspberry fruits

Raspberry fruits represent a rich source of antioxidants and anti-inflammatory phenolic compounds [Xing *et al.*, 2018], such as flavan-3-ols, flavonols, phenolic acids, and anthocyanins [Pap *et al.*, 2021], which are also known to have the ability to induce browning of WAT [Zou *et al.*, 2018]. C57BL/6 mice treated with raspberry fruits for 10 weeks presented decreased iWAT, eWAT, and body weights, with a concomitant increment in BAT mass, greater oxygen uptake and CO_2 excretion, as well as intensified heat production [Zou *et al.*, 2018]. Lowered insulin, triglycerides, total cholesterol and free fatty acids serum levels were also noted. Furthermore, raspberry supplementation enhanced mRNA

and protein expression of *Ucp1*, *Prdm16, Ppargc1a mRNA* and Cyt C, in both BAT and iWAT [Zou *et al.*, 2018]. In iWAT, it upregulated *Elovl3*, *Cd137*, *Tbx1,* and *Tmem26*, while in BAT – *Cidea* and *Cox7al*. Moreover, raspberry administration resulted in diminished adipocyte size in iWAT [Zou *et al.*, 2018] and eWAT [Xing *et al.*, 2018].

Another 12-week study conducted on C57BL/6J high-fat diet mice showed that raspberry fruit administration caused a decline in monocyte chemoattractant protein 1, *Cd14*, *Cd68* mRNAs, as well as IL-6, IL-18, IL-1β concentrations, and macrophages abundance in iWAT [Xing *et al.*, 2018]. What is more, glucose transporter type 4 accretion resulted in improved insulin sensitivity.

It was suggested that raspberry fruits trigger adipocyte beiging by stimulating the AMPK pathway [Xing *et al.*, 2018; Zou *et al.*, 2018] and activating p38 and extracellular signal-regulated kinases 1/2 signaling, which take part in irisin-induced browning [Xing *et al.*, 2018].

Rose hip

Rose hip is the fruit of diverse plants belonging to the genus *Rosa*, which contains a wealth of ascorbic acid [Strålsjö *et al.*, 2003], carotenoids [Hodisan *et al.*, 1997], and phenolic compounds [Daels-Rakotoarison *et al.*, 2002]. The addition of rose hip to high-fat diet of C57BL/6J mice resulted in increased expression of brown and beige adipose tissue-specific genes in inguinal subcutaneous WAT, such as *Ucp1*, *Tbx15*, *Cidea*, *Cpt1,* and bone morphogenetic protein 7, which was mediated by AMPK related pathway [Cavalera *et al.*, 2016]. Surprisingly, neither *Ppargc1a* nor *Prdm16* mRNAs were elevated. Furthermore, no changes in gene expression were found in BAT deposits. Interestingly, feces of mice fed a high-fat diet with rose hip addition had much more energy value than these of mice fed only with the high-fat diet [Cavalera *et al.*, 2016]. Hence, the lower body mass of the rose hip-supplemented group should be attributed not only to elevated energy expenditure because of adipocyte browning but also to reduced effective energy intake due to impaired intestinal absorption. Measurements of fecal content are rarely used in adipocyte browning studies, although they might be useful for providing more comprehensive results of future research.

DIETARY INGREDIENTS OF ANIMAL ORIGIN

Fish oils

DHA, EPA, α-linolenic and linoleic acids are major constituents of fish oil [Kowalski *et al.*, 2019]. The browning-positive effect of fish oil was studied in C57BL/6 mice fed with fish oil-rich diet [Bargut *et al.*, 2016] or DHA/EPA-enriched fish oil [Kim *et al.*, 2015]. Fish oil supplementation elevated UCP1 concentration at both mRNA and protein levels as well as *Prdm16, Cidea, Cpt1b, Adrb3,* and *Fgf21* mRNAs in iWAT and BAT [Kim *et al.*, 2015]. Furthermore, increased transcription and translation of *Ppargc1a, Ppara, Pparg,* and *Adrb3* in BAT [Bargut *et al.*, 2016], and overexpression of *Tbx1* in iWAT, were observed [Kim *et al.*, 2015].

Same as for isolated DHA and EPA, fish oil enhanced glucose transporter type 4 and lipoprotein lipase mRNAs, and therefore lowered blood glucose and improved lipid profile [Bargut *et al.*, 2019; Zhao & Chen, 2014]. Additionally, fish oil elevated serum level of adiponectin and decreased that of leptin [Bargut *et al.*, 2016; Zhuang *et al.*, 2019].

Milk fat globule membrane substances

Milk fat globule membrane is composed of three layers built-up of lipids and proteins, and originates from the apical part of mammary apocrine glands [Fong *et al.*, 2007]. Since a few substances included in milk fat globule membrane may exert beneficial effects, Li *et al.* [2018] studied the outcomes of the whole complex milk fat globule membrane (the naturally ingested from) administration to high-fat diet C57BL/6 mice. They found that milk fat globule membrane reduced fat mass by both inhibiting adipogenesis in eWAT and inducing adipocyte browning in iWAT. Mechanistically, all results of milk fat globule membrane supplementation were mediated by the AMPK pathway, which led to the downregulation of PPARγ, C/EBPα, and sterol regulatory element-binding protein 1c in epididymal WAT as well as increased UCP1 in inguinal WAT and BAT. In addition, milk fat globule membrane altered lipid profile to less atherogenic (↓ triglycerides, LDL-C; ↑ HDL-C/LDL-C) and declined the content of free fatty acids [Li *et al.*, 2018].

Scallop shell

Scallops are a popular delicacy in Japan, therefore, their shells, which are composed of calcium carbonate (98%) and organic ingredients (2%), make up copious industrial waste [Liu *et al.*, 2006; Liu & Hasegawa, 2006]. While looking for a way to use them, it was suggested that they might improve metabolic health. Recent studies revealed that scallop shell powder intensifies lipolysis in 3T3-L1 cells [Liu & Hasegawa, 2006] as well as in Wistar rats [Liu *et al.*, 2006]. Moreover, reduced iWAT, eWAT, perirenal WAT, and body weights, along with no changes in the BAT mass, were observed in the group supplementing scallop shell powder for 5 weeks [Liu *et al.*, 2006; Liu & Hasegawa, 2006]. Furthermore, applying this ingredient resulted in a decreased serum leptin concentration [Liu *et al.*, 2006]. Among scallop shell-treated animals, it was noted that in BAT there were no alterations in the *Ucp1* level, while *Ucp2* was downregulated. However, both of them were elevated in eWAT. Though the exact mechanism leading to metabolic changes caused by scallop shell is not known, it is probably distinct from β_3-adrenergic stimulation and G protein-coupled receptors activation [Liu *et al.*, 2006].

GENERAL DIETARY MODIFICATIONS

Caloric restriction

Limiting caloric intake can prevent obesity, insulin resistance, metabolic and cardiovascular diseases [Golbidi *et al.*, 2017]. A recent study shows that it can also promote adipocyte browning [Fabbiano *et al.*, 2016]. Among the C57BL/6J mice subjected to caloric restriction, increased glucose uptake in WAT, which deposits were smaller and denser, was observed. In the caloric restriction group, the number of adipocytes raised. They were also shrunken and multilocular compared to the control mice in both inguinal subcutaneous

adipose tissue and perigonadal visceral fat. In those deposits, caloric restriction resulted in upregulation of *Ucp1*, *Cidea*, *Ppargc1a*, *Ppara*, *Prdm16*, *Pparg*, *Tbx1,* and fatty acid-binding protein 4 – the BAT hallmarks. *Cd137* and *Tmem26* expression was also enhanced in perigonadal visceral adipose tissue. The above changes appeared after one week of caloric restriction, reached their maximum after 4 weeks, and gradually disappeared after cessation of the diet. Similar consequences were noticed in the caloric restriction group kept in the thermoneutral environment and obese leptin-deficient (ob/ob) mice [Fabbiano *et al.*, 2016].

Moreover, using caloric restriction was connected with lipolysis intensification as a result of improved response to β-adrenergic stimulation [Fabbiano *et al.*, 2016]. Importantly, caloric restriction mice were able to maintain a constant body temperature, unlike the controls. Consequently, it proves the activity of the newly formed beige adipose tissue in caloric restriction mice [Fabbiano *et al.*, 2016].

Interestingly, WAT browning caused by caloric depletion was associated with augmented SIRT1 expression on macrophages and activation of type 2 immune signaling, including enhanced infiltration of eosinophils, macrophages, and increased secretion of cytokines (IL-4, IL-5, IL-13) in both inguinal subcutaneous adipose tissue and perigonadal visceral adipose tissue [Fabbiano *et al.*, 2016]. The study also revealed that caloric restriction-dependent browning occurred regardless of the proportion of diet components.

Dietary macronutrient composition

The influence of low-protein, high-carbohydrate diet on browning processes was studied by Pereira *et al.* [2017]. They found that low-protein, high-carbohydrate diet-fed rats presented a lower body weight but higher iWAT mass compared to the control group, while lipid content was similar in both iWAT and perigonadal WAT. Moreover, expansion of multilocular adipocytes as well as elevated levels of UCP1, TBX1, PRDM16, and β_1-AR were observed in the latter. Besides, the content of β_3-AR and PKA was comparable to control, but it was reduced in iWAT of low-protein, high-carbohydrate diet-fed rats. Additionally, this regimen resulted in adipose triglyceride lipase and phosphoenolpyruvate carboxykinase increment in iWAT, as well as lipoprotein lipase accretion in perigonadal WAT. Among low-protein, high-carbohydrate diet-fed rodents, FGF21 serum level increased, so did pAMPK/AMPK ratio in iWAT, whereas it was lessened in the second fat pad [Pereira *et al.*, 2017].

Effects of a high-carbohydrate diet were also determined in a 6-week study on wild-type and perulipin-2-null mice, treated with a 20% sucrose solution [Libby *et al.*, 2018]. This resulted in an elevated level of genes, such as *Ucp1*, *Elovl3*, *Cidea*, *Dio2*, *Cpt1b*, *Ppargc1a*, and *Ppara*. Moreover, the number of adipocytes with many lipid droplets increased in iWAT. Also, a diminution in iBAT, iWAT, and eWAT weights was demonstrated in animals with perilipin-2 deletion. Additionally, improvement in insulin sensitivity was observed due to, *inter alia*, augmented glucose transporter type 4 expression. It was also revealed that the increase in FGF21, which occurred in iWAT, BAT, and the liver under the influence of sucrose, was probably the underlying mechanism of browning [Libby *et al.*, 2018].

According to recent research, the type of diet may also affect the expression of irisin, fibronectin type III domain-containing protein 5 proteolytic cleavage product produced in muscles and adipocytes both in mice and humans [de Macêdo *et al.*, 2017]. A 60-day study conducted on Friend Virus B NIH mice revealed an increment in fibronectin type III domain-containing protein 5 and irisin concentration induced by a high-protein diet. It also turned out that their elevation was probably modulated by the *Ucp1* and *Ppara* genes, which are typical of BAT, suggesting that high-protein diet might have augmented their expression. Thus, these results differ from the conclusions presented by Pereira *et al.* [2017], who described low-protein, high-carbohydrate diet as the one that leads to browning activation. In addition, it was observed that both high-protein diet and high-carbohydrate diet increased the BAT mass, however, it was more significant in the first group [de Macêdo *et al.*, 2017]. Finally, higher HDL-C concentrations were noted in the high-carbohydrate diet-fed mice compared to the high-protein diet group. Although both high-carbohydrate diet and high-protein diet led to elevated glucose levels, the insulin sensitivity test showed no differences between the groups [de Macêdo *et al.*, 2017].

Intermittent fasting

Fasting is recognized as a factor that positively influences metabolism and prevents insulin resistance or fatty liver disease by leading to WAT browning [Li *et al.*, 2017]. A study conducted on growing C57BL/6N mice subjected to 15-cycle every other day fasting showed higher rectal temperatures compared to the control animals [Li *et al.*, 2017]. It also enhanced lipid utilization and reduced body weight with no effect on food intake. Comparing fat mass, the eWAT mass decreased, while the BAT weight rose. Interestingly, in BAT, there was no increment in the expression of BAT-specific genes, such as *Ucp1*, *Ppargc1a, Dio2*. What is more, every other day fasting inhibited norepinephrine and did not affect *Adrb3* expression [Li *et al.*, 2017]. However, when iWAT was examined, the features of browning, such as the occurrence of multilocular adipocytes and augmented expression of UCP1, were observed. Although every other day fasting discontinuation returned *Ucp1* mRNA to baseline values after 15 days, reduced weight was still observed. Furthermore, it was described that WAT browning was responsible for the increased energy consumption and occurred in the FGF21-independent pathway [Li *et al.*, 2017].

It seems that the intestinal microflora plays an important role in the WAT browning process caused by every other day fasting since an increased abundance of Firmicutes and inhibition of other phyla were observed upon fasting [Li *et al.*, 2017]. Moreover, microbiota in every other day fasting mice was responsible not only for intensification of lactate and acetate production, which are known to be factors leading to the beiging of adipose tissue, but also enhanced expression of the monocarboxylate transporter 1 gene, which encodes the protein transporting those molecules into the adipocytes [Li *et al.*, 2017].

MICROBIOTA

The intestinal microflora is closely related to human physiology and health [Moreno-Navarrete *et al.*, 2018] as it influences various metabolic processes in the body [Suárez--Zamorano *et al.*, 2015]. Its composition is significantly affected by diet or medicines [Moreno-Navarrete *et al.*, 2018]. The dominant types of bacteria are Firmicutes, Bacteroidetes, Proteobacteria, and Actinobacteria. Studies on rodents showed that Firmicutes increment and Bacteroidetes decrease was related to obesity, which was also observed in humans. However, some research has also shown an inverse relationship [Jumpertz *et al.*, 2011; Patil *et al.*, 2012]. According to the study conducted on humans, Firmicutes relative abundance increased the expression of BAT markers such as *UCP1*, *PRDM16,* and *DIO2* in subcutaneous adipose tissue [Moreno-Navarrete *et al.*, 2018]. In contrast, obese people with insulin resistance had lowered Firmicutes and increased Bacteroidetes, which correlated negatively with BAT markers.

It seems that the mechanistic link between Firmicutes relative abundance and brown adipocyte differentiation is connected with the acetate production since its concentration correlated positively with Firmicutes relative abundance, insulin sensitivity, and *PRDM16* mRNA level in subcutaneous adipose tissue [Moreno-Navarrete *et al.*, 2018]. Interestingly, at Firmicutes relative abundance, the levels of acetate, UCP1, and PRDM16 varied with age, gender, BMI, type 2 diabetes, and antihypertensive therapy.

In addition, an experiment on C57BL/6J mice, administered water containing antibiotics, revealed that microbiota depletion led to WAT browning and metabolic changes [Suárez--Zamorano *et al.*, 2015]. According to this study, improved insulin sensitivity and augmented WAT glucose uptake, as well as decreased weight and volume of inguinal subcutaneous adipose tissue and perigonadal visceral adipose tissue, were observed in microbiota-depleted mice despite increased food intake. Besides, their adipocytes were darker and smaller with multilocular phenotype. Furthermore, the upregulation of primary BAT proteins, such as UCP1, was demonstrated. Ten days after recolonization of the antibiotic-treated mice with microbes, the elevated level of browning markers and greater cold resistance were still noted, which was due to the development of functional beige adipocytes promoted by the depletion of microbiota [Suárez-Zamorano *et al.*, 2015]. Moreover, adipocytes derived from microbiota-depleted mice responded more strongly to β-adrenergic stimulation than control mice, indicating higher thermogenic capacity. Described metabolic changes occurred as a result of enhanced type 2 cytokine signaling, including secretion of interleukins IL-4, IL-5, IL-13, and infiltrations from eosinophils in inguinal subcutaneous adipose tissue [Suárez-Zamorano *et al.*, 2015].

CONCLUSIONS

There is a wide range of dietary substances that may participate in adipocyte browning induction, including amino acids, carbohydrates, lipids, phenolic compounds, and many others. Each of the described components upregulated BAT-specific genes in different WAT depots or cell lines. Numerous research also evidenced signs of adipose tissue remodeling associated with britening stimulated by different food ingredients, and increased BAT activation. Moreover, improved metabolic parameters, such as lipid profile or glucose concentration, were frequently observed.

However, the vast majority of the molecules were investigated based on murine models. Nevertheless, most of the papers focused on the impact of dietary intervention in obesity-induced animals, which closely resemble the obese state in humans, albeit interspecies differences should always be taken into consideration when analyzing the results.

Evidence regarding diet-induced adipocyte browning in humans or human cell cultures is rather scarce, including studies on caffeine, EPA, (–)-epicatechin, genistein, or resveratrol. Among them, EPA appears the most promising browning activator, since it upregulated not only the pivotal adipocyte browning genes (*UCP1, PRDM16*), but also genes involved in mitochondrial biogenesis (*NRF1, TFAM*) and β-oxidation (*CPT1A*), being responsible for the complete thermogenesis-related metabolic change. In addition, adipocyte browning upon EPA administration was evidenced with highly-specific beige adipose tissue markers (*CD137, TBX1*). Finally, the browning properties of EPA were investigated on the fully differentiated subcutaneous adipocytes, confirming its ability to stimulate adipocyte transdifferentiation, which seems to be the most relevant when considering potential clinical application in adults. Another optimistic data is associated with resveratrol, which also enhanced the expression of browning-fundamental genes (*UCP1*, *PRDM16*). Furthermore, the research with the use of resveratrol was performed on humans *in vivo* and carefully designed. Moreover, it revealed that even a small dose of resveratrol (500 mg/day) may contribute to adipocyte browning, which appears crucial, concerning its limited bioavailability. Additionally, resveratrol elevated the expression of fibronectin type III domain--containing protein 5, potentially initiating other mechanisms leading to adipocyte browning *via* irisin formation. Favorable outcomes were also reported about (–)-epicatechin, which increased essential proteins concentrations (UCP1, PRDM16) in fully differentiated subcutaneous adipocytes. Apart from adipocyte browning stimulation, the anti-inflammatory effect of (–)-epicatechin was observed. More studies are needed to appropriately establish the role of caffeine and genistein on adipocyte browning in humans. However, limited data indicate their ability to raise the level of UCP1.

In our opinion, future research should elucidate the outcomes of the acknowledged browning activators in human WAT and cell lines to provide novel therapeutic agents for the treatment of obesity and obesity-related diseases. Furthermore, the safety doses of dietary substances should be determined. Simultaneously, more compounds should be screened for browning-positive effects.

ACKNOWLEDGEMENTS

The authors thank Ms. Malwina Malinowska for writing assistance.

RESEARCH FUNDING

The publication of this review paper was funded from the budget of Vice-Rector for Student Affairs at Poznan University of Medical Sciences (ID: 4317).

CONFLICT OF INTERESTS

The authors declare no conflict of interests.

ORCID IDs

M. Gibas-Dorna https://orcid.org/0000-0002-8408-2829
A. Rajczewski https://orcid.org/0000-0001-8022-3148
A. Szumigała https://orcid.org/0000-0002-3591-1539
O.W. Wiśniewski https://orcid.org/0000-0001-6262-5119

REFERENCES

1. Andrade, J.E., Twaddle, N.C., Helferich, W.G., Doerge, D.R. (2010). Absolute bioavailability of isoflavones from soy protein isolate-containing food in female BALB/c mice. *Journal of Agricultural and Food Chemistry, 58*(7), 4529–4536. https://doi.org/10.1021/jf9039843
2. Andrade, J.M.O., Barcala-Jorge, A.S., Batista-Jorge, G.C., Paraíso, A.F., Freitas, K.M. de, Lelis, D. de F., Guimarães, A.L.S., de Paula, A.M.B., Santos, S.H.S. (2019). Effect of resveratrol on expression of genes involved thermogenesis in mice and humans. *Biomedicine & Pharmacotherapy, 112*, art. no. 108634. https://doi.org/10.1016/j.biopha.2019.108634
3. Angeloni, C., Malaguti, M., Barbalace, M.C., Hrelia, S. (2017). Bioactivity of olive oil phenols in neuroprotection. *International Journal of Molecular Sciences, 18*(11), art. no. E2230. https://doi.org/10.3390/ijms18112230
4. Arai, C., Arai, N., Arai, S., Yoshizane, C., Miyata, S., Mizote, A., Suyama, A., Endo, S., Ariyasu, T., Mitsuzumi, H., Ushio, S. (2019). Continuous intake of trehalose induces white adipose tissue browning and enhances energy metabolism. *Nutrition & Metabolism, 16*, art. no. 45. https://doi.org/10.1186/s12986-019-0373-4
5. Arias, N., Picó, C., Teresa Macarulla, M., Oliver, P., Miranda, J., Palou, A., Portillo, M.P. (2017). A combination of resveratrol and quercetin induces browning in white adipose tissue of rats fed an obesogenic diet. *Obesity (Silver Spring, Md.), 25*(1), 111–121. https://doi.org/10.1002/oby.21706
6. Assini, J.M., Mulvihill, E.E., Burke, A.C., Sutherland, B.G., Telford, D.E., Chhoker, S.S., Sawyez, C.G., Drangova, M., Adams, A.C., Kharitonenkov, A., Pin, C.L., Huff, M.W. (2015). Naringenin prevents obesity, hepatic steatosis, and glucose intolerance in male mice independent of fibroblast growth factor 21. *Endocrinology, 156*(6), 2087–2102. https://doi.org/10.1210/en.2014-2003
7. Baba, S., Osakabe, N., Yasuda, A., Natsume, M., Takizawa, T., Nakamura, T., Terao, J. (2000). Bioavailability of (–)-epicatechin upon intake of chocolate and cocoa in human volunteers. *Free Radical Research, 33*(5), 635–641. https://doi.org/10.1080/10715760000301151
8. Baboota, R.K., Singh, D.P., Sarma, S.M., Kaur, J., Sandhir, R., Boparai, R.K., Kondepudi, K.K., Bishnoi, M. (2014). Capsaicin induces "brite" phenotype in differentiating 3T3-L1 preadipocytes. *PLoS One, 9*(7), art. no. e103093. https://doi.org/10.1371/journal.pone.0103093
9. Bai, W., Shen, J., Zhu, Y., Men, Y., Sun, Y., Ma, Y. (2015). Characteristics and kinetic properties of L-rhamnose isomerase from *Bacillus subtilis* by isothermal titration calorimetry for the production of D-allose. *Food Science and Technology Research, 21*(1), 13–22. https://doi.org/10.3136/fstr.21.13
10. Bargut, T.C.L., Martins, F.F., Santos, L.P., Aguila, M.B., Mandarim-de-Lacerda, C.A. (2019). Administration of eicosapentaenoic and docosahexaenoic acids may improve the remodeling and browning in subcutaneous white adipose tissue and thermogenic markers in brown adipose tissue in mice. *Molecular and Cellular Endocrinology, 482*, 18–27. https://doi.org/10.1016/j.mce.2018.12.003
11. Bargut, T.C.L., Silva-e-Silva, A.C.A.G., Souza-Mello, V., Mandarim-de-Lacerda, C.A., Aguila, M.B. (2016). Mice fed fish oil diet and upregulation of brown adipose tissue thermogenic markers. *European Journal of Nutrition, 55*(1), 159–169. https://doi.org/10.1007/s00394-015-0834-0
12. Bártíková, H., Boušová, I., Matoušková, P., Szotáková, B., Skálová, L. (2017). Effect of green tea extract-enriched diets on insulin and leptin levels, oxidative stress parameters and antioxidant enzymes activities in obese mice. *Polish Journal of Food and Nutrition Sciences, 67*(3), 233–240. https://doi.org/10.1515/pjfns-2017-0004
13. Bartoňková, I., Dvořák, Z. (2018). Essential oils of culinary herbs and spices display agonist and antagonist activities at human aryl hydrocarbon receptor AhR. *Food and Chemical Toxicology, 111*, 374–384. https://doi.org/10.1016/j.fct.2017.11.049
14. Berry, D.C., Noy, N. (2009). All-*trans*-retinoic acid represses obesity and insulin resistance by activating both peroxisome proliferation-activated receptor beta/delta and retinoic acid receptor. *Molecular and Cellular Biology, 29*(12), 3286–3296. https://doi.org/10.1128/MCB.01742-08
15. Bershad, S., Poulin, Y.P., Berson, D.S., Sabean, J., Brodell, R.T., Shalita, A.R., Kakita, L., Tanghetti, E., Leyden, J., Webster, G.F., Miller, B.H. (1999). Topical retinoids in the treatment of acne vulgaris. *Cutis, 64*(2 Suppl), 8–20.
16. Bialonska, D., Kasimsetty, S.G., Khan, S.I., Ferreira, D. (2009). Urolithins, intestinal microbial metabolites of *Pomegranate* ellagitannins, exhibit potent antioxidant activity in a cell-based assay. *Journal of Agricultural and Food Chemistry, 57*(21), 10181–10186. https://doi.org/10.1021/jf9025794
17. Binder, E., Bermúdez-Silva, F.J., Elie, M., Leste-Lasserre, T., Belluomo, I., Clark, S., Duchampt, A., Mithieux, G., Cota, D. (2014). Leucine supplementation modulates fuel substrates utilization and glucose metabolism in previously obese mice. *Obesity (Silver Spring, Md.), 22*(3), 713–720. https://doi.org/10.1002/oby.20578
18. Blankson, H., Stakkestad, J.A., Fagertun, H., Thom, E., Wadstein, J., Gudmundsen, O. (2000). Conjugated linoleic acid reduces body fat mass in overweight and obese humans. *The Journal of Nutrition, 130*(12), 2943–2948. https://doi.org/10.1093/jn/130.12.2943

19. Blüher, M. (2013). Adipose tissue dysfunction contributes to obesity related metabolic diseases. *Best Practice & Research. Clinical Endocrinology & Metabolism, 27*(2), 163–177. https://doi.org/10.1016/j.beem.2013.02.005
20. Bonati, M., Latini, R., Galletti, F., Young, J.F., Tognoni, G., Garattini, S. (1982). Caffeine disposition after oral doses. *Clinical Pharmacology and Therapeutics, 32*(1), 98–106. https://doi.org/10.1038/clpt.1982.132
21. Boskou, D., Blekas, G., Tsimidou, M. (2006). Olive oil composition. In D. Boskou (Eds.), *Olive Oil: Chemistry and Technology*, AOCS Press, Boca Raton, USA, pp. 41–72. https://doi.org/10.4324/9781003040217
22. Boström, P., Wu, J., Jedrychowski, M.P., Korde, A., Ye, L., Lo, J.C., Rasbach, K.A., Boström, E.A., Choi, J.H., Long, J.Z., Kajimura, S., Zingaretti, M.C., Vind, B.F., Tu, H., Cinti, S., Højlund, K., Gygi, S.P., Spiegelman, B.M. (2012). A PGC1-α-dependent myokine that drives brown-fat-like development of white fat and thermogenesis. *Nature, 481*(7382), 463–468. https://doi.org/10.1038/nature10777
23. Bounds, S.V., Caldwell, J. (1996). Pathways of metabolism of [1'-14C]-*trans*-anethole in the rat and mouse. *Drug Metabolism and Disposition, 24*(7), 717–724.
24. Burke, A.C., Sutherland, B.G., Telford, D.E., Morrow, M.R., Sawyez, C.G., Edwards, J.Y., Drangova, M., Huff, M.W. (2018). Intervention with citrus flavonoids reverses obesity and improves metabolic syndrome and atherosclerosis in obese Ldlr-/- mice. *Journal of Lipid Research, 59*(9), 1714–1728. https://doi.org/10.1194/jlr.M087387
25. Cavalera, M., Axling, U., Berger, K., Holm, C. (2016). Rose hip supplementation increases energy expenditure and induces browning of white adipose tissue. *Nutrition & Metabolism, 13*, art. no. 91. https://doi.org/10.1186/s12986-016-0151-5
26. Cavallito, C.J., Bailey, J.H. (1944). Allicin, the antibacterial principle of *Allium sativum*. I. Isolation, physical properties and antibacterial action. *Journal of the American Chemical Society, 66*(11), 1950–1951. https://doi.org/10.1021/ja01239a048
27. Chen, H., Chan, K.K., Budd, T. (1998). Pharmacokinetics of D-limonene in the rat by GC-MS assay. *Journal of Pharmaceutical and Biomedical Analysis, 17*(4–5), 631–640. https://doi.org/10.1016/S0731-7085(97)00243-4
28. Chen, L., Lee, M.J., Li, H., Yang, C.S. (1997). Absorption, distribution, elimination of tea polyphenols in rats. *Drug Metabolism and Disposition, 25*(9), 1045–1050.
29. Chen, X., Li, D., Hu, Y., Jin, M., Zhou, L., Peng, K., Zheng, H. (2011). Simultaneous determination of 3,3',4',5,7-pentamethylquercetin and its possible metabolite 3,3',4',7-tetramethylquercetin in dog plasma by liquid chromatography-tandem mass spectrometry and its application to preclinical pharmacokinetic study. *Journal of Chromatography. B, Analytical Technologies in the Biomedical and Life Sciences, 879*(23), 2339–2344. https://doi.org/10.1016/j.jchromb.2011.06.019
30. Chen, Z., Zhu, Q.Y., Tsang, D., Huang, Y. (2001). Degradation of green tea catechins in tea drinks. *Journal of Agricultural and Food Chemistry, 49*(1), 477–482. https://doi.org/10.1021/jf000877h
31. Cheng, Y., Meng, Q., Wang, C., Li, H., Huang, Z., Chen, S., Xiao, F., Guo, F. (2010). Leucine deprivation decreases fat mass by stimulation of lipolysis in white adipose tissue and upregulation of uncoupling protein 1 (UCP1) in brown adipose tissue. *Diabetes, 59*(1), 17–25. https://doi.org/10.2337/db09-0929
32. Cheng, Y., Zhang, Q., Meng, Q., Xia, T., Huang, Z., Wang, C., Liu, B., Chen, S., Xiao, F., Du, Y., Guo, F. (2011). Leucine deprivation stimulates fat loss *via* increasing CRH expression in the hypothalamus and activating the sympathetic nervous system. *Molecular Endocrinology (Baltimore, Md.), 25*(9), 1624–1635. https://doi.org/10.1210/me.2011-0028
33. Choi, J.H., Kim, S.W., Yu, R., Yun, J.W. (2017). Monoterpene phenolic compound thymol promotes browning of 3T3-L1 adipocytes. *European Journal of Nutrition, 56*(7), 2329–2341. https://doi.org/10.1007/s00394-016-1273-2
34. Choi, J.H., Yun, J.W. (2016). Chrysin induces brown fat-like phenotype and enhances lipid metabolism in 3T3-L1 adipocytes. *Nutrition, 32*(9), 1002–1010. https://doi.org/10.1016/j.nut.2016.02.007
35. Choi, M., Mukherjee, S., Kang, N.H., Barkat, J.L., Parray, H.A., Yun, J.W. (2018). L-rhamnose induces browning in 3T3-L1 white adipocytes and activates HIB1B brown adipocytes. *IUBMB Life, 70*(6), 563–573. https://doi.org/10.1002/iub.1750
36. Chondronikola, M., Volpi, E., Børsheim, E., Porter, C., Annamalai, P., Enerbäck, S., Lidell, M.E., Saraf, M.K., Labbe, S.M., Hurren, N.M., Yfanti, C., Chao, T., Andersen, C.R., Cesani, F., Hawkins, H., Sidossis, L.S. (2014). Brown adipose tissue improves whole-body glucose homeostasis and insulin sensitivity in humans. *Diabetes, 63*(12), 4089–4099. https://doi.org/10.2337/db14-0746
37. Chou, Y.-C., Ho, C.-T., Pan, M.-H. (2018). Immature *Citrus reticulata* extract promotes browning of beige adipocytes in high-fat diet-induced C57BL/6 mice. *Journal of Agricultural and Food Chemistry, 66*(37), 9697–9703. https://doi.org/10.1021/acs.jafc.8b02719
38. Contreras, G.A., Lee, Y.-H., Mottillo, E.P., Granneman, J.G. (2014). Inducible brown adipocytes in subcutaneous inguinal white fat: the role of continuous sympathetic stimulation. *American Journal of Physiology. Endocrinology and Metabolism, 307*(9), E793–E799. https://doi.org/10.1152/ajpendo.00033.2014
39. Daels-Rakotoarison, D.A., Gressier, B., Trotin, F., Brunet, C., Luyckx, M., Dine, T., Bailleul, F., Cazin, M., Cazin, J.-C. (2002). Effects of *Rosa canina* fruit extract on neutrophil respiratory burst. *Phytotherapy Research, 16*(2), 157–161. https://doi.org/10.1002/ptr.985
40. Dawson, M.I. (2000). The importance of vitamin A in nutrition. *Current Pharmaceutical Design, 6*(3), 311–325. https://doi.org/10.2174/1381612003401190
41. de Jong, J.M.A., Larsson, O., Cannon, B., Nedergaard, J. (2015). A stringent validation of mouse adipose tissue identity markers. *American Journal of Physiology. Endocrinology and Metabolism, 308*(12), E1085–1105. https://doi.org/10.1152/ajpendo.00023.2015
42. de Macêdo, S.M., Lelis, D. de F., Mendes, K.L., Fraga, C.A. de C., Brandi, I.V., Feltenberger, J.D., Farias, L.C., Guimarães, A.L.S., de Paula, A.M.B., Santos, S.H. de S. (2017). Effects of dietary macronutrient composition on FNDC5 and irisin in mice skeletal muscle. *Metabolic Syndrome and Related Disorders, 15*(4), 161–169. https://doi.org/10.1089/met.2016.0109

43. Doyle, B., Griffiths, L.A. (1980). The metabolism of ellagic acid in the rat. *Xenobiotica, 10*(4), 247–256. https://doi.org/10.3109/00498258009033752
44. Du, J., Shen, L., Tan, Z., Zhang, P., Zhao, X., Xu, Y., Gan, M., Yang, Q., Ma, J., Jiang, A., Tang, G., Jiang, Y., Jin, L., Li, M., Bai, L., Li, X., Wang, J., Zhang, S., Zhu, L. (2018). Betaine supplementation enhances lipid metabolism and improves insulin resistance in mice fed a high-fat diet. *Nutrients, 10*(2), art. no. 131. https://doi.org/10.3390/nu10020131
45. Fabbiano, S., Suárez-Zamorano, N., Rigo, D., Veyrat-Durebex, C., Stevanovic Dokic, A., Colin, D.J., Trajkovski, M. (2016). Caloric restriction leads to browning of white adipose tissue through type 2 immune signaling. *Cell Metabolism, 24*(3), 434–446. https://doi.org/10.1016/j.cmet.2016.07.023
46. Fahey, J.W., Holtzclaw, W.D., Wehage, S.L., Wade, K.L., Stephenson, K.K., Talalay, P. (2015). Sulforaphane bioavailability from glucoraphanin-rich broccoli: control by active endogenous myrosinase. *PLoS One, 10*(11), art. no. e0140963. https://doi.org/10.1371/journal.pone.0140963
47. Farco, J.A., Grundmann, O. (2013). Menthol – pharmacology of an important naturally medicinal "cool." *Mini Reviews in Medicinal Chemistry, 13*(1), 124–131. https://doi.org/10.2174/138955713804484686
48. Felgines, C., Texier, O., Morand, C., Manach, C., Scalbert, A., Régerat, F., Rémésy, C. (2000). Bioavailability of the flavanone naringenin and its glycosides in rats. *American Journal of Physiology. Gastrointestinal and Liver Physiology, 279*(6), G1148–1154. https://doi.org/10.1152/ajpgi.2000.279.6.G1148
49. Fisher, F.M., Kleiner, S., Douris, N., Fox, E.C., Mepani, R.J., Verdeguer, F., Wu, J., Kharitonenkov, A., Flier, J.S., Maratos-Flier, E., Spiegelman, B.M. (2012). FGF21 regulates PGC-1α and browning of white adipose tissues in adaptive thermogenesis. *Genes & Development, 26*(3), 271–281. https://doi.org/10.1101/gad.177857.111
50. Fong, B.Y., Norris, C.S., MacGibbon, A.K.H. (2007). Protein and lipid composition of bovine milk-fat-globule membrane. *International Dairy Journal, 17*(4), 275–288. https://doi.org/10.1016/j.idairyj.2006.05.004
51. Forney, L.A., Lenard, N.R., Stewart, L.K., Henagan, T.M. (2018). Dietary quercetin attenuates adipose tissue expansion and inflammation and alters adipocyte morphology in a tissue-specific manner. *International Journal of Molecular Sciences, 19*(3), art. no. 895. https://doi.org/10.3390/ijms19030895
52. Gandhi, G.R., Vasconcelos, A.B.S., Wu, D.-T., Li, H.-B., Antony, P.J., Li, H., Geng, F., Gurgel, R.Q., Narain, N., Gan, R.-Y. (2020). Citrus flavonoids as promising phytochemicals targeting diabetes and related complications: a systematic review of *in vitro* and *in vivo* studies. *Nutrients, 12*(10), E2907. https://doi.org/10.3390/nu12102907
53. Gao, X., Xie, Q., Kong, P., Liu, L., Sun, S., Xiong, B., Huang, B., Yan, L., Sheng, J., Xiang, H. (2018). Polyphenol- and caffeine-rich postfermented pu-erh tea improves diet-induced metabolic syndrome by remodeling intestinal homeostasis in mice. *Infection and Immunity, 86*(1), art. no. e00601–17. https://doi.org/10.1128/IAI.00601-17
54. García-Alonso, V., López-Vicario, C., Titos, E., Morán-Salvador, E., González-Périz, A., Rius, B., Párrizas, M., Werz, O., Arroyo, V., Clària, J. (2013). Coordinate functional regulation between microsomal prostaglandin E synthase-1 (mPGES-1) and peroxisome proliferator-activated receptor γ (PPARγ) in the conversion of white-to-brown adipocytes. *The Journal of Biological Chemistry, 288*(39), 28230–28242. https://doi.org/10.1074/jbc.M113.468603
55. García-Alonso, V., Titos, E., Alcaraz-Quiles, J., Rius, B., Lopategi, A., López-Vicario, C., Jakobsson, P.-J., Delgado, S., Lozano, J., Clària, J. (2016). Prostaglandin E2 exerts multiple regulatory actions on human obese adipose tissue remodeling, inflammation, adaptive thermogenesis and lipolysis. *PLoS One, 11*(4), art. no. e0153751. https://doi.org/10.1371/journal.pone.0153751
56. Gelal, A., Jacob, P., Yu, L., Benowitz, N.L. (1999). Disposition kinetics and effects of menthol. *Clinical Pharmacology and Therapeutics, 66*(2), 128–135. https://doi.org/10.1053/cp.1999.v66.100455001
57. Golbidi, S., Daiber, A., Korac, B., Li, H., Essop, M.F., Laher, I. (2017). Health benefits of fasting and caloric restriction. *Current Diabetes Reports, 17*(12), art. no. 123. https://doi.org/10.1007/s11892-017-0951-7
58. Górska-Warsewicz, H., Laskowski, W., Kulykovets, O., Kudlińska-Chylak, A., Czeczotko, M., Rejman, K. (2018). Food products as sources of protein and amino acids – The case of Poland. *Nutrients 10*(12), art. no. 1977. https://doi.org/10.3390/nu10121977
59. Grossini, E., Farruggio, S., Raina, G., Mary, D., Deiro, G., Gentilli, S. (2018). Effects of genistein on differentiation and viability of human visceral adipocytes. *Nutrients, 10*(8), art. no. 978. https://doi.org/10.3390/nu10080978
60. Gruenwald, J., Freder, J., Armbruester, N. (2010). Cinnamon and health. *Critical Reviews in Food Science and Nutrition, 50*(9), 822–834. https://doi.org/10.1080/10408390902773052
61. Guo, H., Foncea, R., O'Byrne, S.M., Jiang, H., Zhang, Y., Deis, J.A., Blaner, W.S., Bernlohr, D.A., Chen, X. (2016). Lipocalin 2, a regulator of retinoid homeostasis and retinoid-mediated thermogenic activation in adipose tissue. *The Journal of Biological Chemistry, 291*(21), 11216–11229. https://doi.org/10.1074/jbc.M115.711556
62. Guo, Y.-Y., Li, B.-Y., Peng, W.-Q., Guo, L., Tang, Q.-Q. (2019). Taurine-mediated browning of white adipose tissue is involved in its anti-obesity effect in mice. *The Journal of Biological Chemistry, 294*(41), 15014–15024. https://doi.org/10.1074/jbc.RA119.009936
63. Han, Y., Wu, J.-Z., Shen, J.-Z., Chen, L., He, T., Jin, M.-W., Liu, H. (2017). Pentamethylquercetin induces adipose browning and exerts beneficial effects in 3T3-L1 adipocytes and high-fat diet-fed mice. *Scientific Reports, 7*(1), art. no. 1123. https://doi.org/10.1038/s41598-017-01206-4
64. Hargrave, K.M., Li, C., Meyer, B.J., Kachman, S.D., Hartzell, D.L., Della-Fera, M.A., Miner, J.L., Baile, C.A. (2002). Adipose depletion and apoptosis induced by *trans*-10, *cis*-12 conjugated linoleic acid in mice. *Obesity Research, 10*(12), 1284–1290. https://doi.org/10.1038/oby.2002.174
65. Harms, M., Seale, P. (2013). Brown and beige fat: development, function and therapeutic potential. *Nature Medicine, 19*(10), 1252–1263. https://doi.org/10.1038/nm.3361

66. Helal, A., Tagliazucchi, D., Verzelloni, E., Conte, A. (2014). Bioaccessibility of polyphenols and cinnamaldehyde in cinnamon beverages subjected to *in vitro* gastro-pancreatic digestion. *Journal of Functional Foods, 7*(1), 506–516. https://doi.org/10.1016/j.jff.2014.01.005
67. Hodisan, T., Socaciu, C., Ropan, I., Neamtu, G. (1997). Carotenoid composition of *Rosa canina* fruits determined by thin-layer chromatography and high-performance liquid chromatography. *Journal of Pharmaceutical and Biomedical Analysis, 16*(3), 521–528. https://doi.org/10.1016/S0731-7085(97)00099-X
68. Hostetler, G.L., Ralston, R.A., Schwartz, S.J. (2017). Flavones: food sources, bioavailability, metabolism, and bioactivity. *Advances in Nutrition (Bethesda, Md.), 8*(3), 423–435. https://doi.org/10.3945/an.116.012948
69. Houghton, C.A., Fassett, R.G., Coombes, J.S. (2016). Sulforaphane and other nutrigenomic Nrf2 activators: can the clinician's expectation be matched by the reality? *Oxidative Medicine and Cellular Longevity, 2016*, art. no. 7857186. https://doi.org/10.1155/2016/7857186
70. Hu, J., Kyrou, I., Tan, B.K., Dimitriadis, G.K., Ramanjaneya, M., Tripathi, G., Patel, V., James, S., Kawan, M., Chen, J., Randeva, H.S. (2016). Short-chain fatty acid acetate stimulates adipogenesis and mitochondrial biogenesis *via* GPR43 in brown adipocytes. *Endocrinology, 157*(5), 1881–1894. https://doi.org/10.1210/en.2015-1944
71. Jaiswal, N., Akhtar, J., Singh, S.P., Badruddeen, Ahsan, F. (2019). An overview on genistein and its various formulations. *Drug Research, 69*(6), 305–313. https://doi.org/10.1055/a-0797-3657
72. Jia, T., Qiao, J., Guan, D., Chen, T. (2017). Anti-inflammatory effects of licochalcone A on IL-1β-stimulated human osteoarthritis chondrocytes. *Inflammation, 40*(6), 1894–1902. https://doi.org/10.1007/s10753-017-0630-5
73. Jiang, C., Zhai, M., Yan, D., Li, D., Li, C., Zhang, Y., Xiao, L., Xiong, D., Deng, Q., Sun, W. (2017). Dietary menthol-induced TRPM8 activation enhances WAT "browning" and ameliorates diet-induced obesity. *Oncotarget, 8*(43), 75114–75126. https://doi.org/10.18632/oncotarget.20540
74. Jiang, N., Dillon, F.M., Silva, A., Gomez-Cano, L., Grotewold, E. (2021). Rhamnose in plants - from biosynthesis to diverse functions. *Plant Science, 302*, art. no. 110687. https://doi.org/10.1016/j.plantsci.2020.110687
75. Jiang, Y., Rose, A.J., Sijmonsma, T.P., Bröer, A., Pfenninger, A., Herzig, S., Schmoll, D., Bröer, S. (2015). Mice lacking neutral amino acid transporter B(0)AT1 (Slc6a19) have elevated levels of FGF21 and GLP-1 and improved glycaemic control. *Molecular Metabolism, 4*(5), 406–417. https://doi.org/10.1016/j.molmet.2015.02.003
76. Jiao, J., Han, S.-F., Zhang, W., Xu, J.-Y., Tong, X., Yin, X.-B., Yuan, L.-X., Qin, L.-Q. (2016). Chronic leucine supplementation improves lipid metabolism in C57BL/6J mice fed with a high-fat/cholesterol diet. *Food & Nutrition Research, 60*, art. no. 31304. https://doi.org/10.3402/fnr.v60.31304
77. Jumpertz, R., Le, D.S., Turnbaugh, P.J., Trinidad, C., Bogardus, C., Gordon, J.I., Krakoff, J. (2011). Energy-balance studies reveal associations between gut microbes, caloric load, and nutrient absorption in humans. *The American Journal of Clinical Nutrition, 94*(1), 58–65. https://doi.org/10.3945/ajcn.110.010132
78. Kajimura, S., Spiegelman, B.M., Seale, P. (2015). Brown and beige fat: physiological roles beyond heat generation. *Cell Metabolism, 22*(4), 546–559. https://doi.org/10.1016/j.cmet.2015.09.007
79. Kang, N.H., Mukherjee, S., Min, T., Kang, S.C., Yun, J.W. (2018). *trans*-Anethole ameliorates obesity *via* induction of browning in white adipocytes and activation of brown adipocytes. *Biochimie, 151*, 1–13. https://doi.org/10.1016/j.biochi.2018.05.009
80. Kaşıkcı, M.B., Bağdatlıoğlu, N. (2016). Bioavailability of quercetin. *Current Research in Nutrition and Food Science Journal, 4*(Suppl 2), 146–151. https://doi.org/10.12944/CRNFSJ.4.Special-Issue-October.20
81. Khaled, K.A., El-Sayed, Y.M., Al-Hadiya, B.M. (2003). Disposition of the flavonoid quercetin in rats after single intravenous and oral doses. *Drug Development and Industrial Pharmacy, 29*(4), 397–403. https://doi.org/10.1081/DDC-120018375
82. Kim, H.-J., Choi, E.-J., Kim, H.S., Choi, C.-W., Choi, S.-W., Kim, S.-L., Seo, W.-D., Do, S.H. (2019). Germinated soy germ extract ameliorates obesity through beige fat activation. *Food & Function, 10*(2), 836–848. https://doi.org/10.1039/C8FO02252F
83. Kim, J., Okla, M., Erickson, A., Carr, T., Natarajan, S.K., Chung, S. (2016). Eicosapentaenoic acid potentiates brown thermogenesis through FFAR4-dependent up-regulation of miR-30b and miR-378. *The Journal of Biological Chemistry, 291*(39), 20551–20562. https://doi.org/10.1074/jbc.M116.721480
84. Kim, M., Furuzono, T., Yamakuni, K., Li, Y., Kim, Y.-I., Takahashi, H., Ohue-Kitano, R., Jheng, H.-F., Takahashi, N., Kano, Y., Yu, R., Kishino, S., Ogawa, J., Uchida, K., Yamazaki, J., Tominaga, M., Kawada, T., Goto, T. (2017). 10-Oxo-12(*Z*)-octadecenoic acid, a linoleic acid metabolite produced by gut lactic acid bacteria, enhances energy metabolism by activation of TRPV1. *FASEB Journal, 31*(11), 5036–5048. https://doi.org/10.1096/fj.201700151R
85. Kim, M., Goto, T., Yu, R., Uchida, K., Tominaga, M., Kano, Y., Takahashi, N., Kawada, T. (2015). Fish oil intake induces UCP1 upregulation in brown and white adipose tissue *via* the sympathetic nervous system. *Scientific Reports, 5*, art. no. 18013. https://doi.org/10.1038/srep18013
86. Kim, S.-L., Lee, J.-E., Kwon, Y.-U., Kim, W.-H., Jung, G.-H., Kim, D.-W., Lee, C.-K., Lee, Y.-Y., Kim, M.-J., Kim, Y.-H., Hwang, T.-Y., Chung, I.-M. (2013). Introduction and nutritional evaluation of germinated soy germ. *Food Chemistry, 136*(2), 491–500. https://doi.org/10.1016/j.foodchem.2012.08.022
87. Kishino, S., Takeuchi, M., Park, S.-B., Hirata, A., Kitamura, N., Kunisawa, J., Kiyono, H., Iwamoto, R., Isobe, Y., Arita, M., Arai, H., Ueda, K., Shima, J., Takahashi, S., Yokozeki, K., Shimizu, S., Ogawa, J. (2013). Polyunsaturated fatty acid saturation by gut lactic acid bacteria affecting host lipid composition. *Proceedings of the National Academy of Sciences of the United States of America, 110*(44), 17808–17813. https://doi.org/10.1073/pnas.1312937110
88. Kohlert, C., Schindler, G., März, R.W., Abel, G., Brinkhaus, B., Derendorf, H., Gräfe, E.-U., Veit, M. (2002). Systemic availability and pharmacokinetics of thymol in humans. *Journal of Clinical Pharmacology, 42*(7), 731–737. https://doi.org/10.1177/009127002401102678

89. Kowalski, R., Kałwa, K., Wilczyński, K., Kobus, Z. (2019). The fatty acids composition of selected fish oils used as dietary supplements. *Polish Journal of Natural Sciences, 34*(1), 115–126.
90. Kris-Etherton, P.M., Grieger, J.A., Etherton, T.D. (2009). Dietary reference intakes for DHA and EPA. *Prostaglandins, Leukotrienes, and Essential Fatty Acids, 81*(2–3), 99–104. https://doi.org/10.1016/j.plefa.2009.05.011
91. Krithika, J., Sathiyasree, B., Teodore, B., Ramarajan, C., Gurushankar, K. (2020). Optimization of extraction parameters and stabilization of anthocyanin from onion peel. *Critical Reviews in Food Science and Nutrition,* 1–8. https://doi.org/10.1080/10408398.2020.1856772
92. Kwan, H.Y., Wu, J., Su, T., Chao, X.-J., Liu, B., Fu, X., Chan, C.L., Lau, R.H.Y., Tse, A.K.W., Han, Q.B., Fong, W.F., Yu, Z.-L. (2017). Cinnamon induces browning in subcutaneous adipocytes. *Scientific Reports, 7*(1), art. no. 2447. https://doi.org/10.1038/s41598-017-02263-5
93. Lafontan, M., Barbe, P., Galitzky, J., Tavernier, G., Langin, D., Carpéné, C., Bousquet-Melou, A., Berlan, M. (1997). Adrenergic regulation of adipocyte metabolism. *Human Reproduction (Oxford, England), 12*(Suppl 1), 6–20. https://doi.org/10.1093/humrep/12.suppl_1.6
94. Laidlaw, S.A., Grosvenor, M., Kopple, J.D. (1990). The taurine content of common foodstuffs. *JPEN – Journal of Parenteral and Enteral Nutrition, 14*(2), 183–188. https://doi.org/10.1177/0148607190014002183
95. Laiglesia, L.M., Lorente-Cebrián, S., Prieto-Hontoria, P.L., Fernández-Galilea, M., Ribeiro, S.M.R., Sáinz, N., Martínez, J.A., Moreno-Aliaga, M.J. (2016). Eicosapentaenoic acid promotes mitochondrial biogenesis and beige-like features in subcutaneous adipocytes from overweight subjects. *The Journal of Nutritional Biochemistry, 37*, 76–82. https://doi.org/10.1016/j.jnutbio.2016.07.019
96. Landete, J.M. (2011). Ellagitannins, ellagic acid and their derived metabolites: a review about source, metabolism, functions and healt. *Food Research International (Ottawa, Ont.), 44*(5), 1150–1160. https://doi.org/10.1016/j.foodres.2011.04.027
97. LaRosa, P.C., Miner, J., Xia, Y., Zhou, Y., Kachman, S., Fromm, M.E. (2006). *trans*-10, *cis*-12 Conjugated linoleic acid causes inflammation and delipidation of white adipose tissue in mice: a microarray and histological analysis. *Physiological Genomics, 27*(3), 282–294. https://doi.org/10.1152/physiolgenomics.00076.2006
98. Lawson, L.D., Hunsaker, S.M. (2018). Allicin bioavailability and bioequivalence from garlic supplements and garlic foods. *Nutrients, 10*(7), art. no. E812. https://doi.org/10.3390/nu10070812
99. Lee, C.G., Rhee, D.K., Kim, B.O., Um, S.H., Pyo, S. (2019). Allicin induces beige-like adipocytes *via* KLF15 signal cascade. *The Journal of Nutritional Biochemistry, 64*, 13–24. https://doi.org/10.1016/j.jnutbio.2018.09.014
100. Lee, H.E., Yang, G., Han, S.-H., Lee, J.-H., An, T.-J., Jang, J.-K., Lee, J.Y. (2018). Anti-obesity potential of *Glycyrrhiza uralensis* and licochalcone A through induction of adipocyte browning. *Biochemical and Biophysical Research Communications, 503*(3), 2117–2123. https://doi.org/10.1016/j.bbrc.2018.07.168
101. Lee, S.G., Parks, J.S., Kang, H.W. (2017). Quercetin, a functional compound of onion peel, remodels white adipocytes to brown-like adipocytes. *The Journal of Nutritional Biochemistry, 42*, 62–71. https://doi.org/10.1016/j.jnutbio.2016.12.018
102. Leu, S.-Y., Tsai, Y.-C., Chen, W.-C., Hsu, C.-H., Lee, Y.-M., Cheng, P.-Y. (2018). Raspberry ketone induces brown-like adipocyte formation through suppression of autophagy in adipocytes and adipose tissue. *The Journal of Nutritional Biochemistry, 56*, 116–125. https://doi.org/10.1016/j.jnutbio.2018.01.017
103. Li, G., Xie, C., Lu, S., Nichols, R.G., Tian, Y., Li, L., Patel, D., Ma, Y., Brocker, C.N., Yan, T., Krausz, K.W., Xiang, R., Gavrilova, O., Patterson, A.D., Gonzalez, F.J. (2017). Intermittent fasting promotes white adipose browning and decreases obesity by shaping the gut microbiota. *Cell Metabolism, 26*(4), 672–685.e4. https://doi.org/10.1016/j.cmet.2017.08.019
104. Li, T., Gao, J., Du, M., Song, J., Mao, X. (2018). Milk fat globule membrane attenuates high-fat diet-induced obesity by inhibiting adipogenesis and increasing uncoupling protein 1 expression in white adipose tissue of mice. *Nutrients, 10*(3), art. no. 331. https://doi.org/10.3390/nu10030331
105. Libby, A.E., Bales, E.S., Monks, J., Orlicky, D.J., McManaman, J.L. (2018). Perilipin-2 deletion promotes carbohydrate-mediated browning of white adipose tissue at ambient temperature. *Journal of Lipid Research, 59*(8), 1482–1500. https://doi.org/10.1194/jlr.M086249
106. Lidell, M.E., Betz, M.J., Leinhard, O.D., Heglind, M., Elander, L., Slawik, M., Mussack, T., Nilsson, D., Romu, T., Nuutila, P., Virtanen, K.A., Beuschlein, F., Persson, A., Borga, M., Enerbäck, S. (2013). Evidence for two types of brown adipose tissue in humans. *Nature Medicine, 19*(5), 631–634. https://doi.org/10.1038/nm.3017
107. Liu, J., Li, Y., Yang, P., Wan, J., Chang, Q., Wang, T.T.Y., Lu, W., Zhang, Y., Wang, Q., Yu, L.L. (2017). Gypenosides reduced the risk of overweight and insulin resistance in C57BL/6J mice through modulating adipose thermogenesis and gut microbiota. *Journal of Agricultural and Food Chemistry, 65*(42), 9237–9246. https://doi.org/10.1021/acs.jafc.7b03382
108. Liu, Y.C., Hasegawa, Y. (2006). Reducing effect of feeding powdered scallop shell on the body fat mass of rats. *Bioscience, Biotechnology, and Biochemistry, 70*(1), 86–92. https://doi.org/10.1271/bbb.70.86
109. Liu, Y.C., Satoh, K., Hasegawa, Y. (2006). Feeding scallop shell powder induces the expression of uncoupling protein 1 (UCP1) in white adipose tissue of rats. *Bioscience, Biotechnology, and Biochemistry, 70*(11), 2733–2738. https://doi.org/10.1271/bbb.60349
110. Lone, J., Choi, J.H., Kim, S.W., Yun, J.W. (2016). Curcumin induces brown fat-like phenotype in 3T3-L1 and primary white adipocytes. *The Journal of Nutritional Biochemistry, 27*, 193–202. https://doi.org/10.1016/j.jnutbio.2015.09.006
111. Lone, J., Parray, H.A., Yun, J.W. (2018). Nobiletin induces brown adipocyte-like phenotype and ameliorates stress in 3T3-L1 adipocytes. *Biochimie, 146*, 97–104. https://doi.org/10.1016/j.biochi.2017.11.021

112. Lone, J., Yun, J.W. (2016). Monoterpene limonene induces brown fat-like phenotype in 3T3-L1 white adipocytes. *Life Sciences, 153*, 198–206. https://doi.org/10.1016/j.lfs.2016.04.010
113. Lu, Yuanyuan, Fan, C., Li, P., Lu, Yanfei, Chang, X., Qi, K. (2016). Short chain fatty acids prevent high-fat-diet-induced obesity in mice by regulating G protein-coupled receptors and gut microbiota. *Scientific Reports, 6*, art. no. 37589. https://doi.org/10.1038/srep37589
114. Lund, J., Larsen, L.H., Lauritzen, L. (2018). Fish oil as a potential activator of brown and beige fat thermogenesis. *Adipocyte, 7*(2), 88–95. https://doi.org/10.1080/21623945.2018.1442980
115. Luo, L., Liu, M. (2016). Adipose tissue in control of metabolism. *The Journal of Endocrinology, 231*(3), R77–R99. https://doi.org/10.1530/JOE-16-0211
116. Mao, Z., Liang, Y., Du, X., Sun, Z. (2009). 3,3',4',5,7-Pentamethylquercetin reduces angiotensin II-induced cardiac hypertrophy and apoptosis in rats. *Canadian Journal of Physiology and Pharmacology, 87*(9), 720–728. https://doi.org/10.1139/Y09-069
117. Marcelino, G., Hiane, P.A., Freitas, K. de C., Santana, L.F., Pott, A., Donadon, J.R., Guimarães, R. de C.A. (2019). Effects of olive oil and its minor components on cardiovascular diseases, inflammation, and gut microbiota. *Nutrients, 11*(8), art. no. E1826. https://doi.org/10.3390/nu11081826
118. Mas-Capdevila, A., Teichenne, J., Domenech-Coca, C., Caimari, A., Del Bas, J.M., Escoté, X., Crescenti, A. (2020). Effect of hesperidin on cardiovascular disease risk factors: the role of intestinal microbiota on hesperidin bioavailability. *Nutrients, 12*(5), art. no. E1488. https://doi.org/10.3390/nu12051488
119. Meng-er, H., Yu-chen, Y., Shu-rong, C., Jin-ren, C., Jia-Xiang, L., Lin, Z., Long-jun, G., Zhen-yi, W. (1988). Use of all-*trans* retinoic acid in the treatment of acute promyelocytic leukemia. *Blood, 72*(2), 567–572. https://doi.org/10.1182/blood.V72.2.567.567
120. Mercader, J., Ribot, J., Murano, I., Felipe, F., Cinti, S., Bonet, M.L., Palou, A. (2006). Remodeling of white adipose tissue after retinoic acid administration in mice. *Endocrinology, 147*(11), 5325–5332. https://doi.org/10.1210/en.2006-0760
121. Min, S.Y., Kady, J., Nam, M., Rojas-Rodriguez, R., Berkenwald, A., Kim, J.H., Noh, H.-L., Kim, J.K., Cooper, M.P., Fitzgibbons, T., Brehm, M.A., Corvera, S. (2016). Human 'brite / beige' adipocytes develop from capillary networks and their implantation improves metabolic homeostasis in mice. *Nature Medicine, 22*(3), 312–318. https://doi.org/10.1038/nm.4031
122. Mize, C.E., Avigan, J., Baxter, J.H., Fales, H.M., Steinberg, D. (1966). Metabolism of phytol-U-14C and phytanic acid-U-14C in the rat. *Journal of Lipid Research, 7*(5), 692–697. https://doi.org/10.1016/S0022-2275(20)39252-X
123. Moreno-Navarrete, J.M., Serino, M., Blasco-Baque, V., Azalbert, V., Barton, R.H., Cardellini, M., Latorre, J., Ortega, F., Sabater-Masdeu, M., Burcelin, R., Dumas, M.-E., Ricart, W., Federici, M., Fernández-Real, J.M. (2018). Gut microbiota interacts with markers of adipose tissue browning, insulin action and plasma acetate in morbid obesity. *Molecular Nutrition & Food Research, 62*(3), art. no. 1700721. https://doi.org/10.1002/mnfr.201700721
124. Mosqueda-Solís, A., Sánchez, J., Portillo, M.P., Palou, A., Picó, C. (2018). Combination of capsaicin and hesperidin reduces the effectiveness of each compound to decrease the adipocyte size and to induce browning features in adipose tissue of Western diet fed rats. *Journal of Agricultural and Food Chemistry 66*(37), 9679–9689. https://doi.org/10.1021/acs.jafc.8b02611
125. Murholm, M., Isidor, M.S., Basse, A.L., Winther, S., Sørensen, C., Skovgaard-Petersen, J., Nielsen, M.M., Hansen, A.S., Quistorff, B., Hansen, J.B. (2013). Retinoic acid has different effects on UCP1 expression in mouse and human adipocytes. *BMC Cell Biology, 14*, art. no. 41. https://doi.org/10.1186/1471-2121-14-41
126. Nagata, N., Xu, L., Kohno, S., Ushida, Y., Aoki, Y., Umeda, R., Fuke, N., Zhuge, F., Ni, Y., Nagashimada, M., Takahashi, C., Suganuma, H., Kaneko, S., Ota, T. (2017). Glucoraphanin ameliorates obesity and insulin resistance through adipose tissue browning and reduction of metabolic endotoxemia in mice. *Diabetes, 66*(5), 1222–1236. https://doi.org/10.2337/db16-0662
127. Neyrinck, A.M., Bindels, L.B., Geurts, L., Van Hul, M., Cani, P.D., Delzenne, N.M. (2017). A polyphenolic extract from green tea leaves activates fat browning in high-fat-diet-induced obese mice. *The Journal of Nutritional Biochemistry, 49*, 15–21. https://doi.org/10.1016/j.jnutbio.2017.07.008
128. Okla, M., Kim, J., Koehler, K., Chung, S. (2017). Dietary factors promoting brown and beige fat development and thermogenesis. *Advances in Nutrition (Bethesda, Md.), 8*(3), 473–483. https://doi.org/10.3945/an.116.014332
129. Oku, T., Nakamura, S. (2000). Estimation of intestinal trehalase activity from a laxative threshold of trehalose and lactulose on healthy female subjects. *European Journal of Clinical Nutrition, 54*(10), 783–788. https://doi.org/10.1038/sj.ejcn.1601091
130. Pahlavani, M., Razafimanjato, F., Ramalingam, L., Kalupahana, N.S., Moussa, H., Scoggin, S., Moustaid-Moussa, N. (2017). Eicosapentaenoic acid regulates brown adipose tissue metabolism in high-fat-fed mice and in clonal brown adipocytes. *The Journal of Nutritional Biochemistry, 39*, 101–109. https://doi.org/10.1016/j.jnutbio.2016.08.012
131. Pap, N., Fidelis, M., Azevedo, L., do Carmo, M.A.V., Wang, D., Mocan, A., Pereira, E.P.R., Xavier-Santos, D., Sant'Ana, A., Yang, B., Granato, D. (2021). Berry polyphenols and human health: evidence of antioxidant, anti-inflammatory, microbiota modulation, and cell-protecting effects. *Current Opinion in Food Science, 42*, 167–186. https://doi.org/10.1016/j.cofs.2021.06.003
132. Pascual-Serrano, A., Bladé, C., Suárez, M., Arola-Arnal, A. (2018). Grape seed proanthocyanidins improve white adipose tissue expansion during diet-induced obesity development in rats. *International Journal of Molecular Sciences, 19*(9), art. no. 2632. https://doi.org/10.3390/ijms19092632
133. Patil, D.P., Dhotre, D.P., Chavan, S.G., Sultan, A., Jain, D.S., Lanjekar, V.B., Gangawani, J., Shah, P.S., Todkar, J.S., Shah, S., Ranade, D.R., Patole, M.S., Shouche, Y.S. (2012). Molecular

analysis of gut microbiota in obesity among Indian individuals. *Journal of Biosciences, 37*(4), 647–657. https://doi.org/10.1007/s12038-012-9244-0

134. Peier, A.M., Moqrich, A., Hergarden, A.C., Reeve, A.J., Andersson, D.A., Story, G.M., Earley, T.J., Dragoni, I., McIntyre, P., Bevan, S., Patapoutian, A. (2002). A TRP channel that senses cold stimuli and menthol. *Cell, 108*(5), 705–715. https://doi.org/10.1016/S0092-8674(02)00652-9
135. Pereira, M.P., Ferreira, L.A.A., da Silva, F.H.S., Christoffolete, M.A., Metsios, G.S., Chaves, V.E., de França, S.A., Damazo, A.S., Flouris, A.D., Kawashita, N.H. (2017). A low-protein, high-carbohydrate diet increases browning in perirenal adipose tissue but not in inguinal adipose tissue. *Nutrition, 42*, 37–45. https://doi.org/10.1016/j.nut.2017.05.007
136. Pisani, D.F., Ghandour, R.A., Beranger, G.E., Le Faouder, P., Chambard, J.-C., Giroud, M., Vegiopoulos, A., Djedaini, M., Bertrand-Michel, J., Tauc, M., Herzig, S., Langin, D., Ailhaud, G., Duranton, C., Amri, E.-Z. (2014). The ω6-fatty acid, arachidonic acid, regulates the conversion of white to brite adipocyte through a prostaglandin/calcium mediated pathway. *Molecular Metabolism, 3*(9), 834–847. https://doi.org/10.1016/j.molmet.2014.09.003
137. Quan, H.-Y., Baek, N.I., Chung, S.H. (2012). Licochalcone A prevents adipocyte differentiation and lipogenesis *via* suppression of peroxisome proliferator-activated receptor γ and sterol regulatory element-binding protein pathways. *Journal of Agricultural and Food Chemistry, 60*(20), 5112–5120. https://doi.org/10.1021/jf2050763
138. Quesada-López, T., Cereijo, R., Turatsinze, J.-V., Planavila, A., Cairó, M., Gavaldà-Navarro, A., Peyrou, M., Moure, R., Iglesias, R., Giralt, M., Eizirik, D.L., Villarroya, F. (2016). The lipid sensor GPR120 promotes brown fat activation and FGF21 release from adipocytes. *Nature Communications, 7*, art. no. 13479. https://doi.org/10.1038/ncomms13479
139. Ramiro-Puig, E., Castell, M. (2009). Cocoa: antioxidant and immunomodulator. *The British Journal of Nutrition, 101*(7), 931–940. https://doi.org/10.1017/S0007114508169896
140. Rayalam, S., Yang, J.-Y., Ambati, S., Della-Fera, M.A., Baile, C.A. (2008). Resveratrol induces apoptosis and inhibits adipogenesis in 3T3-L1 adipocytes. *Phytotherapy Research, 22*(10), 1367–1371. https://doi.org/10.1002/ptr.2503
141. Rodriguez Lanzi, C., Perdicaro, D.J., Antoniolli, A., Fontana, A.R., Miatello, R.M., Bottini, R., Vazquez Prieto, M.A. (2016). Grape pomace and grape pomace extract improve insulin signaling in high-fat-fructose fed rat-induced metabolic syndrome. *Food & Function, 7*(3), 1544–1553. https://doi.org/10.1039/C5FO01065A
142. Rodriguez Lanzi, C., Perdicaro, D.J., Landa, M.S., Fontana, A., Antoniolli, A., Miatello, R.M., Oteiza, P.I., Vazquez Prieto, M.A. (2018). Grape pomace extract induced beige cells in white adipose tissue from rats and in 3T3-L1 adipocytes. *The Journal of Nutritional Biochemistry, 56*, 224–233. https://doi.org/10.1016/j.jnutbio.2018.03.001
143. Rodríguez, V.M., Portillo, M.P., Picó, C., Macarulla, M.T., Palou, A. (2002). Olive oil feeding up-regulates uncoupling protein genes in rat brown adipose tissue and skeletal muscle. *The American Journal of Clinical Nutrition, 75*(2), 213–220. https://doi.org/10.1093/ajcn/75.2.213
144. Rondanelli, M., Nichetti, M., Peroni, G., Faliva, M.A., Naso, M., Gasparri, C., Perna, S., Oberto, L., Di Paolo, E., Riva, A., Petrangolini, G., Guerreschi, G., Tartara, A. (2021). Where to find leucine in food and how to feed elderly with sarcopenia in order to counteract loss of muscle mass: practical advice. *Frontiers in Nutrition, 7*, art. no. 622391. https://doi.org/10.3389/fnut.2020.622391
145. Rosenwald, M., Perdikari, A., Rülicke, T., Wolfrum, C. (2013). Bi-directional interconversion of brite and white adipocytes. *Nature Cell Biology, 15*(6), 659–667. https://doi.org/10.1038/ncb2740
146. Ross, A.B., Zangger, A., Guiraud, S.P. (2014). Cereal foods are the major source of betaine in the Western diet – analysis of betaine and free choline in cereal foods and updated assessments of betaine intake. *Food Chemistry, 145*, 859–865. https://doi.org/10.1016/j.foodchem.2013.08.122
147. Rossato, M., Granzotto, M., Macchi, V., Porzionato, A., Petrelli, L., Calcagno, A., Vencato, J., De Stefani, D., Silvestrin, V., Rizzuto, R., Bassetto, F., De Caro, R., Vettor, R. (2014). Human white adipocytes express the cold receptor TRPM8 which activation induces UCP1 expression, mitochondrial activation and heat production. *Molecular and Cellular Endocrinology, 383*(1–2), 137–146. https://doi.org/10.1016/j.mce.2013.12.005
148. Rossi, F., Punzo, F., Umano, G.R., Argenziano, M., Miraglia Del Giudice, E. (2018). Role of cannabinoids in obesity. *International Journal of Molecular Sciences, 19*(9), art. no. 2690. https://doi.org/10.3390/ijms19092690
149. Sae-Tan, S., Rogers, C.J., Lambert, J.D. (2015). Decaffeinated green tea and voluntary exercise induce gene changes related to beige adipocyte formation in high fat-fed obese mice. *Journal of Functional Foods, 14*, 210–214. https://doi.org/10.1016/j.jff.2015.01.036
150. Sarawek, S., Derendorf, H., Butterweck, V. (2008). Pharmacokinetics of luteolin and metabolites in rats. *Natural Product Communications, 3*(12), 2029–2036. https://doi.org/10.1177/1934578X0800301218
151. Sauer, L.A., Dauchy, R.T., Blask, D.E., Krause, J.A., Davidson, L.K., Dauchy, E.M., Welham, K.J., Coupland, K. (2004). Conjugated linoleic acid isomers and *trans* fatty acids inhibit fatty acid transport in hepatoma 7288CTC and inguinal fat pads in Buffalo rats. *The Journal of Nutrition, 134*(8), 1989–1997. https://doi.org/10.1093/jn/134.8.1989
152. Schluter, A., Giralt, M., Iglesias, R., Villarroya, F. (2002). Phytanic acid, but not pristanic acid, mediates the positive effects of phytol derivatives on brown adipocyte differentiation. *FEBS Letters, 517*(1–3), 83–86. https://doi.org/10.1016/S0014-5793(02)02583-8
153. Shabalina, I.G., Petrovic, N., de Jong, J.M.A., Kalinovich, A.V., Cannon, B., Nedergaard, J. (2013). UCP1 in brite/beige adipose tissue mitochondria is functionally thermogenic. *Cell Reports, 5*(5), 1196–1203. https://doi.org/10.1016/j.celrep.2013.10.044
154. Shapiro, T.A., Fahey, J.W., Wade, K.L., Stephenson, K.K., Talalay, P. (2001). Chemoprotective glucosinolates and isothiocyanates of broccoli sprouts: metabolism and excretion in humans. *Cancer Epidemiology, Biomarkers & Prevention, 10*(5), 501–508.
155. Shen, H.-H., Huang, S.-Y., Kung, C.-W., Chen, S.-Y., Chen, Y.-F., Cheng, P.-Y., Lam, K.-K., Lee, Y.-M. (2019). Genistein amelio-

rated obesity accompanied with adipose tissue browning and attenuation of hepatic lipogenesis in ovariectomized rats with high-fat diet. *The Journal of Nutritional Biochemistry, 67*, 111–122. https://doi.org/10.1016/j.jnutbio.2019.02.001

156. Shen, W., McIntosh, M.K. (2016). Nutrient regulation: conjugated linoleic acid's inflammatory and browning properties in adipose tissue. *Annual Review of Nutrition, 36*, 183–210. https://doi.org/10.1146/annurev-nutr-071715-050924
157. Shin, S., Ajuwon, K.M. (2018a). Divergent response of murine and porcine adipocytes to stimulation of browning genes by 18-carbon polyunsaturated fatty acids and beta-receptor agonists. *Lipids, 53*(1), 65–75. https://doi.org/10.1002/lipd.12010
158. Shin, S., Ajuwon, K.M. (2018b). Effects of diets differing in composition of 18-C fatty acids on adipose tissue thermogenic gene expression in mice fed high-fat diets. *Nutrients, 10*(2), art. no. 256. https://doi.org/10.3390/nu10020256
159. Shoaib, M., Shehzad, A., Omar, M., Rakha, A., Raza, H., Sharif, H.R., Shakeel, A., Ansari, A., Niazi, S. (2016). Inulin: properties, health benefits and food applications. *Carbohydrate Polymers, 147*, 444–454. https://doi.org/10.1016/j.carbpol.2016.04.020
160. Shoba, G., Joy, D., Joseph, T., Majeed, M., Rajendran, R., Srinivas, P.S. (1998). Influence of piperine on the pharmacokinetics of curcumin in animals and human volunteers. *Planta Medica, 64*(4), 353–356. https://doi.org/10.1055/s-2006-957450
161. Silvester, A.J., Aseer, K.R., Yun, J.W. (2019). Dietary polyphenols and their roles in fat browning. *The Journal of Nutritional Biochemistry, 64*, 1–12. https://doi.org/10.1016/j.jnutbio.2018.09.028
162. Smedman, A., Vessby, B. (2001). Conjugated linoleic acid supplementation in humans – metabolic effects. *Lipids, 36*(8), 773–781. https://doi.org/10.1007/s11745-001-0784-7
163. Sonnweber, T., Pizzini, A., Nairz, M., Weiss, G., Tancevski, I. (2018). Arachidonic acid metabolites in cardiovascular and metabolic diseases. *International Journal of Molecular Sciences, 19*(11), art. no. E3285. https://doi.org/10.3390/ijms19113285
164. Steck, S.E., Chalecki, A.M., Miller, P., Conway, J., Austin, G.L., Hardin, J.W., Albright, C.D., Thuillier, P. (2007). Conjugated linoleic acid supplementation for twelve weeks increases lean body mass in obese humans. *The Journal of Nutrition, 137*(5), 1188–1193. https://doi.org/10.1093/jn/137.5.1188
165. Stohs, S.J., Preuss, H.G., Keith, S.C., Keith, P.L., Miller, H., Kaats, G.R. (2011). Effects of *p*-synephrine alone and in combination with selected bioflavonoids on resting metabolism, blood pressure, heart rate and self-reported mood changes. *International Journal of Medical Sciences, 8*(4), 295–301. https://doi.org/10.7150/ijms.8.295
166. Stone, K.P., Wanders, D., Calderon, L.F., Spurgin, S.B., Scherer, P.E., Gettys, T.W. (2015). Compromised responses to dietary methionine restriction in adipose tissue but not liver of ob/ob mice. *Obesity (Silver Spring, Md.), 23*(9), 1836–1844. https://doi.org/10.1002/oby.21177
167. Strålsjö, L., Alklint, C., Olsson, M.E., Sjöholm, I. (2003). Total folate content and retention in rosehips (*Rosa* ssp.) after drying. *Journal of Agricultural and Food Chemistry, 51*(15), 4291–4295. https://doi.org/10.1021/jf034208q
168. Suárez-Zamorano, N., Fabbiano, S., Chevalier, C., Stojanović, O., Colin, D.J., Stevanović, A., Veyrat-Durebex, C., Tarallo, V., Rigo, D., Germain, S., Ilievska, M., Montet, X., Seimbille, Y., Hapfelmeier, S., Trajkovski, M. (2015). Microbiota depletion promotes browning of white adipose tissue and reduces obesity. *Nature Medicine, 21*(12), 1497–1501. https://doi.org/10.1038/nm.3994
169. Sun, J. (2007). D-Limonene: safety and clinical applications. *Alternative Medicine Review: A Journal of Clinical Therapeutic, 12*(3), 259–264.
170. Sun, Y., Qiao, L., Shen, Y., Jiang, P., Chen, J., Ye, X. (2013). Phytochemical profile and antioxidant activity of physiological drop of citrus fruits. *Journal of Food Science, 78*(1), C37–42. https://doi.org/10.1111/j.1750-3841.2012.03002.x
171. Suresh, D., Srinivasan, K. (2010). Tissue distribution & elimination of capsaicin, piperine & curcumin following oral intake in rats. *The Indian Journal of Medical Research, 131*, 682–691.
172. Taber, L., Chiu, C.H., Whelan, J. (1998). Assessment of the arachidonic acid content in foods commonly consumed in the American diet. *Lipids, 33*(12), 1151–1157. https://doi.org/10.1007/s11745-998-0317-4
173. Tazoe, H., Otomo, Y., Kaji, I., Tanaka, R., Karaki, S.-I., Kuwahara, A. (2008). Roles of short-chain fatty acids receptors, GPR41 and GPR43 on colonic functions. *Journal of Physiology and Pharmacology, 59*(Suppl 2), 251–262.
174. Tourniaire, F., Musinovic, H., Gouranton, E., Astier, J., Marcotorchino, J., Arreguin, A., Bernot, D., Palou, A., Bonet, M.L., Ribot, J., Landrier, J.-F. (2015). All-*trans* retinoic acid induces oxidative phosphorylation and mitochondria biogenesis in adipocytes. *Journal of Lipid Research, 56*(6), 1100–1109. https://doi.org/10.1194/jlr.M053652
175. Ueland, P.M. (2011). Choline and betaine in health and disease. *Journal of Inherited Metabolic Disease, 34*(1), 3–15. https://doi.org/10.1007/s10545-010-9088-4
176. Unno, Y., Yamamoto, H., Takatsuki, S., Sato, Y., Kuranaga, T., Yazawa, K., Ono, Y., Wakimoto, T. (2018). Palmitoyl lactic acid induces adipogenesis and a brown fat-like phenotype in 3T3-L1 preadipocytes. *Biochimica Et Biophysica Acta. Molecular and Cell Biology of Lipids, 1863*(7), 772–782. https://doi.org/10.1016/j.bbalip.2018.04.003
177. Varela, C.E., Rodriguez, A., Romero-Valdovinos, M., Mendoza-Lorenzo, P., Mansour, C., Ceballos, G., Villarreal, F., Ramirez-Sanchez, I. (2017). Browning effects of (–)-epicatechin on adipocytes and white adipose tissue. *European Journal of Pharmacology, 811*, 48–59. https://doi.org/10.1016/j.ejphar.2017.05.051
178. Vattem, D.A., Shetty, K. (2005). Biological functionality of ellagic acid: a review. *Journal of Food Biochemistry, 29*(3), 234–266. https://doi.org/10.1111/j.1745-4514.2005.00031.x
179. Velickovic, K., Wayne, D., Leija, H.A.L., Bloor, I., Morris, D.E., Law, J., Budge, H., Sacks, H., Symonds, M.E., Sottile, V. (2019). Caffeine exposure induces browning features in adipose tissue *in vitro* and *in vivo*. *Scientific Reports, 9*(1), art. no. 9104. https://doi.org/10.1038/s41598-019-45540-1

180. Verhoeven, N.M., Jakobs, C. (2001). Human metabolism of phytanic acid and pristanic acid. *Progress in Lipid Research, 40*(6), 453–466. https://doi.org/10.1016/S0163-7827(01)00011-X
181. Villarroya, F., Cereijo, R., Villarroya, J., Giralt, M. (2017). Brown adipose tissue as a secretory organ. *Nature Reviews. Endocrinology, 13*(1), 26–35. https://doi.org/10.1038/nrendo.2016.136
182. Vissers, M.N., Zock, P.L., Katan, M.B. (2004). Bioavailability and antioxidant effects of olive oil phenols in humans: a review. *European Journal of Clinical Nutrition, 58*(6), 955–965. https://doi.org/10.1038/sj.ejcn.1601917
183. Walle, T., Hsieh, F., DeLegge, M.H., Oatis, J.E., Walle, U.K. (2004). High absorption but very low bioavailability of oral resveratrol in humans. *Drug Metabolism and Disposition, 32*(12), 1377–1382. https://doi.org/10.1124/dmd.104.000885
184. Walle, T., Otake, Y., Brubaker, J.A., Walle, U.K., Halushka, P.V. (2001). Disposition and metabolism of the flavonoid chrysin in normal volunteers. *British Journal of Clinical Pharmacology, 51*(2), 143–146. https://doi.org/10.1111/j.1365-2125.2001.01317.x
185. Wanders, D., Forney, L.A., Stone, K.P., Burk, D.H., Pierse, A., Gettys, T.W. (2017). FGF21 mediates the thermogenic and insulin-sensitizing effects of dietary methionine restriction but not its effects on hepatic lipid metabolism. *Diabetes, 66*(4), 858–867. https://doi.org/10.2337/db16-1212
186. Wanders, D., Stone, K.P., Dille, K., Simon, J., Pierse, A., Gettys, T.W. (2015). Metabolic responses to dietary leucine restriction involve remodeling of adipose tissue and enhanced hepatic insulin signaling. *BioFactors (Oxford, England), 41*(6), 391–402. https://doi.org/10.1002/biof.1240
187. Wang, B., Fu, X., Liang, X., Deavila, J.M., Wang, Z., Zhao, L., Tian, Q., Zhao, J., Gomez, N.A., Trombetta, S.C., Zhu, M.-J., Du, M. (2017). Retinoic acid induces white adipose tissue browning by increasing adipose vascularity and inducing beige adipogenesis of PDGFRα+ adipose progenitors. *Cell Discovery, 3*, art. no. 17036. https://doi.org/10.1038/celldisc.2017.36
188. Wang, J., Ke, W., Bao, R., Hu, X., Chen, F. (2017). Beneficial effects of ginger *Zingiber officinale Roscoe* on obesity and metabolic syndrome: a review. *Annals of the New York Academy of Sciences, 1398*(1), 83–98. https://doi.org/10.1111/nyas.13375
189. Wang, J., Li, D., Wang, P., Hu, X., Chen, F. (2019). Ginger prevents obesity through regulation of energy metabolism and activation of browning in high-fat diet-induced obese mice. *The Journal of Nutritional Biochemistry, 70*, 105–115. https://doi.org/10.1016/j.jnutbio.2019.05.001
190. Wang, L., Wei, Y., Ning, C., Zhang, M., Fan, P., Lei, D., Du, J., Gale, M., Ma, Y., Yang, Y. (2019). Ellagic acid promotes browning of white adipose tissues in high-fat diet-induced obesity in rats through suppressing white adipocyte maintaining genes. *Endocrine Journal, 66*(10), 923–936. https://doi.org/10.1507/endocrj.EJ18-0467
191. Wang, S., Liang, X., Yang, Q., Fu, X., Rogers, C.J., Zhu, M., Rodgers, B.D., Jiang, Q., Dodson, M.V., Du, M. (2015). Resveratrol induces brown-like adipocyte formation in white fat through activation of AMP-activated protein kinase (AMPK) α1. *International Journal of Obesity, 39*(6), 967–976. https://doi.org/10.1038/ijo.2015.23
192. Wang, Shan, Wang, X., Ye, Z., Xu, C., Zhang, M., Ruan, B., Wei, M., Jiang, Y., Zhang, Y., Wang, L., Lei, X., Lu, Z. (2015). Curcumin promotes browning of white adipose tissue in a norepinephrine-dependent way. *Biochemical and Biophysical Research Communications, 466*(2), 247–253. https://doi.org/10.1016/j.bbrc.2015.09.018
193. Wang, Y., Xin, X., Jin, Z., Hu, Y., Li, X., Wu, J., Jin, M. (2011). Anti-diabetic effects of pentamethylquercetin in neonatally streptozotocin-induced diabetic rats. *European Journal of Pharmacology, 668*(1–2), 347–353. https://doi.org/10.1016/j.ejphar.2011.06.022
194. Watras, A.C., Buchholz, A.C., Close, R.N., Zhang, Z., Schoeller, D.A. (2007). The role of conjugated linoleic acid in reducing body fat and preventing holiday weight gain. *International Journal of Obesity (2005), 31*(3), 481–487. https://doi.org/10.1038/sj.ijo.0803437
195. Weitkunat, K., Stuhlmann, C., Postel, A., Rumberger, S., Fankhänel, M., Woting, A., Petzke, K.J., Gohlke, S., Schulz, T.J., Blaut, M., Klaus, S., Schumann, S. (2017). Short-chain fatty acids and inulin, but not guar gum, prevent diet-induced obesity and insulin resistance through differential mechanisms in mice. *Scientific Reports, 7*(1), art. no. 6109. https://doi.org/10.1038/s41598-017-06447-x
196. Wendel, A.A., Purushotham, A., Liu, L.-F., Belury, M.A. (2009). Conjugated linoleic acid induces uncoupling protein 1 in white adipose tissue of ob/ob mice. *Lipids, 44*(11), 975–982. https://doi.org/10.1007/s11745-009-3348-9
197. Weng, Q., Chen, L., Ye, L., Lu, X., Yu, Z., Wen, C., Chen, Y., Huang, G. (2019). Determination of licochalcone A in rat plasma by UPLC–MS/MS and its pharmacokinetics. *Acta Chromatographica, 31*(4), 262–265. https://doi.org/10.1556/1326.2018.00491
198. Wijerathne, T.D., Kim, J.H., Kim, M.J., Kim, C.Y., Chae, M.R., Lee, S.W., Lee, K.P. (2019). Onion peel extract and its constituent, quercetin inhibits human Slo3 in a pH and calcium dependent manner. *The Korean Journal of Physiology & Pharmacology, 23*(5), 381–392. https://doi.org/10.4196/kjpp.2019.23.5.381
199. Wisniewski, O., Malinowska, M., Gibas-Dorna, M. (2018). Physiologically-induced adipocyte browning. *Advances in Hygiene and Experimental Medicine, 72*, 499–511. https://doi.org/10.5604/01.3001.0012.0757
200. Wisniewski, O.W. (2019). Physiology of adipose tissue. In H. Krauss (Eds.), *Physiology of Nutrition*, PZWL Wydawnictwo Lekarskie, Warsaw, Poland, pp. 25–56.
201. Wong, J.M.W., de Souza, R., Kendall, C.W.C., Emam, A., Jenkins, D.J.A. (2006). Colonic health: fermentation and short chain fatty acids. *Journal of Clinical Gastroenterology, 40*(3), 235–243. https://doi.org/10.1097/00004836-200603000-00015
202. Wu, J., Boström, P., Sparks, L.M., Ye, L., Choi, J.H., Giang, A.-H., Khandekar, M., Nuutila, P., Schaart, G., Huang, K., Tu, H., van Marken Lichtenbelt, W.D., Hoeks, J., Enerbäck, S., Schrauwen, P., Spiegelman, B.M. (2012). Beige adipocytes are a distinct type of thermogenic fat cell in mouse and human. *Cell, 150*(2), 366–376. https://doi.org/10.1016/j.cell.2012.05.016

203. Xing, T., Kang, Y., Xu, X., Wang, B., Du, M., Zhu, M.-J. (2018). Raspberry supplementation improves insulin signaling and promotes brown-like adipocyte development in white adipose tissue of obese mice. *Molecular Nutrition & Food Research, 62*(5), art. no. 1701035. https://doi.org/10.1002/mnfr.201701035

204. Yoneshiro, T., Aita, S., Matsushita, M., Kayahara, T., Kameya, T., Kawai, Y., Iwanaga, T., Saito, M. (2013). Recruited brown adipose tissue as an antiobesity agent in humans. *The Journal of Clinical Investigation, 123*(8), 3404–3408. https://doi.org/10.1172/JCI67803

205. Yuzbashian, E., Zarkesh, M., Asghari, G., Hedayati, M., Safarian, M., Mirmiran, P., Khalaj, A. (2018). Is apelin gene expression and concentration affected by dietary intakes? A systematic review. *Critical Reviews in Food Science and Nutrition, 58*(4), 680–688. https://doi.org/10.1080/10408398.2016.1262325

206. Zhang, F., Ai, W., Hu, X., Meng, Y., Yuan, C., Su, H., Wang, L., Zhu, X., Gao, P., Shu, G., Jiang, Q., Wang, S. (2018). Phytol stimulates the browning of white adipocytes through the activation of AMP-activated protein kinase (AMPK) α in mice fed high-fat diet. *Food & Function, 9*(4), 2043–2050. https://doi.org/10.1039/C7FO01817G

207. Zhang, H.Q., Chen, S.Y., Wang, A.S., Yao, A.J., Fu, J.F., Zhao, J.S., Chen, F., Zou, Z.Q., Zhang, X.H., Shan, Y.J., Bao, Y.P. (2016). Sulforaphane induces adipocyte browning and promotes glucose and lipid utilization. *Molecular Nutrition & Food Research, 60*(10), 2185–2197. https://doi.org/10.1002/mnfr.201500915

208. Zhang, M., Xin, Y., Feng, K., Yin, B., Kan, Q., Xiao, J., Cao, Y., Ho, C.-T., Huang, Q. (2020). Comparative analyses of bioavailability, biotransformation, and excretion of nobiletin in lean and obese rats. *Journal of Agricultural and Food Chemistry, 68*(39), 10709–10718. https://doi.org/10.1021/acs.jafc.0c04425

209. Zhang, X., Zhang, Q.-X., Wang, X., Zhang, L., Qu, W., Bao, B., Liu, C.-A., Liu, J. (2016). Dietary luteolin activates browning and thermogenesis in mice through an AMPK/PGC1α pathway-mediated mechanism. *International Journal of Obesity 40*(12), 1841–1849. https://doi.org/10.1038/ijo.2016.108

210. Zhao, D., Yuan, B., Kshatriya, D., Polyak, A., Simon, J., Bello, N., Wu, Q. (2019). Bioavailability and metabolism of raspberry ketone with potential implications for obesity prevention (OR34–05–19). *Current Developments in Nutrition, 3*(Suppl. 1), art. no. nzz031.OR34–05–19. https://doi.org/10.1093/cdn/nzz031.OR34-05-19

211. Zhao, M., Chen, X. (2014). Eicosapentaenoic acid promotes thermogenic and fatty acid storage capacity in mouse subcutaneous adipocytes. *Biochemical and Biophysical Research Communications, 450*(4), 1446–1451. https://doi.org/10.1016/j.bbrc.2014.07.010

212. Zhuang, P., Lu, Y., Shou, Q., Mao, L., He, L., Wang, J., Chen, J., Zhang, Y., Jiao, J. (2019). Differential anti-adipogenic effects of eicosapentaenoic and docosahexaenoic acids in obesity. *Molecular Nutrition & Food Research, 63*(14), art. no. e1801135. https://doi.org/10.1002/mnfr.201801135

213. Zhuang, P., Shou, Q., Lu, Y., Wang, G., Qiu, J., Wang, J., He, L., Chen, J., Jiao, J., Zhang, Y. (2017). Arachidonic acid sex-dependently affects obesity through linking gut microbiota-driven inflammation to hypothalamus-adipose-liver axis. *Biochimica Et Biophysica Acta. Molecular Basis of Disease, 1863*(11), 2715–2726. https://doi.org/10.1016/j.bbadis.2017.07.003

214. Zou, T., Chen, D., Yang, Q., Wang, B., Zhu, M.-J., Nathanielsz, P.W., Du, M. (2017). Resveratrol supplementation of high-fat diet-fed pregnant mice promotes brown and beige adipocyte development and prevents obesity in male offspring. *The Journal of Physiology, 595*(5), 1547–1562. https://doi.org/10.1113/JP273478

215. Zou, T., Wang, B., Yang, Q., de Avila, J.M., Zhu, M.-J., You, J., Chen, D., Du, M. (2018). Raspberry promotes brown and beige adipocyte development in mice fed high-fat diet through activation of AMP-activated protein kinase (AMPK) α1. *The Journal of Nutritional Biochemistry*, *55*, 157–164. https://doi.org/10.1016/j.jnutbio.2018.02.005

216. Zu, Y., Overby, H., Ren, G., Fan, Z., Zhao, L., Wang, S. (2018). Resveratrol liposomes and lipid nanocarriers: Comparison of characteristics and inducing browning of white adipocytes. *Colloids and Surfaces B: Biointerfaces, 164*, 414–423. https://doi.org/10.1016/j.colsurfb.2017.12.044

Pol. J. Food Nutr. Sci., 2021, Vol. 71, No. 4, pp. 383–392
On-line ISSN: 2083-6007
Print ISSN: 1230-0322
DOI: 10.31883/pjfns/142639
http://journal.pan.olsztyn.pl

Original article
Section: Nutrition

Compositional Characteristics and Antioxidant Activity of Edible Rose Flowers and Their Effect on Phenolic Urinary Excretion

Andrea Devecchi[1], Sonia Demasi[2], Francesca Saba[1], Rosalba Rosato[3], Roberto Gambino[1], Valentina Ponzo[1], Antonella De Francesco[4], Paola Massarenti[4], Simona Bo[1], Valentina Scariot[2]*

[1]*Department of Medical Sciences, University of Turin, Corso Dogliotti 14, 10126, Turin, Italy*
[2]*Department of Agricultural, Forest and Food Sciences, University of Turin, Largo P. Braccini 2, 10095, Grugliasco (TO), Italy*
[3]*Department of Psychology, University of Turin, Via Verdi 10, 10124, Turin, Italy*
[4]*Azienda Ospedaliera Universitaria Città della Salute e della Scienza di Torino, Corso Bramante 88, 10126, Turin, Italy*

Key words: anthocyanins, bioactive compounds, edible flowers, human study, polyphenols

Petals of edible flowers (EF) are rich in biologically active compounds with many proven benefits for human health. However, studies on the effects of EF in humans after consumption are lacking. This pilot explorative study evaluated the changes in urinary phenolic excretion in healthy volunteers to whom different doses of phenolics from edible roses (Gourmet Roses™) have been added to a meal. Rose petals were picked fresh once a week for three weeks, showing significantly increasing values of total phenolic content, total anthocyanin content, and antioxidant activity (measured as ferric reducing antioxidant power (FRAP) and as DPPH$^{\bullet}$ and ABTS$^{\bullet+}$ scavenging activities) from the first to the third week. After the meal, direct associations between urinary phenolics and both the EF phenolic content and the antioxidant activity were found in a multiple regression model. These new insights on EF consumption, to be confirmed by larger trials, suggest that the urinary phenolic excretion of healthy volunteers increases with increasing rose phenolic content.

INTRODUCTION

Edible flowers (EF) have been used in human nutrition for hundreds of years and are popular in the European, Middle-East, Chinese, and Indian cultures [Lim, 2014a,b; Pires *et al*., 2019; Scariot *et al*., 2018], thanks to their taste, beauty, and aromas [Takahashi *et al*., 2020]. EF are consumed either fresh or minimally processed or in the form of different preparations [Fernandes *et al*., 2020; Takahashi *et al*., 2020]. Since the late 1980's, studies revealing the EF chemical composition and properties linked to the presence of several bioactive compounds arose [Demasi *et al*., 2020; Falla *et al*., 2020; Fernandes *et al*., 2020; Grzeszczuk *et al*., 2016; Rop *et al*., 2012; Scariot *et al*., 2018], together with an increased awareness of consumers towards the consumption of natural sources of bioactive compounds [Fernandes *et al*., 2020; Rop *et al*., 2012; Takahashi *et al*., 2020]. Petals of fresh EF are rich in vitamins, minerals, and phenolics, a class of biologically active compounds with many proven benefits [Liu, 2003; Loizzo *et al*., 2016; Navarro-González *et al*., 2015; Takahashi *et al*., 2020]. Adequate intake of phenolics could confer benefits for human health, by reducing the risk of cardiovascular, dysmetabolic, and neurodegenerative diseases, and cancer (in particular gastrointestinal neoplasms), by eliciting anti-inflammatory effects, and by favorably modulating the gut microbiota composition [Fraga *et al*., 2019; Zamora-Ros *et al*., 2013]. Furthermore, phenolics have been reported to be inversely associated with all-cause mortality and cardiovascular events [Del Bo *et al*., 2019]. EF have a low-fat content and are rich in water similarly to leafy vegetables [González-Barrio *et al*., 2018; Rop *et al*., 2012]. It has also been demonstrated that many EF contain high amounts of phenolics, exceeding those found in fresh fruits and vegetables. For instance, *Rosa pendulina* petals have a total phenolic content of ~1,700 mg/100 g, more than double than blackcurrant (~800 mg/100 g) or blackberry (~600 mg/100 g) fruits [Demasi *et al*., 2021a; Pérez-Jiménez *et al*., 2010b]. Looking at single classes of phenolics, petals of *Dianthus pavonius* contain more than 2,000 mg/100 g of flavonols compared to ~100 mg/100 g in spinach, or *Paeonia officinalis* contains ~800 mg/100 g of benzoic acid compared to ~120 mg/100 g in raspberry, or finally *Taraxacum officinale* have ~800 mg/100 g of cinnamic

* Corresponding Author:
E-mail: sonia.demasi@unito.it (S. Demasi)

Submitted: 14 April 2021
Accepted: 28 September 2021
Published on-line: 27 October 2021

© Copyright by Institute of Animal Reproduction and Food Research of the Polish Academy of Sciences
© 2021 Author(s). This is an open access article licensed under the Creative Commons Attribution-NonCommercial-NoDerivs License (http://creativecommons.org/licenses/by-nc-nd/4.0/).

acids compared to the 200 mg/100 g of globe artichoke [Demasi *et al*., 2021a; Pérez-Jiménez *et al*., 2010b]. It is therefore evident that it is important to deepen the knowledge on flowers composition in order to understand the role of their phenolics in human metabolism.

The quantity and quality of secondary metabolites and bioactive compounds in petals, similarly to other anatomical parts of plants, may be influenced by several factors. A wide variability in the amount and composition of metabolites in plants have been recorded depending on the genotype [Fiehn, 2002], the stage of development [Piccolella *et al*., 2018], the environmental conditions [Demasi *et al*., 2018], the cultivation practices [Caser *et al*., 2019a,b; Najar *et al*., 2019], the harvesting time [Pal & Singh, 2013], and storage [Demasi *et al*., 2021b].

To date, a few EF species have been investigated and this number is expected to increase [Fernandes *et al*., 2020; Pires *et al*., 2019]. Rose (*Rosa* spp.) is one of the most beloved and known ornamental plants, with a complex genus classification [Martínez *et al*., 2020; Smulders *et al*., 2019]. It is among the most frequently consumed EF worldwide [Fernandes *et al*., 2020], showing a high phenolic content and antioxidant activity according to the genotype [Demasi *et al*., 2021a; Fernandes *et al*., 2020; Guimarães *et al*., 2010; Li *et al*., 2014; Lu *et al*., 2016; Zheng *et al*., 2018]. At present, the contribution of EF to human metabolism *in vivo* is almost unexplored and data relative to phenolic urinary excretion after EF consumption in humans are lacking. We carried out an exploratory pilot study in a small group of healthy volunteers who were given a week away both a meal and the same meal with the addition of rose petals with different phenolic contents. Then we explored whether the fresh rose characteristics (total phenolic content, total anthocyanin content, and antioxidant activity) were associated with the excretion of phenolics in human urine, after standardization of the meals.

MATERIALS AND METHODS

Chemicals and apparatus

Sodium carbonate, sodium acetate, potassium chloride, potassium persulfate, hydrochloric acid, acetic acid, iron(III) chloride hexahydrate, 2,2'-azino-bis(3-ethylbenzothiazoline-6-sulfonic acid) diammonium salt (ABTS), 2,4,6-tripyridyl-s-triazine (TPTZ), 2,2-diphenyl-1-picrylhydrazyl (DPPH radical), Folin–Ciocalteu phenol reagent, and gallic acid were purchased from Sigma Aldrich (St. Louis, MO, USA). Oaxis MAX Cartridges were purchased from Waters (Milford, CT, USA). A Cary 60 UV-Vis spectrophotometer (Agilent, Santa Clara, CA, USA) was used to perform spectrophotometric readings.

Plant material

Fresh open flowers of Gourmet Roses™ were provided by the organic nursery RaveraBio® (Rzero Group di Orsini L. & C., Albenga, SV, Italy) once a week from 1st to 21st June 2019. From each of the three supplies, part of the fresh petals was used for the human experiment, and part was grinded in a mortar using liquid nitrogen, then prepared for the spectrophotometric analysis of total phenolic and total anthocyanin content, and antioxidant activity. One gram of flower powder was extracted with 50 mL of a water-methanol solution (1:1, *v/v*) at room temperature with ultrasound-assisted extraction (Sarl Reus, Drap, France) at 23 kHz for 30 min. Three different extractions were performed as replicates for each supply. The solution was filtered with one-layer of filter paper (Whatman No. 1, Maidstone, UK) and preserved at -20°C until the spectrophotometric analyses.

Total phenolic content of roses

The total phenolic content was analyzed using the Folin-Ciocalteu reagent [Demasi *et al*., 2021b], by mixing 750 μL of the reagent (diluted 1:10) with 150 μL of the rose extract and 600 μL of Na_2CO_3 (7.5%). The solution was left in a dark room at room temperature for 30 min. Then, its absorbance was read at 765 nm, and results were expressed as g of gallic acid equivalents (GAE) per kg of fresh flower (g GAE/kg).

Total anthocyanin content of roses

The pH-differential method was used for anthocyanin measurement [Demasi *et al*., 2020]. The rose extract (1 mL) was mixed with 9 mL of an aqueous buffer solution at pH 1 (4.026 g KCl + 12.45 mL HCl 37% in a 1 L water volume) in one flask. In another flask, 1 mL of the same rose extract was mixed with an aqueous buffer solution at pH 4.5 (32.82 g $C_2H_3NaO_2$ + 18 mL $C_2H_4O_2$ in a 1 L water volume). The solutions were kept in the dark for 20 min at room temperature, and their absorbance was read at 515 nm and 700 nm. Results were expressed as g of cyanidin 3-*O*-glucoside (C3G) per kg of fresh flower (g C3G/kg).

Antioxidant activity of roses

The antioxidant activity of roses was analyzed using different assays: the ferric reducing antioxidant power (FRAP), DPPH, and ABTS [Demasi *et al*., 2021b]. The FRAP assay was performed by mixing 30 μL of the rose extract with 90 μL of deionized water and 900 μL of the FRAP reagent. The solution was kept for 30 min at 37°C, and then its absorbance was measured at 595 nm, and results were expressed as millimoles of ferrous iron (Fe^{2+}) equivalents per kg (mmol Fe^{2+}/kg). The DPPH assay was performed with the following procedure: a $DPPH^{\bullet}$ solution was obtained by the reaction of 2 mg of $DPPH^{\bullet}$ with 50 mL of MeOH, up to the absorbance of 1.000 at 515 nm. Then, 3 mL of the $DPPH^{\bullet}$ solution was mixed with 40 μL of the rose extract. The mixture was left in the dark at room temperature for 30 min, and then its absorbance was measured at 515 nm. The ABTS assay was performed with the following procedure: the ABTS radical cation solution was obtained by the reaction of 7.0 mM ABTS with 2.45 mM $K_2S_2O_8$, incubated for 12–16 h in the dark at room temperature and diluted with distilled water until the absorbance of 0.70 had been achieved at 734 nm. Then, 2 mL of the diluted $ABTS^{\bullet+}$ solution was mixed with 30 μL of the rose extract. The mixture was left in the dark at room temperature for 10 min, and then its absorbance was measured at 734 nm. In both DPPH and ABTS methods the results were expressed as mmol of Trolox equivalents (TE) per kilogram (mmol TE/kg).

The water-methanol (1:1, *v/v*) extraction solution was used as control in each analysis instead of the rose extract.

The human experiment

Twenty healthy volunteers were enrolled for the experiment. Inclusion criteria were age 20–70 years, and a body mass index (BMI) 20–29 kg/m^2. Exclusion criteria were: treatment with any drugs and/or supplements, subjects in any dietary regimen, pregnant and/or lactating women, the presence of any known disease, active smoking, inability to express informed consent to the study, and known flower allergy. The study was conducted following a randomized cross-over design [Kuntz *et al*., 2015] and all participants received the same meal without (M; meal without EF) or with (EFM; meal + EF) the addition of 17 g of rose petals after 1 week of wash out. Participants were randomized to receive as a first meal either the meal without EF (M) or the same meal with the addition of EF (EFM). Meals were prepared by the same researcher in the same place; each meal consisted of 2 courses, and their composition is reported in Table 1.

In a random order, 7, 8, and 5 participants received the EFM supplied respectively in the first, second, and third week. Randomization sequence was computer-generated by a statistician. Participants were to consume either the M or the EFM in 60-min under researchers' supervision at 1:00 pm at the kitchen of the School of Dietetics (University of Turin). Volunteers had to eat both the two courses each of the two days of the experiment. During each meal, only water was allowed. The same dietary recommendations for the 24-h before each test and the 24-h after each test were given to all participants. The energy content was calculated according to the participant's energy need (range 1500–1900 kcal); the dietary composition was 20 g/100 g proteins, 30 g/100 g lipids, 50 g/100 g carbohydrates. Fiber intake was restricted to 17 g/day, by reducing phenolic-rich foods (no more than 250 g fruit/day -only peeled apple and banana allowed-, no more than 200 g vegetables/day -only lettuce and zucchini allowed-, no wine, no tea, no coffee, no cocoa) in order to avoid interference from dietary polyphenols. The dietary phenolic intake was calculated according to the published database [Neveu *et al*., 2010; Rothwell *et al*., 2013]. Each participant completed both a 1-day food record to collect data relative to food consumption 24-h before each experiment and a validated food-frequency questionnaire to obtain data relative to usual dietary habits. Diet adherence was verified both by the 1-day food recall and by telephone interview with each participant the day before the experiment. Urine collection began from 4:00 pm of the day of the test until 4:00 pm of the day after the test. Each volunteer was asked to urinate before the meal and then to wait until 4:00 pm before the next voiding. All procedures were in agreement with the principles of the Helsinki Declaration; the study protocol, the questionnaires used, the informed consent, the information for the participant and the *curriculum vitae* of the researchers were submitted to the attention of the Local Bioethics Committee of the University of Turin on 25 March 2019. The study protocol was approved by the Local Bioethics Committee of the University of Turin (No.176859, Turin, Italy) on 2 May 2019. Informed consent was obtained from all individual participants included in the study.

Total phenolic content of urine

Urine samples were collected into sterilized 1.5 L bottles, acidified with HCl to preserve the phenolic compounds in line with literature [Roura *et al*., 2006], and processed the following morning to avoid formation of artefacts and loss of phenolic content. The total phenolic content excreted in urine after consumption of the test meals was determined with Folin-Ciocalteu assay after purifying the samples by solid-phase extraction according to literature [Medina-Remón *et al*., 2009], with the difference that the solid-phase extraction was carried out through Oaxis MAX Cartridge Waters containing the same stationary phase as micro titer 96-well plate cartridges. Briefly, 1 mL of acidified urine was applied to an activated Waters Oasis MAX cartridge. The cartridge was rinsed with 4 mL of sodium acetate 50 mM pH 7/5% methanol. The phenolics were eluted with 1.8 mL of 2% (*v/v*) formic acid in methanol. Then, 30 μL of the eluted fractions were mixed with 340 μL of deionized water adding 25 μL

TABLE 1. Composition of the meal (M) received by the participants. The meal with edible flowers (EFM) was the same with the addition of 17 g of rose petals.

Meal	Ingredient	Quantity (g)	Proteins (g)	Lipids (g)	Carbohydrates (g)	Fiber (g)	Total kcal
Vegetable noodles	Noodles	80	7.3	1.7	39.5	1.81	
	Courgettes	60	0.81	0	0.87	0.87	
	Carrots	50	0.55	0	3.8	1.55	
	Ricotta	40	3.5	4.37	1.4	0	
	Olive oil	10	0	10	0	0	
Baked fish fillet with yogurt sauce	Cod	100	17	0.3	0	0	
	Natural yogurt	50	1.9	1.95	2.15	0	
	Cucumbers	15	0.1	0	0.3	0.11	
	Olive oil	5	0	5	0	0	
Intake (*per capita*)			30	23	48	4.34	520

of the Folin-Ciocalteu reagent and 60 μL of sodium carbonate (200 g/L). The mixture was incubated for 1 h at room temperature in the dark. Later, 145 μL of deionized water was added. Absorbance was measured at 765 nm. Results were expressed as mg gallic acid equivalent per liter (mg/L) and per day (mg/day).

Statistical analyses

Flowers' variables and human data were reported as means ± standard deviations. For each rose's phytochemical parameter, differences between the three samples were analyzed by non-parametric analysis of variance using Kruskal-Wallis test, with stepwise comparison, and by Spearman's correlation analyses. Between-group differences in urinary phenolic excretion were analyzed by Kruskal-Wallis test. Analyses were performed using SPSS 24.0 Inc. software (SPSS Inc., Chicago, IL, USA). Crude and adjusted linear regression models were used to examine the urinary phenolic excretion (dependent variable) in relation to each compositional characteristics and antioxidant activity of edible rose flowers: (a) the flower total phenolic, (b) the total anthocyanin contents, and (c) the antioxidant activity. A multiple regression model adjusted for age, sex, BMI, and dietary phenolic intake was estimated for each phytochemical characteristic (a, b, c). These analyses were done with Statistica software (ver. 7.0; StatSoft Inc., Tulsa, OK, USA).

RESULTS AND DISCUSSION

Bioactive compounds in rose petals

The content of phenolics and anthocyanins in rose petals and their antioxidant activity are reported in Table 2. The total phenolic content (6.53, 8.01, and 11.71 g GAE/kg) and the FRAP (298.23, 407.41, 564.77 mmol Fe^{2+}/kg) significantly differed in each sample, increasing from the first to the third week of EF supply. Similarly, anthocyanin content (0.86–1.36 g C3G/kg), DPPH$^{\bullet}$ (26.67–45.58 mmol TE/kg), and $ABTS^{\bullet+}$ (9.49–14.12 mmol TE/kg) scavenging activities were higher in the third sample. All the evaluated parameters of EF were positively highly correlated with each other (p values were always lower than 0.01), as reported in Table 3.

Rosa is an extremely wide and complex genus of plant and comprises more than 150 species and 30,000 cultivars [Smulders *et al*., 2019]. Some of them have already been studied as edible flowers and source of bioactive compounds (*e.g. Rosa* × *hybrida*, *Rosa* × *odorata*, *Rosa centifolia*, *Rosa chinensis*, *Rosa gallica*, *Rosa micrantha*, *Rosa damascena*, *Rosa bourboniana*, *Rosa brunonii,* and *Rosa rugosa*), and results showed a wide variability according to the species [Chen *et al*., 2018; Guimarães *et al*., 2010; Kumar *et al*., 2009; Li *et al*., 2014; Lu *et al*., 2016; Mohsen *et al*., 2020; Rop *et al*., 2012; Zhang *et al*., 2014; Zheng *et al*., 2018]. Different analytical assays

TABLE 2. Total phenolic and total anthocyanin contents, and antioxidant activity measured as ferric reducing antioxidant power (FRAP) and as DPPH$^{\bullet}$ and $ABTS^{\bullet+}$ scavenging activities of edible roses (Gourmet Roses™) supplied in the first, second, and third week of June 2019.

Rose supply	Total polyphenol content (g GAE/kg)	Total anthocyanin content (g C3G/kg)	FRAP (mmol Fe^{2+}/kg)	DPPH$^{\bullet}$ scavenging activity (mmol TE/kg)	$ABTS^{\bullet+}$ scavenging activity (mmol TE/kg)
n.1	6.53 ± 0.70^{c}	0.86 ± 0.09^{b}	298.23 ± 35.75^{c}	26.67 ± 1.47^{b}	9.49 ± 1.92^{b}
n.2	8.01 ± 0.19^{b}	0.97 ± 0.02^{b}	407.41 ± 16.53^{b}	28.36 ± 2.62^{b}	9.96 ± 0.49^{b}
n.3	11.71 ± 0.40^{a}	1.36 ± 0.08^{a}	564.77 ± 6.45^{a}	45.58 ± 0.82^{a}	14.12 ± 0.17^{a}
p	0.00003	0.0004	0.00002	0.00002	0.005

Results are expressed as mean of three replicates ± standard deviation; different letters indicate significant differences in a column according to Kruskal-Wallis stepwise comparisons ($p \leq 0.05$). GAE – gallic acid equivalent; C3G – cyanidin 3-*O*-glucoside; TE – Trolox equivalent.

TABLE 3. Spearman's correlation coefficients between total phenolic content, total anthocyanin content, and antioxidant activity measured as ferric reducing antioxidant power (FRAP) and as DPPH$^{\bullet}$ and $ABTS^{\bullet+}$ scavenging activities of edible roses (Gourmet Roses™).

		FRAP	DPPH$^{\bullet}$ scavenging activity	$ABTS^{\bullet+}$ scavenging activity	Total anthocyanin content
Total phenolic content	Correlation coefficient	0.983	0.850	0.803	0.833
	p	0.000	0.004	0.009	0.005
FRAP	Correlation coefficient		0.883	0.820	0.850
	p		0.002	0.007	0.004
DPPH$^{\bullet}$ scavenging activity	Correlation coefficient			0.887	0.800
	p			0.001	0.010
$ABTS^{\bullet+}$ scavenging activity	Correlation coefficient				0.937
	p				0.000

(*e.g.* FRAP, DPPH, and ABTS, or total phenolic content) are necessary to evaluate the antioxidant activity of matrices. However, different extraction and analytical methods, and sample preparation could make the comparison among different studies difficult [Santos-Buelga *et al*., 2012]. The range of total phenolic content has been reported to vary from 5.00 to 24.00 g GAE/kg in *R.* × *hybrida* and *R.* × *odorata* [Li *et al*., 2014; Rop *et al*., 2012], while other authors [Chen *et al*., 2018] found 74 g GAE/kg in pink *R. rugosa* (on dry weight). Twelve rose cultivars are reported to have a total anthocyanin content ranging from 0 to 2.50 g C3G/kg [Friedman *et al*., 2010]. In four rose species [Zheng *et al*., 2018], ranges of 360–3620 mmol Fe^{2+}/kg were recorded with FRAP, and 239–1037 mmol TE/kg with ABTS assay. $ABTS^{\bullet+}$ scavenging activities of 2–36 mmol TE/kg and 653 mmol TE/kg were reported in fresh flowers of 12 rose cultivars [Friedman *et al*., 2010] and in dry flowers of *R. rugosa* [Zhang *et al*., 2014], respectively. In turn, 101 mmol TE/kg (by ABTS assay) and 451 mmol Fe^{2+}/kg (by FRAP) were recorded in *R.* × *hybrida* petals [Li *et al*., 2014]. Our results on Gourmet Roses™ petals are consistent with the above-mentioned ranges, except for the DPPH assay, which detected lower values than those reported in literature (243–520 mmol TE/kg) [Chen *et al*., 2018; Zheng *et al*., 2018].

The petals of roses harvested at one-week distance during the month of July showed an increasing content over time in bioactive compounds, namely total phenolics, and anthocyanins. Consequently, an increased antioxidant activity was found. These parameters were positively correlated, confirming previous results on edible plants and wildflowers [Demasi *et al*., 2021a; Li *et al*., 2014]. The secondary metabolite content in roses varies among species and may be triggered by various stimuli, which commonly occur because of seasonal variations, or biotic and abiotic stresses. Similarly, also the phenological stage and senescence of the plant could have determined an increased production of antioxidants, such as phenolic compounds, as a defense system that can lead to increments both in the phenolic content and the biological activity over time [Piccolella *et al*., 2018].

Urinary phenolic content

Twenty volunteers participated in the study (12 males, 8 females); their mean age and BMI were 41.2±10.8 years and 22.6±3.2 kg/m^2, respectively. Their usual mean phenolic dietary intake was 931.3±219.1 mg/day. The 24-h before each experiment, the mean phenolic dietary intake was lower (784.5±230.4 mg/day) in line with the given dietary recommendations for those days. Diet adherence was evaluated by 1-day food record and telephone interview the day before each experiment and resulted to be adequate. Out of them, 2 volunteers (1 male and 1 female, both receiving the third EF sample) did not perform a correct 24-h urine collection. Therefore, the urine samples of 18 subjects were analyzed. No adverse effects related to the EF assumption were reported by participants.

The differences in urinary phenolic excretion (expressed as mg/L or mg/day) between the participant consuming EFM and M were -1.8±11.4, 7.0±14.6, 59.1±94.6 mg/L (p=0.15 according to Kruskal-Wallis) and -4.5±20.2, 6.8±10.9, 72.7±124.1 mg/day (p=0.15), respectively from the first, second, and third supply of roses. The associations between the urinary human phenolic excretion (dependent variable) and the EF characteristics, namely total phenolic and total anthocyanin content, and antioxidant activity are shown in Table 4. Direct significant associations were found with all the EF characteristics in both crude and adjusted models, in which four variables potentially impacting the intake or excretion of phenolics (age, gender, body mass index, and dietary phenolic intake) were considered. It is reassuring that the associations remain statistically significant in the adjusted model, despite the small size of the sample (20 participants). This might suggest a potential influence of the rose characteristics on the human absorption of the rose phenolic content.

TABLE 4. Parameters of a regression model for relationships between differences in 24-h urinary phenolic excretion of participants consuming meal with and without edible flower, and the roses (Gourmet Roses™) characteristics.

Characteristics	Model	β_1	SE_1	p_1	β_2	SE_2	p_2
Total phenolic content (g GAE/kg)	Crude	0.11	0.048	0.031	0.15	0.063	0.032
	Adjusted[a]	0.16	0.063	0.030	0.19	0.084	0.044
Total anthocyanin content (g C3G/kg)	Crude	1.21	0.50	0.027	1.58	0.65	0.027
	Adjusted	1.65	0.65	0.026	2.03	0.86	0.035
Ferric reducing antioxidant power (mmol Fe^{2+}/kg)	Crude	0.20	0.09	0.046	0.26	0.12	0.049
	Adjusted	0.28	0.12	0.047	0.32	0.17	0.07
$DPPH^{\bullet}$ scavenging activity (mmol TE/kg)	Crude	3.10	1.24	0.024	4.09	1.62	0.022
	Adjusted	4.27	1.64	0.023	5.40	2.12	0.026
$ABTS^{\bullet+}$ scavenging activity (mmol TE/kg)	Crude	12.85	5.15	0.024	16.90	6.70	0.023
	Adjusted	17.67	6.78	0.023	22.24	8.79	0.026

[a] adjusted – multiple regression model adjusted for age, gender, body mass index, and dietary polyphenol intake. β_1, ES_1, p_1 – parameters for urinary phenolic excretion expressed in mg/L; β_2, ES_2, p_2 – parameters for urinary phenolic excretion expressed in mg/day. β – regression coefficient; SE – standard error; GAE – gallic acid equivalent; C3G – cyanidin 3-*O*-glucoside; TE – Trolox equivalent.

Polyphenols bioavailability varies widely among different classes of phenolics and they can be absorbed and metabolized differently according to their chemical structure [Teng & Chen, 2019]. Briefly, part of them are absorbed by the small intestine, while part are metabolized by microbiota. The metabolites reach the liver to be absorbed by tissues and cells or the kidneys, to be ultimately excreted through urine. Phenolic intake from food has been therefore associated with human total urinary phenolic excretion [Nielsen *et al*., 2002; Mennen *et al*., 2006; Pérez-Jiménez *et al*., 2010a; Roura *et al*., 2006; Spencer *et al*., 2008; Zamora-Ros *et al*., 2011]. A systematic review has suggested that urinary phenolics might be considered as an indicator of phenolic intake [Pérez-Jiménez *et al*., 2010a]. An increased consumption of phenolic compounds with diet has been reported to reduce cardiovascular risk factors [Guo *et al*., 2016; Medina-Remón *et al*., 2017], the incidence of type 2 diabetes mellitus [Wedick *et al*., 2012], cardiovascular events, and all-cause mortality [Agudo *et al*., 2007; Alonso *et al*., 2004; Covas *et al*., 2001; Grassi *et al*., 2005; Manach *et al*., 2005; Tresserra-Rimbau *et al*., 2014a,b], and to decrease blood concentrations of inflammatory biomarkers [Medina-Remón *et al*., 2017]. The beneficial effects of dietary polyphenols may also be due to a bi-directional relationship with the gut microbiota: polyphenols can favorably affect the gut microbiota composition, and the gut microflora could metabolize polyphenols into beneficial bioactive compounds, such as chlorogenic acid and the derived compounds [Fraga *et al*., 2019; Liu *et al*., 2020a; Ozdal *et al*., 2016; Tomas-Barberan *et al*., 2014].

At present, only *in vitro* and animal studies evaluated the effects of EF phenolics. The anti-inflammatory property of extract of *R. canina,* tested on the carrageenin-induced rat paw edema assay, was demonstrated by the inhibition of carrageenin-induced edema, similarly to the effect of indomethacin [Lattanzio *et al*., 2011]. Flower compounds have been reported both to induce cell apoptosis *via* the p53 signalling and p38 MAPK/FasL (mitogen-activated protein kinase--FAS ligand) cascade pathways [Lin *et al*., 2005; Lo *et al*., 2007] and to ameliorate the ROS-mediated mitochondrial dysfunction pathway [Hou *et al*., 2005; Lin *et al*., 2005; Lo *et al*., 2007]. Hibiscus acid from *Hibiscus sabdariffa* (roselle) and (+)-epimagnolin A and (+)-magnolin from *Magnolia denudata* induced weight loss in animals and in *in vitro* experiments, by acting on fat metabolism-related enzymes, down-regulating adipocyte differentiation *via* the modulation of the PI3K (phosphoinositide 3-kinase) and MAP-kinase pathways and inhibiting α-amylase activity and sugar/starch absorption [Hansawasdi *et al*., 2001; Kim *et al*., 2007; Kong *et al*., 2011; Preuss *et al*., 2007]. Similarly, the methanol extract of *Nymphaeaceae* inhibited the lipid storage in adipocytes by promoting lipolysis [Hansawasdi *et al*., 2001; Lee *et al*., 2010; Kong *et al*., 2011; Velusami *et al*., 2013]. *Rosa* spp. are very rich in quercetin, which has been shown to inhibit both α-glucosidase and α-amylase, thus reducing the intestinal absorption of glucose [Lu *et al*., 2016; Oboh *et al*., 2015]. However, different EF showed great variability in their phenolic composition and bio-accessibility through an *in vitro* digestion model coupled to a simulated intestinal barrier [de Morais *et al*., 2020]. Thus, *in vivo* and human studies are needed to define the potential role of EF on human health.

This is the first human study analyzing the relationship between the dietary content of phenolics from EF and the urinary phenolic excretion in healthy volunteers. According to the multiple regression analysis, we found a direct relationship between the increasing rose phenolic content and the phenolic excretion, meaning that phenolics have been absorbed and metabolized by the body [Pérez-Jiménez *et al*., 2010a].

CONCLUSIONS

The preliminary data of this pilot explorative study suggest the importance of carrying out further human trials to characterize the absorption of the phenolics contained in the EF and their impact on the human oxidative status. Indeed, edible roses were confirmed as a rich source of bioactive compounds (total phenolics and total anthocyanins) with high antioxidant activity, and the increasing values of these parameters in flowers corresponded to an increase of the urinary phenolic excretion in healthy volunteers. Interestingly, the amount of EF used in the recipes (17 g) provided an amount of phenolics (111–199 mg GAE) proper to fill the gap between the dietary recommendations during the trial (784 mg/day) and the usual mean dietary intake of the participants (931 mg/day), suggesting that no other supplemented phenolics are required to meet their needs. Though, we cannot exclude the possibility that an absorption plateau could be reached at a specific threshold of phenolic intake by EF supplementation. In order to reduce the risk of bias, the conditions were standardized as much as possible before and during the human experiment and the participants reported an adequate compliance to the given dietary recommendations. Even though for the purposes of a pilot study any sample size from 12 upwards has been considered adequate [Julious, 2005], a larger sample of participants will be needed for future studies to specifically test a dose-response relationship [Shader, 2015]. Moreover, the evaluation, besides urine, also of blood markers of oxidative stress, inflammation, kidney and liver function would be of interest to define the efficiency of phenolics absorption and the potential benefits and safety of adding specific EF in daily diet.

ACKNOWLEDGEMENTS

Authors thank RZero Group s.r.l. for providing rose flowers, and Mina Novello for suggesting the recipes.

RESEARCH FUNDING

This research was partially funded by the program Interreg V-A Francia Italia Alcotra, project n. 1139 "ANTEA – Attività innovative per lo sviluppo della filiera transfrontaliera del fiore edule".

CONFLICT OF INTEREST

The authors declare that this study received component from RZero Group s.r.l. The provider was not involved in the study design, collection, analysis, interpretation of data, the writing of this article or the decision to submit it for publication.

ORCID IDs

S. Bo https://orcid.org/0000-0001-6862-8628
S. Demasi https://orcid.org/0000-0001-6223-5436
A. Devecchi https://orcid.org/0000-0003-2508-1110
R. Rosato https://orcid.org/0000-0002-4921-374X
V. Scariot https://orcid.org/0000-0003-0195-1361

REFERENCES

1. Agudo, A., Cabrera, L., Amiano, P., Ardanaz, E., Barricarte, A., Berenguer, T., Chirlaque, M.D., Dorronsoro, M., Jakszyn, P., Larrañaga, N., Martínez, C., Navarro, C., Quirós, J.R., Sánchez, M.J., Tormo, M.J., González, C.A. (2007). Fruit and vegetable intakes, dietary antioxidant nutrients, and total mortality in Spanish adults: findings from the Spanish cohort of the European Prospective Investigation into Cancer and Nutrition (EPIC-Spain). *The American Journal of Clinical Nutrition*, *85*(6), 1634–1642. https://doi.org/10.1093/ajcn/85.6.1634
2. Alonso, A., de la Fuente, C., Martín-Arnau, A.M., de Irala, J., Alfredo Martínez, J., Martínez-González, M.Á. (2004). Fruit and vegetable consumption is inversely associated with blood pressure in a Mediterranean population with a high vegetable-fat intake: the Seguimiento Universidad de Navarra (SUN) Study. *British Journal of Nutrition*, *92*(2), 311–319. https://doi.org/10.1079/BJN20041196
3. Caser, M., Chitarra, W., D'Angiolillo, F., Perrone, I., Demasi, S., Lovisolo, C., Pistelli, L., Pistelli, L., Scariot, V. (2019a). Drought stress adaptation modulates plant secondary metabolite production in *Salvia dolomitica* Codd. *Industrial Crops and Products*, *129*, 85–96. https://doi.org/10.1016/j.indcrop.2018.11.068
4. Caser, M., Demasi, S., Victorino, Í.M.M., Donno, D., Faccio, A., Lumini, E., Bianciotto, V., Scariot, V. (2019b). Arbuscular mycorrhizal fungi modulate the crop performance and metabolic profile of saffron in soilless cultivation. *Agronomy*, *9*(5), 232. https://doi.org/10.3390/agronomy9050232
5. Chen, G.L., Chen, S.G., Xiao, Y., Fu, N.L. (2018). Antioxidant capacities and total phenolic contents of 30 flowers. *Industrial Crops and Products*, *111*, 430–445. https://doi.org/10.1016/j.indcrop.2017.10.051
6. Covas, M.I., Fitó, M., Marrugat, J., Miró, E., Farré, M., De la Torre, R., Gimeno, E., López-Sabater, M.C., Lamuela-Raventós, R., De la Torre-Boronat, H.C. (2001). Coronary heart disease protective factors: Antioxidant effect of olive oil | Facteurs protecteurs de la maladie coronarienne: Effet antioxydant de l'huile d'olive. *Therapie*, *56*(5), 607–611. Available at: [https://www.ncbi.nlm.nih.gov/pubmed/11806301]
7. de Morais, J.S., Sant'Ana, A.S., Dantas, A.M., Silva, B.S., Lima, M.S., Borges, G.C., Magnani, M. (2020). Antioxidant activity and bioaccessibility of phenolic compounds in white, red, blue, purple, yellow and orange edible flowers through a simulated intestinal barrier. *Food Research International*, *131*, art. no. 109046. https://doi.org/10.1016/j.foodres.2020.109046
8. Del Bo, C., Bernardi, S., Marino, M., Porrini, M., Tucci, M., Guglielmetti, S., Cherubini, A., Carrieri, B., Kirkup, B., Kroon, P., Zamora-Ros, R., Liberona, N.H., Andres-Lacueva, C., Riso, P. (2019). Systematic review on polyphenol intake and health outcomes: is there sufficient evidence to define a health-promoting polyphenol-rich dietary pattern? *Nutrients*, *11*(6), art. no. 1355. https://doi.org/10.3390/nu11061355
9. Demasi, S., Caser, M., Donno, D., Ravetto Enri, S., Lonati, M., Scariot, V. (2021a). Exploring wild edible flowers as a source of bioactive compounds: New perspectives in horticulture. *Folia Horticulturae*, *33*(1), 27–48. https://doi.org/10.2478/fhort-2021-0004
10. Demasi, S., Caser, M., Lonati, M., Cioni, P. L., Pistelli, L., Najar, B., Scariot, V. (2018). Latitude and altitude influence secondary metabolite production in peripheral alpine populations of the mediterranean species *Lavandula angustifolia* Mill. *Frontiers in Plant Science*, *9*, art. no. 983. https://doi.org/10.3389/fpls.2018.00983
11. Demasi, S., Falla, N.M., Caser, M., Scariot, V. (2020). Postharvest aptitude of *Begonia semperflorens* and *Viola cornuta* edible flowers. *Advances in Horticultural Science*, *34*(1S), 13–20. https://doi.org/10.13128/ahsc-7444
12. Demasi, S., Mellano, M.G., Falla, N.M., Caser, M., Scariot, V. (2021b). Sensory profile, shelf life, and dynamics of bioactive compounds during cold storage of 17 edible flowers. *Horticulturae*, *7*(7), art. no. 166. https://doi.org/10.3390/horticulturae7070166
13. Falla, N.M., Contu, S., Demasi, S., Caser, M., Scariot, V. (2020). Environmental impact of edible flower production: A case study. *Agronomy*, *10*(4), 1–17. https://doi.org/10.3390/agronomy10040579
14. Fernandes, L., Casal, S., Pereira, J.A., Saraiva, J.A., Ramalhosa, E. (2020). An overview on the market of edible flowers. *Food Reviews International*, *36*(3), 258–275. https://doi.org/10.1080/87559129.2019.1639727
15. Fiehn, O. (2002). Metabolomics — the link between genotypes and phenotypes. In C. Town (Eds.), *Functional Genomics,* Springer, Dordrecht, The Netherlands, pp. 155–171. https://doi.org/10.1007/978-94-010-0448-0_11
16. Fraga, C.G., Croft, K.D., Kennedy, D.O., Tomás-Barberán, F.A. (2019). The effects of polyphenols and other bioactives on human health. *Food & Function*, *10*(2), 514–528. https://doi.org/10.1039/C8FO01997E
17. Friedman, H., Agami, O., Vinokur, Y., Droby, S., Cohen, L., Refaeli, G., Resnick, N., Umiel, N. (2010). Characterization of yield, sensitivity to *Botrytis cinerea* and antioxidant content of several rose species suitable for edible flowers. *Scientia Horticulturae*, *123*(3), 395–401. https://doi.org/10.1016/j.scienta.2009.09.019
18. González-Barrio, R., Periago, M.J., Luna-Recio, C., Garcia-Alonso, F.J., Navarro-González, I. (2018). Chemical composition of the edible flowers, pansy (*Viola wittrockiana*) and snapdragon (*Antirrhinum majus*) as new sources of bioactive compounds. *Food Chemistry*, *252*, 373–380. https://doi.org/10.1016/j.foodchem.2018.01.102
19. Grassi, D., Necozione, S., Lippi, C., Croce, G., Valeri, L., Pasqualetti, P., Desideri, G., Blumberg, J.B., Ferri, C. (2005). Cocoa reduces blood pressure and insulin resistance and improves endothelium-dependent vasodilation in hypertensives. *Hypertension*, *46*(2), 398–405. https://doi.org/10.1161/01.HYP.0000174990.46027.70

20. Grzeszczuk, M., Stefaniak, A., Pachlowska, A. (2016). Biological value of various edible flower species. *Acta Scientiarum Polonorum Hortorum Cultus*, *15*(2), 109–119.
21. Guimarães, R., Barros, L., Carvalho, A.M., Ferreira, I.C.F.R. (2010). Studies on chemical constituents and bioactivity of *Rosa micrantha*: An alternative antioxidants source for food, pharmaceutical, or cosmetic applications. *Journal of Agricultural and Food Chemistry*, *58*(10), 6277–6284. https://doi.org/10.1021/jf101394w
22. Guo, X., Tresserra-Rimbau, A., Estruch, R., Martínez-González, M.A., Medina-Remón, A., Castañer, O., Corella, D., Salas-Salvadó, J., Lamuela-Raventós, R.M. (2016). Effects of polyphenol, measured by a biomarker of total polyphenols in urine, on cardiovascular risk factors after a long-term follow-up in the PREDIMED study. *Oxidative Medicine and Cellular Longevity*, *2016*, 1–11. https://doi.org/10.1155/2016/2572606
23. Hansawasdi, C., Kawabata, J., Kasai, T. (2001). Hibiscus acid as an inhibitor of starch digestion in the Caco-2 cell model system. *Bioscience, Biotechnology and Biochemistry*, *65*(9), 2087–2089. https://doi.org/10.1271/bbb.65.2087
24. Hou, D.X., Tong, X., Terahara, N., Luo, D., Fujii, M. (2005). Delphinidin 3-sambubioside, a *Hibiscus* anthocyanin, induces apoptosis in human leukemia cells through reactive oxygen species-mediated mitochondrial pathway. *Archives of Biochemistry and Biophysics*, *440*(1), 101–109. https://doi.org/10.1016/j.abb.2005.06.002
25. Julious, S.A. (2005). Sample size of 12 per group rule of thumb for a pilot study. *Pharmaceutical Statistics*, *4*(4), 287–291. https://doi.org/10.1002/pst.185
26. Kim, J.K., So, H., Youn, M.J., Kim, H.J., Kim, Y., Park, C., Kim, S.J., Ha, Y.A., Chai, K.Y., Kim, S.M., Kim, K.Y., Park, R. (2007). *Hibiscus sabdariffa* L. water extract inhibits the adipocyte differentiation through the PI3-K and MAPK pathway. *Journal of Ethnopharmacology*, *114*(2), 260–267. https://doi.org/10.1016/j.jep.2007.08.028
27. Kong, C.S., Lee, J.I., Kim, J.A., Seo, Y. (2011). *In vitro* evaluation on the antiobesity effect of lignans from the flower buds of *Magnolia denudata*. *Journal of Agricultural and Food Chemistry*, *59*(10), 5665–5670. https://doi.org/10.1021/jf200230s
28. Kumar, N., Bhandari, P., Singh, B., Bari, S.S. (2009). Antioxidant activity and ultra-performance LC-electrospray ionization-quadrupole time-of-flight mass spectrometry for phenolics-based fingerprinting of rose species: *Rosa damascena*, *Rosa bourboniana* and *Rosa brunonii*. *Food and Chemical Toxicology*, *47*(2), 361–367. https://doi.org/10.1016/j.fct.2008.11.036
29. Kuntz, S., Rudloff, S., Asseburg, H., Borsch, C., Fröhling, B., Unger, F., Dold, S., Spengler, B., Römpp, A., Kunz, C. (2015). Uptake and bioavailability of anthocyanins and phenolic acids from grape/blueberry juice and smoothie *in vitro* and *in vivo*. *British Journal of Nutrition*, *113*(7), 1044–1055. https://doi.org/10.1017/S0007114515000161
30. Lattanzio, F., Greco, E., Carretta, D., Cervellati, R., Govoni, P., Speroni, E. (2011). *In vivo* anti-inflammatory effect of *Rosa canina* L. extract. *Journal of Ethnopharmacology*, *137*(1), 880–885. https://doi.org/10.1016/j.jep.2011.07.006
31. Lee, E.J., Kim, J.S., Kim, H.P., Lee, J.H., Kang, S.S. (2010). Phenolic constituents from the flower buds of *Lonicera japonica* and their 5-lipoxygenase inhibitory activities. *Food Chemistry*, *120*(1), 134–139. https://doi.org/10.1016/j.foodchem.2009.09.088
32. Li, A.N., Li, S., Li, H.B., Xu, D.P., Xu, X.R., Chen, F. (2014). Total phenolic contents and antioxidant capacities of 51 edible and wild flowers. *Journal of Functional Foods*, *6*(1), 319–330. https://doi.org/10.1016/j.jff.2013.10.022
33. Lim, T.K. (2014a). *Edible Medicinal And Non-Medicinal Plants. Volume 7, Flowers*. Springer, Dordrecht, The Netherlands. https://doi.org/10.1007/978-94-007-7395-0
34. Lim, T. K. (2014b). *Edible Medicinal and Non-Medicinal Plants. Volume 8, Flowers*. Springer, Dordrecht, The Netherlands. https://doi.org/10.1007/978-94-017-8748-2
35. Lin, H.H., Huang, H.P., Huang, C.C., Chen, J.H., Wang, C.J. (2005). *Hibiscus* polyphenol-rich extract induces apoptosis in human gastric carcinoma cells *via* p53 phosphorylation and p38 MAPK/FasL cascade pathway. *Molecular Carcinogenesis*, *43*(2), 86–99. https://doi.org/10.1002/mc.20103
36. Liu, J., He, Z., Ma, N., Chen, Z.Y. (2020a). Beneficial effects of dietary polyphenols on high-fat diet-induced obesity linking with modulation of gut microbiota. *Journal of Agricultural and Food Chemistry*, *68*(1), 33–47. https://doi.org/10.1021/acs.jafc.9b06817
37. Liu, R.H. (2003). Health benefits of fruit and vegetables are from additive and synergistic combinaions of phytochemicals. *The American Journal of Clinical Nutrition*, *78*(3), 517S-520S. https://doi.org/10.1093/ajcn/78.3.517S
38. Lo, C.W., Huang, H.P., Lin, H.M., Chien, C.T., Wang, C.J. (2007). Effect of *Hibiscus* anthocyanins-rich extract induces apoptosis of proliferating smooth muscle cell *via* activation of P38 MAPK and p53 pathway. *Molecular Nutrition & Food Research*, *51*(12), 1452–1460. https://doi.org/10.1002/mnfr.200700151
39. Loizzo, M.R., Pugliese, A., Bonesi, M., Tenuta, M.C., Menichini, F., Xiao, J., Tundis, R. (2016). Edible flowers: a rich source of phytochemicals with antioxidant and hypoglycemic properties. *Journal of Agricultural and Food Chemistry*, *64*(12), 2467–2474. https://doi.org/10.1021/acs.jafc.5b03092
40. Lu, B., Li, M., Yin, R. (2016). Phytochemical content, health benefits, and toxicology of common edible flowers: a review (2000–2015). *Critical Reviews in Food Science and Nutrition*, *56*, S130–S148. https://doi.org/10.1080/10408398.2015.1078276
41. Manach, C., Mazur, A., Scalbert, A. (2005). Polyphenols and prevention of cardiovascular diseases. *Current Opinion in Lipidology*, *16*(1), 77–84. https://doi.org/10.1097/00041433-200502000-00013
42. Martínez, M.C., Santiago, J.L., Boso, S., Gago, P., Álvarez-Acero, I., De Vega, M.E., Martínez-Bartolomé, M., Álvarez-Nogal, R., Molíst, P., Caser, M., Scariot, V., Gómez-García, D. (2020). Narcea – an unknown, ancient cultivated rose variety from northern Spain. *Horticulture Research*, *7*(1), art. no. 44. https://doi.org/10.1038/s41438-020-0266-8
43. Medina-Remón, A., Barrionuevo-González, A., Zamora-Ros, R., Andres-Lacueva, C., Estruch, R., Martínez-González, M.-Á., Diez-Espino, J., Lamuela-Raventos, R.M. (2009). Rapid Fo-

lin–Ciocalteu method using microtiter 96-well plate cartridges for solid phase extraction to assess urinary total phenolic compounds, as a biomarker of total polyphenols intake. *Analytica Chimica Acta*, *634*(1), 54–60. https://doi.org/10.1016/j.aca.2008.12.012

44. Medina-Remón, A., Casas, R., Tressserra-Rimbau, A., Ros, E., Martínez-González, M. A., Fitó, M., Corella, D., Salas-Salvadó, J., Lamuela-Raventos, R.M., Estruch, R. (2017). Polyphenol intake from a Mediterranean diet decreases inflammatory biomarkers related to atherosclerosis: a substudy of the PREDIMED trial. *British Journal of Clinical Pharmacology*, *83*(1), 114–128. https://doi.org/10.1111/bcp.12986
45. Mennen, L.I., Sapinho, D., Ito, H., Bertrais, S., Galan, P., Hercberg, S., Scalbert, A. (2006). Urinary flavonoids and phenolic acids as biomarkers of intake for polyphenol-rich foods. *British Journal of Nutrition*, *96*(1), art. no. 191. https://doi.org/10.1079/BJN20061808
46. Mohsen, E., Younis, I.Y., Farag, M.A. (2020). Metabolites profiling of Egyptian *Rosa damascena* Mill. flowers as analyzed *via* ultra-high-performance liquid chromatography-mass spectrometry and solid-phase microextraction gas chromatography-mass spectrometry in relation to its anti-collagenase skin effect. *Industrial Crops and Products*, *155*, art. no. 112818. https://doi.org/10.1016/j.indcrop.2020.112818
47. Najar, B., Demasi, S., Caser, M., Gaino, W., Cioni, P.L., Pistelli, L., Scariot, V. (2019). Cultivation substrate composition influences morphology, volatilome and essential oil of *Lavandula angustifolia* Mill. *Agronomy*, *9*(8), art. no. 411. https://doi.org/10.3390/agronomy9080411
48. Navarro-González, I., González-Barrio, R., García-Valverde, V., Bautista-Ortín, A.B., Periago, M.J. (2015). Nutritional composition and antioxidant capacity in edible flowers: Characterisation of phenolic compounds by HPLC-DAD-ESI/MSn. *International Journal of Molecular Sciences*, *16*(1), 805–822. https://doi.org/10.3390/ijms16010805
49. Neveu, V., Perez-Jiménez, J., Vos, F., Crespy, V., du Chaffaut, L., Mennen, L., Knox, C., Eisner, R., Cruz, J., Wishart, D., Scalbert, A. (2010). Phenol-Explorer: an online comprehensive database on polyphenol contents in foods. *Database*, *2010*, bap024–bap024. https://doi.org/10.1093/database/bap024
50. Nielsen, S.E., Freese, R., Kleemola, P., Mutanen, M. (2002). Flavonoids in human urine as biomarkers for intake of fruits and vegetables. *Cancer Epidemiology Biomarkers and Prevention*, *11*(5), 459–466. Available at: [https://www.ncbi.nlm.nih.gov/pubmed/12010860]
51. Oboh, G., Ademosun, A.O., Ayeni, P.O., Omojokun, O.S., Bello, F. (2015). Comparative effect of quercetin and rutin on α-amylase, α-glucosidase, and some pro-oxidant-induced lipid peroxidation in rat pancreas. *Comparative Clinical Pathology*, *24*(5), 1103–1110. https://doi.org/10.1007/s00580-014-2040-5
52. Ozdal, T., Sela, D.A., Xiao, J., Boyacioglu, D., Chen, F., Capanoglu, E. (2016). The reciprocal interactions between polyphenols and gut microbiota and effects on bioaccessibility. *Nutrients*, *8*(2), art. no. 78. https://doi.org/10.3390/nu8020078
53. Pal, P.K., Singh, R.D. (2013). Understanding crop-ecology and agronomy of *Rosa damascena* Mill. for higher productivity. *Australian Journal of Crop Science*, *7*(2), 196–205.
54. Pérez-Jiménez, J., Hubert, J., Hooper, L., Cassidy, A., Manach, C., Williamson, G., Scalbert, A. (2010a). Urinary metabolites as biomarkers of polyphenol intake in humans: a systematic review. *The American Journal of Clinical Nutrition*, *92*(4), 801–809. https://doi.org/10.3945/ajcn.2010.29924
55. Pérez-Jiménez, J., Neveu, V., Vos, F., Scalbert, A. (2010b). Identification of the 100 richest dietary sources of polyphenols: an application of the Phenol-Explorer database. *European Journal of Clinical Nutrition*, *64*(S3), S112–S120. https://doi.org/10.1038/ejcn.2010.221
56. Piccolella, S., Crescente, G., Pacifico, F., Pacifico, S. (2018). Wild aromatic plants bioactivity: a function of their (poly)phenol seasonality? A case study from Mediterranean area. *Phytochemistry Reviews*, *17*(4), 785–799. https://doi.org/10.1007/s11101-018-9558-0
57. Pires, T.C.S.P., Barros, L., Santos-Buelga, C., Ferreira, I.C.F.R. (2019). Edible flowers: Emerging components in the diet. *Trends in Food Science & Technology*, *93*, 244–258. https://doi.org/10.1016/j.tifs.2019.09.020
58. Preuss, H.G., Echard, B., Bagchi, D., Stohs, S. (2007). Inhibition by natural dietary substances of gastrointestinal absorption of starch and sucrose in rats and pigs: 1. Acute studies. *International Journal of Medical Sciences*, *4*(4), 196–202. https://doi.org/10.7150/ijms.4.196
59. Rop, O., Mlcek, J., Jurikova, T., Neugebauerova, J., Vabkova, J. (2012). Edible flowers – A new promising source of mineral elements in human nutrition. *Molecules*, *17*(6), 6672–6683. https://doi.org/10.3390/molecules17066672
60. Rothwell, J.A., Perez-Jimenez, J., Neveu, V., Medina-Remon, A., M'Hiri, N., Garcia-Lobato, P., Manach, C., Knox, C., Eisner, R., Wishart, D.S., Scalbert, A. (2013). Phenol-Explorer 3.0: a major update of the Phenol-Explorer database to incorporate data on the effects of food processing on polyphenol content. *Database*, *2013*, art. no. bat070. https://doi.org/10.1093/database/bat070
61. Roura, E., Andrés-Lacueva, C., Estruch, R., Lamuela-Raventós, R.M. (2006). Total polyphenol intake estimated by a modified folin-ciocalteu assay of urine. *Clinical Chemistry*, *52*(4), 749–752. https://doi.org/10.1373/clinchem.2005.063628
62. Santos-Buelga, C., Gonzalez-Manzano, S., Dueñas, M., Gonzalez-Paramas, A.M. (2012). Extraction and isolation of phenolic compounds. *Methods in Molecular Biology*, *864*, 427–464. https://doi.org/10.1007/978-1-61779-624-1_17
63. Scariot, V., Gaino, W., Demasi, S., Caser, M., Ruffoni, B. (2018). Flowers for edible gardens: combinations of species and colours for northwestern Italy. *Acta Horticulturae*, *1215*, 363–368. https://doi.org/10.17660/ActaHortic.2018.1215.67
64. Shader, R.I. (2015). Proof of feasibility: what a pilot study is and is not. *Clinical Therapeutics*, *37*(7), 1379–1380. https://doi.org/10.1016/j.clinthera.2015.06.011
65. Slinkard, K., Singleton, V.L. (1977). Total phenol analysis: automation and comparison with manual methods. *American Journal of Enology and Viticulture*, *28*(1), 49–55
66. Smulders, M.J.M., Arens, P., Bourke, P.M., Debener, T., Linde, M., De Riek, J., Leus, L., Ruttink, T., Baudino, S., Hibrant Saint-Oyant, L., Clotault, J., Foucher, F. (2019). In the name of the rose: a roadmap for rose research in the genome era. *Horticulture Research*, *6*(1), art. no. 65. https://doi.org/10.1038/s41438-019-0156-0

67. Spencer, J.P.E., Abd El Mohsen, M.M., Minihane, A.M., Mathers, J.C. (2008). Biomarkers of the intake of dietary polyphenols: strengths, limitations and application in nutrition research. *British Journal of Nutrition*, *99*(1), 12–22. https://doi.org/10.1017/S0007114507798938
68. Takahashi, J.A., Rezende, F.A.G.G., Moura, M.A.F., Dominguete, L.C.B., Sande, D. (2020). Edible flowers: Bioactive profile and its potential to be used in food development. *Food Research International*, *129*, art. no. 108868. https://doi.org/10.1016/j.foodres.2019.108868
69. Teng, H., Chen, L. (2019). Polyphenols and bioavailability: an update. *Critical Reviews in Food Science and Nutrition*, *59*(13), 2040–2051. https://doi.org/10.1080/10408398.2018.1437023
70. Tomas-Barberan, F., García-Villalba, R., Quartieri, A., Raimondi, S., Amaretti, A., Leonardi, A., Rossi, M. (2014). *In vitro* transformation of chlorogenic acid by human gut microbiota. *Molecular Nutrition & Food Research*, *58*(5), 1122–1131. https://doi.org/10.1002/mnfr.201300441
71. Tresserra-Rimbau, A., Rimm, E.B., Medina-Remón, A., Martínez-González, M.A., de la Torre, R., Corella, D., Salas-Salvadó, J., Gómez-Gracia, E., Lapetra, J., Arós, F., Fiol, M., Ros, E., Serra-Majem, L., Pintó, X., Saez, G.T., Basora, J., Sorlí, J.V., Martínez, J.A., Vinyoles, E., Ruiz-Gutiérrez, V., Estruch, R., Lamuela-Raventós, R.M. (2014a). Inverse association between habitual polyphenol intake and incidence of cardiovascular events in the PREDIMED study. *Nutrition, Metabolism and Cardiovascular Diseases*, *24*(6), 639–647. https://doi.org/10.1016/j.numecd.2013.12.014
72. Tresserra-Rimbau, A., Rimm, E.B., Medina-Remón, A., Martínez-González, M.A., López-Sabater, M.C., Covas, M.I., Corella, D., Salas-Salvadó, J., Gómez-Gracia, E., Lapetra, J., Arós, F., Fiol, M., Ros, E., Serra-Majem, L., Pintó, X., Muñoz, M.A., Gea, A., Ruiz-Gutiérrez, V., Estruch, R., Lamuela-Raventós, R.M. (2014b). Polyphenol intake and mortality risk: a re-analysis of the PREDIMED trial. *BMC Medicine*, *12*(1), art. no. 77. https://doi.org/10.1186/1741-7015-12-77
73. Velusami, C.C., Agarwal, A., Mookambeswaran, V. (2013). Effect of *Nelumbo nucifera* petal extracts on lipase, adipogenesis, adipolysis, and central receptors of obesity. *Evidence-Based Complementary and Alternative Medicine*, *2013*, art. no. 145925. https://doi.org/10.1155/2013/145925
74. Wedick, N.M., Pan, A., Cassidy, A., Rimm, E.B., Sampson, L., Rosner, B., Willett, W., Hu, F.B., Sun, Q., van Dam, R.M. (2012). Dietary flavonoid intakes and risk of type 2 diabetes in US men and women. *The American Journal of Clinical Nutrition*, *95*(4), 925–933. https://doi.org/10.3945/ajcn.111.028894
75. Zamora-Ros, R., Rabassa, M., Cherubini, A., Urpí-Sardà, M., Bandinelli, S., Ferrucci, L., Andres-Lacueva, C. (2013). High concentrations of a urinary biomarker of polyphenol intake are associated with decreased mortality in older adults. *The Journal of Nutrition*, *143*(9), 1445–1450. https://doi.org/10.3945/jn.113.177121
76. Zamora-Ros, R., Rabassa, M., Cherubini, A., Urpi-Sarda, M., Llorach, R., Bandinelli, S., Ferrucci, L., Andres-Lacueva, C. (2011). Comparison of 24-h volume and creatinine-corrected total urinary polyphenol as a biomarker of total dietary polyphenols in the Invecchiare InCHIANTI study. *Analytica Chimica Acta*, *704*(1–2), 110–115. https://doi.org/10.1016/j.aca.2011.07.035
77. Zhang, J., Rui, X., Wang, L., Guan, Y., Sun, X., Dong, M. (2014). Polyphenolic extract from *Rosa rugosa* tea inhibits bacterial quorum sensing and biofilm formation. *Food Control*, *42*, 125–131. https://doi.org/10.1016/j.foodcont.2014.02.001
78. Zheng, J., Yu, X., Maninder, M., Xu, B. (2018). Total phenolics and antioxidants profiles of commonly consumed edible flowers in China. *International Journal of Food Properties*, *21*(1), 1524–1540. https://doi.org/10.1080/10942912.2018.1494195

Pol. J. Food Nutr. Sci., 2021, Vol. 71, No. 4, pp. 393–401
On-line ISSN: 2083-6007
Print ISSN: 1230-0322
DOI: 10.31883/pjfns/142835
http://journal.pan.olsztyn.pl

Original article
Section: Nutrition Research

Tumor Anti-Initiation and Anti-Progression Properties of Sulphated-Extract of *Colocasia esculenta*

Amira M. Gamal-Eldeen[1], Hassan Amer[2], Cinderella A. Fahmy[3,4], Haytham Dahlawi[1], Basem H. Elesawy[1], Nahla L. Faizo[5], Bassem M. Raafat[5]*

[1]*Clinical Laboratory Sciences Department, College of Applied Medical Sciences, Taif University, P.O. Box 11099, Taif 21944, Saudi Arabia*
[2]*Department of Natural and Microbial Products Chemistry, National Research Centre, Dokki, Cairo 12622, Egypt*
[3]*Cancer Biology and Genetics Laboratory, Centre of Excellence for Advanced Sciences, National Research Centre, 33 El Buhouth St. Dokki, Cairo, 12622, Egypt*
[4]*Biochemistry Department, National Research Centre, 33 El Buhouth St. Dokki, Cairo, 12622, Egypt*
[5]*Radiological Sciences Department, College of Applied Medical Sciences, Taif University, P.O. Box 11099, Taif 21944, Saudi Arabia*

Key words: *Colocasia esculenta*, CYP1A, cancer chemoprevention & tumor anti-initiating, HDAC, macrophage function, breast MCF-7 carcinoma

Colocasia esculenta (Taro) is an edible tuberous plant; however, corms are its most worldwide consumed part while the corm powder is widely used in food industries. In this work, a sulphated polysaccharide extract of *C. esculenta* corm (SCE) was prepared and its cancer chemopreventive properties were explored. The amending of carcinogen metabolism and radical scavenging affinity revealed that SCE is a strong tumor anti-initiation agent *via* suppressing cytochrome P450–1A and enhancing glutathione and the carcinogen detoxification enzyme; glutathione *S*-transferase. SCE exhibited a strong scavenging affinity towards critical radicals (hydroxyl and peroxyl). It induced lymphocyte growth and modulated the macrophage functions into an anti-inflammatory profile, *via* elevating macrophage proliferation and its binding affinity of fluorescein isothiocyanate-lipopolysaccharide (FITC-LPS) and inhibiting nitric oxide and tumor necrosis factor-α generation. Furthermore, SCE showed a potent cytotoxicity against human breast MCF-7 carcinoma cells (IC_{50} 27.73 μg/mL), whereas SCE treatment inhibited the activity of histone deacetylase (HDAC IC_{50} 37.70 μg/mL) and disturbed the pattern of cell cycle phases. An arrest in both S- and G2/M-phases was linked with shifted cell populations towards late apoptosis and necrosis, as detected by flow cytometry. SCE is a promising cancer chemopreventive agent to be used in healthy food industries and for the high breast cancer-risk population.

INTRODUCTION

Colocasia esculenta (Liliatae, Araceae), traditionally called taro, is a tuberous plant classified as monocotyledonous and distributed in humid subtropics and tropics. All of the plant parts are edible; however, corms are its most worldwide consumed part [Lim, 2015]. The corms afford various nutrients, including proteins, carbohydrates, vitamins (niacin, riboflavin, and thiamine), minerals (iron, potassium, sodium, calcium, and phosphorus) and fibers [Temesgen & Retta, 2015]. Additionally, many bioactive compounds were extracted from *C. esculenta; e.g.*, phenolic compounds (including anthocyanins and tannins), sterols, organic acids, bioactive proteins, phytocystatin, alkaloids, terpenes, and saponins [Ferreres *et al*., 2012; Lim, 2015; Reyad-ul-Ferdous *et al*., 2015]. Preclinical studies reported that *C. esculenta* corm extracts exerted antitumoral and antimetastatic [Kundu *et al*., 2012; Park *et al*., 2013], antihyperlipidemic [Sakano *et al*., 2005], antioxidant [Lee *et al*., 2011], wound healing [Gonçalves *et al*., 2013], antidiabetic [Eleazu *et al*., 2013], and antiviral [Keyaerts *et al*., 2007] properties.

The widespread traditional usages of *C. esculenta* are for many health disorders including: gastrointestinal diseases, diabetes mellitus, alopecia, internal hemorrhages, anemia, body ache, snakebite, and additionally for immune system stimulation [Lim, 2015, Nwauzoma & Dappa, 2013]. *C. esculenta* corm powder is marketed as an ingredient and as a food supplement, worldwide. The flour constituents of *C. esculenta* are comparable to corn, potato, and soybean ones; it has a high fiber a low fat content, which makes the flour a satisfactory substitute for market flours as an economic alternative in developing countries [reviewed in Pereira *et al*., 2018]. *C. esculenta* flour may be utilized in numerous preparations, such as bread, noodle, cookies, paste, and infant formulations,

* Corresponding Author:
E-mail: amabdulaziz@tu.edu.sa, aeldeen7@yahoo.com. (A.M. Gamal-Eldeen)

Submitted: 25 May 2021
Accepted: 1 October 2021
Published on-line: 26 October 2021

© Copyright by Institute of Animal Reproduction and Food Research of the Polish Academy of Sciences
© 2021 Author(s). This is an open access article licensed under the Creative Commons Attribution-NonCommercial-NoDerivs License (http://creativecommons.org/licenses/by-nc-nd/4.0/).

especially for dietary restriction cases (*e.g*., gluten intolerance and allergenic disorders) [Kaushal *et al*., 2015; Noorfarahzilah *et al*., 2014].

The defensive mechanisms that provide prevention of the carcinogenesis cascade are defined as chemoprevention perception. Chemopreventive agents are capable to prevent, reverse or postpone carcinogenesis cascade. Daily consumption of these agents represents a hopeful approach to suppress or prevent carcinogenesis [Mollakhalili *et al*., 2017]. A variety of phytochemicals originated from dietary plants are proved to hinder specific carcinogenesis stages through the inhibition of tumor initiation, promotion, and progression, which among others, encompassed the modulation of the cancer cell cycle, proliferation inhibition, and initiation of apoptosis [Mollakhalili *et al*., 2017].

In our previous studies, we reported that the sulphated forms of natural polysaccharides showed promising tumor cancer chemopreventive potentials [Gamal-Eldeen *et al.*, 2006; 2007a,b 2009; 2021]. In continuation, the current study was planned to explore the cancer chemopreventive mechanisms of a sulphated extract of *C. esculenta* corms, targeting to function as a cancer chemopreventive alternative in the healthy food industries for high-risk populations.

MATERIAL AND METHODS

Preparation of the sulphated *C. esculenta* extract

C. esculenta tubers (2 kg) were purchased from the local market (Dokki, Giza). Corms were washed and cleaned from the foreign substances, peeled, and chopped into smaller pieces (~1 cm^3). Afterward, the pieces were macerated with distilled water in a kitchen blender, and then extracted for 1 h with hot water under reflux. A filtration was carried out to discard insoluble material, and the filtrate was dialyzed for 48 h against running distilled water, prior overnight incubation with cold ethanol (1:4; *v/v*). The precipitate was gathered by centrifugation before vacuum drying (crude polysaccharides). Sulphated *C. esculenta* extract (SCE) was prepared rendering to published methods [Mähner *et al*., 2001; Yang *et al*., 2003]. In brief, the sulphating agent was developed by dropping 20 mL of fuming sulphuric acid into 100 mL of formamide, in a cooling chamber. The crude polysaccharides (4 g) were mixed with formamide and then mixed with the sulphation solution (120 mL) under overnight stirring. After cooling, consecutive steps were carried out including neutralization by 1 N NaOH, dialysis against distilled water for 48 h, and finally lyophilization. All of the chemicals were purchased from Sigma-Aldrich (Saint Louis, MO, USA), unless otherwise mentioned.

Characterization of the sulphated *C. esculenta* extract

The total carbohydrate content of SCE was estimated by the phenol–H_2SO_4 protocol [DuBois *et al*., 1956]. The total protein was determined with the Lowry method [Lowry *et al*., 1951]. The sugar composition was estimated after a complete hydrolysis of polysaccharides with H_2SO_4 (2 M) at 100°C for 8 h. The hydrolysate was neutralized by $BaCO_3$ and then Dowex 50 resin (H^+ form) was used. The chromatography for 24 h on Whatmann no. 1 paper with butanol: acetone: water (4:5:1, *v/v/v*) as a mobile phase was applied to separate the individual sugars [Partridge *et al.*, 1949]. The spots were sprayed with aniline phthalate for visualization. The total sulphate content was determined after hydrolysis with HCl [Larsen *et al.*, 1966] and the liberated sulphate ions were estimated by $BaCl_2$ turbidimetric method [Hunt, 1980].

Cell culture

Various cell lines were utilized through the study, including human breast carcinoma (MCF-7), human hepatocellular carcinoma (Hep G2), human lymphoblastic leukemia (1301) and raw murine macrophages (RAW 264.7); purchased from the American Type Culture Collections (ATCC, Manassas, VA, USA). RAW 264.7 cells were cultured in Roswell Park Memorial Institute Medium-1640 (RPMI-1640), while the other cell lines were routinely cultured in Dulbecco's Modified Eagle Medium (DMEM). Media were supplemented with 10% fetal bovine serum (FBS), 2 mM L-glutamine, 100 U/mL streptomycin sulfate, 100 U/mL penicillin G sodium, and 250 ng/mL amphotericin B. Cells were maintained in humidified air containing 5% CO_2 at 37°C. Extracts were dissolved in the cell matching medium. The extract stocks were examined, before assay dilutions, for endotoxins by the Pyrogent® Ultra gel clot assay to confirm endotoxin-free status. Materials for cell culture were purchased from Lonza (Morristown, NJ, USA). All of the cellular experiments were repeated (n=8), except flow cytometry analysis (n=4).

Tumor anti-initiation activity

The total cellular capacity for scavenging the physiologically dangerous radicals; peroxyl ($ROO^{\bullet}$) and hydroxyl ($OH^{\bullet}$); was investigated by the oxygen radical absorbance capacity (ORAC) assay, which is an indication of the total antioxidant activity of the cells [Cao & Prior, 1999; Gamal-Eldeen *et al*., 2004]. Hep-G2 cells were treated with 10 μg/mL of SCE for 24 h. The protein content of the cell lysate was measured and only 1 μg protein/mL was subjected to ORAC assay. β-Naphthoflavone-treated Hep-G2 cells were used as cytochrome P450 1A1 (CYP1A1) source, which was further treated with SCE (1 μg/mL), and then CYP1A1 was assessed by the dealkylation rate of 3-cyano-7-ethoxycoumarin into 3-cyano-7-hydroxycoumarin [Crespi *et al*., 1997; Gerhäuser, *et al*., 2003]. Glutathione *S*-transferase (GST) activity was estimated in 1×10^6 Hep G2 cells after being incubated with SCE (10 and 20 μg/mL) for 48 h [Habig *et al*., 1974]. The kinetic analysis was traced at 340 nm, and then GST concentration was normalized to the protein content. The total thiol content was estimated by an enzymatic method [Griffith, 1980].

Tumor anti-promoting activity and macrophage functions

To select a safe dose, the macrophage proliferation index was calculated for RAW 264.7 cells (0.5×10^5 cells/well) after being seeded with SCE (0–40 μg/mL) for 48 h. Cell viability was assessed by MTT test. RAW 264.7 cells were cultured in phenol red-free RPMI, to estimate both of the secreted tumor necrosis factor-α (TNF-α) by ELISA kit (R&D Systems, Minneapolis, MN) and the generated nitric oxide (NO), as assayed by Griess reagent in Moorcroft *et al*. [2001]. Macrophages were treated with bacterial lipopolysaccharide

(LPS, 1 μg/mL) for 24 h and with/without SCE (10 μg/mL and 20 μg/mL). Additionally, the SCE influence on the binding affinity of FITC-conjugated LPS to macrophages was evaluated [Carracedo *et al*., 2002]. Cells were seeded with SCE (10 and 20 μg/mL) in phenol red-free RPMI with 10% FBS (source of CD14 and LPS-binding protein), then incubated for 1 h, and the FITC-LPS binding affinity was detected *via* microplate fluorometer (FluoStarOptima, BMG, USA).

Tumor anti-progression effect

Cytotoxicity of SCE against human cancer cells was evaluated by the 3-[4,5-dimethyl-2-thiazolyl)-2,5-diphenyl-2H--tetrazolium bromide (MTT) assay after 48 h after the treatment of 0.5×10^5 cells/well with SCE (0–40 μg/mL) for 48 h. Thereafter, the media were discarded and 40 μL MTT solution/well were added and incubated for 4 h. MTT crystals were solubilized by acidified isopropanol [Hansen, *et al*., 1989]. Photometric readings were recorded at 570 nm using a microplate ELISA reader. The analysis of cell cycle phases in 5×10^5 MCF-7 cells/mL after being treated with SCE (IC_{50}) for 12 h was carried out by flow cytometry after cell staining with propidium iodide (PI), using a flow cytometer (Becton Dickinson, San Jose, CA, USA). The PI/FITC-anti-Annexin V Kit (Invitrogen, Waltham, MA, USA) was used to estimate apoptosis/necrosis by flow cytometry. MCF-7 cells were treated with SCE (0–40 μg/mL) for 48 h, and then the activity of histone deacetylase (HDAC) was measured in the cell lysate by a colorimetric kit (BioVision, Milpitas, CA, USA) according to the manufacturer's instructions.

Data analysis

Data were statistically analyzed by Student's unpaired t-test and one-way ANOVA test. The differences between mean values were considered insignificant at $p>0.05$.

RESULTS AND DISCUSSION

Halting, suppressing, retarding or reversing the sequence of carcinogenesis stages is regularly called "cancer chemoprevention", which is mostly achieved *via* using natural semi--natural, or synthetic chemicals to neutralize carcinogens [Tan *et al*., 2011]. Plant extracts are known to possess wide-range mechanistic chemopreventive activity, through blocking the enzymatic carcinogen-activation process in tumor initiation stage or inhibiting the growth of the pre-neoplastic and neoplastic cells [Tan *et al*., 2011]. The current study is an attempt to recognize whether SCE acts as a blocking or a suppressing agent.

Characterization of sulphated *C. esculenta* extract

The analysis of the chemical composition of SCE revealed that after the sulphation process, the sulphate substitution in SCE was 48% with a sulphation degree of 2.3 (molar ratio to monosaccharide unit) (Table 1) that indicated the accomplishment of the sulphation reaction. Chromatography analysis of SCE acid hydrolysates revealed the occurrence of a significant amount of glucose, and smaller amounts of mannose, galactose and uronic acids, as well as traces of arabinose, xylose, and rhamnose (Table 1).

Tumor anti-initiation activity

In oxidative stress status and inflammatory condition, extreme generation of reactive oxygen (ROS) and nitrogen (RNS) species occurs and causes DNA damage that ignites tumor initiation and promotion cascade [Sun *et al*., 2004]. Accordingly, eliminating the excess of physiologically-pertinent ROS, such as $ROO^{\bullet}$ and $OH^{\bullet}$, affords an effective approach to halt tumor initiation and promotion. Likewise, the augmentation of the non-enzymatic antioxidants; total thiols, supports the attenuation of ROS harmful effect. The total cell lysate capacity for scavenging the radicals; $OH^{\bullet}$ and $ROO^{\bullet}$; was assessed by ORAC assay in HepG2 cells. The results indicated that SCE remarkably enhanced the total cellular capacity to scavenge both radicals (Figure 1a). However, the affinity to scavenge $OH^{\bullet}$ was higher than $ROO^{\bullet}$, as concluded from their ORAC units in comparison with Trolox, where one ORAC unit is equivalent to the protection of the fluorescence decay of α-phycoerythrin (α-PE) achieved by Trolox (1.0 μM).

To antagonize xenobiotics and toxic agents, cells emerged a panel of responding genetic amendments that help them to repress the damaging effect of toxicants. Those amendments include upregulation of drug-metabolizing enzymes, cytoprotective proteins, and drug transporters, that facilitate clearance of toxicants from the body and restore normal homeostasis. Nuclear factor-erythroid 2–related factor 2 (Nrf2) as well as aryl hydrocarbon receptor (AhR) are transcription factors that mediate the enzymatic response towards xenobiotics [Hayes *et al*., 2009]. Among others, transcription factor AhR regulates CYP1A1 expression, which is triggered by its conjugation with polycyclic aromatic hydrocarbons. The metabolizing of exogenous and endogenous substrates is regulated by monooxygenase, which is primarily encoded by CYP1A1 gene. CYP1A1 is a pivotal player in the metabolism of benzo[α]pirene and linked polycyclic aromatic hydrocarbons, transferring both into strongly dangerous carcinogens. Accordingly, the enhanced expression of CYP1A1

TABLE 1. Chemical composition of a sulphated water-soluble extract of *C. esculenta* (SCE).

Chemical composition	Value
Carbohydrate (g/100 g)	35.4
Protein (g/100 g)	0.8
Sulphate (g/100 g)	48.0
Degree of sulphation	2.3
Relative monosaccharide contents (g/100 g)	
Uronic acid	1.15
Galactose	4.0
Glucose	83.5
Mannose	11.0
Arabinose	Traces
Xylose	Traces
Rhamnose	Traces

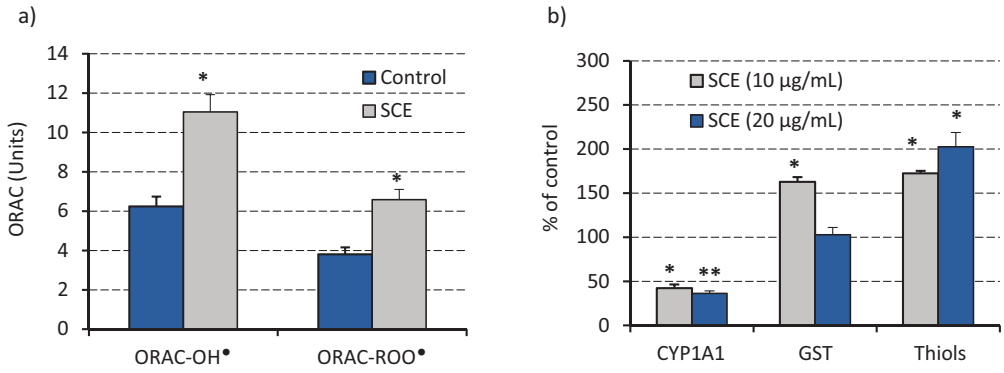

FIGURE 1. Tumor anti-initiating activity: (a) Oxygen radical absorbance capacity (ORAC) was used to investigate the radical scavenging (antioxidant) activity against OH• and ROO• in Hep-G2 cell lysate after being treated with a sulphated *C. esculenta* extract (SCE) in comparison with control cells. Data are expressed in ORAC units. (b) The modulation of the carcinogen metabolism: The effect of SCE (10 and 20 μg/mL) on the purified cytochrome P450 1A1 (CYP1A1; 1 μg protein/mL) and the cellular levels of glutathione *S*-transferase (GST) and total thiol content in Hep-G2 cells was investigated. Data was expressed as mean percentage ± standard error and control represents 100% of the scale. In control cells, GST and total thiol contents were 118 nmol/min/mg protein and 84 nmol/min/mg protein, respectively. *$p<0.05$ and **$p<0.01$.

gene is an indicator for AHR stimulation and is associated with the metabolism and toxicity of xenobiotics [Mescher & Haarmann-Stemmann, 2018]. Therefore, CYP1A1 is considered as a potential molecular target to modulate and prevent chemically-induced carcinogenesis.

Alteration of different enzymes that participate in the metabolic activation of carcinogens (phase I enzymes) and in the detoxification of carcinogens (phase II enzymes), is an effective strategy for recognizing cancer anti-tumor initiation agents. The estimation of the inhibitory effect of SCE on CYP1A1 enzyme, as one of the phase I-enzymes participating in the transformation of procarcinogens into active carcinogens, revealed that SCE (10 μg/mL and 20 μg/mL) can be recognized as a strong inhibitor of CYP1A1 activity ($p<0.01$) with inhibition of 57% and 64%, respectively (Figure 1b), in comparison to control.

In carcinogenesis, the initiation is the very early and crucial event, where it functionally promotes the clonal cell growth under the control of promoters and ends eventually with consequent preneoplastic cell generations [Bertram, 2000]. Retarding or stopping the initiation stage through suppressing the activators of carcinogen metabolism (*e.g.*, CYP1A), enhancing the carcinogen detoxification (*e.g.*, glutathione (GSH) and GSTs), and increasing cellular antioxidant activity are efficient operative strategies. A fundamental indicator of the cellular defense against the oxidative stress is the total thiol level, especially GSH, the key cytosolic thiol, that supports the elimination of peroxides and other free radicals [Aggarwal & Shishodia, 2006]. GSH homeostasis depends on its binding to GSTs, which is a panel of enzymes that regulates xenobiotic detoxification and defends the cells against carcinogens. GSTs generally amend the cellular GSH levels according to the ROS generation level [Prabhu & Guruvayoorappan, 2010]. In Hep-G2 cells, GST was explored (as one of phase II enzymes) after 48 h of cell seeding with SCE (10 μg/mL). Its activity was elevated up to 162.47% of the control ($p<0.05$), as shown in Figure 1b, while it remained unaffected by the higher SCE. The assessment of the total thiol level indicated that SCE dramatically increased the thiol content in cells in both of the tested doses (Figure 1b).

Our results revealed that SCE is an effective tumor anti-initiating agent, since it dramatically suppressed CYP1A activity. Cellular antioxidants guard the cells from the harm of dangerous physiological radicals, such as hydroxyl and peroxyl radicals, that can attack critical protein and DNA molecules. The cellular antioxidants maintain the homeostatic balance of cellular ROS [Bertram, 2000], whenever this balance is impaired, it directly disturbs cellular growth, apoptosis, and senescence. Our findings indicated that SCE strongly increased the total cellular scavenging activity, as estimated in the cell lysate of SCE-treated Hep-G2 cells, against OH• and ROO•, with higher affinity towards OH•, compared with the scavenging activity of cell lysate of untreated cells.

Tumor anti-promoting activity and modulation of macrophage function

As a key player in innate and adaptive immune responses, macrophages are regularly engulfing and then digesting pathogens *via* discharging mediators of inflammation including NO that is a potential RNS that in turn transforms into many oxidation products which are capable to trigger the carcinogenesis initiation and promotion [Prabhu & Guruvayoorappan, 2010]. The strong affinity of SCE to scavenge variable radicals including its suppressing of the LPS-induced NO may indicate that the suppression was because of a direct NO scavenging or *via* inhibiting iNOS pathway. The macrophage growth induced after SCE treatment may be associated with an elevation in the expression of the macrophage growth factor; IL-12. The outer membrane of Gram-negative bacteria enclosed LPS that is an essential molecule in septic shock pathogenesis.

LPS regularly conjugates the serum acute-phase reactant LPS-binding protein (LBP) that transports LPS to CD14 (a primary LPS receptor in serum) and as a glycophosphatidylinositol-linked agent on mononuclear phagocytes surface. LPS-CD14 activates the generation of the inflammatory cytokines [Kitchens, 2000]. Subsequently, the effective

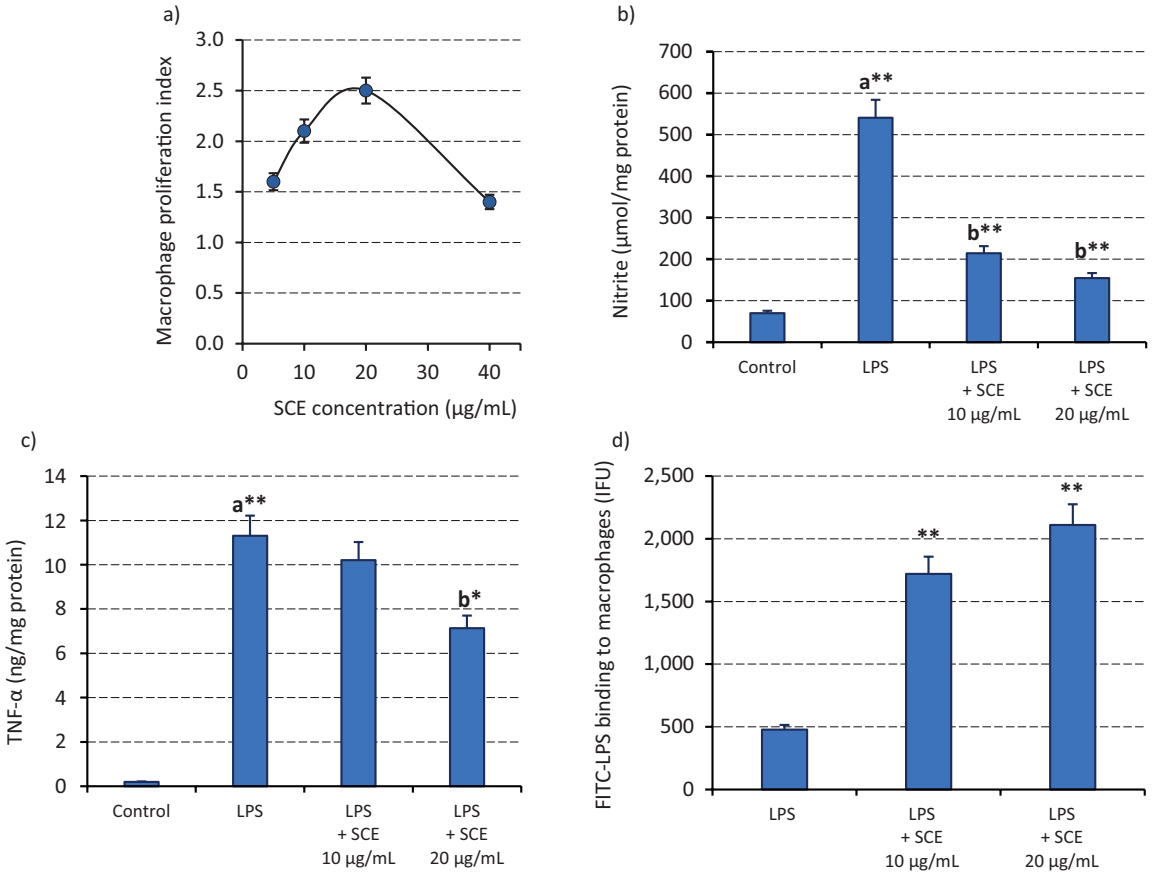

FIGURE 2. Modulation of macrophage function: (a) Macrophage proliferation index (folds of control) in sulphated *C. esculenta* extract (SCE) treated Raw 264.7 cells. (b) Nitric oxide (NO) production (µmol/mg protein). (c) Tumor necrosis factor (TNF-α) concentration (ng/mg protein) were estimated in the supernatants of Raw 264.7 after being stimulated by bacterial lipopolysaccharide (LPS) before being treated with/without 10 & 20 µg/mL SCE. (d) Analysis of fluorescein isothiocyanate-LPS (FITC-LPS) binding affinity to Raw 264.7 cells by flow cytometry. Data was expressed as mean percentage ± standard error. *$p<0.05$ and **$p<0.01$; [a]compared to control macrophages and [b]compared to LPS-treated macrophages.

enhancement of the macrophages/LPS binding affinity by SCE may ultimately result in enhanced LPS-LBP conjugation and/or LPS-CD14 conjugation. *C. esculenta* extract treatment for Her-2/neu negative murine mammary tumor cell line (410.4) showed antimetastatic activity, which suggested to be due to its inhibition of the inflammatory mediators including the suppression of prostaglandin E_2 (PGE_2) synthesis and downregulation of cyclooxygenase (COX) 1 and 2 expressions [Kundu *et al.*, 2012].

The influence of SCE on the macrophage proliferation and its functionality was explored. The results demonstrated that SCE displayed a gradual dose-dependent immunoproliferative outcome on macrophages (Figure 2a) to the highest level of 2.51-fold of control at 20 µg/mL ($p<0.05$), but not in the highest dose used. This high macrophage proliferation led to the interest of further investigations to check if this proliferation was concurrently accompanied with elevated macrophage functions. Bacterial LPS was used to induce inflammation cascade in the RAW 264.7 cells before being further treated with SCE. Interestingly, treating RAW 264.7 cells with SCE (10 µg/mL and 20 µg/mL) resulted in a significant inhibition ($p<0.01$) in the LPS-stimulated NO production, where it inhibited 60.32% and 71.43% of the LPS-generated NO, respectively (Figure 2b). While only the dose of 20 µg/mL of SCE significantly inhibited ($p<0.05$) the TNF-α release from LPS-treated macrophages (Figure 2c). The affinity of macrophages to bind a tumor surface antigen or a pathogen is their essential mechanistic activation function. That binding was traced after the seeding of macrophages with FITC-LPS with/without SCE (10 µg/mL and 20 µg/mL). The results revealed that both doses of SCE dramatically suppressed ($p<0.01$) the macrophage binding affinity to FITC--LPS (Figure 2d).

Anti-progression activity

Exploring the cytotoxicity of SCE against solid tumor cell lines showed a remarkable dose-dependent cytotoxicity in breast MCF-7 cells (IC_{50} 27.73 µg/mL) and a lower cytotoxicity extent in the case of Hep-G2 cells (IC_{50} 64.32 µg/mL), as shown in Figure 3a. However, the treatment of the hematopoietic tumor cells (1301 leukemia) with SCE resulted in a gradual increment in the lymphocyte proliferation, up to 1.5-fold at 40 µg/mL (Figure 3a).

Consequently, the effect of SCE on MCF-7 cell cycle phases was investigated, whereas the untreated MCF-7 cells exhibited an intact pattern of cell cycle stages, as 96.3% of the cell's population appeared in G0/G1 phase (Figure 3b). SCE treatment resulted in a significant arrest

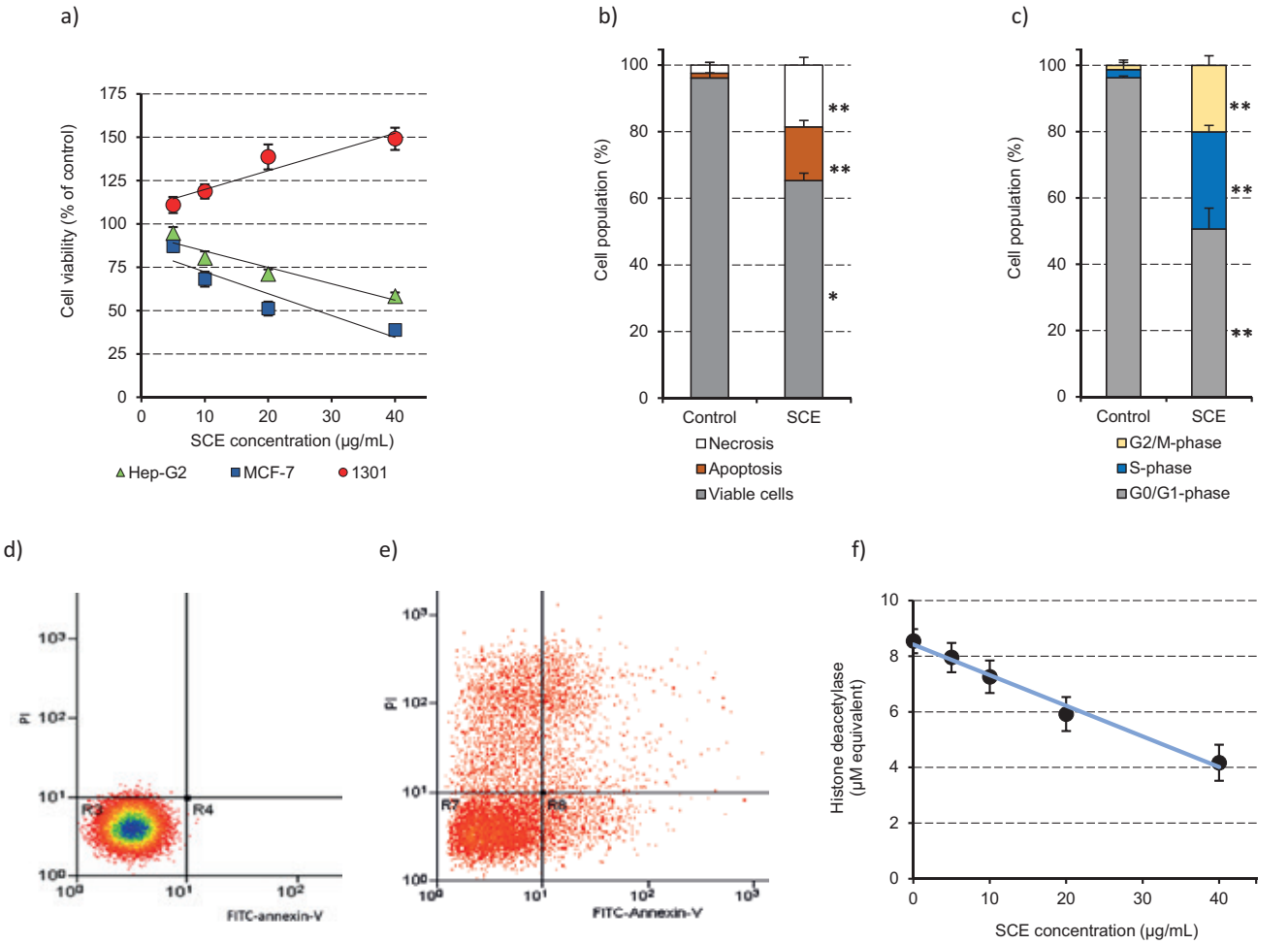

FIGURE 3. Anti-progression activity: (a) Cytotoxicity of a sulphated *C. esculenta* extract (SCE) against different human cancer cell lines. (b) Cell cycle analysis of breast MCF-7 cells after being treated with SCE (20% IC_{50}; 48 h), compared with control cells. (c-e) The analysis of apoptosis and necrosis (by anti-annexin V-FITC/PI) in MCF-7 cells that were seeded without/with 20% IC_{50} of SCE for 12 h. The data are presented as percentages of the cell population, while in (e) the flow cytometry dot plots for the cells are presented. (f) Histone deacetylase (HDAC) inhibition in SCE-treated MCF-7 cells. Data were presented as mean percentage ± standard error. $^{*}p<0.05$ and $^{**}p<0.01$.

($p<0.01$) in S-phase (29.2%), and G2/M phase (20.1%) and subsequently a concomitant significant decrease in cell population in G0/G1 phase, as shown in Figure 3b. Due to the noticed disturbance in cell cycle phases and SCE-induced cytotoxicity in MCF-7 cells, the meanwhile cell death mode stimulated by SCE was analyzed. The findings indicated that SCE encourages necrosis as much as apoptosis (Figure 3c, Figure 3e), as concluded from their total population percentages (18.5%, and 16.1%, respectively), compared to the control pattern (Figure 3c, Figure 3d).

Our results indicate the cytotoxicity of SCE against breast carcinoma MCF-7 cells and hepatocellular Hep-G2 carcinoma but not with lymphoblastic leukemia, signifying the SCE specificity to solid tumor cells. Rendering the polysaccharides high molecular weight, SCE IC_{50} of MCF-7 cells (27.73 μg/mL) provides a dramatic low molar concentration of SCE. In a parallel previous report, *C. esculenta* extract was reported to similarly reduce the proliferation of some breast as well as prostate cancer cell lines [Kundu *et al*., 2012]. Rounded cells with morphologic alterations were recorded, where cell migration was totally jammed by taro extract [Kundu *et al*., 2012]. Cell death may occur due to different death mechanisms, among them are the necrosis and apoptosis that are characterized by variable morphological and biochemical events, including cell swelling, disruption, and rapid cell membrane fragmentation in necrosis and elegant nuclear and cytoplasmic disintegration and formation of apoptotic bodies [Xu *et al*., 2019].

In the current study, SCE induced both necrosis and apoptosis in MCF-7 cells that was activated by a parallel disorder in cell cycle phases; arrested cell population in S- and G2/M phases. The rate of cell growth can interfere in the carcinogenesis stages by multiple mechanisms; among them the cell population *per se* may be carcinogenic through fixing of miscoding lesion in the freshly synthesized DNA [Lund, 2011]. Cells retort to cytotoxic stress and DNA impairment by arresting cell-cycle phases, repairing DNA or enduring apoptotic cell death. A wide array of cancer chemopreventive agents displayed their antitumor activity in association with disturbing cell cycle and arrested growth, with apoptosis [Tanaka & Ishigamori, 2011]. Subsequently, the ability of SCE to inhibit S-phase in breast cell cycle may diminish the frequency of DNA miscoding lesions. Anticancer therapeutics eliminate

cancer cells by targeted mechanisms including damaging cell membrane, interactions with DNA, suppressing DNA replication, and attacking cells by free radicals.

Since HDAC is one of the apoptosis-regulating factors, the acetylation of histone was estimated in the MCF-7 cell lysate after being treated with different concentrations of SCE. The results revealed that SCE is a potent inhibitor of HDAC, in dose--dependent linear profile, whereas the half maximal inhibitory concentration of SCE to HDAC (HDAC IC_{50}) was 37.7 μg/mL (Figure 3f). In the current study, the apoptosis was associated with a remarkable inhibition in HDAC (IC_{50} 37.7 μg/mL). It is known that the post-translational histone modification "histone acetylation" is regulated by histone acetyltransferases and HDACs. By eliminating the acetyl groups, HDACs opposite the acetylation of chromatin and amend tumor suppressor genes and oncogenes transcriptions [Li & Seto, 2016]. Interestingly, HDACs deacetylate other non-histone substrates that regulate a battery of biological pathways such as tumor initiation and progression. The therapeutic approach of HDAC inhibitors (HDACi) is an emerging cancer treatment [Li & Seto, 2016]. *Via* hyperacetylation of histone/non-histone, HDACi permit the restoration of cellular acetylation homeostasis and re-establish the normal expression of proteins and inverse the processes of tumor initiation and progression [Li &d Seto, 2016]. Accordingly, the strong inhibitory activity of SCE for HDAC is one of the mechanisms of SCE as a potential tumor anti-initiating agent.

CONCLUSION

Recently, due to their flexibility, cost-effectiveness, and desirable drug release and regulatory acceptance, many biotechnological approaches have been focused on hydrophilic polymers in pharmaceuticals. The current study findings propose SCE as a promising candidate for food industries as a functional and healthy food supplement and as an alternative of CE itself, to offer a cancer chemopreventive properties and evoke anti--inflammatory activity in targeted breast cancer-high risk communities. This study is an innovative trial to prepare a sulphated water extract of *C. esculenta*. Taken together, SCE is a strong tumor anti-initiation agent *via* suppressing cytochrome P450–1A and enhancing the total thiol content and the carcinogen detoxification enzyme (GST). SCE exhibited a strong scavenging affinity towards critical radicals ($OH^{\bullet}$ and $ROO^{\bullet}$). Also, it induced lymphocyte growth and modulated the macrophage functions into an anti-inflammatory profile, *via* elevating macrophage proliferation, its binding affinity of FITC-LPS and, to different extent, its inhibition of NO and TNF-α generation. Furthermore, it showed a potent cytotoxicity against MCF-7 cells, disturbed cell cycle phases (S- and G2/M-phases), and enhanced late apoptosis and necrosis. SCE is a promising cancer chemopreventive agent to be used in healthy food industries and for the high breast cancer-risk population, an assumption that needs to be validated in forthcoming *in vivo* studies.

ACKNOWLEDGEMENT

The authors gratefully acknowledge the support of the Deanship of Scientific Research, Taif University.

RESEARCH FUNDING

This work was supported by Taif University Researchers Supporting Project Number (TURSP- 2020/103).

CONFLICT OF INTEREST

We declare that there is no conflict of interest.

ORCID IDs

H. Amer https://orcid.org/0000-0002-9595-110
H. Dahlawi https://orcid.org/0000-0002-4406-4554
B.H. Elesawy https://orcid.org/0000-0002-2581-265X
C.A. Fahmy https://orcid.org/0000-0002-2629-2473
N.L. Faizo https://orcid.org/0000-0003-4451-7602
A.M. Gamal-Eldeen https://orcid.org/0000-0002-4423-5616
B.M. Raafat https://orcid.org/0000-0003-4612-8811

REFERENCES

1. Aggarwal, B.B., Shishodia, S. (2006). Molecular targets of dietary agents for prevention and therapy of cancer. *Biochemical Pharmacology*, *71*(10),1397–1421. https://doi.org/10.1016/j.bcp.2006.02.009
2. Bertram, J.S. (2000). The molecular biology of cancer. *Molecular Aspects of Medicine*, *21*(6), 167–223. https://doi.org/10.1016/S0098-2997(00)00007-8
3. Bose, D.S., Sudharshan, M., Chavhan, S.W. (2005). New protocol for Biginelli reaction – a practical synthesis of monastrol. *Arkivoc*, *iii*, 228–236.
4. Cao, G., Prior, R.L. (1999). Measurement of oxygen radical absorbance capacity in biological samples. *Methods in Enzymology*, *299*, 50–62. https://doi.org/10.1016/s0076-6879(99)99008-0
5. Carracedo, J., Ramirez, R., Martin-Malo, A., Rodriguez, M., Aljama, P. (2002). The effect of LPS, uraemia, and haemodialysis membrane exposure on CD14 expression in mononuclear cells and its relation to apoptosis. *Nephrology Dialysis Transplantation*, *17*(3), 428–434. https://doi.org/10.1093/ndt/17.3.428
6. Crespi, C.L., Miller, V.P., Penman, B.W. (1997). Microtiter plate assays for inhibition of human, drug-metabolizing cytochromes P450. *Analytical Biochemistry*, *248*(1), 188–190. https://doi.org/10.1006/abio.1997.2145
7. DuBois, M., Gilles, K.A., Hamilton, J.K., Rebers, P.A., Smith, F. (1956). Colourimetric method for determination of sugars and related substances. *Analytical Chemistry*, *28*(3), 350–356. https://doi.org/10.1021/ac60111a017
8. Eleazu, C.O., Iroaganachi, M., Eleazu, K.C. (2013). Ameliorative potentials of cocoyam (*Colocasia esculenta* L). and unripe plantain (*Musa paradisiaca* L). on the relative tissue weights of streptozotocin-induced diabetic rats. *Journal of Diabetes Research*, *2013*, art. no. 160964. https://doi.org/10.1155/2013/160964
9. Ferreres, F., Gonçalves, R.F., Gil-Izquierdo, A., Valentão, P., Silva, A.M.S., Silva, J.B. (2012). Further knowledge on the phenolic profile of *Colocasia esculenta* (L). Schott. *Journal of Agricultural and Food Chemistry*, *60*(28), 7005–7015. https://doi.org/10.1021/jf301739q

10. Gamal-Eldeen, A.M., Amer, H., Alrehaili, A.A., Saleh, A., Al Ghamdi, A, Hawsawi, N.M., Salman, A., Raafat, B. (2021). Cancer chemopreventive properties of sulfated *Enterolobium cyclocarpum* extract. *Nutrition and Cancer*, *73*, 856–868. https://doi.org/10.1080/01635581.2020.1773512
11. Gamal-Eldeen, A.M., Ahmed, E.F., Abo-Zeid, M.A. (2009). *In vitro* cancer chemopreventive properties of polysaccharide extract from the brown alga, *Sargassum latifolium*. *Food and Chemical Toxicology*, *47*(6), 1378–1384. https://doi.org/10.1016/j.fct.2009.03.016
12. Gamal-Eldeen, A.M., Amer, H., Helmy, W.A. (2006). Cancer chemopreventive and anti-inflammatory activities of chemically modified guar gum. *Chemico-Biological Interactions*, *161*(3), 229–240. https://doi.org/10.1016/j.cbi.2006.03.010
13. Gamal-Eldeen, A.M., Amer, H., Helmy, W.A., Ragab, H.M., Talaat, R.M. (2007a). Antiproliferative and cancer-chemopreventive properties of sulfated glycosylated extract derived from *Leucaena leucocephala*. *Indian Journal of Pharmaceutical Sciences*, *69*(6), 805–811. https://doi.org/10.4103/0250-474X.39438
14. Gamal-Eldeen, A.M., Amer, H., Helmy, W.A., Talaat, R.M., Ragab, H. (2007b). Chemically-modified polysaccharide extract derived from *Leucaena leucocephala* alters RAW 2647 murine macrophage functions. *International Immunopharmacology*, *7*(6), 871–878. https://doi.org/10.1016/j.intimp.2007.02.002
15. Gamal-Eldeen, A.M., Kawashty, S., Ibrahim, L., Shabana, M., El-Negoumy, S. (2004). Evaluation of antioxidant, anti-inflammatory, and antinociceptive properties of aerial parts of *Vicia sativa* and its flavonoids. *Journal of Natural Remedies*, *4*, 81–96. https://doi.org/10.18311/JNR/2004/388
16. Gerhäuser, C., Klimo, K., Heiss, E., Neumann, I., Gamal-Eldeen, A., Knauft, J., Liu, G.Y., Sitthimonchai, S., Frank, N. (2003). Mechanism-based *in vitro* screening of potential cancer chemopreventive agents. *Mutation Research*, *523–524*, 163–172. https://doi.org/10.1016/s0027-5107(02)00332-9
17. Gonçalves, R.F., Silva, A.M., Silva, A.M., Valentão, P., Ferreres, F., Gil-Izquierdo, A., Silva, J.B., Santos, D., Andrade, P.B. (2013). Influence of taro (*Colocasia esculenta* L Schott). growth conditions on the phenolic composition and biological properties. *Food Chemistry*, *141*(4), 3480–3485. https://doi.org/10.1016/j.foodchem.2013.06.009
18. Griffith, O.W. (1980). Determination of glutathione and glutathione disulfide using glutathione reductase and 2-vinylpyridine. *Analytical Biochemistry, 106*(1), 207–212. https://doi.org/10.1016/0003-2697(80)90139-6
19. Habig, W.H., Pabst, M.J., Jakoby, W.B. (1974). Glutathione S-transferases: The first enzymatic step in mercapturic acid formation. *Journal of Biological Chemistry*, *249*(22), 7130–7139. https://doi.org/10.1016/S0021-9258(19)42083-8
20. Hansen, M.B., Nielsen, S.E., Berg, K. (1989). Re-examination and further development of a precise and rapid dye method for measuring cell growth/cell kill. *Journal of Immunological Methods, 119*(2), 203–210. https://doi.org/10.1016/0022-1759(89)90397-9
21. Hayes, J.D., Dinkova-Kostova, A.T., McMahon, M. (2009). Cross-talk between transcription factors AhR and Nrf2, lessons for cancer chemoprevention from dioxin. *Toxicological Sciences*, *111*(2), 199–201. https://doi.org/10.1093/toxsci/kfp168
22. Hunt, J. (1980). Determination of total sulfur in small amounts of plant material. *The Analyst, 105*(1246), 83–85. https://doi.org/10.1039/an9800500083
23. Kaushal, P., Kumar, V., Sharma, H.K. (2015). Utilization of taro (*Colocasia esculenta*). A review. *Journal of Food Science and Technology*, *52,* 27–40. https://doi.org/10.1007/s13197-013-0933-y
24. Keyaerts, E., Vijgen, L., Pannecouque, C., Van Damme, E., Peumans, W., Egberink, H., Balzarini, J., Van Ranst, M. (2007). Plant lectins are potent inhibitors of coronaviruses by interfering with two targets in the viral replication cycle. *Antiviral Research*, *75*(3), 179–187. https://doi.org/10.1016/j.antiviral.2007.03.003
25. Kitchens, R.L. (2000). Role of CD14 in cellular recognition of bacterial lipopolysaccharides. *Chemical Immunology*, *74*, 61–67. https://doi.org/10.1159/000058750
26. Kundu, N., Campbell, P., Hampton, B., Lin, C.Y., Ma, X., Ambulos, N., Zhao, X.F., Goloubeva, O., Holt, D., Fulton, A.M. (2012). Antimetastatic activity isolated from *Colocasia esculenta* (taro). *Anticancer Drugs*, *23*(2), 200–211. https://doi.org/10.1097/CAD.0b013e32834b85e8
27. Larsen, B., Haug, A., Painter, J.T.J. (1966). Sulfated polysaccharides in brown algae. I. Iisolation and preliminary characterization of three sulfated polysaccharides from *Ascophylum nodosum*. *Acta Chemica Scandinavica*, *20*, 219–230. https://doi.org/10.3891/acta.chem.scand.20-0219
28. Lee, S., Wee, W., Yong, J., Syamsumir, D. (2011). Antimicrobial, antioxidant, anticancer property and chemical composition of different parts (corm, stem and leaves) of *Colocasia esculenta* extract. *Annales Universitatis Mariae Curie-Sklodowska, Lublin – Polonia, Sectio DDD, Pharmacia*, *24*(3), 9–16.
29. Li, Y., Seto, E. (2016). HDACs and HDAC inhibitors in cancer, development and therapy. *Cold Spring Harbor Perspectives in Medicine*, *6*(10), art. no. a026831. https://doi.org/10.1101/cshperspect.a026831
30. Lim, T.K. (2015). *Colocasia esculenta in Edible Medicinal and Non-Medicinal Plants*. Springer, Germany. Vol. 9, pp. 454– 492. https://doi.org/10.1007/978-94-017-9511-1_13
31. Lowry, O.H., Rosenbrough, N.J., Farr, A.L., Randall, R.J. (1951). Protein measurement with the Folin–phenol reagent. *Journal of Biological Chemistry*, *193*(1), 265–275. https://doi.org/10.1016/S0021-9258(19)52451-6
32. Lund, E. (2011). An exposure driven functional model of carcinogenesis. *Medical Hypotheses*, *77*(2), 195–198. https://doi.org/10.1016/j.mehy.2011.04.009
33. Mähner, C., Lechner, M.D., Nordmeier, E. (2001). Synthesis and characterization of dextran and pullulan sulfate. *Carbohydrate Research*, *331*(2), 203–208. https://doi.org/10.1016/s0008-6215(00)00315-3
34. Mescher, M., Haarmann-Stemmann, T. (2018). Modulation of CYP1A1 metabolism, from adverse health effects to chemoprevention and therapeutic options. *Pharmacology, Therapeutics*, *187*, 71–87. https://doi.org/10.1016/j.pharmthera.2018.02.012

35. Mollakhalili, M.N., Mortazavian, A.M., Bahadori, M.A., Sohrabvandi, S., Aghaei, M.F. (2017). Phytochemicals in cancer prevention, a review of the evidence. *International Journal of Cancer Management*, *10*(1), art. no. e7219. https://doi.org/10.17795/ijcp-7219
36. Moorcroft, M., Davis, J., Compton, R.G. (2001). Detection and determination of nitrate and nitrite, a review. *Talanta*, *54*(5), 785–803. https://doi.org/10.1016/s0039-9140(01)00323-x
37. Noorfarahzilah, M., Lee, J.S., Sharifudin, M., MohdFadzelly, A., Hasmadi, M. (2014). Applications of composite flour in development of food products. *International Food Research Journal*, *21*(6), 2061– 2074.
38. Nwauzoma, A., Dappa, M.S. (2013). Ethnobotanical studies of Port Harcourt Metropolis, Nigeria. *ISRN Botany*, *2013*, art. no. 829424. https://doi.org/10.1155/2013/829424
39. Park, H.R., Lee, H.S., Cho, S.Y., Kim, Y.S., Shin, K.S. (2013). Antimetastatic effect of polysaccharide isolated from *Colocasia esculenta* is exerted through immunostimulation. *International Journal of Molecular Medicine*, *31*(2), 361–368. https://doi.org/10.3892/ijmm.2012.1224
40. Partridge, S.M. (1949). Aniline hydrogen phthalate as spraying reagent for chromatography of sugars. *Nature*, *164*, 443–446. https://doi.org/10.1038/164443a0
41. Pereira, P.R., Corrêa, A., Vericimo, M.A., Paschoalin, V. (2018). Tarin, a potential immunomodulator and COX-inhibitor lectin found in taro (*Colocasia esculenta*). *Comprehensive Reviews in Food Science and Food Safety, 17*(4), 878–891. https://doi.org/10.1111/1541-4337.12358
42. Prabhu, V., Guruvayoorappan, C. (2010). Nitric oxide, pros and cons in tumor progression. *Immunopharmacology and Immunotoxicology*, *32*(3), 387–392. https://doi.org/10.3109/08923970903440192
43. Reyad-ul-Ferdous, M., Arman, M.S.I., Tanvir, M.M.I., Sumi, S., Siddique, K.M.M.R., Billah, M.M., Islam, S. (2015). Biologically potential for pharmacologicals and phytochemicals of medicinal plants of *Colocasia esculenta*, A comprehensive review. *American Journal of Clinical and Experimental Medicine*, *3*(5–1), 7–11. https://doi.org/10.11648/j.ajcem.s.2015030501.12
44. Sakano, Y., Mutsuga, M., Tanaka, R., Suganuma, H., Inakuma, T., Toyoda, M. (2005). Inhibition of human lanosterol synthase by the constituents of *Colocasia esculenta* (taro). *Biological and Pharmaceutical Bulletin*, *28*(2), 299– 304. https://doi.org/10.1248/BPB.28.299
45. Sun, S.Y., Hail, N. J.R., Lotan, R. (2004). Apoptosis as a novel target for cancer chemoprevention. *Journal of the National Cancer Institute, 9*6(5), 662–672. https://doi.org/10.1093/jnci/djh123
46. Tan, A.C., Konczak, I., Sze, D.M., Ramzan, I. (2011). Molecular pathways for cancer chemoprevention by dietary phytochemicals. *Nutrition and Cancer*, *63*(4), 495–505. https://doi.org/10.1080/01635581.2011.538953
47. Tanaka, T., Ishigamori, R. (2011). Understanding carcinogenesis for fighting oral cancer. *Journal of Oncology*, *2011*, art. no. 603740. https://doi.org/10.1155/2011/603740
48. Temesgen, M., Retta, N. (2015). Nutritional potential, health and food security benefits of taro *Colocasia esculenta* (L)., A review. *Food Science and Quality Management, 36*, 23–30.
49. Xu, X., Lai, Y., Hua, Z.-C. (2019). Apoptosis and apoptotic body, disease message and therapeutic target potentials. *Bioscience Reports*, *39*(1), art. no. BSR20180992. https://doi.org/10.1042/BSR20180992
50. Yang, J., Du, Y., Wen, Y., Li, T., Hu, L. (2003). Sulfation of Chinese lacquer polysaccharides in different solvents. *Carbohydrate Polymers, 52*(4), 397–403. https://doi.org/10.1016/S0144-8617(02)00330-2

Pol. J. Food Nutr. Sci., 2021, Vol. 71, No. 4, pp. 403–410
On-line ISSN: 2083-6007
Print ISSN: 1230-0322
DOI: 10.31883/pjfns/142879
http://journal.pan.olsztyn.pl

Original article
Section: Food Chemistry

Non-Destructive Quantitative Analysis of Azodicarbonamide Additives in Wheat Flour by High-Throughput Raman Imaging

Xiaobin Wang[1, 2, 3, 4, 5]*, *Chunjiang Zhao*[2, 3, 4, 5]

[1]*School of Physics and Electronic Information, Nanchang Normal University, Nanchang 330032, China*
[2]*Beijing Research Center of Intelligent Equipment for Agriculture, Beijing 100097, China*
[3]*National Research Center of Intelligent Equipment for Agriculture, Beijing 100097, China*
[4]*Key Laboratory of Agri-informatics, Ministry of Agriculture, Beijing 100097, China*
[5]*Beijing Key Laboratory of Intelligent Equipment Technology for Agriculture, Beijing 100097, China*

Key words: azodicarbonamide, wheat flour, Raman imaging, image classification, quantitative model

Azodicarbonamide (ADA) additives are limited or prohibited from being added to wheat flour by various countries because they may produce carcinogenic semicarbazide in humid and hot conditions. This study aimed to realize the non-destructive detection of ADA additives in wheat flour using high-throughput Raman imaging and establish a quantitative analysis model. Raman images of pure wheat flour, pure ADA, and wheat flour-ADA mixed samples were collected respectively, and the average Raman spectra of each sample were calculated. A partial least squares (PLS) model was established by using the linear combination spectra of pure wheat flour and pure ADA and the average Raman spectra of mixed samples. The regression coefficients of the PLS model were used to reconstruct the 3D Raman images of mixed samples into 2D grayscale images. Threshold segmentation was used to classify wheat flour pixels and ADA pixels in grayscale images, and a quantitative analysis model was established based on the number of ADA pixels. The results showed that the minimum detectable content of ADA in wheat flour was 100 mg/kg. There was a good linear relationship between the ADA content in the mixed sample and the number of pixels classified as ADA in the grayscale image in the range of 100 – 10,000 mg/kg, and the correlation coefficient was 0.9858. This study indicated that the combination of PLS regression coefficients with threshold segmentation had provided a non-destructive method for quantitative detection of ADA in Raman images of wheat flour-ADA mixed samples.

INTRODUCTION

Wheat is the staple food for more than one-third of the world's population. Flour is the main product of wheat processing, which is often used to make steamed buns, noodles, bread, instant noodles, dumplings and other kinds of food. The wheat flour quality differs due to the effects of wheat varieties, growth environment, storage and transportation, processing methods and other factors [Lancelot *et al*., 2021; Liu *et al*., 2015; Lv *et al*., 2013]. To meet the market demand for different wheat flour products, the company needs to add various types of additives in the course of processing. The use of additives is directly related to the wheat flour quality and people's dietary safety.

As a wheat flour quality improver, azodicarbonamide (ADA) is used to increase the strength and flexibility of dough and has a certain bleaching effect [Yasui *et al*., 2016]. ADA acts as an oxidizing agent when wheat flour is stirred into dough with water, and may be transformed into semicarbazide after heat treatment [Becalski *et al*., 2004; Ye *et al*., 2011]. Some experiments have shown the potential carcinogenicity of semicarbazide in animals [Tian *et al*., 2014]. Therefore, the international restrictions on the use of ADA vary. The European Union, Australia, New Zealand, Singapore, and Japan have all banned the use of ADA in food, but it can be used as a wheat flour additive in the United States, Brazil, Canada, and China at the maximum dose of 45 mg/kg [Chen *et al*., 2018].

At present, the conventional detection methods of ADA in wheat flour are mainly high-performance liquid chromatography (HPLC) [Li *et al*., 2015; Wei *et al*., 2017] and liquid chromatography-mass spectrometry (LC-MS) [Noonan *et al*., 2005; Wang *et al*., 2014]. These two chromatographic methods can accurately detect the ADA content in wheat flour, and have the advantages of low detection limit, strong specificity, and high sensitivity. However, they require a series of complex pretreatments, and the selection of chromatographic conditions, such as chromatography column, flow rate of carrier gas, and sample size, also needs to be taken into account. The entire operation process requires skilled operators and has complicated, time- and cost-consuming, and destructive procedures.

* Corresponding Author:
E-mail: tawangxiaobin@126.com (X. Wang)

Submitted: 17 April 2021
Accepted: 4 October 2021
Published on-line: 26 October 2021

© Copyright by Institute of Animal Reproduction and Food Research of the Polish Academy of Sciences
© 2021 Author(s). This is an open access article licensed under the Creative Commons Attribution-NonCommercial-NoDerivs License (http://creativecommons.org/licenses/by-nc-nd/4.0/).

As the optoelectronic technology develops, some spectroscopy methods have been shown reliable in the detection of wheat flour additives, such as fluorescence spectroscopy [Chen *et al*., 2011], Raman spectroscopy [Cebi *et al*., 2017], near-infrared spectroscopy [Che *et al*., 2017; Gao *et al*., 2016], and terahertz spectroscopy [Hu *et al*., 2020; Sun *et al*., 2019]. However, these spectral methods only obtain the information of a single sampling point, which poses the problem of sampling representativeness. In addition, only the spectral signal of the sample can be obtained, and the distribution of the substance inside the sample cannot be known. High-throughput Raman imaging integrates the advantages of Raman spectroscopy and digital imaging, which can obtain Raman spectra and spatial distribution information simultaneously during sample scanning [Qin *et al*., 2010; Wang *et al*., 2017a; Zhai *et al*., 2017]. There are three ways to acquire Raman images: point-scan, line-scan, and plane-scan [Lohumi *et al*., 2017]. Among them, the detection speed of line-scan mode is faster than that of the point-scan, which can be applied to the detection of samples with flat surface, and shows a good prospect to be used for powdered food safety assessment. Currently, the related reports on the detection of wheat flour additives by line-scan Raman imaging focus on benzoyl peroxide (BPO) [Li *et al*., 2019; Qin *et al*., 2017; Wang *et al*., 2017b]. All these reports provided the spatial distribution and quantitative detection model of BPO in wheat flour, but the data processing method is achieved by selecting the grayscale image corresponding to the Raman peak with the highest intensity in the additive Raman spectrum combined with the threshold segmentation method, ignoring the influence of other bands in the Raman spectrum of the additive on the detection results. In this way, in order to consider the influence of each band of the Raman spectrum on the detection of ADA in wheat flour, we applied the regression coefficients of the partial least squares (PLS) model to all the bands of the sample Raman spectrum to enable the quantitative analysis of ADA in wheat flour.

This study aimed to achieve the non-destructive quantitative analysis of ADA additives in wheat flour by high-throughput Raman imaging. Specific objectives were to: 1) acquire Raman images of wheat flour, ADA, and wheat flour-ADA mixed samples, and find the Raman characteristic peaks of wheat flour and ADA; 2) establish a PLS model and extract the regression coefficients to reconstruct the Raman image into a grayscale image; and 3) create a binary image to classify wheat flour pixels and ADA pixels, and establish a quantitative analysis model for ADA detection in wheat flour.

MATERIALS AND METHODS

Instruments and reagents

The high-throughput Raman imaging system was assembled by Isuzu Optics Corp. (Shanghai, China), and its detailed description can be found in Wang *et al*. [2017a]. Electronic balance (FA2204B) was obtained from Shanghai Precision and Scientific Instrument Corp. (Shanghai, China), with a weighing range of 0–220 g and an accuracy of 0.1 mg. Vortex Mixer (Vortex-Genie 2) was purchased from Scientific Industries Inc. (New York, NY, USA), with a 600–3,200 rpm speed range. Customized square aluminum alloy container had the internal size of 45×45×2 mm (we have determined in the previous study that the effective penetration depth of line laser to wheat flour is 2 mm).

ADA (97%) was purchased from Xiya Chemical Technology Co. Ltd. (Linyi, China). Wheat flour was obtained from a local supermarket in Beijing (China), and was determined by HPLC to be ADA free.

Sample preparation

The electronic balance was used to accurately weigh 0.1 g of ADA and 9.9 g of wheat flour, that were transferred into a 50 mL centrifuge tube and mixed evenly with a vortex mixer to obtain a wheat flour-ADA mixed sample containing 10,000 mg of ADA per kg of wheat flour. The mass of ADA and wheat flour was adjusted to keep the total mass of each mixed sample at 10 g, and the mixed samples with 9 different ADA contents in wheat flour (100; 200; 500; 800; 1,000; 2,000; 5,000; 8,000; and 10,000 mg/kg) were prepared. The mass of the mixed sample in the square container was about 2.1 g. To make full use of the mixed samples, each mixed sample was put into four identical square containers to obtain four subsamples. Meanwhile, the pure wheat flour sample and pure ADA sample were prepared and divided into four subsamples for Raman image acquisition.

Raman image collection

The sample was placed on a single-axis moving platform, and the height was adjusted to ensure that the sample surface was 20 cm away from the lens. The exposure time of the camera was 1,000 ms, and the spatial resolution was 0.125 mm/pixel. The Raman spectrum collection range was 785–1,000 nm (corresponding to the Raman shift was 0–2,728 cm^{-1}), and the spectral resolution was 0.54 nm. The moving speed of the single-axis moving platform was 0.0823 mm/s. The acquisition area of the camera was 128×45 mm (spatial information was 1,024×360 pixels), and the data was saved as 1,024 pixels×360 pixels×512 wavelengths Raman image cube.

Data processing

To reduce the data volume and quickly extract target information, it was necessary to determine the region of interest (ROI) and spectral range of the Raman image. The center of the sample Raman image was taken as the center of ROI, and a 40×40 mm square area (corresponding to 320×320 pixels, a total of 102,400 pixels) was selected to ensure that only the sample area was included and the background area was excluded. The Raman peak of ADA was mainly located in 400–2000 cm^{-1}, and this spectral range was selected for subsequent analysis. The mixed sample was irradiated by laser to generate Raman signals and accompanied by fluorescence signals, and the high fluorescence directly interfere with the identification of Raman peak. The adaptive iteratively reweighted penalized least squares method can fit the Raman spectrum to eliminate the interference of the background signal, so this method was selected for the correction of the Raman spectrum [Zhang *et al*., 2010].

The PLS model was established using the ADA content and Raman spectra of wheat flour-ADA mixed samples,

in which the calibration set was the average Raman spectra of mixed samples, and the prediction set was the new Raman spectrum obtained by combining the Raman spectrum of wheat flour and ADA. The new Raman spectrum as given in equation (1):

$$S_i^{new} = S_a C_i + \frac{S_f}{1\text{-}C_i} \quad (1)$$

where: S_i^{new} is the new Raman spectrum; S_a is the Raman spectrum of ADA; S_f is the Raman spectrum of wheat flour; C_i is the ADA content of the mixed sample; a total of 9 ADA contents (100; 200; 500; 800; 1,000; 2,000; 5,000; 8,000; 10,000 mg/kg) was used.

The coefficient of determination (calibration set is R_c^2, prediction set is R_p^2) and root mean square error (RMSE) (calibration set is RMSEC; prediction set is RMSEP) was used to evaluate the performance of the PLS model. The regression coefficient of the optimal PLS model was extracted and used to calculate the intensity of each pixel in the Raman image of the mixed sample. The intensity of each pixel was computed according to equation (2):

$$I = R_1X_1 + R_2X_2 + \ldots\ldots + R_nX_n + R_0 \quad (2)$$

where: I is the intensity; R_1-R_n are the regression coefficients of each band in the PLS model; X_1-X_n are the Raman intensity of each band in the Raman spectrum of the mixed sample; R_0 is the intercept.

To obtain the PLS model with high predictive performance, different methods were used to preprocess the Raman spectra of the calibration set and the prediction set, including normalization, and multiplicative scatter correction (MSC), standard normal variate transformation (SNV), first derivative (1st), and second derivative (2nd).

The threshold segmentation method was used to create binary images to classify ADA pixels and wheat flour pixels in grayscale images of mixed samples, and the threshold was determined by the maximum gray value in the grayscale image of pure wheat flour. Those with gray values above and below the threshold were classified as ADA pixels and wheat flour pixels, respectively. PLS model establishment and spectral pretreatment were performed by The Unscrambler X10.4 Software (Camo Software AS, Oslo, Norway), and the rest of the process was completed using MATLAB 7.11 program (Math Works Inc., Natick, MA, USA).

RESULTS AND DISCUSSION

Average Raman spectra of wheat flour and ADA

The average Raman spectra of wheat flour and ADA are shown in Figure 1. The Raman spectra of the two are significantly different. There was a high fluorescence background in the Raman spectrum of wheat flour (Figure 1a), which causes the baseline to drift. The peak with the highest intensity was located at 481 cm^{-1} in the corrected Raman spectrum, which was consistent with the results obtained by other researchers [Czaja *et al*., 2016]. This Raman peak was assigned to the coupling of C-C-C skeleton bending vibration and C-O deformation vibration [Wiercigroch *et al*., 2017].

The Raman spectrum of ADA had a flat baseline and many Raman peaks (Figure 1b). Three obvious peaks could be observed at 1,121; 1,335; and 1,577 cm^{-1}, respectively. Among them, the 1,335 cm^{-1} peak had the highest intensity. The model of the molecular structure of ADA with C–N, C=O, N=N, N–H and other bonds is shown in Figure 1b (upper left diagram). Its molecular formula is $C_2H_4N_4O_2$. Each bond of the functional group has its characteristic vibration frequency, and the Raman peaks can be assigned according to the different vibration frequencies. The wavenumber of 1,121 cm^{-1} was assigned to the in-plane bending vibration of H–N–H; 1,335 cm^{-1} was assigned to the asymmetric stretching vibration of N–C–N, which was also accompanied by the in-plane bending vibration of N–H; and 1,577 cm^{-1} was assigned to the N=N stretching vibration [Li *et al*., 2015; Xie *et al*., 2013].

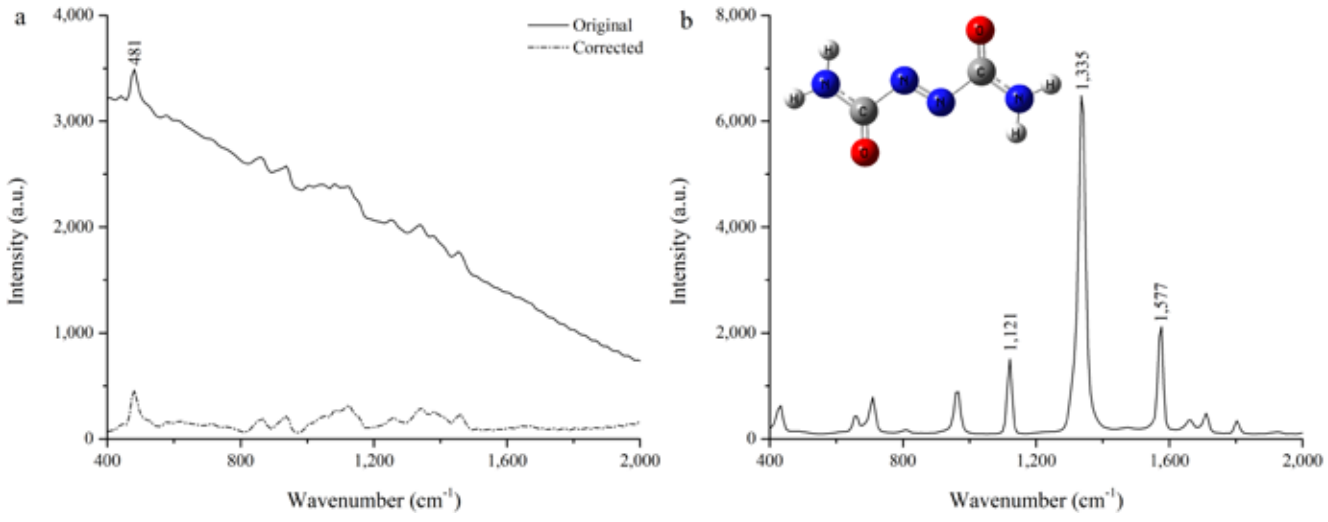

FIGURE 1. Average Raman spectra of (a) wheat flour and (b) azodicarbonamide (ADA). ADA structure model is presented in left upper corner of Figure 1b.

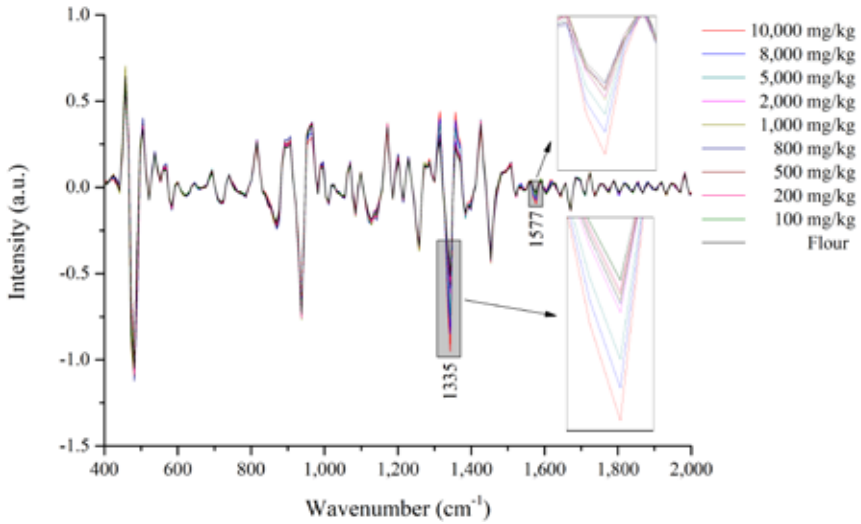

FIGURE 2. Average Raman spectra of wheat flour-azodicarbonamide mixed samples with different contents of azodicarbonamide (pretreated with second derivative).

Average Raman spectra of wheat flour-ADA mixed samples

Figure 2 shows the average Raman spectra of wheat flour-ADA mixed samples with different ADA contents in wheat flour (pretreated with the 2nd). The Raman spectrum of each mixed sample contained the signals from both wheat flour and ADA. The two peaks of ADA (1,335 and 1,577 cm^{-1}) could be observed in the spectra, but their intensity was lower than that of wheat flour, because the ADA content in mixed samples was low. The mixed sample with ADA content of 10,000 mg/kg showed the highest intensity of the Raman characteristic peaks of ADA. When the ADA content in the mixed samples decreased from 10,000 to 1,000 mg/kg, the intensity of these peaks decreased continuously. The intensity of peaks recorded for samples with ADA content lower than 1,000 mg/kg was not significantly different. This indicated that the average spectrum of the mixed samples could not be used to detect ADA content in wheat flour effectively. On the other hand, Huang *et al*. [2016] found that the spectra corresponding to pixels can be used to effectively detect additive particles in food when detecting food additives by near-infrared hyperspectral imaging. Therefore, in the next step of our study, the Raman spectrum of each pixel in ROI was analyzed to realize the effective detection of ADA in wheat flour.

Establishment of PLS model

A total of 9 wheat flour-ADA mixed samples were prepared, and Raman images of 4 subsamples corresponding to each mixed sample were collected; then those 4 subsamples were aggregated and remixed, and divided into 4 new subsamples to collect Raman images. The process was repeated once more. The average Raman spectrum of each subsample was calculated, and a total of 108 spectra (9×4×3) were obtained as the calibration set of the PLS model. The average Raman spectra of wheat flour and ADA (based on 4 subsamples of each) were also calculated and applied to equation (1) to obtain the 36 new Raman spectra (for 9 different ADA contents; 4×9) as the prediction set of the PLS model.

Table 1 shows the PLS model results established by different pretreated Raman spectra. The R_c^2 of the PLS model established by the original spectra was higher than that of normalized, 1st and 2nd derivative spectra, while the R_c^2 of the PLS model established by MSC and SNV spectra was higher than that of original spectra. Among all PLS models, SNV spectra had the best prediction result, and the R_p^2 and RMSEP values of the prediction set were 0.9212 and 0.0967%, respectively. SNV was used to eliminate the interference caused by surface scattering, solid particle size, and light intensity changes on the Raman spectrum of wheat flour particles and this pretreatment method had a good correction effect [Huang *et al*., 2011]. The regression coefficients of the PLS model established by SNV spectra were extracted, as shown in Figure 3. Higher or lower coefficients indicate the wavenumbers that have a significant impact on the PLS model [Esquerre *et al*., 2011].

TABLE 1. Partial least squares model results established by different pretreated Raman spectra.

Pretreatment	Calibration set		Prediction set		Factor
	R_c^2	RMSEC	R_p^2	RMSEP	
Original	0.9934	0.0280	0.9071	0.1050	5
Normalized	0.9933	0.0282	0.9086	0.1042	3
MSC	0.9950	0.0244	0.9205	0.0972	3
SNV	0.9951	0.0242	0.9212	0.0967	3
1st derivative	0.9882	0.0374	0.8899	0.1144	2
2nd derivative	0.9930	0.0288	0.9087	0.1041	4

MSC: multiplicative scatter correction; SNV: standard normal variate transformation; RMSEC: root-mean-square error of calibration set; RMSEP: root-mean-square error of prediction set.

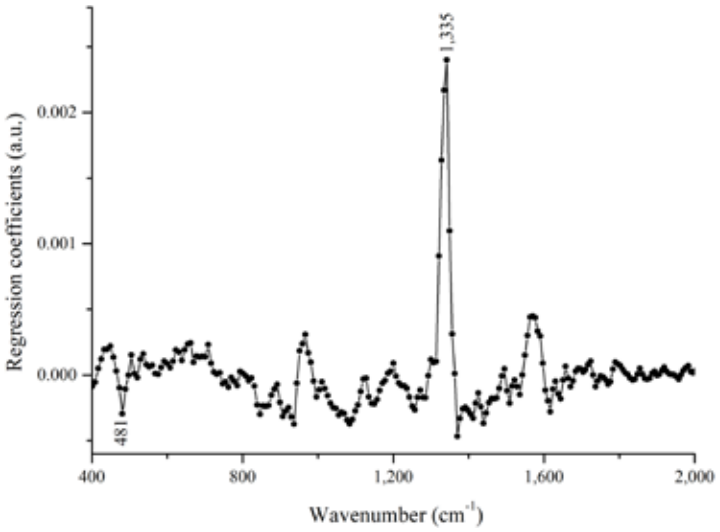

FIGURE 3. Regression coefficient of partial least squares model.

In our study, the highest regression coefficient was located at 1,335 cm^{-1} (Figure 3), which corresponds with the significant Raman peak of ADA (Figure 1b). The regression coefficient at 481 cm^{-1} (significant peak of wheat flour Raman spectrum) also had a certain impact on the PLS model.

Quantitative analysis of ADA in wheat flour

The absolute value of each regression coefficient in the PLS model was applied to the Raman image of wheat flour-ADA mixed sample, and the intensity of each pixel was calculated by equation (2) to convert the 3D Raman image into a 2D grayscale image. Wheat flour pixels and ADA pixels were still difficult to identify in the grayscale image of the mixed sample. Therefore, the threshold segmentation method was used to create the grayscale image as a binary image to classify wheat flour pixels and ADA pixels. The PLS model regression coefficient was also used to determine the threshold. The intensity of each pixel in the wheat flour Raman image was calculated by equation (2), and its maximum intensity was 6.9382, which was selected as the threshold. The pixels with intensity above the threshold (white pixels) were classified as ADA, whereas those with intensity below the threshold (black ones) were classified as wheat flour. No pixels classified as wheat flour were found in the pure ADA image, and no pixels classified as ADA were found in the pure wheat flour image, which indicated that the threshold can correctly classify wheat flour pixels and ADA pixels.

The number of pixels classified as ADA in 4 subsamples of each mixed sample was counted (Table 2). The values decreased with the decrease of ADA content in each subsample. The number of pixels classified as ADA in the mixed sample with the lowest ADA content was 7, 6, 9, and 8, as shown in Figure 4. This indicated that the minimum detectable content of ADA in wheat flour by this method was 100 mg/kg, which was lower than the limit of detection of ADA in flour by near-infrared hyperspectral imaging (200 mg/kg) [Wang *et al*., 2018]. Differences in the number of ADA pixels among subsamples were probably caused by the random distribution of ADA particles in the mixed sample. Also, the differences in the number of ADA pixels indicate that multiple subsamples need to be used for the quantitative analysis of wheat flour-ADA mixed samples. The average number of ADA pixels of subsamples was used to establish a quantitative model (Figure 5). There was a good linear correlation between the ADA content and the average number of ADA pixels, and the coefficient of determination was 0.9858, which indicated that the method established in this study could be used for the quantitative analysis of ADA additives in wheat flour.

Raman characteristic peak method (based on Raman imaging) was commonly used for detecting additives in food products [Dhakal *et al*., 2016; Qin *et al*., 2018; Wang *et al*., 2017b]. In our study, this method was used to detect ADA in wheat flour-ADA mixed samples. The single-band image corresponding to the Raman peak with the highest intensity in the ADA Raman spectrum was selected from the Raman image of the mixed sample, and the thresholding segmentation method was used to achieve the classification of wheat flour pixels and ADA pixels. The results are shown in Table 3. In all wheat flour-ADA mixed samples, the number

TABLE 2. Number of azodicarbonamide pixels classified in the four subsamples of each wheat flour-azodicarbonamide mixed sample.

Content (mg/kg)	Subsample 1	Subsample 2	Subsample 3	Subsample 4	Average
100	7	6	9	8	7.50
200	24	23	28	25	25.00
500	78	76	75	77	76.50
800	114	105	107	105	107.75
1,000	158	149	159	165	157.75
2,000	316	310	308	319	313.25
5,000	724	691	706	694	703.75
8,000	1152	1097	1122	1118	1122.25
10,000	1694	1642	1722	1653	1677.75

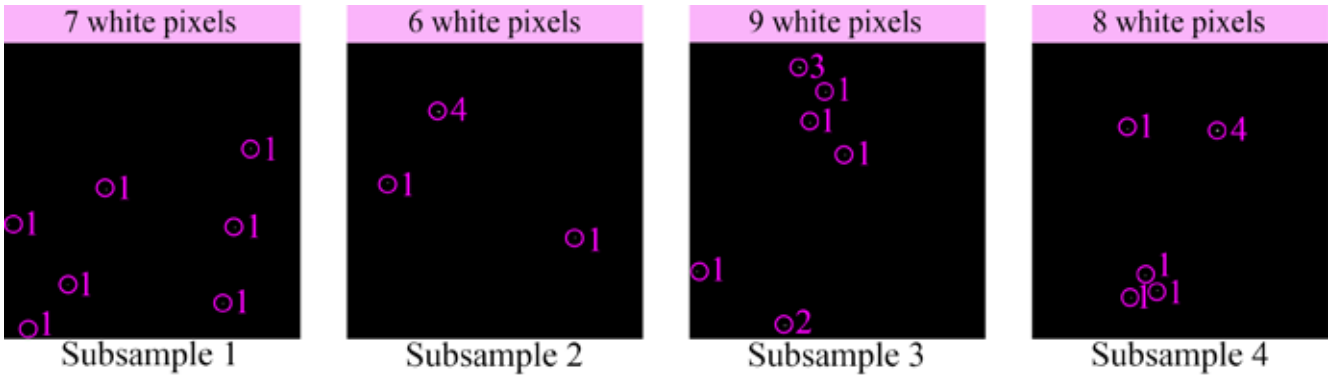

FIGURE 4. Classification image of wheat flour-azodicarbonamide mixed samples with the azodicarbonamide content of 100 mg/kg.

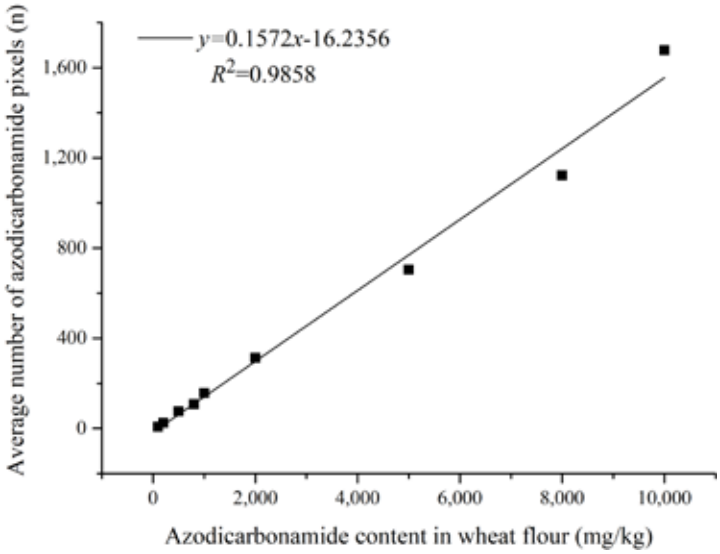

FIGURE 5. Linear relationship model between azodicarbonamide content in wheat flour and average number of azodicarbonamide pixels.

TABLE 3. Detection results of azodicarbonamide in wheat flour-azodicarbonamide mixed samples by Raman characteristic peak method.

Content (mg/kg)	Subsample 1	Subsample 2	Subsample 3	Subsample 4	Average
100	8	6	7	8	7.25
200	24	22	27	24	24.25
500	76	75	72	73	74
800	109	105	103	105	105.5
1,000	153	147	157	165	155.5
2,000	309	307	303	316	308.75
5,000	699	676	696	687	689.5
8,000	1120	1080	1097	1110	1101.75
10,000	1650	1621	1687	1641	1649.75

of pixels classified as ADA by the PLS model regression coefficient method established in this paper (Table 2) was higher than determined with the Raman characteristic peak method. In the Raman characteristic peak method, the intensity of a single Raman peak was used as an index for determination, and the threshold was the maximum intensity of the wheat flour sample at this band. But some pixels were not detected due to their low Raman scattering intensity of ADA, which could lead to false negative results. In the PLS model regression coefficient method, the intensities of all bands of each mixed sample were used for calculation, which provided more comprehensive information and had higher detection accuracy. The linear correlation between ADA content in wheat flour-ADA mixed samples and the number of ADA pixels in Raman images proves the potential of high-throughput Raman imaging for the quantitative analysis of ADA in wheat flour. In the next research, the improvement of hardware equipment performance and spectral pretreatment methods will help to achieve lower concentration detection, and will lay a theoretical foundation for the market-oriented application of high-throughput Raman imaging.

CONCLUSIONS

In this study, the large-area detection, visual identification and non-destructive quantitative analysis of ADA additives

in wheat flour were achieved by high-throughput Raman imaging. The average Raman spectra of wheat flour-ADA mixed samples showed that the three Raman characteristic peaks of ADA (1,121; 1,335; and 1,577 cm^{-1}) were ineffective in evaluating the ADA content in wheat flour. Different spectral pretreatment methods were used for Raman spectra of mixed sample images, and the PLS model established by SNV pretreatment had a good predictive effect. All the regression coefficients of the PLS model were applied to the Raman spectra of the mixed sample images to convert them into grayscale images, but wheat flour pixels and ADA pixels were still difficult to identify. Threshold segmentation was used to classify wheat flour pixels and ADA pixels in grayscale images. The classification results showed that the minimum detection content of ADA in wheat flour was 100 mg/kg, and that there was a good linear correlation between the ADA content in the mixed sample and the number of ADA pixels in the Raman image, with a determination coefficient of 0.9858. This study provides the method for the quantitative analysis of ADA additives in wheat flour as well as a technical reference for large-scale rapid screening. This method also appears to have the potential in future applications for the analysis of contaminants in other powdered food products.

RESEARCH FUNDING

This work was supported by the Project supported by the National Natural Science Foundation of China (No. 32160417), the Science and Technology Project of Jiangxi Provincial Department of Education (No. GJJ212605), the Doctoral Research Funds of Nanchang Normal University (No. NSBSJJ2018016), and the Scientific research project of Nanchang Normal University (No. N21KJYB02).

CONFLICT OF INTEREST

Authors declare no conflict of interest.

ORCID IDs

X. Wang https://orcid.org/0000-0002-0402-6895
C. Zhao https://orcid.org/0000-0002-8641-2254

REFERENCES

1. Becalski, A., Lau, B.P.Y., Lewis, D., Seaman, S.W. (2004). Semicarbazide formation in azodicarbonamide-treated flour: A model study. *Journal of Agricultural and Food Chemistry, 52*(18), 5730–5734. https://doi.org/10.1021/jf0495385
2. Cebi, N., Dogan, C.E., Develioglu, A., Yayla, M.E.A., Sagdic, O. (2017). Detection of L-cysteine in wheat flour by Raman microspectroscopy combined chemometrics of HCA and PCA. *Food Chemistry*, *228*, 116–124. https://doi.org/10.1016/j.foodchem.2017.01.132
3. Che, W.K., Sun, L.J., Zhang, Q., Zhang, D., Ye, D.D., Tan, W.Y., Wang, L.K., Dai, C.J. (2017). Application of visible/near-infrared spectroscopy in the prediction of azodicarbonamide in wheat flour. *Journal of Food Science*, *82*(10), 2516–2525. https://doi.org/10.1111/1750-3841.13859
4. Chen, W., Shi, W., Li, Z., Ma, H.M., Liu, Y., Zhang, J.H., Liu, Q.J. (2011). Simple and fast fluorescence detection of benzoyl peroxide in wheat flour by *N*-methoxy rhodamine-6G spirolactam based on consecutive chemical reactions. *Analytica Chimica Acta*, *708*(1–2), 84–88. https://doi.org/10.1016/j.aca.2011.10.002
5. Chen, Z.Q., Chen, L., Lin, L., Wu, Y.N., Fu, F.F. (2018). A colorimetric sensor for the visual detection of azodicarbonamide in flour based on azodicarbonamide-induced anti-aggregation of gold nanoparticles. *ACS Sensors*, *3*(10), 2145–2151. https://doi.org/10.1021/acssensors.8b00705
6. Czaja, T., Mazurek, S., Szostak, R. (2016). Quantification of gluten in wheat flour by FT-Raman spectroscopy. *Food Chemistry, 211*, 560–563. https://doi.org/10.1016/j.foodchem.2016.05.108
7. Dhakal, S., Chao, K.L., Qin, J.W., Kim, M., Chan, D.N. (2016). Raman spectral imaging for quantitative contaminant evaluation in skim milk powder. *Journal of Food Measurement and Characterization, 10*(2), 374–386. https://doi.org/10.1007/s11694-016-9316-1
8. Esquerre, C., Gowen, A.A., Downey, G., O'Donnell, C.P. (2011). Selection of variables based on most stable normalised partial least squares regression coefficients in an ensemble Monte Carlo procedure. *Journal of Near Infrared Spectroscopy, 19*(6), 443–450. https://doi.org/10.1255/jnirs.962
9. Gao, S., Sun, L.J., Hui, G.Y., Wang, L.K., Dai, C.J., Wang, J.A. (2016). Prediction of azodicarbonamide in flour using near-infrared spectroscopy technique. *Food Analytical Methods*, *9*(9), 2642–2648. https://doi.org/10.1007/s12161-016-0441-6
10. Hu, J., Liu, Y.D., He, Y., Sun, X.D., Li, B. (2020). Optimization of quantitative detection model for benzoic acid in wheat flour based on CARS variable selection and THz spectroscopy. *Journal of Food Measurement and Characterization*, *14*(5), 2549–2558. https://doi.org/10.1007/s11694-020-00501-5
11. Huang, C.W., Dai, L.K., Dong, X.F. (2011). The application of piecewise direct standardization with SNV in calibration transfer of Raman spectra. *Spectroscopy and Spectral Analysis, 31*(5), 1279–1282. https://doi.org/10.3964/j.issn.1000-0593(2011)05-1279-04
12. Huang, M., Kim, M.S., Delwiche, S.R., Chao, K., Qin, J.W., Mo, C., Esquerre, C., Zhu, Q.B. (2016). Quantitative analysis of melamine in milk powders using near-infrared hyperspectral imaging, and band ratio. *Journal of Food Engineering, 181*, 10–19. https://doi.org/10.1016/j.jfoodeng.2016.02.017
13. Lancelot, E., Fontaine, J., Grua-Priol, J., Le-Bail, A. (2021). Effect of long-term storage conditions on wheat flour and bread baking properties. *Food Chemistry, 346*, art. no. 128902. https://doi.org/10.1016/j.foodchem.2020.128902
14. Li, G.L., Tang, C.H., Wang, Y., Yang, J., Wu, H.L., Chen, G., Kong, X.J., Kong, W.H., Liu, S.C., You, J.M. (2015). A rapid and sensitive method for semicarbazide screening in foodstuffs by HPLC with fluorescence detection. *Food Analytical Methods, 8*(7), 1804–1811. https://doi.org/10.1007/s12161-014-0063-9
15. Li, M.H., Guo, X.Y., Wang, H., Wen, Y., Yang, H.F. (2015). Rapid and label-free Raman detection of azodicarbonamide with asthma risk. *Sensors and Actuators B-Chemical*, *216*, 535–541. https://doi.org/10.1016/j.snb.2015.04.103

16. Li, Y., Peng, Y.K., Chao, K.L., Qin, J.W., Dhakal, S. (2019). Nondestructive rapid detection of benzoyl peroxide in flour based on Raman hyperspectral technique. *Proceedings of SPIE*, *11016*, art. no. 110160G. https://doi.org/10.1117/12.2517454
17. Liu, C., Liu, L., Li, L.M., Hao, C.M., Zheng, X.L., Bian, K., Zhang, J., Wang, X.X. (2015). Effects of different milling processes on whole wheat flour quality and performance in steamed bread making. *LWT – Food Science and Technology, 62*(1), 310–318. https://doi.org/10.1016/j.lwt.2014.08.030
18. Lohumi, S., Kim, M.S., Qin, J.W., Cho, B.K. (2017). Raman imaging from microscopy to macroscopy: Quality and safety control of biological materials. *TrAC – Trends in Analytical Chemistry*, *93*, 183–198. https://doi.org/10.1016/j.trac.2017.06.002
19. Lv, J.L., Lu, Y.J., Niu, Y.G., Whent, M., Ramadan, M.F., Costa, J., Yu, L.L. (2013). Effect of genotype, environment, and their interaction on phytochemical compositions and antioxidant properties of soft winter wheat flour. *Food Chemistry, 138*(1), 454–462. https://doi.org/10.1016/j.foodchem.2012.10.069
20. Noonan, G.O., Warner, C.R., Hsu, W., Begley, T.H., Perfetti, G.A., Diachenko, G.W. (2005). The determination of semicarbazide (N-Aminourea) in commercial bread products by liquid chromatography-mass spectrometry. *Journal of Agricultural and Food Chemistry*, *53*(12), 4680–4685. https://doi.org/10.1021/jf050480j
21. Qin J., Chao K., Kim M.S. (2010). Raman chemical imaging system for food safety and quality inspection. *Transactions of the ASABE*, *53*(6), 1873–1882. https://doi.org/ 10.13031/2013.35796
22. Qin, J.W., Kim, M.S., Chao, K.L., Bellato, L., Schmidt, W.F., Cho, B.K., Huang, M. (2018). Inspection of maleic anhydride in starch powder using line-scan hyperspectral Raman chemical imaging technique. *International Journal of Agricultural and Biological Engineering, 11*(6), 120–125. https://doi.org/10.25165/j.ijabe.20181106.4339
23. Qin, J.W., Kim, M.S., Chao, K.L., Gonzalez, M., Cho, B.K. (2017). Quantitative detection of benzoyl peroxide in wheat flour using line-scan macroscale Raman chemical imaging. *Applied Spectroscopy*, *71*(11), 2469–2476. https://doi.org/10.1177/0003702817706690
24. Sun, X.D., Zhu, K., Liu, J.B., Hu, J., Jiang, X.G., Liu, Y.D., Gong, Z.Y. (2019). Terahertz spectroscopy determination of benzoic acid additive in wheat flour by machine learning. *Journal of Infrared Millimeter and Terahertz Waves*, *40*(4), 466–475. https://doi.org/10.1007/s10762-019-00579-z
25. Tian, W.R., Sang, Y.X., Wang, X.H. (2014). Semicarbazide – from state-of-the-art analytical methods and exposure to toxicity: a review. *Food Additives and Contaminants Part A-Chemistry Analysis Control Exposure & Risk Assessment*, *31*(11), 1850–1860. https://doi.org/10.1080/19440049.2014.953012
26. Wang, X.B., Zhao, C.J., Huang, W.Q., Wang, Q.Y., Liu, C., Yang, G.Y. (2017a). Effective detection of benzoyl peroxide in flour based on parameter selection of Raman hyperspectral system. *Spectroscopy Letters*, *50*(7), 364–369. https://doi.org/10.1080/00387010.2017.1332649
27. Wang, X.B., Huang, W.Q., Zhao, C.J., Wang, Q.Y., Liu, C., Yang, G.Y. (2017b). Quantitative analysis of BPO additive in flour *via* Raman hyperspectral imaging technology. *European Food Research and Technology*, *243*(12), 2265–2273. https://doi.org/10.1007/s00217-017-2928-9
28. Wang, X.B., Zhao, C.J., Huang, W.Q., Wang, Q.Y., Liu, C., Yang, G.Y. (2018). Near-infrared hyperspectral imaging for detection and quantification of azodicarbonamide in flour. *Journal of the Science of Food and Agriculture*, *98*(7), 2793–2800. https://doi.org/10.1002/jsfa.8776
29. Wang, Y., Wang, J., Xiang, L., Xi, C., Chen, D., Peng, T., Wang, G., Mu, Z. (2014). Determination of biurea in flour and its products by liquid chromatography-tandem mass spectrometry. *Chinese Journal of Chromatography, 32*(5), 513–518. https://doi.org/10.3724/SP.J.1123.2013.12023
30. Wei, T.F., Li, G.K., Zhang, Z.M. (2017). Rapid determination of trace semicarbazide in flour products by high-performance liquid chromatography based on a nucleophilic substitution reaction. *Journal of Separation Science*, *40*(9), 1993–2001. https://doi.org/10.1002/jssc.201700045
31. Wiercigroch, E., Szafraniec, E., Czamara, K., Pacia, M.Z., Majzner, K., Kochan, K., Kaczor, A., Baranska, M., Malek, K. (2017). Raman and infrared spectroscopy of carbohydrates: A review. *Spectrochimica Acta Part A – Molecular and Biomolecular Spectroscopy, 185*, 317–335. https://doi.org/10.1016/j.saa.2017.05.045
32. Xie Y.F., Li P., Zhang J., Wang H.Y., Qian H., Yao W.R. (2013). Comparative studies by IR, Raman, and surface-enhanced Raman spectroscopy of azodicarbonamide, biurea and semicarbazide hydrochloride. *Spectrochimica Acta Part A – Molecular and Biomolecular Spectroscopy*, *114*, 80–84. https://doi.org/10.1016/j.saa.2013.05.055
33. Yasui, A., Oishi, M., Hayafuji, C., Kobayashi, C., Shindo, T., Ozawa, H., Nakazato, M. (2016). Analysis of azodicarbonamide in wheat flour and prepared flour mixes. *Food Hygiene and Safety Science*, *57*(5), 133–138. https://doi.org/10.3358/shokueishi.57.133
34. Ye, J., Wang, X.H., Sang, Y.X., Liu, Q. (2011). Assessment of the determination of azodicarbonamide and its decomposition product semicarbazide: investigation of variation in flour and flour products. *Journal of Agricultural and Food Chemistry, 59*(17), 9313–9318. https://doi.org/10.1021/jf201819x
35. Zhai, C., Peng, Y.K., Li, Y.Y., Zhao, J. (2017). Detection of chemical additives in food using Raman chemical imaging system. *Chemical Journal of Chinese Universities*, *38*(3), 369–375. https://doi.org/10.7503/cjcu20160640
36. Zhang, Z.M., Chen, S., Liang, Y.Z. (2010). Baseline correction using adaptive iteratively reweighted penalized least squares. *Analyst*, *135*(5), 1138–1146. https://doi.org/10.1039/b922045c

Pol. J. Food Nutr. Sci., 2021, Vol. 71, No. 4, pp. 411–421
On-line ISSN: 2083-6007
Print ISSN: 1230-0322
DOI: 10.31883/pjfns/142926
http://journal.pan.olsztyn.pl

Original article
Section: Food Quality and Functionality

Effect of Glucosamine and Ascorbic Acid Addition on Beef Burger Textural and Sensory Attributes

Philip O. Soladoye[1], Yuliya Hrynets[2], Mirko Betti[2], Zeb Pietrasik[3]*

[1]Agriculture and Agri-Food Canada, Lacombe Research and Development Centre, Lacombe, Alberta, T4L 1W1, Canada
[2]Department of Agricultural, Food and Nutritional Science, University of Alberta 410 Agriculture/Forestry Centre, Edmonton Alberta, T6G 2P5, Canada
[3]Food Processing Development Centre, Food and Bio Processing Branch, Alberta Agriculture and Forestry, Government of Alberta, Leduc, Alberta, T9E 7C5, Canada

Key words: glucosamine, ascorbic acid, beef burger, consumer acceptability, quality attributes

Aside from the possible health benefit of dietary consumption of glucosamine (GlcN), studies have also reported its flavour enhancing properties in varying food products. However, the impact of its inclusion on other quality attributes of meat products has been under-assessed. The present study examined the effect of the addition of ascorbic acid (0.1%) and varying levels of GlcN (0.75, 1.5 and 3.0%) on colour stability, textural as well as sensory attributes of beef burger. Except for L^* (lightness) value, significant interaction ($p<0.01$) between storage time and added ingredient was observed for all colour parameters (a^*; redness, b^*; yellowness, chroma, and hue angle) in beef burger. Generally, although ascorbic acid preserved the colour attributes of beef burgers during storage, addition of GlcN resulted in the deterioration of these colour parameters. Whereas the present result did not confirm any flavour enhancing attributes of GlcN compared to control, GlcN improved beef burger's yield and reduced product cook loss. However, level of GlcN above 1.5% resulted in significant flavour and textural deterioration ($p<0.05$), leading to decline in consumer acceptability of beef burger. This study showed that a moderate level of glucosamine could be used in meat products as a functional ingredient with some additional technological benefits and limited impact on sensory attributes. Ascorbic acid adequately protected the colour of beef burger during refrigerated storage.

INTRODUCTION

In recent years, epidemiological studies are associating red and processed meat with several human disease conditions including cardiovascular disease, colorectal/colon cancer, diabetes and thrombosis, among others [Chan *et al*., 2011; Micha *et al*., 2010]. The attributes of red and processed meat largely implicated in this disease associative effect may include their saturated fatty acid content, sodium salt content as well as the severity of their processing. Considering these recent trends, consumers tend to scrutinize their meat consumption; demanding for clean label, minimally processed and reduced salt meat products. One of many possible strategies for sodium salt reduction in meat products is the incorporation of flavour enhancer in place of salt in meat product formulation [Hong *et al.*, 2016].

Glucosamine (GlcN, 2-amino-2-deoxy-D-glucose), also referred to as chitosamine, is a naturally occurring amino sugar found around the bone joints and plays a vital function in cartilage building. GlcN is also made available as dietary supplement through the hydrolysis and deacetylation of chitin mainly derived from the exoskeleton of marine crustaceans and shellfishes [Hong & Betti, 2016]. GlcN supplement has been used in the prevention and treatment of osteoarthritis symptoms [Bruyere & Reginster, 2007; Hrynets *et al*., 2016; McAlindon *et al*., 2000]. Although not without debates, other health claims reported for GlcN include improvement and ease of inflammatory bowel diseases (3–6 g of *N*-acetyl glucosamine administered orally or rectally to children daily for unspecified period) [Salvatore *et al*., 2000]; bone healing and pain alleviation (230 mg/kg glucosamine-sulfate daily intraperitoneal for 4 weeks to Wistar rats) [Uğraş *et al*., 2013]; as well as treatment of immunological diseases (10 μg/mL of 5–40 mM D-GlcN or deoxyfructosazines on Jurkat cells) [Zhu *et al*., 2007]. Aside from these potential health benefits associated with GlcN, this amino sugar could also find applications in the food industry since several studies have reported its antimicrobial [Hrynets *et al*., 2016], antioxidant [Gottardi *et al.*, 2014; Hong & Betti, 2016; Xing *et al*., 2006] and flavour/taste enhancing potentials [Fu *et al.*, 2020], especially when incubated at moderate temperatures (between 25 and 50°C). Jia *et al*. [2014] have proposed a one-pot dehydration process

* Corresponding Author:
Tel.: +1 587–334–1812;
E-mail: philip.soladoye@agr.gc.ca (O.P. Soladoye)

Submitted: 18 August 2021
Accepted: 7 October 2021
Published on-line: 27 October 2021

© Copyright by Institute of Animal Reproduction and Food Research of the Polish Academy of Sciences
© 2021 Author(s). This is an open access article licensed under the Creative Commons Attribution-NonCommercial-NoDerivs License (http://creativecommons.org/licenses/by-nc-nd/4.0/).

for the conversion of GlcN into fructosazine and deoxyfructosazine which can be used as a flavoring agent in the food industry. GlcN can also be used to modify proteins with the aim of enhancing their functionalities [Hrynets *et al.,* 2013]. Other studies have used GlcN to enrich beverages and milk with the aim of creating functional products [Kralovec & Barrow, 2007; Uzzan *et al.,* 2007].

The flavour enhancing attributes of GlcN can be largely attributed to its unique chemical structure which makes it unstable [Hong & Betti, 2016] and prone for self-condensation to form non-volatile hydroxyalkyl pyrazines including, fructosazine [2,5-bis(D-arabino-tetrahydroxybutyl)pyrazine] and deoxyfructosazine [2-(D-arabino-tetrahydroxybutyl)-5-(D-erythro--2,3,4-trihydroxybutyl)pyrazine], which have been identified as flavour compounds in some selected foods (including roasted soy sauce, nuts, and caramel) and are recognized to be the precursors of the aromatic volatile pyrazines [Hrynets *et al*., 2016]. Additionally, Maillard reaction compounds have been reported to possess some taste enhancing potentials [Hong, 2016]. Given that GlcN is capable of triggering a fast Maillard reaction with peptides or proteins at moderate temperature especially between 25 and 50°C, further makes this compound very attractive as flavour enhancer in an array of food applications [Dhungel *et al*., 2018]. In fact, GlcN can also undergo degradative reactions at 37°C forming reactive α-dicarbonyls (α-DCs) including glucosone, 3-deoxyglucosone, methylgyoxal, glyoxal and diacetyl which are important precursors of some desirable flavours [Hong, 2016; Hrynets *et al*., 2016].

Ascorbic acid (ASC) is a proven antioxidant widely used in meat processing although it can act either as pro- or antioxidant depending on the concentration, the presence of metal ion as well as the presence of other components [Schaefer *et al.,* 1995]. Several studies have reported the effectiveness of ascorbic acid in maintaining the stability of beef colour and lipid [Ahn & Nam, 2004; Sen *et al*., 2014]. Given that the colour of meat is considered the most important quality characteristics influencing consumer appeal and purchasing decision, several intervention strategies to prevent meat discoloration and oxidation have been proposed. However, the recent concerns about safety and consumers' heightened interest in natural antioxidant has resulted in more researchers exploring ascorbic acid as replacement for conventional antioxidants. This antioxidant enhances quality attributes of meat, prevents discoloration, and extends the shelf life significantly.

Following these aforementioned studies, aside from its acclaimed health benefits, it seems promising that GlcN can significantly enhance the flavour of meat products. However, the consequences of their inclusion on other important meat products' quality attributes remain unknown. The present study hence intends to evaluate the impact of GlcN and ASC addition on sensory and quality attributes of beef burger. Specific flavour effects of GlcN and ASC on beef burger will be examined. Other possible effects of the inclusion levels of these compounds on meat technological/processing attributes will also be considered.

MATERIALS AND METHODS

Burgers manufacturing

Fresh beef trimmings (shoulder clod and beef plates) were purchased from local processors. Glucosamine in the form of D-glucosamine hydrochloride and ascorbic acid were purchased from Pure Bulk Inc. (Roseburg, OR, United States). Commercially available toasted wheat crumb (Breader B34216 White #50, Newly Weds, Edmonton, AB, Canada) was produced and supplied by Newly Weds Foods (Edmonton, AB, Canada).

Five different burger formulations were processed on the same day at the Food Processing Development Centre in Leduc, Alberta, Canada (Table 1). Before processing, beef trimmings were separately ground *via* a 4 mm plate (Model AW114, K & G Wetter, Mississauga, ON, Canada). Samples were withdrawn from each batch of the ground beef and proximate composition analysis was conducted with the aid of Foss FoodScan analyzer (FoodScan Lab, Type 78800, FOSS, Hillerød, Denmark) according to the method of Anderson [2007]. Pre-determined quantities of ground beef, wheat crumb, spices (*i.e*. 0.8 g/100 g salt, 0.15 g/100 g onion powder, 0.1 g/100 g black pepper), water (12 g/100 g), and depending on specific treatment, ASC or GlcN were combined and mixed slowly in a mixer (A-200T, Hobart, Trot, OH, United States) for 45 s (Table 1). The overall weight of each treatment batch was 8 kg. The mixture was thereafter moulded into 140 g (5 oz) burger patties using a patty forming machine (Super 54 Patty machine, Hollymatic, Countryside, IL, United States).

Following burger forming, three burger patties from each treatment were packaged individually on Styrofoam® trays

TABLE 1. Burger treatment formulations.

Ingredient (g/100 g)	Control	ASC	0.75% GlcN	1.5% GlcN	3.0% GlcN
Ground beef	81.95	81.85	81.2	80.45	78.95
Water	12	12	12	12	12
Seasoning mix	1.05	1.05	1.05	1.05	1.05
Wheat crumb	5	5	5	5	5
Ascorbic acid	-	0.1	-	-	-
Glucosamine	-	-	0.75	1.5	3.0

ASC – ascorbic acid; GlcN – glucosamine.

enclosed with an O_2-permeable film (8,000 cm^3/m^2/24 h; Vitafilm, Huntsman Film Products of Canada, Toronto, ON, Canada). The burgers were then placed on double-tier display cabinet (MPM-72, Master-Bilt® Refigeration Solutions, Albany, MS, United States) kept at 4.0±1°C under 24 h fluorescent lighting with an average light intensity of 1,630 lx (CRI=85) to monitor instrumental colour change for 5 days. The rest of the burgers were packaged in cardboard boxes separated with plastic liners, frozen and stored at –20°C until subsequent analyses including sensory evaluation.

Evaluation of raw burgers during retail display

Instrumental colour evaluation of raw patties during retail display

Colour of beef patties was objectively assessed using a hand-held Minolta spectrophotometer (Minolta CM-2500C, Osaka, Japan) with a 10° observer angle, 8 mm aperture and illuminant A, after being calibrated against a white tile prior to readings being taken. Colour observations for lightness (L^* refers to light reflected), redness (a^* refers to positive red and negative green), and yellowness (b^* refers to positive yellow and negative blue) were taken daily for up to 5 days of simulated retail display under aerobic environments. The reported L^*, a^*, b^* values for each patty were average of six separate readings. Hue angle was also calculated as: $\tan^{-1}(b^*/a^*)$, and the saturation index (chroma) was calculated as: $(a^*2+b^*2)^{0.5}$.

Evaluation of patties following frozen storage

Cooking measurements

Cooking loss for the burger was evaluated following our previously described method [Pietrasik *et al.,* 2020]. Briefly, frozen patties were placed on an electric grill (Garland ED-42B electric broiler, Russell Food Equipment Ltd, Edmonton, AB, Canada) earlier pre-heated to 190°C. The patties were cooked on the grill while flipping every 3 min, until the internal temperature has reached 71°C. Following cooking, the cooked burgers were allowed to stand for 5 min at room temperature and weighed. Cooking loss was estimated based on the weight of the initial frozen patty. Diameter of each burger patty was measured for both raw and cooked patty in two directions at 90° angle to each other. The dimensional changes were assessed based on the initial diameter of the frozen patty. The diameter and thickness were determined using an electronic calliper. Two diameter readings were taken in two orthogonal directions and four thickness readings were taken 90° apart from each other from the bottom to the top. Means for each parameter of burger were used to calculate the dimensional shrinkage as:

$$\text{Dimensional shrinkage} = \frac{\text{raw thickness-cooked thickness + raw diameter-cooked diameter}}{\text{raw thickness+raw diameter}} \times 100\%$$

pH measurement

pH measurements for both raw and cooked products were performed in duplicate with a pH meter (Hanna Instruments FC240, Canadawide Scientific, Ottawa, ON, Canada). This was done by homogenizing 20 g sample in 80 mL deionized water as previously described by Pietrasik *et al.* [2016a]. pH was measured on this homogenized sample.

Textural properties

The textural attributes of beef burgers were evaluated according to texture profile analysis procedure (TPA) [Bourne, 1982] *via* an Instron texture system (Model 5565, Instron Corporation, Burlington, ON, Canada). Core samples of 22 mm diameter were excised from the center of each burger and compressed twice to 30% of their initial height with a 9 cm flat ended steel plunger at a constant cross-head speed of 60 mm/min. The TPA parameters; hardness (peak force on first compression (N)), cohesiveness (ratio of the active work done under the second force-displacement curve to that done under the first compression curve (dimensionless)), springiness (distance the sample recovered after the first compression (mm)), and chewiness (hardness × cohesiveness × springiness (N×mm)) were computed [Pietrasik *et al.,* 2016b].

The shear force analysis of cooked beef burgers was carried out for each treatment using an Instron texture system. Burgers were cooked as earlier described and allowed to cool down for about 1 h at room temperature. Thereafter, a 2.5 cm wide strip was cut from the middle of each burger patty, making sure that the edges of the burgers were avoided. Samples were sheared with a straight-edge blade fixture at three different sample locations using a crosshead speed of 250 mm/min. Results of shear force measurements were reported in N.

Consumer acceptability

Consumer sensory evaluations were performed at the Consumer Product Testing Centre (CPTC), Edmonton, Alberta, Canada. Exactly 108 consumer panelists (54 male and 54 female, age between 18 and 65) were recruited from the CPTC's consumer testing database with the eligibility criteria being that they are regular consumers of grilled beef burgers at least once per month. Consumer panelists were provided monetary compensation for their participation. During cooking, cook chart was drawn to randomize the placement of beef patties on the grill. After the burger reached the required internal temperature (71°C), patties were cut into 1/3 pieces, wrapped in foil, and placed into a 60°C environment chamber to maintain the temperature of the sample until served to panelists. Burgers were served between 1–10 min following cooking. Using a fully randomized block design, consumer panelists received the portioned piece of the patty monadically. The overall acceptability of cooked burger patty as well as the acceptability of appearance, flavour, texture and aftertaste was evaluated using 9-point hedonic scales (1 = dislike extremely, 9 = like extremely). A *Just-About-Right* (JAR) scaling was employed to provide additional understanding into acceptability results. JAR gauges the level of intensity that consumer panelists associate with each specific attribute and can assist in determining areas of opportunity for product improvement. JAR attributes were customized for both flavour and textural attributes. *Check-All-That-Apply* (CATA) was also used to capture the frequency of consumers' selection of various terms. Terms were generated by the Sensory Evaluation team to assist with targeted insight into certain areas of interest. Presentation of CATA terms was randomized

for each panelist, with the option provided for panelists to create their own CATA term(s). To avoid carryover of flavour, a 90 s break was ensured between sample presentation during which panelists cleaned their palate with unsalted crackers and room temperature water.

Statistical analysis

Three separate replications were conducted for this study. Processing and instrumental data were analysed using the PROC MIXED procedure of SAS (v. 9.1.3, SAS Institute Inc., Cary, NC, United States). The analyses included both the formulation treatment (the fixed) and the processing replication (random) effects. For colour stability data, a simulated retail display day was included in the model. For consumer panel data, XLSTAT (v.XLSTAT 2019.1.3.58109) was used for data analysis. Sensory evaluation day and panelists within each evaluation day were included in the analysis as random factors. Least-squares means were calculated for all main effects or interactions (where applicable) and means separation was done using the Tukey adjustment when the respective F-tests were significant at $p<0.05$. CATA frequency data for texture and flavour were also summarized in a contingency table and subjected to correspondence analysis using chi-square distances and only attributes that came out significant at $p<0.05$ were reported.

RESULTS AND DISCUSSION

Instrumental colour evaluation

The colour characteristics of raw meat and meat products largely influence consumer first appeal and overall acceptability of the product. No significant interaction was observed between storage period and treatments for L^* value, suggesting that lightness/brightness of burgers was not affected by the tested ingredients over duration of retail display. Although interactions were not significant for L^* value, the main effects were significant (Table 2). As aerobic display time increased, there was a gradual decline in L^* value, signifying darker meat with storage time. This result is consistent with progressive colour deterioration due to oxidation that could occur in meat or meat products with days in refrigerated storage [Ganhão *et al.,* 2010; Shivas *et al*., 1984]. Only ASC and 0.75% GlcN burgers had L^* values that were significantly different from each other ($p<0.01$) while L^* values for other treatments were similar. Given the similarities of these values however, the practical significance of this result may be very subtle.

There were significant ($p<0.05$) interactions between treatments and storage time for a^*, b^*, chroma (saturation index; how vivid or dull the colour is) and hue values (reflected wavelength or colour as seen by the eyes; larger value indicates less red and more metmyoglobin), indicating that color stability was affected by addition of ingredients (Figure 1A-D). Burgers formulated with ASC maintained the highest a^* values (*i.e*., a brightest red colour) for much longer period compared to control and those processed with GlcN. With ASC treatment, the significant reduction in burger red colour was observed only after day 4 of storage, whereas, a more rapid discolouration was observed in the other treatments where a significant colour change occurred as early as on day 1 (in 1.5% GlcN) or day 2 (in control, 0.75% and 3.0% GlcN) (Figure 1A). Similar pattern was observed with other colour parameters where significant change in b^*, chroma and hue was only evident on day 4 or 5 in ASC treatment whereas these changes occurred rapidly on day 1 or 2 in control and other GlcN treatments. This result further highlights the reports from other studies which showed the effectiveness of ascorbic acid in preventing the oxidation of oxymyoglobin to metmyoglobin, evading rapid meat discoloration [Ahn & Nam, 2004; Ismail *et al.,* 2009; Mitsumoto *et al*., 1991a,b]. Generally, there was a tendency for faster discoloration with increased incorporation level of GlcN leading to decreasing a^*, b^* and chroma as well as increasing hue value in the burger. This could simply be due to the impact of the colour of GlcN solution itself. Moreover, while GlcN has been reported to show some antioxidant activity [Xing *et al*., 2006] in some food systems, its ability to also generate reactive oxygen species during incubation [Hrynets *et al*., 2016] may also suggest some prooxidative factors that could result in oxidative instability of myoglobin as observed in this study and is also worth exploring. It is possible that, depending on the nature of food, the level of inclusion as well as the nature of GlcN in food system, it could serve as either antioxidant or a prooxidant. While this may be speculative to a large extent, the underlining chemistry of this change requires future exploration.

TABLE 2. Lightness (L^*) value of fresh burgers as a function of refrigeration time and glucosamine (GlcN) inclusion level and ascorbic acid (ASC) addition.

	L^* value
Treatment	
Control	53.3^{ab}
ASC	52.3^{b}
0.75% GlcN	53.7^{a}
1.5% GlcN	53.3^{ab}
3.0% GlcN	52.5^{ab}
SEM	0.38
p-value	*0.01*
Storage time (days)	
0	54.0^{a}
1	53.9^{a}
2	53.8^{ab}
3	52.4^{c}
4	52.2^{c}
5	51.9^{c}
SEM	0.40
p-value	*<0.01*

$^{a-f}$Means with different letter in the same column are significantly different at $p<0.01$. SEM – standard error of the mean.

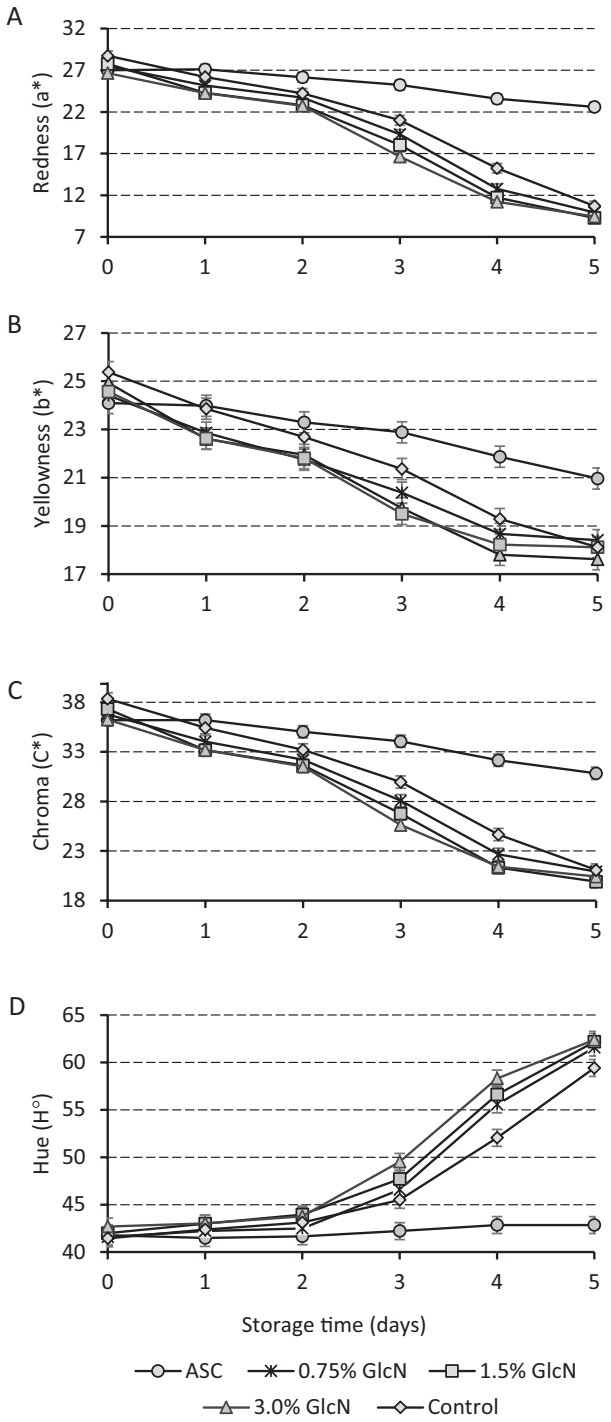

FIGURE 1. Instrumental colour measurements of beef burgers with glucosamine (GlcN) and ascorbic acid (ASC) inclusion levels and time during refrigerated retail display for 5 days under aerobic packaging. A) redness; B) yellowness; C) chroma and D) hue angle. Values are expressed as means of three independent determinations ± standard deviation.

Cooking and textural characteristics of beef patties

Of all the burger treatments, the highest cook loss was recorded in ASC samples followed by wheat crumb controls and those processed with 0.75% GlcN ($p<0.05$, Table 3). Generally speaking, although other factors can also play a role, pH has been regarded as a crucial factor in the meat ability to hold water [Bendall & Swatland, 1988]. This is because pH can influence both the net charge and the steric effects in meat system, the additive effect of which can impact meat water holding capacity (WHC). The low pH of raw ASC treatment (Table 4) can explain the high cook loss reported for this formulation (Table 3). The addition of ASC to the formulation led to more acidic environment which could bring the pH of meat protein close to its isoelectric point. This mechanism will result in reduced net charge on meat protein that could bind water molecules. The consequence is the reduced WHC and greater cook loss. Although antioxidants would be expected to limit oxidative changes and as such, improve water holding capacity and reduce cooking loss in meat system, the net charge effect due to reduced pH could have overpowered its subsequent protective effects. While the effect of ASC on cooking loss in beef has been scarcely reported, similar to the present study, Mitsumoto *et al*. [1995] have reported increased cooking loss in *longissimus dorsi* from cattle fed dietary vitamin E supplementation. A previous study by Mancini *et al*. [2015] however, found no significant difference in cooking loss between ASC and control treatments of rabbit burgers whereas, Peña *et al*. [2008] showed that increasing supplementation of ascorbic acid for broilers led to increasing cooking loss in broilers' breasts. It also seems consistent that, while antioxidant supplementation may improve drip loss and WHC in raw meat, this protective effect may be lost during subsequent meat cooking.

On the other hand, cooking losses were found to significantly decrease with increasing GlcN levels in burger formulations (Table 3). Thus, the more GlcN added, the less weight was lost during cooking. This could be explained by elevated ionic charges with increased addition of GlcN in burger system. Puolanne & Halonen [2010] have previously reported that one amino acid of an ionic side chain could bind up to 4–7 water molecules. This higher concentration of ions will increase the solute concentration that may enhance water trapping in the burger system during cooking. Furthermore, the addition of GlcN to burger formulation appeared to enhance more protein extraction which may also support the elevated ionic charge with GlcN addition to the meat mixture. While this was not objectively quantified in this study, it was visually evident as GlcN led to increased stickiness of beef burger mixture during formulation and processing. Also, the increased GlcN in the meat system could have also resulted in elevated levels of hydroxyl hydrophilic groups which have the potential to attract more water molecules, further enhancing water retention during cooking. As observed, burgers with 1.5 and 3.0% GlcN also had significantly lower shrinkage for all dimensional parameters evaluated following cooking compared to all other treatment groups (Table 3). This signifies the potential of GlcN to enhance water holding capacity and increase yield in meat products on cooking.

The burgers formulated with GlcN were significantly ($p<0.05$) softer as compared to controls processed with wheat crumb (Table 5). As previously explained and also evident with pH change with GlcN addition in cooked burger (Table 4), GlcN could have shifted the isoelectric point of protein in beef burger making more similar electric charges available to trap/immobilize water molecules. The repulsive energy created by these like charges may also create more structural spaces for water holding [Huff-Lonergan & Lonergan, 2005].

TABLE 3. Cook loss and dimensional parameters for cooked beef burgers as affected by glucosamine (GlcN) and ascorbic acid (ASC) inclusion.

Treatment	Cook loss (%)	Diameter change (%)	Thickness change (%)	Total dimensional change (%)
Control	30.2[b]	16.7[a]	12.1[a]	14.3[ab]
ASC	33.3[a]	16.6[a]	14.6[a]	15.6[a]
0.75% GlcN	29.7[b]	16.4[a]	12.9[a]	14.6[ab]
1.5% GlcN	25.3[c]	14.1[b]	12.6[a]	13.4[b]
3.0% GlcN	19.0[d]	12.2[c]	8.6[b]	10.4[c]
SEM	1.94	1.53	2.85	1.54
p-value	<0.01	<0.01	<0.01	<0.01

[a-d]Means with different letter in the same column are significantly different at $p<0.01$. SEM – standard error of the mean.

TABLE 4. pH values of raw and cooked burgers with glucosamine (GlcN) and ascorbic acid (ASC) inclusion.

Treatment	Raw	Cooked
Control	5.70[a]	5.88[a]
ASC	5.54[c]	5.73[b]
0.75% GlcN	5.66[b]	5.67[b]
1.5% GlcN	5.65[b]	5.54[c]
3.0% GlcN	5.64[b]	5.23[d]
SEM	0.02	0.01
p-value	<0.01	<0.01

[a-d]Means with different letter in the same column are significantly different at $p<0.01$. SEM – standard error of the mean.

The effect of these processes had both textural and water binding implication of the beef burger in this study resulting in softer product. Hardness values showed a decreasing trend as the GlcN incorporation level increased from 0.75 to 3.0%. Chewiness results followed a similar pattern with control burgers being the chewiest and with gradual decrease in chewiness with increased addition of GlcN. Neither ASC nor GlcN affected ($p>0.05$) cohesiveness or shear force of beef burgers, whereas the treatments containing ASC or 0.75% GlcN had the lowest or highest ($p<0.05$) springiness, respectively. Springiness however, tended to decrease with an increased incorporation of GlcN (Table 5). It is worth noting that, while cooking typically results in increased pH as observed for both ASC and control treatments (Table 4), addition of GlcN disrupted this trend. This disruption could be due to the degradation products of GlcN during heat treatment. Previous reports have also reported the reduction of pH values during GlcN thermal degradation [Hrynets *et al.*, 2015; 2016; Dhungel *et al*., 2018]. This observation was claimed to be due to the formation of carboxylic and hydrocarboxylic acids during monosaccharide decomposition. Other studies have also reported the formation of acetic and formic acid due to the splitting of 1- and 3-deoxyglucosone, respectively [Brands & van Boekel, 2001].

Consumer acceptability of burgers

The overall acceptability for burgers formulated with increasing levels of GlcN was only significantly affected at the 3.0% level GlcN (Figure 2). Similar result was observed for flavour, texture and aftertaste liking (results not shown). At this 3.0% level of GlcN inclusion, consumers' liking for these attributes significantly decreased. Although other studies have reported tendency for improved flavour enhancement of food product with GlcN inclusion [Hong *et al*., 2016], similar observation was not evident for consumer flavour attributes liking of beef burger in this study. This could be due to the fact

TABLE 5. Textural properties for cooked burger as affected by glucosamine (GlcN) and ascorbic acid (ASC) addition.

Treatment	Hardness (N)	Cohesiveness	Springiness (mm)	Chewiness (N×mm)	Shear force (N)
Control	114.9[a]	0.26	6.1[b]	187.5[a]	23.1
ASC	107.3[ab]	0.28	5.8[c]	172.4[ab]	21.9
0.75% GlcN	100.5[bc]	0.26	6.4[a]	170.0[ab]	21.5
1.5% GlcN	93.7[cd]	0.28	6.2[ab]	159.2[b]	22.3
3.0% GlcN	86.8[d]	0.27	6.1[b]	145.5[b]	23.9
SEM	8.72	0.02	0.17	16.76	2.23
p-value	<0.01	0.08	<0.01	<0.01	0.28

[a-d]Means with different letter in the same column are significantly different at $p<0.01$. SEM – standard error of the mean.

that all treatments had similar levels of seasoning mix minimizing the impact of GlcN. Furthermore, the flavour enhancing claims from GlcN have been largely attributed to its self-condensation products; fructosazine and deoxyfructosazine as well as degradation products such as α-dicarbonyls [Hrynets *et al*., 2016; Magaletta & Ho, 1996; Tsuchida *et al*., 1990], and optimal conditions to enhance these reactions may not have been achieved in this study. Also, the impact may vary between different model food systems. A recent result from our laboratory has shown an increased consumer flavour liking score when glucosamine and glucosamine caramel (1%) were added to breakfast sausage compared to control samples [Soladoye *et al.,* 2021]. A recent study has also shown that glycation by GlcN can alter the taste profile of protein hydrolysates further highlighting the potential impact of GlcN on sensory attributes of food products [Fu *et al.*, 2020].

Upon further exploration of the consumer acceptability rating of these burger formulations using the *Check-All-That--Apply* procedure, it became evident that the decrease in consumer liking was the combination of deteriorating texture (as described in previous section) as well as flavour attributes. Figure 3a and Figure 3b, respectively, showed the flavour and texture variables that were selected by consumer to describe the different burger treatments. Employing a factor analysis for all the selected attributes, two factors that, respectively explained up to 95 and 89% of the variation in flavour and texture attributes in the burgers were computed. Factor 1 that explained up to 91% of flavour attributes adequately separated 3.0% GlcN from the other treatments and was largely associated with attributes such as bitter, tangy, off-flavour as well as some unacceptable sweetness level and fruity note (Figure 3a). Other burger treatments (especially the controls, ASC and 0.75% GlcN) formed a cluster with descriptors such as "good beef flavour", "tasty", "grilled flavour", and "spicy/seasoning". Attributes such as "metallic", "bland", "salty" and "livery" were not statistically significant based on consumer selection and as such did not impact the overall acceptability of any of the burger treatment. According to penalty analysis, up to 53% of the panelists were averse to the too sweet, too sour and low beef flavour of 3.0% GlcN burgers.

Texture descriptors associated with 3.0% GlcN include "greasy" and "rubbery" while the other treatments were largely described as "beefy", "crumbly" and "granular" texture (Figure 3b). Other textural attributes did not significantly affect consumer acceptability of the products. This was also evident in the penalty analysis where up 56 and 36% of the panelists, respectively adjudged the 3.0% GlcN burgers as too much fatty/oily mouth coating and too soft firmness, significantly decreasing the products' overall acceptability score (Table 6).

Similarly, on the *Just-About-Right* (JAR) scale, between 33 and 53% of the panelists described the saltiness, sweetness and sourness of 3.0% GlcN as "too strong" while up to 54% of the panelists described the burger's beefy flavour as "too weak" (Table 7). On the other hand, between 50 and 73% of the consumer panelists described saltiness, sweetness and sourness of other treatments as JAR. While the overall beef flavour in the treatment has been penalized as being too weak, the beef flavour attribute of the 3.0% GlcN has been described as JAR by the least number of consumers (22%), with significantly higher penalty. It is important to note that, the magnitude of the penalty generally increases with an

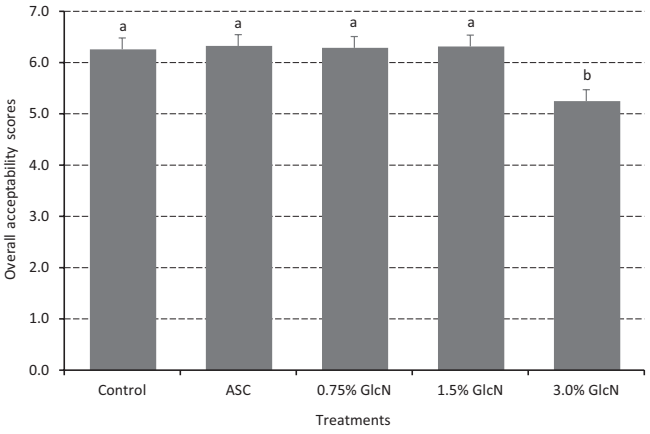

FIGURE 2. Mean consumer scores for overall acceptability of beef burger with varying levels of glucosamine (GlcN) and (ascorbic acid) ASC inclusion; [a-b]Means with different letter on the same bar are significantly different at $p<0.001$.

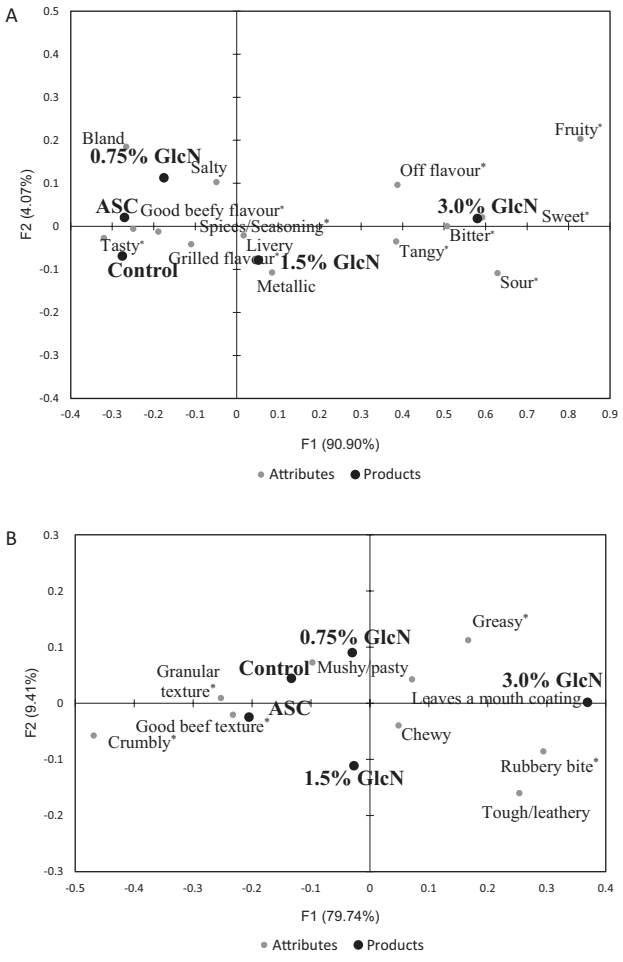

FIGURE 3. *Check-All-That-Applies* analyses for A) flavour and B) texture attributes defined by consumers as affected by glucosamine (GlcN) and ascorbic acid (ASC) inclusion. Only attributes with asterisks were significant at $p<0.05$.

TABLE 6. Penalty analysis and mean drop for texture attributes of beef burgers with glucosamine (GlcN) and ascorbic acid (ASC).

	Levels	Control		ASC		0.75% GlcN		1.5% GlcN		3.0% GlcN	
		Selection %[1]	Mean OA[2]	Selection %	Mean OA	Selection %	Mean OA	Selection %	Mean OA	Selection %	Mean OA
Firmness	Too soft	23.2	4.4***	27.8	4.6***	28.7	4.5***	15.7	4.5	36.1	3.9***
	JAR	56.5	6.5	53.7	6.7	48.2	6.7	56.5	6.7	43.5	6.0
	Too firm	20.4	5.1**	18.5	5.4	23.2	5.4**	27.8	5.5**	20.4	4.4**
Overall penalty		1.785***		1.750***		1.725***		1.567***		1.913***	
Juiciness	Too dry	26.9	5.3*	21.3	5.3*	23.2	5.1	25.0	5.3*	13.0	4.5
	JAR	53.7	6.1	68.5	6.3	50.0	5.9	57.4	6.3	46.3	5.2
	Too juicy	19.4	5.2	10.2	4.3	26.9	6.0	17.6	6.4	40.7	4.7
Overall penalty		0.878*		1.370**		0.333		0.551		1.285	
Fatty/Oily mouth coating	Too little	9.3	5.1	15.7	5.1	16.7	5.6	14.8	5.1	7.4	4.1
	JAR	48.2	6.1	51.9	6.4	38.0	6.1	50.9	6.5	37.0	5.5
	Too much	42.6	5.4	32.4	5.5*	45.4	5.6	34.3	5.8	55.6	4.6*
Overall penalty		0.740*		0.992**		0.467		0.924*		0.956*	

[1]Selection %: The percentage of consumers corresponding to the different collapsed *Just-About-Right* (JAR) levels; [2]Mean OA; Mean overall acceptability corresponding to each JAR levels. ***mean drop with level of significance <0.001, **mean drop with level of significance between 0.001 and 0.01 and *mean drop with level between significance >0.01 and <0.05.

TABLE 7. Penalty analysis and mean drop for flavour/taste attributes of beef burgers with glucosamine (GlcN) and ascorbic acid (ASC).

	Levels	Control		ASC		0.75% GlcN		1.5% GlcN		3.0% GlcN	
		Selection %[1]	Mean OA[2]	Selection %	Mean OA	Selection %	Mean OA	Selection %	Mean OA	Selection %	Mean OA
Beef flavour	Too strong	35.2	6.6	45.4	6.7	41.7	6.6	36.1	6.7	24.1	6.3
	JAR	38.9	7.0	31.5	6.7	31.5	6.7	39.8	6.9	22.2	7.1
	Too weak	25.9	5.4***	23.2	5.1**	26.9	5.3**	24.1	4.9***	53.7	3.8***
Overall penalty		0.870**		0.557		0.627		0.907*		2.542***	
Saltiness	Too strong	19.4	6.0	25.9	5.5***	34.3	5.6***	28.7	5.9*	33.3	4.3**
	JAR	64.8	6.8	61.1	6.8	50.0	7.2	58.3	6.8	43.5	6.2
	Too weak	15.7	5.7	13.0	5.8	15.7	5.1	13.0	4.9	25.1	4.3**
Overall penalty		0.929**		1.193***		1.685***		1.263***		1.923***	
Sweetness	Too strong	10.2	5.8	11.1	5.0	19.4	5.6	28.7	5.7*	52.8	4.4***
	JAR	68.5	6.7	63.9	6.6	57.4	6.8	50.0	6.7	33.3	6.7
	Too weak	21.3	5.9*	25.0	6.2	23.2	5.6**	21.3	6.3	13.9	4.4
Overall penalty		0.820*		0.828*		1.214***		0.741*		2.319***	
Sourness	Too strong	11.1	5.4	11.1	4.8	17.6	5.4	30.6	5.1***	52.8	4.1***
	JAR	73.2	6.8	72.2	6.6	67.6	6.6	61.1	6.9	35.2	6.8
	Too weak	15.7	5.7	16.7	6.1	14.8	5.9	8.3	6.7	12.0	4.9
Overall penalty		1.220**		1.049**		0.959		1.489**		2.614***	

[1]Selection %: The percentage of consumers corresponding to the different collapsed *Just-About-Right* (JAR) levels; [2]Mean OA; Mean overall acceptability corresponding to each JAR levels. ***mean drop with level of significance <0.001, **mean drop with level of significance between 0.001 and 0.01 and *mean drop with level between significance >0.01 and <0.05.

increasing level of GlcN (Table 7). The firmness and juiciness of all other burger formulations except 3.0% GlcN have been largely described by panelists (48–69%) as JAR while between 41 and 56% of the panelists described 3.0% GlcN as too juicy and too much oily mouth coating. It therefore seems reasonable to conclude that excessive inclusion of glucosamine above 1.5% in burger formulation may be detrimental to the texture and greasy/oily attributes of the product as well as resulting in tangy, sour and off--flavoured burger, leading ultimately to consumer rejection of the product.

The impact of GlcN addition on the appearance liking of GlcN burgers was not significantly different from ASC and control treatment. Given that all the treatments were ranked between 6.0 and 6.6 on a 9-point hedonic scale, it generally seems that the appearance of burgers was more influenced by the variation inherent in the cooking process rather than the subjected treatments.

CONCLUSION

Aside from the health benefits of GlcN, which could qualify meat with GlcN as functional food, its moderate inclusion in various meat products formulation may also provide some technological advantages. GlcN may enhance meat products' water holding capacity and overall yield. While this may be beneficial to certain extent, inclusion above 1.5% may negatively affect consumer overall acceptability as a result of texture and flavour deterioration. In addition, GlcN may have impact on colour stability of meat products during refrigerated storage, however, this does not seem to affect consumer overall acceptability as this effect becomes irrelevant following cooking. Ascorbic acid preserved the colour attributes of beef burgers during refrigerated storage. It remains to be assessed if the colour change with GlcN will influence consumer first appeal of the raw/fresh products and hence, subsequent purchase. Given the novelty of this ingredient in meat application, other studies are still required to evaluate important technological impact of glucosamine in meat processing and quality.

ACKNOWLEDGEMENTS

Authors are grateful to the technical staff at the Food Processing Development Centre for their assistance.

RESEARCH FUNDING

The financial support by the Alberta Agriculture and Forestry's Strategic Research & Development Program is greatly appreciated by the authors.

CONFLICT OF INTEREST

None to declare.

ORCID IDs

M. Betti https://orcid.org/0000-0002-4256-7174
P.O. Soladoye https://orcid.org/0000-0002-4446-2149

REFERENCES

1. Ahn, D.U., Nam, K.C. (2004). Effects of ascorbic acid and antioxidants on color, lipid oxidation and volatiles of irradiated ground beef. *Radiation Physics and Chemistry, 71*(1–2), 151–156. https://doi.org/10.1016/j.radphyschem.2004.04.012
2. Anderson, S. (2007). Determination of fat, moisture, and protein in meat and meat products by using the FOSS FoodScan near--infrared spectrophotometer with FOSS artificial neural network calibration model and associated database: collaborative study. *Journal of AOAC International, 90*(4), 1073–1083. https://doi.org/10.1093/jaoac/90.4.1073
3. Bendall, J.R., Swatland, H.J. (1988). A review of the realtionship of pH with physical aspects of pork quality. *Meat Science*, *24*, 85–126. https://doi.org/10.1016/0309-1740(88)90052-6
4. Bourne, M.C. (Ed.) (1982). Texture, viscosity and food. *Food Texture and Viscosity*, Academic Press, pp. 1–23. https://doi.org/10.1016/B978-0-12-119060-6.50006-X
5. Brands, C.M., van Boekel, M.A. (2001). Reactions of monosaccharides during heating of sugar−casein systems: Building of a reaction network model. *Journal of Agricultural and Food Chemistry, 49*(10), 4667–4675. https://doi.org/10.1021/jf001430b
6. Bruyere, O., Reginster, J.Y. (2007). Glucosamine and chondroitin sulfate as therapeutic agents for knee and hip osteoarthritis. *Drugs & Aging, 24*(7), 573–580. https://doi.org/10.2165/00002512-200724070-00005
7. Chan, D.S.M., Lau, R., Aune, D., Vieira, R., Greenwood, D.C., Kampman, E., Norat, T. (2011). Red and processed meat and colorectal cancer incidence: meta-analysis of prospective studies. *PloS One, 6*(6), art. no. e20456. https://doi.org/10.1371/journal.pone.0020456
8. Dhungel, P., Hrynets, Y., Betti, M. (2018). *Sous-vide* non-enzymatic browning of glucosamine at different temperatures. *Journal of Agricultural and Food Chemistry*, *66*(17), 4521–4530. https://doi.org/10.1021/acs.jafc.8b01265
9. Fu, Y., Liu, J., Zhang, W., Wæhrens, S.S., Tøstesen, M., Hansen, E.T., Bredie, W.L.P., Lametsch, R. (2020). Exopeptidase treatment combined with Maillard reaction modification of protein hydrolysates derived from porcine muscle and plasma: Structure–taste relationship. *Food Chemistry, 306*, art. no. 125613. https://doi.org/10.1016/j.foodchem.2019.125613
10. Ganhão, R., Morcuende, D., Estévez, M. (2010). Protein oxidation in emulsified cooked burger patties with added fruit extracts: Influence on colour and texture deterioration during chill storage. *Meat Science, 85*(3), 402–409. https://doi.org/10.1016/j.meatsci.2010.02.008
11. Gottardi, D., Hong, P.K., Ndagijimana, M., Betti, M. (2014). Conjugation of gluten hydrolysates with glucosamine at mild temperatures enhances antioxidant and antimicrobial properties. *LWT – Food Science and Technology, 57*(1), 181–187. https://doi.org/10.1016/j.lwt.2014.01.013
12. Hong, P.K. (2016). Non-enzymatic browning in glucosamine and glucosamine-peptides reaction systems as a source of antioxidant and flavouring compounds. *Doctoral Dissertation*. University of Alberta, pp. 164 [https://era.library.ualberta.ca/items/6fca2b48–4f56–4f39–9298–8e5f32618675].

13. Hong, P.K., Betti, M. (2016). Non-enzymatic browning reaction of glucosamine at mild conditions: Relationship between colour formation, radical scavenging activity and α-dicarbonyl compounds production. *Food Chemistry, 212*, 234–243. https://doi.org/10.1016/j.foodchem.2016.05.170
14. Hong, P.K., Ndagijimana, M., Betti, M. (2016). Glucosamine--induced glycation of hydrolysed meat proteins in the presence or absence of transglutaminase: Chemical modifications and taste--enhancing activity. *Food Chemistry, 197*, 1143–1152. https://doi.org/10.1016/j.foodchem.2015.11.096
15. Hrynets, Y., Bhattacherjee, A., Ndagijimana, M., Hincapie Martinez, D.J., Betti, M. (2016). Iron (Fe^{2+})-catalyzed glucosamine browning at 50° C: identification and quantification of major flavor compounds for antibacterial activity. *Journal of Agricultural and Food Chemistry, 64*(16), 3266–3275. https://doi.org/10.1021/acs.jafc.6b00761
16. Hrynets, Y., Ndagijimana, M., Betti, M. (2015). Studies on the formation of Maillard and caramelization products from glucosamine incubated at 37°C. *Journal of Agricultural and Food Chemistry*, *63*, 6249–6261. https://doi.org/10.1021/acs.jafc.5b02664
17. Hrynets, Y., Ndagijimana, M., Betti, M. (2013). Non-enzymatic glycation of natural actomyosin (NAM) with glucosamine in a liquid system at moderate temperatures. *Food Chemistry, 139*(1–4), 1062–1072. https://doi.org/10.1016/j.foodchem.2013.02.026
18. Huff-Lonergan, E., Lonergan, S.M. (2005). Mechanisms of water-holding capacity of meat: The role of *postmortem* biochemical and structural changes. *Meat Science, 71*(1), 194–204. https://doi.org/10.1016/j.meatsci.2005.04.022
19. Ismail, H.A., Lee, E.J., Ko, K., Paik, H.D., Ahn, D.U. (2009). Effect of antioxidant application methods on the color, lipid oxidation, and volatiles of irradiated ground beef. *Journal of Food Science, 74*(1), C25-C32. https://doi.org/10.31274/ans_air-180814-1036
20. Jia, L., Wang, Y., Qiao, Y., Qi, Y., Hou, X. (2014). Efficient one-pot synthesis of deoxyfructosazine and fructosazine from D-glucosamine hydrochloride using a basic ionic liquid as a dual solvent-catalyst. *RSC Advances, 4*(83), 44253–44260. https://doi.org/10.1039/C4RA06832G
21. Kralovec, J.A., Barrow, C.J. (2007). Glucosamine production and health benefits. In: C. Barrow, F. Shahidi (Eds.). *Marine Nutraceuticals and Functional Foods*, CRC Press, pp. 197–229. https://doi.org/10.1201/9781420015812.ch8
22. Magaletta, R.L., Ho, C.T. (1996). Effect of roasting time and temperature on the generation of nonvolatile (polyhydroxyalkyl) pyrazine compounds in peanuts, as determined by high--performance liquid chromatography. *Journal of Agricultural and Food Chemistry, 44*(9), 2629–2635. https://doi.org/10.1021/jf960148v
23. Mancini, S., Preziuso, G., Dal Bosco, A., Roscini, V., Szendrő, Z., Fratini, F., Paci, G. (2015). Effect of turmeric powder (*Curcuma longa* L.) and ascorbic acid on physical characteristics and oxidative status of fresh and stored rabbit burgers. *Meat Science, 110*, 93–100. https://doi.org/10.1016/j.meatsci.2015.07.005
24. McAlindon, T.E., LaValley, M.P., Gulin, J.P., Felson, D.T. (2000). Glucosamine and chondroitin for treatment of osteoarthritis: a systematic quality assessment and meta-analysis. *JAMA, 283*(11), 1469–1475. https://doi.org/10.1001/jama.283.11.1469
25. Micha, R., Wallace, S.K., Mozaffarian, D. (2010). Red and processed meat consumption and risk of incident coronary heart disease, stroke, and diabetes mellitus: a systematic review and meta--analysis. *Circulation, 121*(21), 2271–2283. https://doi.org/10.1161/CIRCULATIONAHA.109.924977
26. Mitsumoto, M., Arnold, R.N., Schaefer, D.M., Cassens, R.G. (1995). Dietary vitamin E supplementation shifted weight loss from drip to cooking loss in fresh beef *longissimus* during display. *Journal of Animal Science, 73*(8), 2289–2294. https://doi.org/10.2527/1995.7382289x
27. Mitsumoto, M., Cassens, R.G., Schaefer, D.M., Arnold, R.N., Scheller, K.K. (1991a). Improvement of color and lipid stability in beef *longissimus* with dietary vitamin E and vitamin C dip treatment. *Journal of Food Science, 56*(6), 1489–1492. https://doi.org/10.1111/j.1365-2621.1991.tb08622.x
28. Mitsumoto, M., Faustman, C., Cassens, R.G., Arnold, R.N., Schaefer, D.M., Scheller, K.K. (1991b). Vitamins E and C improve pigment and lipid stability in ground beef. *Journal of Food Science, 56*(1), 194–197. https://doi.org/10.1111/j.1365-2621.1991.tb08010.x
29. Peña, J.E.M., Vieira, S.L., López, J., Reis, R.N., Barros, R., Furtado, F.V.F., Silva, P.X. (2008). Ascorbic acid and citric flavonoids for broilers under heat stress: effects on performance and meat quality. *Revista Brasileira de Ciência Avícola, 10*(2), 125–130. https://doi.org/10.1590/S1516-635X2008000200008
30. Puolanne, E., Halonen, M. (2010). Theoretical aspects of water--holding in meat. *Meat Science, 86*(1), 151–165. https://doi.org/10.1016/j.meatsci.2010.04.038
31. Pietrasik, Z., Gaudette, N.J., Johnston, S.P. (2016a). The use of high pressure processing to enhance the quality and shelf life of reduced sodium naturally cured restructured cooked hams. *Meat Science, 116*, 102–109. https://doi.org/10.1016/j.meatsci.2016.02.009
32. Pietrasik, Z., Gaudette, N.J., Klassen, M. (2016b). Effect of hot water treatment of beef trimmings on processing characteristics and eating quality of ground beef. *Meat Science, 113*, 41–50. https://doi.org/10.1016/j.meatsci.2015.11.011
33. Pietrasik, Z., Sigvaldson, M., Soladoye, O.P., Gaudette, N.J. (2020). Utilization of pea starch and fibre fractions for replacement of wheat crumb in beef burgers. *Meat Science, 161*, art. no. 107974. https://doi.org/10.1016/j.meatsci.2019.107974
34. Salvatore, S., Heuschkel, R., Tomlin, S., Davies, S.E., Edwards, S., Walker-Smith, J.A., French, I., Murch, S.H. (2000). A pilot study of *N*-acetyl glucosamine, a nutritional substrate for glycosaminoglycan synthesis, in paediatric chronic inflammatory bowel disease. *Alimentary Pharmacology & Therapeutics, 14*(12), 1567–1579. https://doi.org/10.1046/j.1365-2036.2000.00883.x
35. Schaefer, D.M., Liu, Q., Faustman, C., Yin, M.C. (1995). Supranutritional administration of vitamins E and C improves oxidative stability of beef. *The Journal of Nutrition, 125*(suppl_6), 1792S-1798S. https://doi.org/10.1093/jn/125.suppl_6.1792S
36. Sen, A.R., Muthukumar, M., Naveena, B.M., Ramanna, D.B.V. (2014). Effects on colour characteristics of buffalo meat dur-

ing blooming, retail display and using vitamin C during refrigerated storage. *Journal of Food Science and Technology, 51*(11), 3515–3519. https://doi.org/10.1007/s13197-012-0882-x

37. Shivas, S.D., Kropf, D.H., Hunt, M.C., Kastner, C.L., Kendall, J.L.A., Dayton, A.D. (1984). Effects of ascorbic acid on display life of ground beef. *Journal of Food Protection, 47*(1), 11–15. https://doi.org/10.4315/0362-028X-47.1.11
38. Soladoye, O.P., Pietrasik, Z., Hrynets, Y., Betti, M. (2021). The effect of glucosamine and glucosamine caramel on quality and consumer acceptability of regular and reduced salt breakfast sausages. *Meat Science, 172*, art. no. 108310. https://doi.org/10.1016/j.meatsci.2020.108310
39. Tsuchida, H., Komoto, M., Mizuno, S. (1990). Isolation and identification of polyhydroxyalkylpyrazines in soy sauce. *Nippon Shokuhin Kogyo Gakkaishi, 37*(2), 154–161. https://doi.org/10.3136/nskkk1962.37.154
40. Uzzan, M., Nechrebeki, J., Labuza, T.P. (2007). Thermal and storage stability of nutraceuticals in a milk beverage dietary supplement. *Journal of Food Science, 72*(3), E109-E114. https://doi.org/10.1111/j.1750-3841.2007.00284.x
41. Uğraş, A., Güzel, E., Korkusuz, P., Kaya, İ., Dikici, F., Demirbaş, E., Çetinus, E. (2013). Glucosamine-sulfate on fracture healing. *Ulus Travma Acil Cerrahi Derg, 19*(1), 8–12. https://doi.org/10.5505/tjtes.2013.03256
42. Xing, R., Liu, S., Guo, Z., Yu, H., Li, C., Ji, X., Feng, J., Li, P. (2006). The antioxidant activity of glucosamine hydrochloride *in vitro*. *Bioorganic & Medicinal Chemistry, 14*(6), 1706–1709. https://doi.org/10.1016/j.bmc.2005.10.018
43. Zhu, A., Huang, J.B., Clark, A., Romero, R., Petty, H.R. (2007). 2, 5-Deoxyfructosazine, a D-glucosamine derivative, inhibits T-cell interleukin-2 production better than D-glucosamine. *Carbohydrate Research, 342*(18), 2745–2749. https://doi.org/10.1016/j.carres.2007.08.025

Pol. J. Food Nutr. Sci., 2021, Vol. 71, No. 4, pp. 423–440
On-line ISSN: 2083-6007
Print ISSN: 1230-0322
DOI: 10.31883/pjfns/143057
http://journal.pan.olsztyn.pl

Original article
Section: Nutrition

Strawberry Polyphenol-Rich Fractions Can Mitigate Disorders in Gastrointestinal Tract and Liver Functions Caused by a High-Fructose Diet in Experimental Rats

Ewa Żary-Sikorska[1], Bartosz Fotschki[2], Monika Kosmala[3], Joanna Milala[3], Paulius Matusevicius[4], Aleksandra Rawicka[5], Jerzy Juśkiewicz[2]*

[1]Department of Microbiology and Food Technology, Faculty of Agriculture and Biotechnology, Bydgoszcz University of Science and Technology, Kaliskiego 7, 85–796 Bydgoszcz, Poland
[2]Department of Biological Functions of Food, Institute of Animal Reproduction and Food Research of the Polish Academy of Sciences, Tuwima 10, 10–748 Olsztyn, Poland
[3]Institute of Food Technology and Analysis, Łódź University of Technology, Stefanowskiego 4/10, 90–924 Łódź, Poland
[4]Department of Animal Nutrition, Lithuanian University of Health, Kaunas, Tilzes 18, LT-47181 Kaunas, Lithuania
[5]Policlinico Veterinario Roma Sud, Ophthalmology, 00173 Rome, Italy

Key words: rat model, strawberry, bioactive compounds, anthocyanins, ellagitannins, gastrointestinal tract

In the current study, it was hypothesized that the addition of strawberry polyphenol-rich fractions to a high-fructose diet mitigates disorders in liver functions, lipid metabolism, and in the antioxidant and pro-inflammatory status of rats. Therefore, a fraction rich in ellagitannins and proanthocyanidins (EP), and a fraction containing compounds of both mentioned classes of polyphenols and additionally anthocyanins (EPA), in doses of 0.28 and 0.70 g/100 g, respectively, were added to a standard or a high-fructose diet administered to rats for six weeks. The EPA fraction was more beneficial in alleviating the consequences of consuming excess fructose in the diet than the EP fraction. Probably, that fraction containing considerable amounts of carbohydrates was more extensively metabolized by intestinal bacteria, which resulted in higher levels of cecal short chain fatty acids (SCFAs) as well as cecal and urinal ellagitannin metabolites. As a further consequence, diet supplementation with the EPA fraction caused more favorable changes in the levels of serum interleukin 6 and serum antioxidant capacity of water-soluble substances (ACW), in atherogenicity index lg((triglyceride/high-density lipoprotein cholesterol), hepatic oxidized glutathione as well as reduced to oxidized glutathione ratio). Efforts should be made to develop strawberry polyphenol-rich preparations containing the preferred anthocyanins, which is, however, difficult due to the instability of this class of phenolic compounds during the technological process.

INTRODUCTION

Free fructose intake has increased significantly in the Western type diet over the past two decades due to the raised consumption of fructose-rich beverages. The widespread use of fructose corn syrup sweeteners in food production means that consumers ingest free fructose also in such products as corn flakes, sweet snacks, ready-made desserts, and sauces [Tappy & Lê, 2010]. It has been shown that a diet overloaded with fructose causes adverse changes in the composition of the intestinal microflora by reducing the abundance of beneficial *Bifidobacterium* and *Lactobacillus* strains [Horne *et al.*, 2020]. Additionally, unfavorable changes in the population of beneficial intestinal microbiota increase the level of lipopolysaccharides circulating in the blood, causing pro-inflammatory responses that precede the development of insulin resistance and obesity [Fuke *et al*., 2019]. Moreover, high levels of fructose in the diet are the main drivers of liver lipogenesis, by increasing the amount of microbial short-chain fatty acids – SCFAs (*e.g.* acetic acid), and contribute to the development of non-alcoholic fatty liver disease [Park *et al*., 2021]. Moreover, a fructose-rich diet contributes to weight gain, increased blood glucose levels, and adverse changes in the lipid profile, such as decreased high-density lipoprotein (HDL) / increased low-density lipoprotein (LDL) cholesterol levels and increased triglyceride content [Horne *et al*., 2020].

Strawberries (*Fragaria ananassa*) are commonly consumed both fresh and processed. They are a rich source of vitamins and bioactive compounds, such as folates, ascorbic acid, and phenolic compounds. The main class of phenolic compounds found in fresh strawberries is flavonoids, mainly anthocyanins (ACs), which account for over 75% of total phenolic compounds [Sirijan *et al*., 2020]. Their content can range from 150 to 600 mg/kg of fresh weight depending

* Corresponding Author:
E-mail: ezary@pbs.edu.pl (E. Żary-Sikorska)

Submitted: 21 July 2021
Accepted: 13 October 2021
Published on-line: 15 November 2021

© Copyright by Institute of Animal Reproduction and Food Research of the Polish Academy of Sciences
© 2021 Author(s). This is an open access article licensed under the Creative Commons Attribution-NonCommercial-NoDerivs License (http://creativecommons.org/licenses/by-nc-nd/4.0/).

on plant genetic factors and growing conditions. Irrespective of the mentioned factors, which influence the total anthocyanin content in strawberries, the major anthocyanins of strawberries include pelargonidin 3-glucoside (89–95%), followed by cyanidin 3-glucoside (3.9–10.6%) [Sirijan *et al*., 2020]. In unripe strawberries, the flavonoids are mainly represented by proanthocyanidins (PAs), which are polymeric flavan-3-ols. The content of PAs in strawberries ranges from 0.539 to 1.632 mg/g of fresh weight [Sirijan *et al*., 2020]. Another group of strawberry phenolic compounds is ellagitannins (ETs), which are monomeric, oligomeric, and complex polymers of various combinations of gallic and hexahydroxydiphenic acid with glucose. Agrimoniin is indicated as the main ET both in the fresh fruits and particularly in pomace from the strawberry juice production [Nowicka *et al.,* 2019]. Strawberry bioactive compounds, including ACs, Pas, and ETs, can play an important role in the prevention of civilization diseases caused by the Western type diet, like type 2 diabetes, obesity, cancer, cardiovascular diseases as well as oxidative stress, and pro-inflammatory and neurodegenerative conditions [Giampieri *et al.,* 2012].

Consumption of fresh strawberry is seasonal, hence they are widely processed into juices or jams. It has been proved that strawberry processing reduces the content of bioactive compounds, including polyphenols. For example, during the industrial production of strawberry juice, most of the anthocyanins pervade to the juice, while majority of the ellagitannins remain in the pomace [Ertan *et al.*, 2020]. The bioavailability of phenolic compounds is the basic factor determining their health-promoting activity. Studies have shown low ACs absorption and excretion with urine and feces after oral ingestion (>2%), indicating that they undergo extensive biotransformation in the gastrointestinal tract. Thus, most anthocyanins are not absorbed in the upper small intestine, but pass to the colon, where they are metabolized by microflora [Aura *et al*., 2005]. *In vitro* studies with human fecal microflora have shown that the bacterial metabolism of anthocyanin glycosides is based on the cleavage of the sugar moiety and breakdown of the anthocyanidin heterocycle, resulting in the formation of aglycones followed by smaller phenolic acids [Aura *et al.,* 2005]. A study by Hidalgo *et al.* [2012], in which the human colon microflora and anthocyanins were incubated under controlled conditions similar to those in the distal parts of the large intestine, showed 85% reduction of anthocyanins after 4 h of incubation. Moreover, the anthocyanins significantly increased the growth dynamics of the probiotic intestinal microflora such as *Bifidobacterium* and *Lactobacillus-Enterococcus* genera [Hidalgo *et al*., 2012]. Furthermore, anthocyanin extracts have exhibited antibacterial activity against pathogenic bacteria such as *Salmonella enterica, Staphyloccocus aureus, Clostridium perfringens*, or *Helicobacter pylori* [Bauza-Kaszewska *et al*., 2021].

Only about 5% of ETs are metabolized by the host's digestive enzymes, while most ETs are converted by colonic microbiota. ETs show different susceptibility to bacterial transformations, depending on many factors, including the chemical structure (polymerization degree) or the composition of the host microflora [Milala *et al.,* 2017]. The microbial conversion of ETs and ellagic acid (EA) leads to the formation of a number of derivative compounds named urolithins (URs) and/or nasutins (NSs). Milala *et al.* [2017] found that NSs were the main metabolites in the rats' urine, feces, and blood serum after administration of experimental diet supplemented with strawberry ETs with a higher degree of polymerization. In the case of diet supplementation with ETs having a lower degree of polymerization, it was URs, then NSs. Selma *et al.* [2014] identified two strains of the genus *Gordonibacter* in human feces that were capable of converting EA to urolithin. Many studies have proven that ETs have a probiotic effect, promoting the growth of *Lactobacillus* and *Bifidobacterium* [Buzzini *et al*., 2008]. However, there are also contradictory reports supporting the hypothesis that ET metabolism is a counter-reaction of the intestinal microflora to the antibacterial activity of these compounds, as evidenced by the lack of trihydroxybenzoyl groups in the structure of metabolites, which determine the antibacterial activity of ETs [Buzzini *et al*., 2008].

In the present *in vivo* study, it was hypothesized that the dietary inclusion of strawberry bioactive compounds in the form of polyphenol-rich fractions would beneficially affect the intestinal and hepatic homeostasis as well as the blood redox and lipids status, especially in rats administered the high-fructose diet. Besides ETs and PAs, the authors investigated the effects of ACs, the most unstable phenolic compounds. Therefore, two types of dietary strawberry fractions obtained from fruit pomace (containing ETs and PAs – EP) and juice (containing ACs beside ETs and PAs – EPA) were investigated.

MATERIALS AND METHODS

Preparation of the EP strawberry fraction

Strawberry pomace was collected during strawberry juice production in the Alpex Company (Łęczeszyce, Poland). After drying at 70±2°C for 24 h, the strawberry by-product was separated into a seed fraction and a seedless fraction (particle diameter of 0.5–1 mm and 1–3 mm, respectively) using proper screens.

The seedless fraction was used to obtain the crude extracts. To this end, 20 L of 65% (*v/v*) ethanol and 6 kg of the seedless fraction were put into a 30-L volume extractor made of stainless steel at 20–25°C. After 48 h, the mixture was separated on a laboratory press resulting in an ethanol extract (14.7 L) and wet pomace (10.2 kg). The solvent was recovered by distillation, which gave 6 L of the polyphenol-rich residue, which contained 15% of ethanol. Then, a second step of extraction was conducted. The wet pomace from the first step of extraction and 15 L of 65% (*v/v*) acetone were put into the extractor at 20°C for 24 h. Then, 15 L of an acetone-ethanol extract was separated from 10 kg of pomace (wet weight) on a laboratory press. In the third step of extraction, the mixture of resulting pomace and 10 L of water was pressed after 1 h to result in 11 kg of wet pomace and 8 L of an acetone-ethanol-water extract. The solvents (acetone and ethanol) were evaporated from combined acetone extracts (15 L and 8 L) to give 6 L of the residue containing *ca*. 15% ethanol. The 3-step extraction was performed in duplicate and the extracts from both replicates were combined. Then, 12 L of the extract containing

600 g of dry matter were filtered on a cellulose filter and next purified by chromatography on an Amberlite XAD resin using 20 L column with 15 L of the adsorption bed. The process consisted in sorbent conditioning, adsorption of the polyphenols in the column bed with the flow rate of 1 BV/h (BV – bed volume), removing ions and saccharides with the low molecular weight off the bed using 8% (*v/v*) ethanol with the flow rate of 2 BV, and gradual desorption of the fractions with opposite flow direction, at a flow rate of 0.2 BV/h, and increasing ethanol concentration, *i.e.* by 30% (*v/v*) – 1 BV, and by 55% (*v/v*) – until the desorption has been completed. Fractions collected during the desorption were analyzed for polyphenol contents. The fractions which had similar compositions were mixed, concentrated, and freeze-dried. Taking into consideration the content of major polyphenols, the fraction with ETs as the dominant compounds and with a lower content of PAs and flavan-3-ols was selected for future *in vivo* experiments. The lyophilized product was placed in PET boxes and stored at -4°C in the dark.

Preparation of the EPA strawberry fraction

The concentrated to total soluble solids of 62°Bx, fresh, commercial strawberry juice (Alpex Company, Łęczeszyce, Poland) was used to obtain the EPA fraction. In the juice, which was used for fraction preparation, the content of pelargonidin 3-glucoside was 1.1 g/kg of the dry matter of the concentrated strawberry juice. After diluting the juice to 25°Bx, it was purified on an Amberlite XAD resin. The column chromatography conditions were the same as those described above for the purification of strawberry pomace extract. The EPA fraction was eluted in the column using 30% (*v/v*) ethanol with a flow rate of 0.2 BV/h. The collected fraction was concentrated and freeze-dried. The lyophilized product was placed in PET boxes and stored at -4°C in the dark. Apart from ETs, PAs, and flavan-3-ols, the EPA strawberry fraction contained ACs.

Proximate chemical composition of fractions

The Association of Official Analytical Chemists (AOAC) methods 920.151, 940.26, 920.152, 930.09 were used to determine the dry matter, ash and lipid contents, respectively [AOAC, 2019]. The carbohydrate content was determined using the following formula: carbohydrate = total solids – (lipid + ash).

Determination of polyphenol content in the fractions

According to the procedure described by Sójka *et al.* [2013], the contents of ETs, EA, ACs, and flavonols were determined in the fractions using an HPLC system with a photodiode array detector (Knauer Smartline, Berlin, Germany) coupled with a Gemini C18 column (110 Å, 250×4.60 mm, 5 μm; Phenomenex, Torrance, CA, USA). The standards were agrimoniin (obtained from the Institute of Food Technology and Analysis, Łódź, Poland), EA and pelargonidin 3-glucoside (Extrasynthese, Genay, France). Detection was performed for ETs at 250 nm, for EA and flavonols at 360 nm, and for ACs at 520 nm. The column temperature was 35°C, and the mobile phase flow rate was 1.25 mL/min. Mobile phase consisted of solvent A – 0.05% (*v/v*) phosphoric acid in water, and solvent B – 0.05% (*v/v*) phosphoric acid in acetonitrile. Gradient was as follows: 0–5 min 4% B; 5–12.5 min 4–15% B; 12.5–42.5 min 15–40% B; 42.5–51.8 min 40–50% B; 51.8–53.4 min 50–55% B; and 53.4–55 min 4% B.

The determination of proanthocyanidins was performed after acid hydrolysis of the PAs with an excess of phloroglucinol according to the method of Kennedy & Jones [2001]. The separation conditions have previously been described by Kosmala *et al.* [2015]. The following standards were used: (–)-epicatechin, (+)-catechin, (–)-epigallocatechin and their respective phloroglucinol adducts. The quantification was made based on the peak areas registered by the fluorescence detector (excitation wavelength: 278 nm; emission wavelength: 360 nm). The standard curves of (–)-epicatechin, (+)-catechin, and (–)-epicatechin-phloroglucinol adduct were used to quantify the breakdown products of the terminal units and extender units, respectively.

Animal study

The experiment was carried out using six experimental groups, each consisting of eight randomly assigned male Wistar rats, giving a total of 48 animals weighing 176±1.051 g. The rats were housed individually in metabolic cages in a 12-h light: 12-h dark cycle, at a stable temperature (21–22°C), in a ventilated room (15 air changes per h). They were used in accordance with the legal guidelines regulated by EU Directive (2010/63/EU). The experimental protocol was approved by the Local Institutional Animal Care and Use Committee (Olsztyn, Poland, approval no. 10/2018). During the 6-week experiment, the rats had free access to food (stored at 4°C in hermetic containers until the end of the experiment) and tap water (details are provided in Table 1). The diets were modifications of a casein diet for laboratory rodents recommended by the American Institute of Nutrition [Reeves, 1997]. All diets had equilibrated amounts of dietary protein, fiber, and polyphenols, if any, and were based on corn starch or on fructose. The corn starch diets were: corn starch (C_S group), corn starch and EP fraction (EP_S group), corn starch and EPA fraction (EPA_S group), whereas fructose diets were fructose (C_F), fructose and EP fraction (EP_F), fructose and EPA fraction (EPA_F). Strawberry fractions were added to treatment diets at the expense of corn starch, *i.e.*: EP or EPA in doses of 0.28 g and 0.70 g/100 g of diet, respectively. The calculation of experimental diets with the aid of the body surface area normalization method [Reagan-Shaw *et al*., 2008] and literature data for polyphenol content in the strawberry were used to represent a realistic amount of fresh strawberries consumed by humans. The composition of each group-specific diet is displayed in Table 1.

The body weight (BW) gain and individual feed consumption of rats were estimated. Rats were anesthetized with a ketamine/xylazine solution (100/10 mg per one kg BW). Before anesthesia, the rats were deprived of feed overnight (10–12 h).

Sample collection and basic analyses

Blood analysis

After a laparotomy, blood samples were collected from the caudal vein into 2.5-mL heparinized test tubes, and serum was then obtained by solidification and low-speed centrifugation (350×*g*, 10 min, 4°C). Serum samples were kept

TABLE 1. Diet composition (g/100 g).

	C_S	C_F	EP_S	EP_F	EPA_S	EPA_F
Casein	14.8	14.8	14.8	14.8	14.8	14.8
Cellulose[1]	6	6	6	6	6	6
Rapeseed oil	8	8	8	8	8	8
Mineral mix[2]	1	1	1	1	1	1
Vitamin mix[3]	3.5	3.5	3.5	3.5	3.5	3.5
Choline chloride	0.2	0.2	0.2	0.2	0.2	0.2
DL-methionine	0.2	0.2	0.2	0.2	0.2	0.2
Cholesterol	0.5	0.5	0.5	0.5	0.5	0.5
Extract EP	0	0	0.28	0.28	0	0
Extract EPA	0	0	0	0	0.70	0.70
Fructose	0	65.0	0	65.0	0	65.0
Corn starch	65.8	0.8	65.52	0.52	65.1	0.1
Calcd dietary polyphenols*	0	0	0.199	0.199	0.198	0.198
Calcd dietary ellagitannins (mono:dimers)*	0	0	0.121 (55:45)	0.121 (55:45)	0.096 (54:46)	0.096 (54:46)
Calcd dietary proanthocyanidins*	0	0	0.069	0.069	0.071	0.071
Calcd dietary flavonols*	0	0	0.009	0.009	0.013	0.013
Calcd dietary anthocyanins*	0	0	0	0	0.018	0.018
Calcd dietary metabolized carbohydrates*	0	0	0.05	0.05	0.46	0.46

* from the composition of fraction with ellagitannins and proanthocyanidins (EP) or fraction with ellagitannins, proanthocyanidins and anthocyanins (EPA) (see Table 1).

[1]α-cellulose preparation was obtained from Sigma-Aldrich (No. C8002). [2]AIN-93G [Reeves, 1997], g per kg mix: 357 g anhydrous calcium carbonate (40.04% Ca), 196 g monobasic potassium phosphate (22.76% P, 28.73% K), 70.78 g potassium citrate and tripotassium monohydrate (36.16% K), 74 g sodium chloride (39.34% Na, 60.66% Cl), 46.6 g potassium sulfate (44.87% K, 18.39% S), 24 g magnesium oxide (60.32% Mg), 6.06 g ferric citrate (16.5% Fe), 1.65 g zinc carbonate (52.14% Zn), 1.45 g sodium meta-silicate 9 $9H_2O$ (9.88% Si), 0.63 g manganous carbonate (47.79% Mn), 0.3 g cupric carbonate (57.47% Cu), 221.026 g powdered sucrose, and 0.275 g chromium potassium sulfate × $12H_2O$ (10.42% Cr). The following components were added in mg per kg mix quantities: 81.5 mg boric acid (17.5% B), 63.5 mg sodium fluoride (45.24% F), 31.8 mg nickel carbonate (45% Ni), 17.4 mg lithium chloride (16.38% Li), 10.25 mg anhydrous sodium selenate (41.79% Se), 10 mg potassium iodate (59.3% I), 7.95 mg ammonium paramolybdate × $4H_2O$ (54.34% Mo), and 6.6 mg ammonium vanadate (43.55% V). [3]AIN-93G [Reeves 1997], g per kg mix: 3.0 g nicotinic acid, 1.6 g Ca pantothenate, 0.7 g pyridoxine–HCl, 0.6 g thiamin–HCl, 974.655 g powdered sucrose, 0.6 g riboflavin, 0.2 g folic acid, 0.02 g biotin, 2.5 g vit. B_{12} (cyanocobalamin, 0.1% in mannitol). The following components were added in IU per g quantities: 15.0 IU vit. E (all-*rac*-α-tocopheryl acetate, 500), 0.8 IU vit. A (all-*trans*-retinyl palmitate, 500000), 0.25 IU vit. D_3 (cholecalciferol, 400,000), and 0.075 IU vit. K_1 (phylloquinone). Diets: C_S, control diet with corn starch; C_F, control diet with 65% fructose; EP_S, corn starch diet with the EP strawberry fraction; EP_F, fructose diet with the EP fraction; EPA_S, corn starch diet with the EPA strawberry fraction; EPA_F, fructose diet with the EPA fraction.

frozen at -70°C for further analysis. Blood samples were used to analyze total white blood cell count (WBC), granulocyte percentage (GRA), medium-sized cell percentage (MID), lymphocyte percentage (LYM), red blood cell count (RBC), hemoglobin (HGB), hematocrit (HCT), mean corpuscular hemoglobin (MCH), mean corpuscular volume (MCV), mean corpuscular hemoglobin concentration (MCHC), red cell distribution width (RDWc), platelet count (PLT), platelet percentage (PCT), mean platelet volume (MPV), and platelet distribution width (PDWc) using the ABACUS Junior Vet hematological analyzer (Diatron MI PLC, Budapest, Hungary). The photochemiluminescence method was used to determine the serum antioxidant capacity of water-soluble and lipid-soluble substances (ACW and ACL, respectively). Particularly, a Photochem device and respective kits (ACW-Kit and ACL-Kit, Analytik Jena AG, Jena, Germany), and ascorbic acid and Trolox as standards were used to determine ACW and ACL, respectively. The concentrations of HDL cholesterol (HDL), LDL cholesterol (LDL), total cholesterol (TC), and triglyceride (TG) fractions were determined using a biochemical analyzer (Pentra C200, Horiba, Tokyo, Japan). The same analyzer was used to determine serum levels of glucose, urea, and fructosamine (FRC) as well as the activity of aminotransferases: aspartate (AST) and alanine (ALT). The rat serum level of adiponectin was determined by enzyme immunoassay (Rat adiponectin ELISA Kit, Cusabio Biotech Co., Ltd., Wuhan, Hubei, China). Whereas, a validated rat insulin ELISA kit (Demeditec Diagnostics GmbH, Kiel, Germany) was used to determine the insulin concentration. The Thermo Scientific assays (Rockford, IL, USA) were used to determine the serum concentrations of interleukin 6 (IL-6) and tumor necrosis

factor-α (TNF-α). The formula: homeostatic model assessment for insulin resistance (HOMA-IR) = [fasting glycemia (mM) × fasting insulinemia (mU/L)/22.5] was used to calculate the HOMA-IR index, while the following formulas: AI = lg(TG/HDL) and AII = (TC–HDL)/HDL were used to calculate the atherogenicity indexes of serum. Values for TG, TC, and HDL were expressed as mM.

Small intestine and ceca evaluation

Selected intestinal segments (small intestine, cecum, colon) were removed and weighed. The pH was immediately measured in the ileal, cecal, and colonic digesta, using a microelectrode and a pH/ION meter (model 301; Hanna Instruments, Vila do Conde, Portugal). The mucosa from the second quarter of the small intestine was collected by scrapping with glass slides onto an iced glass plate. The mucosa samples were homogenized with four parts of a cold physiological saline (*v/w*) and centrifuged for 10 min (10,000×*g*, 4°C). The obtained supernatant was stored at -40°C until analysis. The procedure described by Jurgoński *et al.* [2013] was used to assay the activities of mucosal disaccharidases – sucrase, maltase, and lactase, which were expressed as μmol of glucose liberated from the respective disaccharide per min per g of protein. The Bradford method with bovine serum albumin as the standard was used to determine the mucosal protein content. In turn, contents of ammonia (microdiffusion method in Conway's dishes) and dry matter (at 105°C) were determined in the fresh cecal digesta. Also, SCFAs were measured using a gas chromatograph (Shimadzu GC-2010, Kyoto, Japan) and a capillary column (SGE BP21, 30 m×0.53 mm; SGE Europe Ltd., Milton Keynes, UK) as described earlier by Kosmala *et al.* [2015]. The concentrations of cecal putrefactive SCFAs (PSCFAs) were calculated as the sum of iso-valeric, iso-butyric, and valeric acids. All SCFAs analyses were performed in duplicate. The mix of pure acetic, propionic, butyric, iso-butyric, iso-valeric, and valeric acids (individually obtained from Sigma, St. Louis, MO, USA) was used to plot a standard curve and then to calculate the contents of individual acids. To maintain the calibration, there was an additional set of pure acids included in each GC run of samples at five sample intervals. Cecal fermentation processes were also analyzed based on the activities of bacterial enzymes, like: α- and β-glucosidase, α- and β-galactosidase, and β-glucuronidase. According to the method described earlier by Fotschki *et al.* [2016], the activities of bacterial enzymes were measured by the rate of release of *p*-nitrophenol (PNP) or *o*-nitrophenol (ONP) from the respective nitrophenylglucosides. Intracellular (IEA) and extracellular enzyme activity (EEA) was also calculated. EEA was determined as the rate of enzyme release, expressed as a percentage of total enzyme activity (TEA), while IEA was calculated by comparing TEA with the activities of bacterial enzymes secreted into the intestinal environment, and expressed as μmol product of PNP or ONP formed per h per g of digesta. The model curves for PNP and ONP (PNP or ONP standard solution in 100 mM phosphate buffer pH 7.0, 40 mg/L) were used to prepare calculation formulas and derive suitable equations. All analyses were performed in duplicate.

Heart, kidney, and liver evaluation

Selected internal organs (heart, kidneys, liver) were removed and weighed. After storage at -70°C, they were determined for the content of thiobarbituric acid-reactive substances (TBARS) according to the spectrophotometrical procedure described by Botsoglou *et al.* [1994]. TBARS contents were expressed in μg malondialdehyde per g of tissue. Reduced glutathione (GSH) and oxidized glutathione (GSSG) contents were determined in stored liver samples using an enzymatic recycling method described by Rahman *et al.* [2006]. Liver lipids were extracted with the method of Folch *et al.* [1957]. After extraction, TC and TG contents were determined enzymatically using commercial kits (Cholesterol DST, Triglycerides DST, Alpha Diagnostics Ltd, Reinach, Switzerland). In accordance with the manufacturer's instructions, total RNA was extracted from liver samples using the TRI Reagent (Sigma-Aldrich, St. Louis, MO, USA). The quantity and quality of RNA were measured spectrophotometrically using a NanoDrop1000 (Thermo Fisher Scientific, Waltham, MA, USA) and agarose gel electrophoresis, respectively. Total RNA (500 ng) was used to synthesize cDNA using a High-Capacity cDNA Reverse Transcription Kit with RNase Inhibitor (Applied Biosystem, Waltham, MA, USA). Glyceraldehyde 3-phosphate dehydrogenase (GAPDH) was applied as a reference gene. The levels of peroxisome proliferator-activated receptor α (PPARα) and GAPDH mRNA expression were analyzed using Single Tube TaqManVR Gene Expression Assays (Life Technologies, Carlsbad, CA, USA) and a 7900HT Fast Real-Time PCR System. The amplification conditions were as follows: initial denaturation for 10 min at 95°C; 40 cycles of 15 s at 95°C, and 1 min at 60°C. All samples were analyzed in duplicate, and each run included a standard curve, which was based on portions of combined liver RNA. The mRNA expression levels of PPARα were normalized to GAPDH and multiplied by 10.

Quantification of ellagic acid and ET metabolites

An HPLC system (Knauer Smartline system with a photodiode array detector) coupled with a Gemini C18 column (110 Å, 250×4.60 mm; 5 μm) was used to determine ellagic acid concentration in the cecal digesta after their hydrolysis with trifluoroacetic acid. Phase A was 0.05% (*v/v*) phosphoric acid in water, phase B was 0.05% (*v/v*) phosphoric acid in 80% (*v/v*) acetonitrile, the flow rate was 1.25 mL/min, the sample volume was 20 μL, and the temperature was 35°C. The gradient was as follows: 0–10 min 10–25% B, 10–20 min 25–40% B, 20–25 min 40–80% B, 25–30 min 80% B, 30–32 min 80–10% B, and 32–40 min 10% B. Ellagic acid was used as a standard, whereas the identification and quantification were performed at 360 nm.

The concentrations of ET metabolites were determined in the cecal digesta and urine. A frozen sample of the digesta (0.5–1 g) was mixed with 2 mL of acetone, then sonicated for 10 min, and centrifuged for 5 min (10,000×*g*). The supernatant was collected into a test tube. The procedure was repeated twice with 2 mL and 1 mL of 70% (*v/v*) acetone. The extract was concentrated using a vacuum concentrator (ScanSpeed 40, Labogene, Allerød, Denmark). In the next step of the procedure,

TABLE 2. Proximate chemical and polyphenol compositions of the strawberry fractions (g/100 g).

	EP fraction[1]	EPA fraction[2]
Dry matter	93.3	99.1
Ash	0.36	0.05
Lipids	0.0	0.0
Metabolized carbohydrates[3]	21.0	70.5
including SDF	0.0	0.0
Polyphenols (HPLC-DAD)	71.8	28.6
Ellagic acid	0.7	0.3
Ellagitannins	43.2	13.7
monomers	23.5	7.4
dimers	19.7	6.4
Proanthocyanidins	24.8	10.1
Flavonols	3.2	1.9
Anthocyanins	0.0	2.6

[1]Fraction with ellagitannins and proanthocyanidins. [2]Fraction with ellagitannins, proanthocyanidins and anthocyanins. [3]Low-molecular carbohydrates and structural components of plant cell walls.

it was dissolved in methanol (1 mL). The HPLC system coupled with a Gemini C18 column was used to determine concentrations of ET metabolites. The same separation conditions were used as for ETs determination in dietary fractions. ET metabolites were identified by comparing their UV spectra with available literature data [Gonzales-Barrio *et al.*, 2011] and additionally confirmed by the mass spectrometry (MS) method described by Fotschki *et al.* [2018]. Urolithin-A, isolated from human urine in accordance with a semipreparative HPLC procedure previously described by Fotschki *et al.* [2016], was used as a standard for the quantification of ET metabolites.

Statistical analysis

The statistical analysis was performed using STATISTICA software, version 12.0 (StatSoft Corp., Krakow, Poland). The distribution of the data for normality was checked prior to further statistical analyses. A two-way analysis of variance (ANOVA) was used to determine the effect of the fraction addition (F; none, EP or EPA fraction) and the diet type (T; corn starch and fructose as the main dietary carbohydrate), and the interaction between these two factors (F×T). The Duncan's post hoc test, which purpose is to determine differences among the respective treatment groups, was used when an interaction was significant ($p<0.05$). The results were expressed as the means and pooled standard error of the mean (SEM).

RESULTS AND DISCUSSION

The chemical composition of strawberry fractions (EP and EPA), including the polyphenol composition, is presented in Table 2. The main differences between the EP and EPA strawberry fractions concern the qualitative and quantitative composition of the polyphenols. The EP fraction contained more polyphenols than the EPA fraction, 71.8 *vs*. 28.6 g/100 g, respectively. On the other hand, the EPA fraction contained additionally ACs, apart from ETs, PAs and flavan-3-ols, also present in the EP fraction.

Feeding the rats for 4 weeks with high-fructose diets did not affect feed intake and body weight gain (Table 3). Tappy & Lê [2010] demonstrated a significant effect of a fructose diet on the body weight of rodents over a long feeding period. The lack of weight gain may also be due to the thermogenic effect of fructose, previously noted in rodents [DeBosch *et al*., 2013] and in human studies [Mizobe *et al*., 2006]. The two-way ANOVA showed that, irrespective of fraction addition, the dietary fructose significantly increased small intestinal mass with contents, ileal digesta pH value, and the mucosal activity of maltase and lactase (Table 3). A significant fraction × diet type interaction revealed that the highest activity of sucrase in the jejunal mucosa followed the C_F treatment ($p<0.05$ *vs.* all remaining groups). Additionally, the lowest sucrase activity was noted in the C_S, EP_S, and EPA_S groups ($p<0.05$ *vs.* all three fructose groups) (Table 3). Intestinal glucose transporter 5 (GLUT5) is remarkably responsive to its substrate fructose. Lower sucrase activity is associated with a lower intestinal content of fructose, which is an activator of intestinal GLUT5. However, a high fructose intake suppresses the activity of the GLUT5 transporter in colonocytes' membrane in the small intestine. Unabsorbed fructose is fermented by bacteria in the lower parts of the gastrointestinal tract, wherein the population of fructophilic bacteria and masses of colonic tissue and digesta (bulk effect) increase [Tappy & Lê, 2010]. Anthocyanins are implied to stimulate the growth of *Lactobacillus* spp., *Bifidobacterium* spp., or the butyrate-producing *C. coccoides – Eubacterium rectale* [Hidalgo *et al*., 2012]. In the current study, strawberry fractions alleviated adverse changes in the ceca induced by a high fructose intake, including greater masses of the cecal digesta, which are related to the more intense fermentation in the colon. Moreover, the presence of anthocyanins in the EPA fraction positively influenced the concentration of ammonia in the cecal digesta of rats, regardless of diet type ($p<0.05$ *vs*. C and EP; Table 4). Increased ammonia utilization is a beneficial change. An increase in ammonia levels is related to an increased incidence of colonic viral infections. Likewise, this bacterial protein degradation product can induce the growth of cancer cells and damage the intestinal epithelium [Hambly *et al*., 1997].

The two-way ANOVA analysis revealed that, regardless the fraction addition, the dietary application of 65% fructose caused a significant reduction in the cecal extracellular and total activities of bacterial α- and β-glucosidase, α- and β-galactosidase in comparison to the rats fed diets based on corn starch (Table 5 and Table 6). Such a decrease was also noted in the case of cecal intracellular activity of the aforementioned bacterial enzymes, except α-glucosidase. Irrespective of diet type, the dietary addition of both fractions significantly enhanced the activity of bacterial α-glucosidase (extracellular and total), β-galactosidase (intracellular), and β-glucosidase (extracellular, intracellular, total) when

TABLE 3. Growth parameters and small intestinal indices of rats fed experimental diets*.

	Start BW (g)	Final BW (g)	Gain (g)	Intake (g)	Small intestine				
					Mass (g/100 g BW)[1]	pH	Sucrase (μmol/min/g protein)	Maltase (μmol/min/g protein)	Lactase (μmol/min/g protein)
Group (n=8)									
C_S	176	343	168	644	1.95	7.27	6.58[c]	42.8	1.87
C_F	176	347	172	621	2.15	7.64	10.6[a]	52.9	2.92
EP_S	176	336	160	640	1.86	7.15	6.86[c]	46.3	2.25
EP_F	175	329	154	640	2.16	7.45	8.77[b]	51.9	2.63
EPA_S	176	343	167	655	2.01	7.18	6.58[c]	46.3	2.38
EPA_F	175	337	161	655	2.13	7.37	8.24[b]	48.6	2.90
SEM	*1.354*	*2.300*	*1.995*	*8.454*	*0.025*	*0.050*	*0.271*	*1.283*	*0.083*
Fraction (F)									
C (without)	176	345	170	633	2.05	7.45	8.60	47.8	2.39
EP	176	332	157	640	2.01	7.30	7.82	49.1	2.44
EPA	176	341	165	657	2.07	7.29	7.29	48.0	2.63
p value	*0.998*	*0.069*	*0.058*	*0.526*	*0.537*	*0.297*	*0.045*	*0.910*	*0.341*
Diet type (T)									
Starch	176	341	165	648	1.94[b]	7.21[b]	6.73	45.5[b]	2.16[b]
FRU	175	338	162	639	2.15[a]	7.49[a]	9.21	51.1[a]	2.82[a]
p value	*0.851*	*0.429*	*0.428*	*0.608*	**	*0.005*	**	*0.031*	**
Interaction F×T									
p value	*0.989*	*0.473*	*0.411*	*0.851*	*0.231*	*0.626*	*0.012*	*0.371*	*0.120*

*C_S, control diet with corn starch; C_F, control diet with 65% fructose (FRU); EP_S, corn starch diet with the strawberry fraction with ellagitannins and proanthocyanidins (EP); EP_F, fructose diet with the EP fraction; EPA_S, corn starch diet with the strawberry fraction with ellagitannins, proanthocyanidins and anthocyanins (EPA); EPA_F, fructose diet with the EPA fraction.

[a,b,c] Mean values within a column with unlike superscript letters were shown to be significantly different ($p<0.05$); differences among the groups C_S, C_F, EP_S, EP_F, EPA_S, and EPA_F were indicated with superscripts only in the case of a statistically significant interaction F×T ($p<0.05$) and in that case the differences for the main factors F and T are not shown. **$p<0.001$.

[1]Mass with contents; BW, body weight.

compared to the C treatment ($p<0.05$) (Table 5 and Table 6). Additionally, the EP treatment was accompanied by the highest extracellular and total activity of β-galactosidase ($p<0.05$ *vs*. C and EPA). As indicated by a significant F×T interaction, the highest release rate of bacterial β-galactosidase into the cecal environment was determined in the C_F rats while the lowest one in the EPA_S and EPA_F groups (in both cases $p<0.05$ *vs.* remaining treatments). The C_F group had also the highest value of β-glucosidase release rate ($p<0.05$ *vs.* all other treatments except EP_F; see: significant F×T interaction). The F×T interaction revealed the highest extracellular as well as total activity of bacterial β-glucuronidase in the C_F as well as C_F and EP_F groups, respectively ($p<0.05$ *vs.* all remaining groups; Table 6). The lowest β-glucuronidase activity (extracellular and total) was noted in the cecum of EPA_F rats ($p<0.05$ *vs.* all other groups). The intracellular β-glucuronidase activity was the highest in EP_F rats compared to all other groups (see: significant F×T interaction). When comparing the three starch-fructose counterparts, only C_F group excelled the C_S one when the calculated release rate of bacterial β-glucuronidase is considered (see F×T interaction). Excessive fructose consumption contributes to dysbiosis and adverse changes in the quantitative and qualitative composition of the intestinal microflora. There is mainly an increase in the number of *Bacteroides* and an increase of *Firmicutes*. These unfavorable changes in the *Firmicute/Bacteroidetes* ratio, a measure commonly associated with metabolic dysfunction and changes in enzymatic activity of microflora, occur with a high fructose diet [Horne *et al.*, 2020]. A decrease in the enzymatic activities of intestinal bacteria results from this antibacterial effect of high-fructose diets on large intestine microflora. The decrease of the activity of galactosidases may intensify fermentation processes in the colon and underlay increased gas production and increased dyspeptic ailments in patients with irritable bowel syndrome [Hillilä *et al.*, 2016]. Simultaneously, the high energy load of undigested fructose increases the extracellular activity of cecal bacterial enzymes, which, when released directly into the environment

TABLE 4. Large intestine indices of rats fed experimental diets*.

	Caecum					Colon		
	Tissue (g/100 g BW)[1]	Digesta (g/100 g BW)[1]	DM (%)	NH_3 (mg/g)	pH	Tissue (g/100 g BW)[1]	Digesta (g/100 g BW)[1]	pH
Group (n=8)								
C_S	0.163	0.518	24.5	0.239	7.39	0.293	0.324	7.65
C_F	0.171	0.654	25.4	0.255	7.46	0.340	0.518	7.66
EP_S	0.169	0.547	25.7	0.265	7.54	0.284	0.343	7.60
EP_F	0.173	0.551	25.7	0.253	7.63	0.283	0.383	7.70
EPA_S	0.177	0.546	26.3	0.218	7.31	0.271	0.360	7.69
EPA_F	0.174	0.578	26.9	0.209	7.48	0.300	0.381	7.72
SEM	*0.003*	*0.015*	*0.313*	*0.006*	*0.037*	*0.006*	*0.022*	*0.032*
Fraction (F)								
C (without)	0.167	0.586	24.9	0.247[a]	7.42	0.316[a]	0.421	7.65
EP	0.171	0.549	25.7	0.259[a]	7.58	0.284[b]	0.363	7.65
EPA	0.176	0.564	26.4	0.215[b]	7.41	0.287[b]	0.372	7.70
p value	*0.431*	*0.605*	*0.152*	*0.014*	*0.097*	*0.035*	*0.486*	*0.765*
Diet type (T)								
Starch	0.170	0.538	25.4	0.241	7.42	0.284[b]	0.343[b]	7.64
FRU	0.173	0.593	26.0	0.239	7.52	0.308[a]	0.427[a]	7.69
p value	*0.557*	*0.073*	*0.310*	*0.789*	*0.170*	*0.034*	*0.048*	*0.499*
Interaction F×T								
p value	*0.695*	*0.171*	*0.802*	*0.549*	*0.905*	*0.210*	*0.197*	*0.846*

*C_S, control diet with corn starch; C_F, control diet with 65% fructose (FRU); EP_S, corn starch diet with the strawberry fraction with ellagitannins and proanthocyanidins (EP); EP_F, fructose diet with the EP fraction; EPA_S, corn starch diet with the strawberry fraction with ellagitannins, proanthocyanidins and anthocyanins (EPA); EPA_F, fructose diet with the EPA fraction.

[a,b,c] Mean values within a column with unlike superscript letters were shown to be significantly different ($p<0.05$); differences among the groups C_S, C_F, EP_S, EP_F, EPA_S, and EPA_F were indicated with superscripts only in the case of a statistically significant interaction F×T ($p<0.05$) and in that case the differences for the main factors F and T are not shown.

[1] mass with contents; BW, body weight.

of the large intestine, affect the rate of bacterial digestion of nutrients in lower parts of the digestive tract [Horne *et al*., 2020]. In both human [Bialonska *et al.*, 2010] and animal studies [Molan *et al.*, 2010], extracts of anthocyanins of various plant origins, have been found to increase the probiotic microflora and regulate the abundance of intestinal microflora, which corresponds to the research hypothesis that the addition of an anthocyanin-containing fraction (EPA) to a high-fructose diet reduced the adverse changes in the enzymatic activity of the intestinal microflora, especially with regard to the potentially harmful β-glucuronidase. Furthermore, flavonoids favorably modified the activity of glucosidases and galactosidases in the cecal digesta of rats in other studies [Fotschki *et al*., 2016; Zduńczyk *et al.,* 2006]. In the case of the EP fraction containing mainly ellagitannins, which are ascribed both antibacterial and growth-promoting properties of beneficial microflora, the decrease in the bacterial enzymatic activity was limited in the group fed the high-fructose diet, although the highest β-glucuronidase activity was noted in that group compared to all others groups (Table 6). Enhanced β-glucuronidase activity is claimed to be an initiator of colorectal cancer and a useful biomarker in disease diagnosis [Awolade *et al*., 2020].

The two-way ANOVA showed that, regardless of fraction addition, the fructose treatment lowered the cecal concentration of total SCFAs, including acetic acid concentration, in comparison to the starch dietary treatment (Table 7). Our study results indicate that fructose consumption influences the gut microflora and thus SCFA production through microbial fermentation. Irrespective of diet type, the EPA treatment caused a significant increase in the cecal concentration of isobutyric acid, valeric acid, total PSCFAs, and total SCFAs as well as in the cecal SCFA pool in comparison to the C and EP treatments ($p<0.05$). The F×T interaction showed the lowest cecal propionic and butyric acid concentrations in the C_F group ($p<0.05$ *vs.* all other groups). In the case of butyric acid, its highest cecal concentration followed the ingestion of EPA_S diet ($p<0.05$ *vs*. all other groups). The calculated

TABLE 5. Activities of bacterial enzymes (α-glucosidase, α- and β-galactosidase) and their release rate into the cecal environment in rats*.

	α-Glucosidase				α-Galactosidase				β-Galactosidase			
	Extracellular (μmol/h/g digesta)	Intracellular (μmol/h/g digesta)	Total (μmol/h/g digesta)	Release rate (%)	Extracellular (μmol/h/g digesta)	Intracellular (μmol/h/g digesta)	Total (μmol/h/g digesta)	Release rate (%)	Extracellular (μmol/h/g digesta)	Intracellular (μmol/h/g digesta)	Total (μmol/h/g digesta)	Release rate (%)
Group (n=8)												
C_S	10.3	2.45^{ab}	12.8	81.0	9.79	2.68	12.5	78.6	28.5	9.08	37.6	76.4^{b}
C_F	6.63	0.83^{c}	7.46	88.8	6.18	1.03	7.21	85.4	16.7	1.69	18.4	91.0^{a}
EP_S	12.2	2.74^{a}	15.0	82.0	8.35	3.56	1.9	70.5	30.9	12.3	43.1	72.2^{b}
EP_F	7.82	1.31^{bc}	9.13	85.6	7.28	2.07	9.34	79.1	26.1	7.72	33.9	78.0^{b}
EPA_S	12.6	1.96^{abc}	14.6	86.8	8.40	2.61	11.0	76.3	18.7	10.5	29.2	64.2^{c}
EPA_F	8.75	1.94^{abc}	10.7	83.7	6.47	2.33	8.80	73.9	14.8	7.93	22.7	65.2^{c}
SEM	*0.424*	*0.183*	*0.527*	*1.222*	*0.302*	*0.190*	*0.396*	*1.439*	*1.173*	*0.682*	*1.663*	*1.594*
Fraction (F)												
C (without)	8.47^{b}	1.64	10.1^{b}	84.9	7.98	1.86	9.84	82.0	22.6^{b}	5.39^{b}	28.0^{b}	83.7
EP	10.0^{a}	2.02	12.0^{a}	83.8	7.82	2.81	10.6	74.8	28.5^{a}	9.99^{a}	38.5^{a}	75.1
EPA	10.7^{a}	1.80	12.5^{a}	85.3	7.68	2.39	10.1	76.4	17.3^{c}	9.37^{a}	26.6^{b}	65.2
p value	*0.012*	*0.624*	*0.025*	*0.753*	*0.885*	*0.067*	*0.560*	*0.067*	**	*0.001*	**	**
Diet type (T)												
Starch	11.7^{a}	2.29	14.0^{a}	83.8	9.01^{a}	2.90^{a}	11.9^{a}	76.0	26.4^{a}	10.7^{a}	37.1^{a}	71.3
FRU	7.73^{b}	1.36	9.09^{b}	86.0	6.64^{b}	1.81^{b}	8.45^{b}	79.4	19.2^{b}	5.78^{b}	25.0^{b}	78.1
p value	**	*0.007*	**	*0.370*	**	*0.002*	**	*0.190*	**	**	**	**
Interaction F×T												
p value	*0.876*	*0.044*	*0.449*	*0.123*	*0.122*	*0.138*	*0.132*	*0.080*	*0.132*	*0.216*	*0.113*	*0.012*

*C_S, control diet with corn starch; C_F, control diet with 65% fructose (FRU); EP_S, corn starch diet with the strawberry fraction with ellagitannins and proanthocyanidins (EP); EP_F, fructose diet with the EP fraction; EPA_S, corn starch diet with the strawberry fraction with ellagitannins, proanthocyanidins and anthocyanins (EPA); EPA_F, fructose diet with the EPA fraction.

^{a,b,c} Mean values within a column with unlike superscript letters were shown to be significantly different ($p<0.05$); differences among the groups C_S, C_F, EP_S, EP_F, EPA_S, and EPA_F were indicated with superscripts only in the case of a statistically significant interaction F×T ($p<0.05$) and in that case the differences for the main factors F and T are not shown. **$p<0.001$.

Release rate, extracellular as % of total activity.

SCFA profile values for acetic, propionic, and butyric acids were attributed to a significant F×T interaction. The highest percentage share of acetic acid *vs*. total SCFAs was in the C_F group ($p<0.05$ *vs*. C_S, EP_F, EPA_S), and that of propionic acid in the EP_F group ($p<0.05$ *vs*. other groups), and that of butyric acid in the C_S and EPA_S groups ($p<0.05$ *vs*. remaining groups). Adverse changes in the production of three key SCFAs, namely butyric, acetic, and propionic acids, are considered risk factors of the development of such diseases as type 2 diabetes or non-alcoholic fatty liver disease (NAFLD) [Markowiak-Kopeć & Śliżewska, 2020]. When using a high-fructose diet, a negative decrease in the cecal concentration of SCFAs as well as propionic and butyric acids was noted (Table 7). Butyric acid is the main source of energy for colonocytes, which influences the correctness of their division, as well as the overall health of the intestines, being a factor that protects against the development of inflammation and cancer of the colon wall [Loke *et al*., 2020]. When supplementing diet with a fraction containing ETs and ACs, favorable modifications of SCFAs were concluded, regardless of whether the diet was based on fructose or starch (Table 7). Moreover, the highest concentration of butyric acid in relation to all groups was also determined in the EPAs group. Our previous studies have shown similar effects in experiments with Wistar rats using ET-rich extracts [Fotschki *et al*., 2014] and extracts of ETs and ACs from strawberries [Fotschki *et al*., 2016].

In the present study, an excess of fructose in the diet of experimental rats caused negative changes in the blood parameters of the antioxidant and proinflammatory status. Chronic excess of fructose in the diet promotes the multiplication of pro-inflammatory intestinal microflora that produces endotoxins and reduces the tightness of the intestinal barrier [Lu *et al.,* 2020]. The C_F group had the highest blood serum TNFα and IL-6 concentrations (Figure 1). Regardless

TABLE 6. Activities of bacterial enzymes (β-glucosidase β-glucuronidase) and the rate of their release into the cecal environment in rats*.

	β-Glucosidase				β-Glucuronidase			
	Extracellular (μmol/h/g digesta)	Intracellular (μmol/h/g digesta)	Total (μmol/h/g digesta)	Release rate (%)	Extracellular (μmol/h/g digesta)	Intracellular (μmol/h/g digesta)	Total (μmol/h/g digesta)	Release rate (%)
Group (n=8)								
C_S	1.93	0.87	2.80	70.4^{b}	12.2^{b}	5.60^{b}	17.8^{b}	69.4^{bc}
C_F	0.73	0.15	0.88	83.2^{a}	18.0^{a}	4.07^{b}	22.0^{a}	82.1^{a}
EP_S	2.39	0.77	3.15	74.3^{b}	12.8^{b}	4.64^{b}	17.4^{b}	72.6^{abc}
EP_F	1.82	0.57	2.39	77.2^{ab}	14.0^{b}	8.39^{a}	22.4^{a}	63.1^{c}
EPA_S	2.86	1.12	3.97	73.7^{b}	12.7^{b}	4.39^{b}	17.1^{b}	74.0^{ab}
EPA_F	2.14	0.85	2.99	72.1^{b}	8.77^{c}	3.90^{b}	12.7^{c}	68.9^{bc}
SEM	*0.131*	*0.078*	*0.187*	*1.555*	*0.560*	*0.370*	*0.721*	*1.492*
Fraction (F)								
C (without)	1.33^{b}	0.508^{c}	1.84^{b}	76.8	15.1	4.83	19.9	75.8
EP	2.10^{a}	0.669^{b}	2.77^{a}	75.8	13.4	6.51	19.9	67.8
EPA	2.47^{a}	0.933^{a}	3.40^{a}	73.6	10.7	3.93	14.7	72.2
p value	**	*0.045*	**	*0.697*	**	*0.006*	**	*0.053*
Diet type (T)								
Starch	2.37^{a}	0.884^{a}	3.26^{a}	73.3	12.6	4.74	17.3	72.5
FRU	1.56^{b}	0.523^{b}	2.08^{b}	77.5	13.6	5.45	19.0	71.4
p value	**	*0.010*	**	*0.180*	*0.245*	*0.255*	*0.144*	*0.663*
Interaction F×T								
p value	*0.364*	*0.173*	*0.150*	*0.048*	**	*0.003*	*0.005*	*0.002*

*C_S, control diet with corn starch; C_F, control diet with 65% fructose (FRU); EP_S, corn starch diet with the strawberry fraction with ellagitannins and proanthocyanidins (EP); EP_F, fructose diet with the EP fraction; EPA_S, corn starch diet with the strawberry fraction with ellagitannins, proanthocyanidins and anthocyanins (EPA); EPA_F, fructose diet with the EPA fraction.

^{a,b,c} Mean values within a column with unlike superscript letters were shown to be significantly different ($p<0.05$); differences among the groups C_S, C_F, EP_S, EP_F, EPA_S, and EPA_F were indicated with superscripts only in the case of a statistically significant interaction F×T ($p<0.05$) and in that case the differences for the main factors F and T are not shown. **$p<0.001$.

Release rate, extracellular as % of total activity.

of fraction addition, the dietary fructose treatment was associated with increased blood serum glucose, FRC, insulin, and calculated HOMA-IR value in comparison to the starch treatment (Table 8). Irrespective of diet type, the dietary addition of the EPA fraction caused a significant decrease in the blood serum IL-6 concentration ($p<0.05$ *vs*. C). In studies with strawberry preparations, their anti-inflammatory effect was proven by the enhancement of IL-10 (an anti-inflammatory cytokine) and the attenuation of IL-1β, IL-6, and TNF-α (pro-inflammatory cytokines) [Liu & Lin, 2013]. Strawberries are a source of anti-inflammatory ingredients, such as vitamin C, anthocyanins, ellagitannins, and ellagic acid [Sirijan *et al*., 2020]. Nowicka *et al.* [2019] have demonstrated that the anti-inflammatory effect of strawberries is chiefly due to the presence of large amounts of pelargonidin 3-*O*-glucoside (P3G). The anti-inflammatory effects of P3G involve the nuclear factor kappa-light-chain-enhancer of activated B cells (NF-κB) and mitogen-activated protein kinase (MAPK) pathways. Hassimotto *et al.* [2013] pointed that the anthocyanin extract obtained from wild mulberry elicited anti-inflammatory effects by reducing the activity of myeloperoxidase (MPO), an enzyme that plays a key role in the pro-inflammatory process. In turn, Xu *et al.* [2018] observed a strong anti-inflammatory effect of urolithins A and B consisting in the inhibition of the activation of the NF-κB, MAPK (p38 and Erk1/2), and Akt signaling pathways mediated by urolithin. In our previous study with strawberry extracts rich in ETs [Żary-Sikorska *et al.,* 2020], we observed a decrease in TNF-α, IL-1, and IL-6 rat blood levels.

The fructose dietary treatment significantly enhanced the blood serum concentration of TC, LDL, TG, and calculated values of the HDL profile, atherogenicity indexes lg(TG/HDL) and (TC–HDL)/HDL, regardless of fraction addition (Table 8). The two-way ANOVA showed that both fractions added to a diet, irrespective of its type, caused a significant

TABLE 7. Short chain fatty acid (SCFA) concentration (μmol/g digesta), total pool (μmol/100 g body weight) and profile (% of total) in the cecal digesta.

	SCFA concentration								SCFA pool	SCFA profile		
	C2	C3	C4i	C4	C5i	C5	PSCFA	SCFA		C2	C3	C4
Group (n=8)												
C_S	92.9	22.0^{a}	2.17	15.8^{b}	2.35	2.16	6.68	137	70.2	67.5^{c}	16.1^{b}	11.5^{a}
C_F	73.7	14.1^{b}	1.86	7.10^{d}	2.53	2.29	6.68	102	66.7	72.4^{a}	14.0^{b}	7.00^{c}
EP_S	98.1	21.3^{a}	2.07	12.7^{bc}	1.34	2.15	5.56	138	75.2	71.0^{ab}	15.7^{b}	9.16^{b}
EP_F	82.0	22.4^{a}	2.45	10.6^{c}	1.55	2.19	6.20	121	66.6	67.6^{c}	18.6^{a}	8.58^{bc}
EPA_S	109	22.5^{a}	2.54	19.9^{a}	2.06	2.67	7.27	158	86.1	68.6^{bc}	14.2^{b}	12.5^{a}
EPA_F	99.9	21.6^{a}	2.97	13.0^{bc}	2.05	2.58	7.60	142	83.8	70.2^{ab}	15.4^{b}	9.08^{b}
SEM	*2.667*	*0.575*	*0.102*	*0.742*	*0.094*	*0.066*	*0.180*	*3.637*	*2.603*	*0.495*	*0.362*	*0.374*
Fraction (F)												
C (without)	83.3^{b}	18.0	2.01^{b}	11.4	2.44^{a}	2.23^{b}	6.68^{b}	119^{b}	68.4^{b}	69.9	15.0	9.27
EP	90.0^{b}	21.8	2.26^{b}	11.6	1.45^{c}	2.17^{b}	5.88^{c}	127^{b}	70.9^{b}	69.3	17.2	8.87
EPA	104^{a}	22.0	2.75^{a}	16.6	2.05^{b}	2.65^{a}	7.45^{a}	150^{a}	85.1^{a}	69.3	14.8	10.9
p value	*0.002*	**	*0.010*	**	**	*0.007*	*0.002*	**	*0.023*	*0.809*	*0.005*	*0.012*
Diet type (T)												
Starch	99.7^{a}	21.9	2.26	16.2	1.92	2.34	6.52	144^{a}	77.3	69.0	15.3	11.1
FRU	85.2^{b}	19.3	2.43	10.2	2.04	2.36	6.82	122^{b}	72.4	70.1	16.0	8.22
p value	*0.002*	*0.004*	*0.375*	**	*0.430*	*0.902*	*0.354*	**	*0.337*	*0.232*	*0.295*	**
Interaction F×T												
p value	*0.593*	**	*0.214*	*0.025*	*0.834*	*0.710*	*0.728*	*0.260*	*0.875*	*0.001*	*0.006*	*0.014*

*C_S, control diet with corn starch; C_F, control diet with 65% fructose (FRU); EP_S, corn starch diet with the strawberry fraction with ellagitannins and proanthocyanidins (EP); EP_F, fructose diet with the EP fraction; EPA_S, corn starch diet with the strawberry fraction with ellagitannins, proanthocyanidins and anthocyanins (EPA); EPA_F, fructose diet with the EPA fraction.

^{a,b,c} Mean values within a column with unlike superscript letters were shown to be significantly different ($p<0.05$); differences among the groups C_S, C_F, EP_S, EP_F, EPA_S, and EPA_F were indicated with superscripts only in the case of a statistically significant interaction F×T ($p<0.05$) and in that case the differences for the main factors F and T are not shown. **$p<0.001$.

PSCFA, putrefactive SCFA (the sum of iso-butyric, iso-valeric and valeric acids).

increase in the blood serum ACL (Figure 2), and a significant decrease in the blood serum TC and TG concentrations, and the (TC–HDL)/HDL index value ($p<0.05$ *vs*. C). Additionally, regardless of diet type, the dietary EPA fraction significantly increased blood serum ACW and decreased the value of atherogenicity index lg(TG/HDL), in comparison to the C treatment. According to the adopted hypothesis, the dietary application of EPA noticeably reduced unwanted changes in antioxidant parameters and blood lipid profile. In the study by Forbes-Hernández *et al.* [2017], the anthocyanin-enriched fraction from strawberries modified the parameters of antioxidant and lipid status in human hepatocellular carcinoma (HepG2) cells more favorably than the whole methanolic strawberry extract. The mechanism of the regulatory effect of polyphenols from berries on lipid metabolism was extensively investigated in the *in vitro* and *in vivo* studies. Prior *et al* [2009] indicated the anthocyanin extract of strawberries to be a viable preparation in preventing the development of dyslipidemia and obesity in mice. Moreover, in studies with obese mice, they demonstrated no anti-obesity effect or even increased obesity when whole strawberries were used in feeding. Aboonabi & Aboonabi [2020] showed that the hypolipidemic effect of anthocyanins mighty be associated with upregulating mRNA expression of peroxisome proliferator-activated receptor-γ (PPAR-γ). In turn, Jarosławska *et al.* [2011] demonstrated the inhibition of pancreatic lipase activity by berry polyphenols, which significantly reduced the absorption of fat from the intestinal lumen. In our previous studies addressing the preparations of black carrots rich in anthocyanins [Żary-Sikorska *et al*., 2019] and preparations of strawberries containing ETs with various degrees of polymerization [Żary-Sikorska *et al*., 2020], a favorable modulation of the blood lipid profile of experimental rats was also noted. The metabolites of phenolic compounds that circulate in the blood and reach various target tissues are responsible for the hypolipidemic effects of phenolic compounds from

TABLE 8. Biochemical indicators of the blood serum of rats fed experimental diets*.

	GL (mmol/L)	FRC (μmol/L)	Insulin (pmol/L)	HOMA-IR	TC (mmol/L)	HDL (mmol/L)	LDL (mmol/L)	HDL profile (% of TC)	TG (mmol/L)	Atherogenicity index	
										lg (TG/HDL)	(TC-HDL)/ HDL
Group (n=8)											
C_S	9.70	160	28.9	1.78	2.28	0.631	0.449	27.9	2.16	2.62	0.521
C_F	14.0	173	38.7	3.48	3.41	0.675	0.651	19.9	3.41	4.06	0.694
EP_S	10.5	157	28.1	1.86	2.09	0.594	0.409	28.6	1.64	2.55	0.437
EP_F	13.0	168	39.4	3.27	3.09	0.641	0.605	21.8	2.88	4.07	0.655
EPA_S	10.3	159	28.8	1.89	2.18	0.640	0.469	29.5	1.94	2.48	0.486
EPA_F	13.3	163	34.8	2.98	2.99	0.705	0.591	24.1	2.95	3.37	0.621
SEM	*0.304*	*1.763*	*1.164*	*0.136*	*0.092*	*0.014*	*0.021*	*0.824*	*0.114*	*0.158*	*0.018*
Fraction (F)											
C (without)	11.8	166	33.8	2.63	2.84^a	0.653	0.550	23.9	2.78^a	3.34^a	0.608^a
EP	11.8	162	33.7	2.57	2.58^b	0.618	0.507	25.2	2.26^b	3.31^{ab}	0.546^b
EPA	11.9	161	31.2	2.42	2.61^b	0.671	0.531	26.4	2.46^b	2.97^b	0.557^b
p value	*0.971*	*0.437*	*0.491*	*0.666*	*0.048*	*0.328*	*0.602*	*0.344*	*0.009*	*0.045*	*0.031*
Diet type (T)											
Starch	10.2^b	158^b	28.2^b	1.84^b	2.20^b	0.621	0.443^b	28.4^a	1.92^b	2.58^b	0.484^b
FRU	13.4^a	168^a	37.6^a	3.24^a	3.16^a	0.674	0.616^a	21.9^b	3.08^a	3.83^a	0.657^a
p value	**	*0.008*	**	**	**	*0.078*	**	**	**	**	**
Interaction F×T											
p value	*0.155*	*0.553*	*0.696*	*0.486*	*0.448*	*0.939*	*0.577*	*0.576*	*0.705*	*0.173*	*0.378*

*C_S, control diet with corn starch; C_F, control diet with 65% fructose (FRU); EP_S, corn starch diet with the strawberry fraction with ellagitannins and proanthocyanidins (EP); EP_F, fructose diet with the EP fraction; EPA_S, corn starch diet with the strawberry fraction with ellagitannins, proanthocyanidins and anthocyanins (EPA); EPA_F, fructose diet with the EPA fraction.

[a,b,c] Mean values within a column with unlike superscript letters were shown to be significantly different ($p<0.05$); differences among the groups C_S, C_F, EP_S, EP_F, EPA_S, and EPA_F were indicated with superscripts only in the case of a statistically significant interaction F×T ($p<0.05$) and in that case the differences for the main factors F and T are not shown. **$p<0.001$. GL, glucose; FCR, fructosamine; HOMA-IR, homeostatic model assessment for insulin resistance [fasting glycemia (mmol/L) × fasting insulinemia (mU/L)/22.5]; TC, total cholesterol; HDL, high-density lipoprotein; LDL, low-density lipoprotein; TG, triglycerides.

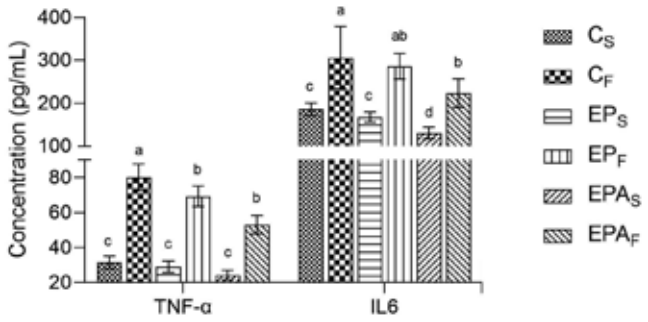

FIGURE 1. Blood serum tumor necrosis factor-α (TNF-α) and interleukin-6 (IL-6) concentrations of rats fed experimental diets: C_S, control diet with corn starch; C_F, control diet with 65% fructose; EP_S, corn starch diet with the strawberry fraction with ellagitannins and proanthocyanidins (EP); EP_F, fructose diet with the EP fraction; EPA_S, corn starch diet with the strawberry fraction with ellagitannins, proanthocyanidins and anthocyanins (EPA); EPA_F, fructose diet with the EPA fraction. Bars with unlike letters show significantly different values ($p<0.05$).

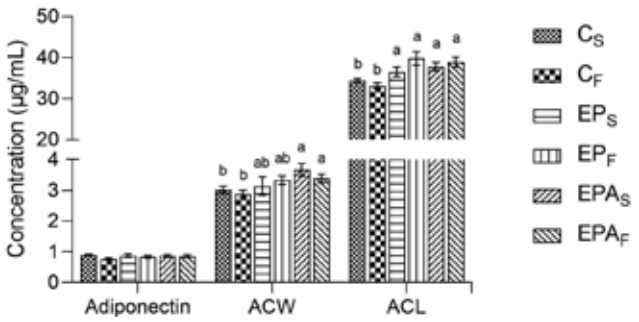

FIGURE 2. Blood serum antioxidant capacity of water-soluble (ACW), and lipid-soluble (ACL) substances, and adiponectin concentration of rats fed experimental diets: C_S, control diet with corn starch; C_F, control diet with 65% fructose; EP_S, corn starch diet with the strawberry fraction with ellagitannins and proanthocyanidins (EP); EP_F, fructose diet with the EP fraction; EPA_S, corn starch diet with the strawberry fraction with ellagitannins, proanthocyanidins and anthocyanins (EPA); EPA_F, fructose diet with the EPA extract. Bars with unlike letters show significantly different values ($p<0.05$).

TABLE 9. Blood serum AST and ALT activity as well as hepatic, heart, and kidneys metabolic indices of rats fed experimental diets*.

	Serum		Liver						Heart		Kidneys	
	AST (U/L)	ALT (U/L)	Mass (g/100g BW)	TBARS (μg/g)	GSH+GSSG (μmol/g)	GSH (μmol/g)	GSSG (μmol/g)	GSH/ GSSG	Mass (g/100g BW)	TBARS (μg/g)	Mass (g/100g BW)	TBARS (μg/g)
Group n=8												
C_S	61.9^{b}	23.7^{b}	3.99^{d}	3.65	38.7	26.5	12.2^{d}	2.19^{a}	0.241	5.67	0.539^{c}	6.69
C_F	83.4^{a}	45.0^{a}	4.97^{a}	4.55	54.0	29.5	24.5^{a}	1.21^{c}	0.251	6.62	0.700^{a}	8.34
EP_S	63.4^{b}	27.2^{b}	4.02^{cd}	3.32	42.3	27.8	14.5^{cd}	2.01^{a}	0.241	5.83	0.569^{c}	6.44
EP_F	67.1^{b}	29.8^{b}	4.89^{a}	4.00	48.1	27.2	20.9^{ab}	1.39^{bc}	0.261	6.39	0.699^{ab}	8.05
EPA_S	67.9^{b}	24.6^{b}	4.12^{cd}	3.20	46.3	30.4	15.8^{cd}	1.97^{a}	0.250	5.82	0.564^{c}	6.58
EPA_F	64.7^{b}	33.5^{b}	4.56^{b}	3.73	50.0	31.3	18.7^{bc}	1.79^{ab}	0.252	6.04	0.633^{b}	7.50
SEM	*1.828*	*1.595*	*0.069*	*0.097*	*1.311*	*0.799*	*0.833*	*0.082*	*0.003*	*0.099*	*0.011*	*0.169*
Fraction (F)												
C (without)	72.6	34.3	4.48	4.10^{a}	46.4	28.0	18.4	1.70	0.246	6.14	0.619	7.51
EP	65.3	65.3	4.45	3.66^{b}	45.2	27.5	17.7	1.70	0.251	6.11	0.619	7.25
EPA	67.2	67.2	4.29	3.48^{b}	47.9	30.6	17.3	1.85	0.253	5.97	0.600	7.04
p value	*0.155*	*0.139*	*0.056*	*0.007*	*0.641*	*0.268*	*0.803*	*0.585*	*0.415*	*0.732*	*0.429*	*0.407*
Diet type (T)												
Starch	65.0	25.2	4.01	3.40^{b}	42.3^{b}	28.0	14.2	2.04	0.245	5.80^{b}	0.559	6.57^{b}
FRU	71.7	36.1	4.81	4.10^{a}	50.7^{a}	29.3	21.4	1.46	0.255	6.35^{a}	0.667	7.96^{a}
p value	*0.041*	**	**	**	*0.001*	*0.425*	**	**	*0.054*	*0.005*	**	**
Interaction F×T												
p value	*0.006*	*0.017*	*0.032*	*0.593*	*0.121*	*0.647*	*0.012*	*0.048*	*0.174*	*0.205*	*0.020*	*0.501*

*C_S, control diet with corn starch; C_F, control diet with 65% fructose (FRU); EP_S, corn starch diet with the strawberry fraction with ellagitannins and proanthocyanidins (EP); EP_F, fructose diet with the EP fraction; EPA_S, corn starch diet with the strawberry fraction with ellagitannins, proanthocyanidins and anthocyanins (EPA); EPA_F, fructose diet with the EPA fraction.

^{a,b,c} Mean values within a column with unlike superscript letters were shown to be significantly different ($p<0.05$); differences among the groups C_S, C_F, EP_S, EP_F, EPA_S, and EPA_F were indicated with superscripts only in the case of a statistically significant interaction F×T ($p<0.05$) and in that case the differences for the main factors F and T are not shown. **$p<0.001$. ALT, alanine transaminase; AST, aspartate transaminase; TBARS, thiobarbituric acid reactive substances; GSH, reduced glutathione; GSSG, oxidized glutathione; BW, body weight.

berries. Urolithins (A, C, D), which are metabolites of ETs, favorably change the concentration of triglycerides and fatty acid oxidation in adipocytes and liver cells, as demonstrated by Kang *et al.* [2016].

Unfavorable changes in liver, kidney, and heart parameters were noted in our study with the high-fructose diet. A significant F×T interaction showed that, among all experimental groups, the highest hepatic TC and TG concentrations as well as blood serum AST and ALT activities were found in the C_F group ($p<0.05$ *vs*. all other groups; Table 9 and Figure 3). The highest concentration of hepatic GSSG was noted in the C_F group ($p<0.05$ *vs*. remaining groups except EP_F; see: interaction F×T). As a result, the lowest value of GSH/GSSG ratio followed the consumption of the C_F diet ($p<0.05$ *vs*. remaining groups except EP_F; interaction F×T). The two-way ANOVA showed that, irrespective of fraction addition, the fructose treatment significantly decreased the hepatic expression of PPARα (Figure 4), increased hepatic TBARS and total glutathione concentrations as well as increased TBARS concentrations in heart and kidney tissues in comparison to the starch treatment. When the fraction addition is considered regardless of diet type, both EP and EPA dietary fractions significantly increased the expression of PPARα and decreased TBARS concentration in the liver tissue ($p<0.05$ *vs*. C). The addition of EPA to the high-fructose diet more favorably reduced the increase in liver and kidney mass, as well as GSH/GSSG ratio in the liver than the fraction without anthocyanins, which corresponds to the research hypothesis. Regardless ACs presence in the preparation, both strawberry fractions reduced lipid peroxidation and pro-inflammatory processes in the liver. Long-term and high-fructose diet consumption results in non-normative lipid accumulation in the liver and liver weight gain. Moreover, excessive fructose intake promotes glucose metabolism disorders and oxidative stress, which correlate with the possibility of liver damage [Lu *et al*., 2020]. The metabolites of strawberry polyphenols, formed as a result of microbiological biotransformation in the intestine, are largely metabolized in the liver, and liver

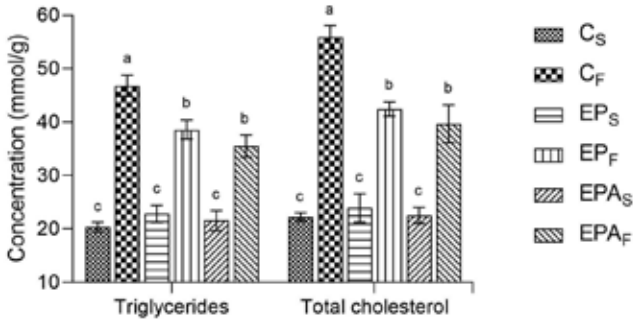

FIGURE 3. Liver triglyceride and total cholesterol concentrations of rats fed experimental diets: C_S, control diet with corn starch; C_F, control diet with 65% fructose; EP_S, corn starch diet with the strawberry fraction with ellagitannins and proanthocyanidins (EP); EP_F, fructose diet with the EP fraction; EPA_S, corn starch diet with the strawberry fraction with ellagitannins, proanthocyanidins and anthocyanins (EPA); EPA_F, fructose diet with the EPA fraction. Bars with unlike letters show significantly different values ($p<0.05$).

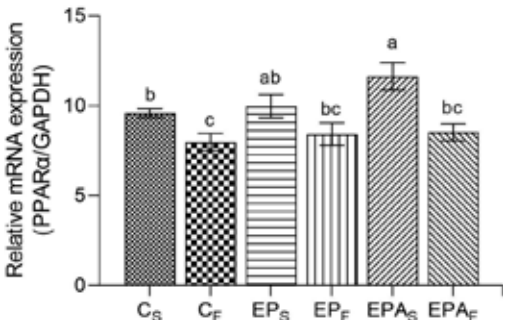

FIGURE 4. Hepatic peroxisome proliferator-activated receptor α (PPARα) expression of rats fed experimental diets: C_S, control diet with corn starch; C_F, control diet with 65% fructose; EP_S, corn starch diet with the strawberry fraction with ellagitannins and proanthocyanidins (EP); EP_F, fructose diet with the EP extract; EPA_S, corn starch diet with the strawberry fraction with ellagitannins, proanthocyanidins and anthocyanins (EPA); EPA_F, fructose diet with the EPA extract. Bars with unlike superscript letters show significantly different values ($p<0.05$).

functions could be modified under the influence of polyphenol metabolic derivatives. In the Elkhadragy & Abdel Moneim [2017] study, the strawberry ethanolic extract significantly alleviated adverse changes in liver function in rats administered hepatotoxic cadmium chloride. Anthocyanin-rich extract from *F. ananassa* effectively lowered cadmium accumulation in the liver, increased the activity of antioxidant enzymes, including superoxide dismutase (SOD), catalase (CAT), GSH peroxidase and GSH reductase, inhibited lipid peroxidation processes, lowered the content of nitric oxide (NO) in the liver, and reduced the apoptosis of hepatocytes. In the acrylamide-treated mice, adverse changes in the activity of antioxidant enzymes in the liver and destruction of hepatocyte DNA were mitigated by a diet supplemented with freeze-dried strawberries [Zhao *et al*., 2015]. Strawberry preparations rich in ETs investigated in the experiment of Fotschki *et al.* [2018] with rats fed a fructose-rich diet also caused beneficial changes in the liver GSSG concentration and the desired increase in the GSH/ GSSG ratio.

The application of fructose and strawberry fractions in the experimental diets did not significantly affect the hematological parameters of rats' blood, except for the erythrocyte volumetric variability index (RDWc), whose value increased significantly when the diet was loaded with fructose (data not shown). RDW corresponds to anisocytosis, a factor that indicates the variability of the red blood cell volume distribution. Recent studies have indicated that the RDW can be used as a laboratory parameter in such diseases as prostate cancer, inflammatory bowel diseases, and cardiovascular diseases [Cheng *et al*., 2017]. The RDW is now a commonly used laboratory marker of an inflammatory condition in the body. An elevated anisocytosis may indicate anemia caused by iron deficiency. According to the latest research with rats [Wang *et al*., 2021], a high-fructose diet causes systemic iron deficiency and hepatic iron overload possibly as a result of activation of a pro-inflammatory state, which may explain the increase in RDW in the fructose groups in our study.

Irrespective of fraction addition, the fructose treatment significantly reduced the cecal concentration of nasutin A and urinal concentration of nasutin A glucuronide, in comparison to the starch treatment (Figure 5). Considering dietary fraction addition, the EPA treatment excelled the EP one in cecal nasutin A and urinal nasutin A glucuronide concentrations ($p<0.05$). A high-fructose diet leads to changes in the intestinal microflora, which to a large extent determines the qualitative and quantitative composition of polyphenol metabolites in intestinal digesta and body fluids. Milala *et al*. [2017] have indicated NS to be the main metabolite in the digestive tract and in the faces, blood serum, and urine of rats fed a diet with ET-rich strawberry extracts. NSs, as well as other metabolites of ETs, such as UTs, are believed to elicit anti-inflammatory, antioxidant, chemopreventive, and anti-carcinogenic effects [Stanisławska *et al.,* 2016]. Mazzone *et al*. [2013] have demonstrated a strong antioxidant effect of nasutin A in a study using density functional theories across three different response mechanisms: hydrogen atom transfer (HAT), electron transfer followed by proton transfer (SET-PT), and sequential proton loss electron transfer (SPLET). In the study by Stanisławska *et al.* [2016], nasutin A inhibited the proliferation of prostate cancer cells *in vitro*. In the discussed studies, the fructose diet adversely

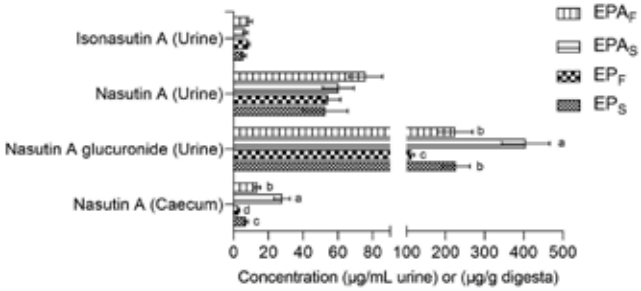

FIGURE 5. Ellagitannins' metabolite concentrations in the caecal digesta and in the urine of rats fed experimental diets: EP_S, corn starch diet with the strawberry fraction with ellagitannins and proanthocyanidins (EP); EP_F, fructose diet with the EP fraction; EPA_S, corn starch diet with the strawberry fraction with ellagitannins, proanthocyanidins and anthocyanins (EPA); EPA_F, fructose diet with the EPA fraction. Bars with unlike superscript letters were show significantly different values ($p<0.05$).

affected the cecal concentration of nasutin A and urinal concentration of nasutin A glucuronide. According to the research hypothesis, the presence of ACs in the EPA fraction probably limited the adverse impact of the high-fructose diet on the intestinal microflora, and thus on the processes of polyphenol transformation by the beneficial intestinal microbiome, which resulted in higher concentrations of nasutin A and nasutin A glucuronide in rats' cecum and urine in the EPA groups.

CONCLUSIONS

To sum up, the high-fructose diet administered to rats in this study led to disorders in their gastrointestinal tract and adverse changes in the antioxidant and pro-inflammatory status of their bodies, as well as in their liver and lipid metabolism. Nevertheless, the addition of strawberry EP fraction, containing mostly ellagitannins and proanthocyanidins, mitigated the negative effects of consuming the high-fructose diet, like the reduction in TC and TG and the increase in ACW and ACL in blood serum. Interestingly, the EPA fraction containing anthocyanins more distinctly alleviated the negative effects of consuming excess fructose in the diet, as manifested by a decreased serum IL-6 concentration, atherogenicity index lg(TG/HDL) and hepatic GSSG as well as by an increased serum level of ACW and hepatic GSH/GSSG ratio. Part of these effects can be probably attributed to the increased activity of cecal microbiota leading to higher concentrations of cecal SCFAs and urinal bioactive ellagitannin metabolites. The biotransformation of anthocyanins by the intestinal microbiota probably intensified the beneficial effects of the EPA fraction. However, the metabolism of phenolic compounds, including ACs and ETs, depends on many factors, including both the species- and the individual-specific ones. Future studies need to be conducted with other experimental models, including especially human trials.

RESEARCH FUNDING

This research was supported by statutory funds from the Department of Biological Functions of Food, Institute of Animal Reproduction and Food Research, Polish Academy of Sciences, Olsztyn, Poland; and Department of Microbiology and Food Technology, Faculty of Agriculture and Biotechnology, University of Science and Technology, Bydgoszcz, Poland.

CONFLICTS OF INTEREST

The authors declare no conflict of interest.

ORCID IDs

B. Fotschki https://orcid.org/0000-0002-9727-7481
J. Juśkiewicz https://orcid.org/0000-0003-0068-5970
M. Kosmala https://orcid.org/0000-0002-9018-3028
P. Matusevicius https://orcid.org/0000-0002-6612-2479
J. Milala https://orcid.org/0000-0002-4732-1907
E. Żary-Sikorska https://orcid.org/0000-0001-8140-3861

REFERENCES

1. Aboonabi, A., Aboonabi, A. (2020). Anthocyanins reduce inflammation and improve glucose and lipid metabolism associated with inhibiting nuclear factor-kappaB activation and increasing PPAR-γ gene expression in metabolic syndrome subjects. *Free Radical Biology and Medicine*, 150, 30–39. https://doi.org/10.1016/j.freeradbiomed.2020.02.004
2. AOAC, Official Methods of Analysis, 21st Edition – AOAC International. 2019. Available online: [https://www.aoac.org/official-methods-of-analysis-21st-edition-2019] (accessed 23 June 2020).
3. Aura, A.M., Martin-Lopez, P., O'Leary, K.A., Williamson, G., Oksman-Caldentey, K.-M., Poutanen, K., Santos-Buelga, C. (2005). *In vitro* metabolism of anthocyanins by human gut microflora. *European Journal of Nutrition*, *44*(3), 133–142. https://doi.org/10.1007/s00394-004-0502-2
4. Awolade, P., Cele, N., Kerru, N., Gummidi, L., Oluwakemi, E., Singh, P. (2020). Therapeutic significance of β-glucuronidase activity and its inhibitors: A review. *European Journal of Medicinal Chemistry*, 187, art. no. 111921. https://doi.org/10.1016/j.ejmech.2019.111921
5. Bauza-Kaszewska, J., Żary-Sikorska, E., Gugolek, A., Ligocka, A., Kosmala, M., Karlińska, E., Fotschki, B., Juśkiewicz, J. (2021). Synergistic antimicrobial effect of raspberry (*Rubus idaeus* L., Rosaceae) preparations and probiotic bacteria on enteric pathogens. *Polish Journal of Food and Nutrition Sciences, 71*(1), 51–59. https://doi.org/10.31883/pjfns/132897
6. Bialonska, D., Ramnani, P., Kasimsetty, S.G., Muntha, K.R., Gibson, G.R., Ferreira, D. (2010). The influence of pomegranate by-product and punicalagins on selected groups of human intestinal microbiota. *International Journal of Food Microbiology*, *140*(2–3), 175–182. https://doi.org/10.1016/j.ijfoodmicro.2010.03.038
7. Botsoglou, N.A., Fletouris, D.J., Papageorgiou, G.E., Vassilopoulos, V.N., Mantis, A.J., Trakatellis, A.G. (1994). Rapid, sensitive, and specific thiobarbituric acid method for measuring lipid peroxidation in animal tissue, food and feedstuff samples. *Journal of Agricultural and Food Chemistry, 42*(9), 1931–1937. https://doi.org/10.1021/jf00045a019
8. Buzzini, P., Arapitsas, P., Goretti, M., Branda, E., Turchetti, B., Pinelli, P., Ieri, F., Romani, A. (2008). Antimicrobial and antiviral activity of hydrolysable tannins. *Mini-Reviews in Medicinal Chemistry*, *8*(12), 1179–1187. https://doi.org/10.2174/138955708786140990
9. Cheng, S., Han, F., Wang, Y., Xu, Y., Qu, T., Ju, Y., Lu, Z. (2017). The red distribution width and the platelet distribution width as prognostic predictors in gastric cancer. *BMC Gastroenterology*, *17*(1), art. no. 163. https://doi.org/10.1186/s12876-017-0685-7
10. DeBosch, B.J., Chen, Z., Finck, B.N., Chi, M., Moley, K.H. (2013). Glucose transporter-8 (GLUT8) mediates glucose intolerance and dyslipidemia in high-fructose diet-fed male mice. *Molecular Endocrinology*, *27*(11), 1887–1896. https://doi.org/10.1210/me.2013-1137
11. Elkhadragy, M.F., Abdel Moneim, A.E. (2017). Protective effect of *Fragaria ananassa* methanolic extract on cadmium chloride (CdCl2)-induced hepatotoxicity in rats. *Toxicology Mechanisms and Methods*, *27*(5), 335–345. https://doi.org/10.1080/15376516.2017.1285973

12. EU Directive (2010/63/EU). Directive 2010/63/EU of the European Parliament and of the Council of 22 September 2010 on the protection of animals used for scientific purposes.
13. Ertan, K., Türkyılmaz, M., Özkan, M. (2020). Color and stability of anthocyanins in strawberry nectars containing various co-pigment sources and sweeteners. *Food Chemistry*, *310*, art. no. 125856. https://doi.org/10.1016/j.foodchem.2019.125856
14. Folch, J., Lees, M., Sloane Stanley, G.H. (1957). A simple method for the isolation and purification of total lipids from animal tissues. *Journal of Biological Chemistry*, *226*(1), 497–509. https://doi.org/10.1016/S0021-9258(18)64849-5
15. Forbes-Hernández, T.Y., Gasparrin, M., Afrin, S., Cianciosi, D., González-Paramás, A.M., Santos-Buelga, C., Mezzetti, B., Quiles, J.L., Battino, M., Giampieri, F., Bompadre, S. (2017). Strawberry (cv. Romina) methanolic extract and anthocyanin-enriched fraction improve lipid profile and antioxidant status in HepG2 cells. *International Journal of Molecular Sciences, 18*(6), art. no. 1149. https://doi.org/10.3390/ijms18061149
16. Fotschki, B., Milala, J., Jurgoński, A., Karlińska, E., Zduńczyk, Z., Juśkiewicz, J. (2014). Strawberry ellagitannins thwarted the positive effects of dietary fructooligosaccharides in rat cecum. *Journal of Agricultural and Food Chemistry*, *62*(25), 5871–5880. https://doi.org/10.1021/jf405612a
17. Fotschki, B., Juśkiewicz, J., Jurgoński, A., Kołodziejczyk, K., Milala, J., Kosmala, M., Zduńczyk, Z. (2016). Anthocyanins in strawberry polyphenolic extract enhance the beneficial effects of diets with fructooligosaccharides in the rat cecal environment. *PLoS ONE*, *11*(2), art. no. e0149081. https://doi.org/10.1371/journal.pone.0149081
18. Fotschki, B., Juśkiewicz, J., Kołodziejczyk, K., Jurgoński, A., Kosmala, M., Milala, J., Ognik, K., Zduńczyk, Z. (2018). Protective effects of ellagitannin-rich strawberry extracts on biochemical and metabolic disturbances in rats fed a diet high in fructose. *Nutrients*, *10*(4), art. no. 445. https://doi.org/10.3390/nu10040445
19. Fuke, N., Nagata, N., Suganuma, H., Ota, T. (2019). Regulation of gut microbiota and metabolic endotoxemia with dietary factors. *Nutrients*, *11*(10), art. no. 2277. https://doi.org/10.3390/nu11102277
20. Giampieri, F., Tulipani, S., Alvarez-Suarez, J.M., Quiles, J.L., Mezzetti, B., Battino, M. (2012). The strawberry: Composition, nutritional quality, and impact on human health. *Nutrition*, *28*(1), 9–19. https://doi.org/10.1016/j.nut.2011.08.009
21. Gonzalez-Barrio, R., Truchado P., Ito, H., Espín, J.C., Tomas-Barberan, F. (2011). UV and MS identification of urolithins and nasutins, the bioavailable metabolites of ellagitannins and ellagic acid in different mammals. *Journal of Agricultural and Food Chemistry*, *59*(4), 1152–1162. https://doi.org/10.1021/jf103894m
22. Hambly, R.J., Rumney, C.J., Cunningham, M., Fletcher, J.M.E., Rijken, P., Rowland, I.R. (1997). Influence of diets containing high and low risk factors for colon cancer on early stages of carcinogenesis in human-flora-associated (HFA) rats. *Carcinogenesis*, *18*(8), 1535–1539. https://doi.org/10.1093/carcin/18.8.1535
23. Hassimotto, N., Moreira, V., Nascimento, N., Souto, P., Teixeira, C., Lajolo, F.M. (2013). Inhibition of carrageenan-induced acute inflammation in mice by oral administration of anthocyanin mixture from wild mulberry and cyanidin-3-glucoside. *BioMed Research International, 2013*, art. no. 146716. https://doi.org/10.1155/2013/146716
24. Hidalgo, M., Oruna-Concha, M.J., Kolida, S., Walton, G.E., Kallithraka, S., Spencer, J.P.E., Gibson, G.R., de Pascual-Teresa, S. (2012). Metabolism of anthocyanins by human gut microflora and their influence on gut bacterial growth. *Journal of Agricultural and Food Chemistry, 60*(15), 3882–3890. https://doi.org/10.1021/jf3002153
25. Hillilä, M., Färkkilä, M.A., Sipponen, T., Rajala, J., Koskenpato, J. (2016). Does oral galactosidase relieve irritable bowel symptoms?. *Scandinavian Journal of Gastroenterology*, *51*(1), 16–21. https://doi.org/10.3109/00365521.2015.1063156
26. Horne, R.G., Yu, Y., Zhang, R., Abdalqadir, N., Rossi, L., Surette, M., Sherman, P.M., Adeli, K. (2020). High fat-high fructose diet-induced changes in the gut microbiota associated with dyslipidemia in Syrian hamsters. *Nutrients*, *12*(11), art. no. 3557. https://doi.org/10.3390/nu12113557
27. Jarosławska, J., Juśkiewicz, J., Wróblewska, M., Jurgoński, A., Król, B., Zduńczyk, Z. (2011). Polyphenol-rich strawberry pomace reduces serum and liver lipids and alters gastrointestinal metabolite formation in fructose-fed rats. *Journal of Nutrition*, *141*(10), 1777–1783. https://doi.org/10.3945/jn.111.143677
28. Jurgoński, A., Juśkiewicz, J., Zduńczyk, Z. (2013). An anthocyanin-rich extract from Kamchatka honeysuckle increases enzymatic activity within the gut and ameliorates abnormal lipid and glucose metabolism in rats. *Nutrition*, *29*(6), 898–902. https://doi.org/10.1016/j.nut.2012.11.006
29. Kang, I., Kim, Y.E., Tomás-Barberán, F.A., Espín, J.C., Chung, S. (2016). Urolithin A, C, and D, but not iso-urolithin A and urolithin B, attenuate triglyceride accumulation in human cultures of adipocytes and hepatocytes. *Molecular Nutrition and Food Research*, *60*(5), 1129–1138. https://doi.org/10.1002/mnfr.201500796
30. Kennedy, J.A., Jones, G.P. (2001). Analysis of proanthocyanidin cleavage products following acid-catalysis in the presence of excess phloroglucinol. *Journal of Agricultural and Food Chemistry*, *49*(4), 1740–1746. https://doi.org/10.1021/jf001030o
31. Kosmala, M., Zduńczyk, Z., Juśkiewicz, J., Jurgoński, A., Karlińska, E., Macierzyński, J., Jańczak, R., Rój, E. (2015). Chemical composition of defatted strawberry and raspberry seeds and the effect of these dietary ingredients on polyphenol metabolites, intestinal function, and selected serum parameters in rats. *Journal of Agricultural and Food Chemistry*, *63*(11), 2989–2996. https://doi.org/10.1021/acs.jafc.5b00648
32. Liu, C.J., Lin, J.Y. (2013). Anti-inflammatory effects of phenolic extracts from strawberry and mulberry fruits on cytokine secretion profiles using mouse primary splenocytes and peritoneal macrophages. *International Immunopharmacology*, *16*(2), 165–170. https://doi.org/10.1016/j.intimp.2013.03.032

33. Loke, Y.L., Chew, M.T., Ngeow, Y.F., Lim, W.W.D., Peh, S.C. (2020). Colon carcinogenesis: the interplay between diet and gut microbiota. *Frontiers in Cellular and Infection Microbiology, 10*, art. no. 603086. https://doi.org/10.3389/fcimb.2020.603086
34. Lu, Y., Wu, Y., Chen, X., Yang, X., Xiao, H. (2020). Water extract of shepherd's purse prevents high-fructose induced-liver injury by regulating glucolipid metabolism and gut microbiota. *Food Chemistry*, *16*(342), art. no. 128536. https://doi.org/10.1016/j.foodchem.2020.128536
35. Markowiak-Kopeć, P., Śliżewska, K. (2020). The effect of probiotics on the production of short-chain fatty acids by human intestinal microbiome. *Nutrients, 12*(4), art. no. 1107. https://doi.org/10.3390/nu12041107
36. Mazzone, G., Marirosa, T., Nino, R. (2013). Density functional predictions of antioxidant activity and UV spectral features of nasutin a, isonasutin, ellagic acid, and one of its possible derivatives. *Journal of Agricultural and Food Chemistry*, *61*(40), 9650–9657. https://doi.org/10.1021/jf403262k
37. Milala, J., Kosmala, M., Karlińska, E., Juśkiewicz, J., Zduńczyk, Z., Fotschki, B. (2017). Ellagitannins from strawberries with different degree of polymerization showed different metabolism through gastrointestinal tract of rats. *Journal of Agricultural and Food Chemistry*, *65*(49), 10738–10748. https://doi.org/10.1021/acs.jafc.7b04120
38. Molan, A.L., Liu, Z., Kruger, M. (2010). The ability of blackcurrant extracts to possitively modulate key markers of gastrointestinal function in rats. *World Journal of Microbiology and Biotechnology*, *26*(10), 1735– 1743. https://doi.org/10.1007/s11274-010-0352-4
39. Mizobe, T., Nakajima, Y., Ueno, H., Sessler, D.I. (2006). Fructose administration increases intraoperative core temperature by augmenting both metabolic rate and the vasoconstriction threshold. *Anesthesiology*, *104*(6), 1124–1130. https://doi.org/10.1097/00000542-200606000-00005
40. Nowicka, A., Kucharska, A.Z., Sokół-Łętowska, A., Fecka, I. (2019). Comparison of polyphenol content and antioxidant capacity of strawberry fruit from 90 cultivars of *Fragariaananassa* Duch. *Food Chemistry*, *270*, 32–46. https://doi.org/10.1016/j.foodchem.2018.07.015
41. Park, G., Jung, S., Wellen, K.E., Jang, Ch. (2021). The interaction between the gut microbiota and dietary carbohydrates in nonalcoholic fatty liver disease. *Experimental & Molecular Medicine*, *53*, 809–822. https://doi.org/10.1038/s12276-021-00614-x
42. Prior, R.L., Wu, X., Gu, L., Hager, T., Hager, A., Wilkes, S., Howard, L. (2009). Purified berry anthocyanins but not whole berries normalize lipid parameters in mice fed an obesogenic high fat diet. *Molecular Nutrition and Food Research*, *53*(11), 1406–1418. https://doi.org/10.1002/mnfr.200900026
43. Rahman, I., Kode, A., Biswas, S.K. (2006). Assay for quantitative determination of glutathione and glutathione disulfide levels using enzymatic recycling method. *Nature Protocols*, *1*(6), 3159–3165. https://doi.org/10.1038/nprot.2006.378
44. Reagan-Shaw, S., Nihal, M., Ahmad, N. (2008.) Dose translation from animal to human studies revisited. *The FASEB Journal*, *22*(3), 659–661. https://doi.org/10.1096/fj.07-9574LSF
45. Reeves, P.G. (1997). Components of the AIN-93 diets as improvements in the AIN-76A diet. *Journal of Nutrition*, *127*(5), 838S-841S. https://doi.org/10.1093/jn/127.5.838S
46. Selma, M.V., Beltrán, D., García-Villalba, R., Espín, J.C., Tomás-Barberán, F.A. (2014). Description of urolithin production capacity from ellagic acid of two human intestinal *Gordonibacter* species. *Food and Function*, *5*(8), 1779–1784. https://doi.org/10.1039/C4FO00092G
47. Sirijan, M., Pipattanawong, N., Saeng-on, B., Chaiprasart, P. (2020). Anthocyanin content, bioactive compounds and physico-chemical characteristics of potential new strawberry cultivars rich in-anthocyanins. *Journal of Berry Research, 10*(3), 397–410. https://doi.org/10.3233/JBR190487
48. Sójka, M., Klimczak, E., Macierzyński, J., Kołodziejczyk, K. (2013). Nutrient and polyphenolic composition of industrial strawberry press cake. *European Food Research and Technology*, *237*(6), 995–1007. https://doi.org/10.1007/s00217-013-2070-2
49. Stanisławska, I.J., Granica, S., Piwowarski, J.P., Szawkało, J., Wiązecki, K., Czarnocki, Z., Kiss A.K. (2016). 5-(3',4',5'-trihydroxyphenyl)-γ-valerolactone and nasutin A inhibit LNCaP prostate cancer cell proliferation. *Planta Medica*, *82*(S01), S1-S381. https://doi.org/10.1055/s-0036-1596836
50. Tappy, L., Lê, K.A., (2010). Metabolic effects of fructose and the worldwide increase in obesity. *Physiological Reviews*, *90*(1), 23– 46. https://doi.org/10.1152/physrev.00019.2009
51. Wang, Ch., Wang, X., Song, G., Xing, H., Linquan, Y., Han, K., Chang, Y-Z. (2021). A high-fructose diet in rats induces systemic iron deficiency and hepatic iron overload by an inflammation mechanism. *Journal of Food Biochemistry, 45*(1), art. no. e13578. https://doi.org/10.1111/jfbc.13578
52. Xu, J., Yuan, Ch., Wang, G., Ma, H., Jiaming L., Xu, L., Li, L., Seeram N.P., Huang X., Mu, Y., Li, Y. (2018). Urolithins attenuate LPS-induced neuroinflammation in BV2Microglia *via* MAPK, Akt, and NF-κB signaling pathways. *Journal of Agricultural and Food Chemistry, 66*(3), 571–580. https://doi.org/10.1021/acs.jafc.7b03285
53. Zduńczyk, Z., Juśkiewicz, J., Estrella, I. (2006). Caecal parameters of rats fed diets containing grapefruit polyphenols and inulin as single supplements or in a combination. *Nutrition*, *22*(9), 898–904. https://doi.org/10.1016/j.nut.2006.05.010
54. Zhao, M., Liu, X., Luo, Y., Guo, H., Hu, X., Chen, F. (2015). Evaluation of protective effect of freeze-dried strawberry, grape, and blueberry powder on acrylamide toxicity in mice. *Journal of Science*, *80*(4), H869–H874. https://doi.org/10.1111/1750-3841.12815
55. Żary-Sikorska, E., Fotschki, B., Fotschki, J., Wiczkowski, W., Juśkiewicz, J. (2019). Preparations from purple carrots contain-

ing anthocyanins improved intestine microbial activity, serum lipid profile and antioxidant status in rats. *Journal of Functional Foods*, *60*, art. no. 103442.
https://doi.org/10.1016/j.jff.2019.103442

56. Żary-Sikorska, E., Fotschki, B., Jurgoński, A., Kosmala, M., Milala, J., Kołodziejczyk, K., Majewski, M., Ognik, K., Juśkiewicz, J. (2020). Protective effects of a strawberry ellagitannin-rich extract against pro-oxidative and pro-inflammatory dysfunctions induced by a high-fat diet in a rat model. *Molecules*, *25*(24), art. no. 5874.
https://doi.org/10.3390/molecules25245874

Pol. J. Food Nutr. Sci., 2021, Vol. 71, No. 4, pp. 441–449
On-line ISSN: 2083-6007
Print ISSN: 1230-0322
DOI: 10.31883/pjfns/143574
http://journal.pan.olsztyn.pl

Original article
Section: Food Quality and Functionality

Sinigrin Encapsulation in Liposomes: Influence on *In Vitro* Digestion and Antioxidant Potential

Ivana Drvenica[1], *Ivica Blažević*[2], *Perica Bošković*[3], *Andre Bratanić*[4], *Branko Bugarski*[5], *Tea Bilušić*[1]*

[1]*Institute for Medical Research, University of Belgrade, Dr Subotića 4, 11000 Belgrade, Serbia*
[2]*Faculty of Chemistry and Technology, University of Split, Ruđera Boškovića 35, 21000 Split, Croatia*
[3]*Faculty of Science, University of Split, Ruđera Boškovića 33, 21000 Split, Croatia*
[4]*Division of Gastroenterology and Hepatology, University Hospital Split, Spinčićeva 1, 21000 Split, Croatia*
[5]*Faculty of Technology and Metallurgy, University of Belgrade, Karnegijeva 4, 11000 Belgrade, Serbia*

Key words: sinigrin, liposomes, oxidative stability, gastric digestion, duodenal digestion, antioxidant potential

Encapsulation of sinigrin in liposomes with the proliposomal method was performed in order to evaluate the effect of this process on *in vitro* simulated digestion and antioxidant potential of sinigrin. The recovery of sinigrin after simulated gastric and duodenal digestion of its free and liposomal forms was determined with HPLC-UV using human digestive juices. The antioxidant potential of sinigrin and sinigrin-loaded liposomes was determined with the Rancimat test as their ability to prolong oxidative stability of edible oil. The efficiency of 62% was obtained by encapsulating sinigrin in liposomes. The values of mean diameter, polydispersity index and zeta potential showed satisfactory size uniformity and physical stability of the liposomes containing sinigrin. Liposomes were shown to inhibit the digestion of sinigrin in both human gastric and intestinal juices, clearly enabling its prolonged release. Moreover, sinigrin in the liposomal form significantly prolonged the induction time of edible oil oxidation compared to its free form. The results obtained are encouraging from the point of view of a possible incorporation of the sinigrin-loaded liposomes in real functional food systems or their use as nutraceuticals.

INTRODUCTION

Glucosinolates (GSLs) are water-soluble plant secondary metabolites with an *S*-β-D-glucopyrano unit, an *O*-sulphated anomeric (*Z*)-thyohydroximate function, and a variable aglucon side chain. To date, 140 structurally different GSLs have been reported, although over 30% of them have not yet been characterized by nuclear magnetic resonance (NMR) and mass spectrometry (MS) techniques [Blažević *et al*., 2020]. GSLs are typical of Brassicaceae plants including mustard, radish, cabbage, broccoli, Brussels sprouts, cauliflower, horseradish. They are also found in other families of Brassicales, *e.g.* Capparaceae, Cleomaceae, Caricaeae [Mithen *et al*., 2010]. Due to the activity of myrosinase (β-thioglucosidase), and depending on their variable chain, GSLs break down into different products, including mostly biologically active isothiocyanates, which exhibit potent antimicrobial, antioxidant and anticancer activities [Melrose, 2019].

Sinigrin (allyl GSL or prop-2-enyl GSL, Figure 1) is one of the first known GSLs, whose name is derived from "*Sinapis nigra*" (currently known as *Brassica nigra*). It is one of the most abundant GSLs found in *Brassica* vegetables. The correct structure was proposed by Ettlinger & Lundeen [1956] while the structural issue of the geometrical isomerism at the C=N bond was shown to be *Z* (or anti-) by X-ray crystallographic analysis by Waser & Watson [1963]. It is one of the most studied GSLs thanks to its degradation product, the pharmacologically active allyl isothiocyanate, a volatile sulphur-containing compound [Blažević *et al*., 2019; Corrales *et al*., 2014]. A very important aspect of the biological activity of isothiocyanates is their antimicrobial potential against human pathogens, especially against bacteria

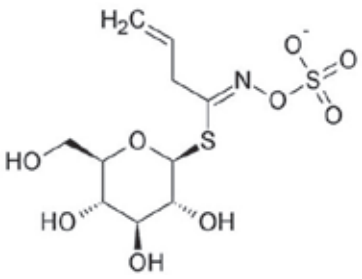

FIGURE 1. Chemical structure of sinigrin.

* Corresponding Author:
E-mail: tea@ktf-split.hr (T. Bilušić)

Submitted: 21 June 2021
Accepted: 3 November 2021
Published on-line: 26 November 2021

© Copyright by Institute of Animal Reproduction and Food Research of the Polish Academy of Sciences
© 2021 Author(s). This is an open access article licensed under the Creative Commons Attribution-NonCommercial-NoDerivs License (http://creativecommons.org/licenses/by-nc-nd/4.0/).

with multi-drug-resistance phenotypes [Romeo *et al*., 2018]. Moreover, many studies have shown that isothiocyanates exhibit anti-tumour activity by affecting multiple pathways including apoptosis, mitogen-activated protein kinase (MAPK) signaling, oxidative stress, and cell cycle progression [Jie *et al.*, 2014; Mitsioginanni *et al*., 2019; Wu *et al*., 2009]. There are many examples of the use of encapsulation techniques to enhance/protect the biological activities of GSLs and isothiocyanates: the antitumor effect against glial tumour cells by broccoli extracts [Radünz *et al*., 2020]; the antimicrobial activity of allyl isothiocyanate using different carriers such as gum Arabic, chitosan, sodium polyacrylate-coated halloysite, mesoporous silica particles [Park *et al*., 2012; Maruthupandy & Seo, 2019]; the cytotoxic activity of sinigrin-loaded phytosomes (phytolipid delivery system) against A-375 cells (human melanoma cell line) [Mazumder *et al*., 2016]; or the cytotoxic and apoptotic potential of silver nanoparticles with sinigrin [Yuan *et al*., 2018]. However, there is no study on sinigrin encapsulated in liposomes. Liposomes, *i.e.* lipid bilayers with a diameter of 50–1000 nm, are particularly attractive encapsulation systems that offer increased stability of encapsulated materials against a range of environmental, enzymatic, and chemical stresses [Emami *et al*., 2016]. What distinguishes liposomes from other encapsulation systems is their ability to encapsulate both hydrophobic (within the membrane of the particle) and hydrophilic (within the core of the liposome) substances [Gaede & Gawrisch, 2003]. The possibility of industrial production is also of great importance for their use in the food industry. However, the fact that liposomes can be produced from natural components (biocompatible, biodegradable and non-toxic) makes these systems attractive from the point of view of faster and easier implementation in cosmetic and food end products [Malheiros *et al*., 2010]. There are several reports demonstrating improved stability of liposomal formulations of commonly used nutraceuticals, such as vitamin C [Wechtersbach *et al*., 2012; Yang *et al*., 2012] during storage or processing conditions (*e.g.*, heat treatment), compared to the solutions of free nutraceuticals. Due to the delayed release of active ingredients, liposomes can improve the bioavailability of antioxidants [Takahashi *et al*., 2009] and reduce their cytotoxicity [Isailović *et al*., 2013]. Enhanced antimicrobial (*e.g.*, *Citrus limon*), antifungal (*e.g.*, *Eucalyptus camaldulensis*) and other biological activities (*e.g.*, *Artemisia arborescens* L.) of essential oils incorporated into liposomes have also been reported [Gortzi *et al*., 2007; Moghimipour *et al*., 2012]. Previously, liposomes were reported to be quite effective in enhancing the chemopreventive efficacy of phenethyl isothiocyanate [Pulliero *et al*., 2015; Sun *et al*., 2019]. This is the first report on the gastrointestinal stability of the sinigrin-loaded liposomes in the simulated two-phase digestion model (gastric and duodenal) with human digestive enzymes. There are few studies on the stability and bioaccessibility of sinigrin after a simulated gastrointestinal process and some of them evaluated the influence of human microflora in the bioconversion of sinigrin [Cheng *et al*., 2004; Girgin & Nehir, 2015]. The aim of this study was to monitor the recovery of free sinigrin and sinigrin released from liposomes after a simulated two-phase digestion process using high-performance liquid chromatography with UV detector (HPLC-UV). The effect of the liposomal form of sinigrin on the prolongation of oxidative stability of edible oil was measured with Rancimat test.

MATERIAL AND METHODS

Chemicals

Sinigrin hydrate (≥99.0% (TLC)) was obtained from Sigma Aldrich (St. Louis, MA, USA). Phospholipon 90G was supplied by Natterman Phospholipids GmbH (Köln, Germany). All other reagents and solvents were of analytical grade.

Preparation of sinigrin-loaded liposomes

Liposomes with sinigrin were prepared with the proliposome method, which allows to easily increase the scale of production to the industrial level [Liović *et al*., 2019]. We used soy lecithin Phosholipon 90G which is purified phosphatidylcholine (min 94.0% by weight), with a low content of lysophosphatidylcholine (max. 4.0% by weight) and tocopherol (max. 0.3% by weight). Phosholipon 90G was mixed with ethanol and water (1:0.8:2, *w/w/w*) at the temperature up to 60°C under continuous stirring at 800 rpm to form a homogenous mixture. The mixture was cooled down to room temperature, and sinigrin was added to the homogenous mixture under continuous stirring at 800 rpm during the next 30 min to obtain the final liposomal formulation.

Determination of the encapsulation efficiency of sinigrin by liposomes

The proportion of sinigrin entrapped within liposomes was determined according to the following procedure. Centrifugation of 10 times diluted suspension of liposome at 21,952×*g* for 1 h at 10°C (Eppendorf centrifuge 5804R, Hamburg, Germany) was used to separate supernatant (containing non-encapsulated sinigrin) from the precipitate (liposomes with encapsulated sinigrin). The resulting precipitate was dissolved in 10 mL of methanol, filtered through 0.2 μm pore size filter and transferred to a clean tube for further analysis on HPLC-UV. Based on HPLC-UV analysis, the percentage of encapsulated sinigrin was calculated, as the percentage of sinigrin entrapped in liposomes relative to the total amount of added sinigrin.

In vitro release kinetics of sinigrin from liposomes

In vitro monitoring of the release kinetics of sinigrin from the liposome formulation was performed in a Franz diffusion cell (PermeGear, Inc., Hellertown, PA, USA), containing donor and receptor cell separated with an acetate-cellulose membrane, based on the procedure given in Isailović *et al*. [2013]. In brief, after Franz cell thermostating, we placed 1 mL of liposome dispersions containing sinigrin as a donor phase in diffusion cell chamber. Magnetic stirring speed and temperature were set at 600 rpm and 37°C, respectively. During the next 6 h, an aliquot of the sample (0.5 mL for each time point) was taken from the receptor section at different time intervals (5, 10, 15, 30, 45, 60, 90, 120, 180, 200, 240 and 360 min) for HPLC-UV analysis and replaced by the same volume of distilled water. The results were expressed as C/C_e against time (where C is sinigrin concentration at time t and C_e is sinigrin

equilibrium concentration). The release profile of sinigrin from liposomes was compared with the profile of a sinigrin aqueous solution that was used as a control (with identical sinigrin concentration as the one used for liposomes preparation).

Size and zeta potential measurements

The average particle size (hydrodynamic weighted mean diameter, z-average) and polydispersity index (PDI) of 1000 times diluted liposome suspension was measured on a Zetasizer Nano ZS (Malvern Instruments, Malvern, UK) at 25±0.1°C, using the dynamic light scattering (DLS), so-called photon correlation spectroscopy (PCS). The same instrument was used for the zeta-potential measurement as described in Liović *et al*. [2019]. The physical stability test was performed during 14 days with the liposomal preparation stored at 4°C.

Light microscopy analysis

Empty liposomes and liposomes loaded with sinigrin were viewed under a Motic light microscope (BA 210, Xiamen, China) equipped with a Moticam digital camera (1 SP, 1,3 MP) and a Motic Images Plus 2.0 software.

***In vitro* digestion method**

Prior to the *in vitro* digestion procedure, the collection of human digestive juices from the stomach and duodenum of healthy donors was carried out using an endoscope. The collected juices were stored in a sterile tube and then centrifuged in a mySpin 12 microcentrifuge (Thermo Scientific, Waltham, MA, USA) at room temperature, for 10 min at 7,700×*g* to remove mucus and cell debris. To reduce inter-individual variations, batches of pooled gastric and duodenal juices were prepared and then stored at –20°C until use. The enzymatic activity of collected digestive juices was determined using the spectrophotometric method described by Almaas *et al*. [2006]. According to this method, one unit of enzyme activity (U) is defined as the amount of enzyme that causes the absorbance change of 1 between the blank and the sample, after 20 min at 37°C. The *in vitro* digestion procedure was performed according to Furlund *et al*. [2013]. The incubation temperature was 37°C. The simulated digestion process was carried out in a horizontal shaking bath (1,200 rpm). The adjustment of appropriate pH (2.5 for gastric phase and 7.5 for duodenal phase) was done using 1 M HCl and 2 M NaOH. Incubation intervals were 60 min for the gastric phase, and 120 min for the duodenal phase. Due to the liquid nature of the sample, the incubation interval of 60 min for gastric phase was long enough. According to the previously mentioned spectrophotometric method, the enzymatic activity of 1 U was equivalent to 20 μL of human gastric juice and 25 μL of human duodenal juice. The quantities of digestive juices used in this experiment were as follows: 200 mL for the gastric phase, and 800 mL for the duodenal phase. The *in vitro* digestion process was stopped on ice for the period of 5 min. After the digestion, the samples were centrifuged at room temperature, for 10 min at 13,000×*g*. The undigested sample (control) and digested samples were kept at –20°C. All digestive processes were run in duplicate. The recovery of sinigrin was calculated as follows [Girgin & Nehir, 2015]:

$$\text{Recovery of sinigrin (\%)} = (S/C) \times 100$$

where: S – sinigrin content after *in vitro* digestion; C – sinigrin content before *in vitro* digestion.

HPLC-UV analysis

The identification and quantification of the encapsulated sinigrin, as well as the monitoring of its release from the obtained formulations, was performed using HPLC-UV according to the modified procedure by Tsao *et al*. [2000]. The analysis was performed on the Ultimate 3000 UHPLC system (Thermo Fisher Scientific, Schwerte, Germany). By optimizing the elution conditions (flow rate 1 mL/min, isocratic conditions) and selecting the mobile phase (acetonitrile/0.025 M ammonium acetate, 1:99, *v/v*), the detection and quantification of sinigrin in the tested formulations at 228 nm (λ_{max}) was successfully performed using the obtained standard curve in methanol and water (80:20). Prior to HPLC-UV analysis, all samples were filtered through 0.2 μm syringe filters and prepared as described above.

Antioxidant potential evaluation

The antioxidant potential of sinigrin, and sinigrin-loaded liposomes was determined as their ability to inhibit the olive oil oxidation. The oxidation of olive oil (pure and with antioxidants) was carried out using the Rancimat apparatus (Methrom 743, Herisau, Switzerland) [ISO 6886:1996] at 120°C (DT=1.4°C) and the constant airflow of 20 L/h. The quantity of olive oil used for this experiment was 2.5 g. Concentrations of samples (sinigrin, liposomes with sinigrin, and pure liposomes) in the olive oil were 0.2 and 0.1% (*w/w*). The conductivity was measured as a function of time, and the results were expressed as induction time. All measurements were performed in triplicate, and the results were expressed as mean value ± standard deviation.

RESULTS AND DISCUSSION

Nowadays, encapsulation technologies have proved to be competitive tools in the development of new nutraceuticals or the properties and functions of commonly used ingredients in the food industry, as they are able to protect active ingredients, improve their stability and prolong their release in the gastrointestinal tract. Encapsulation in liposomes has a number of advantages that are important for the food industry. These include the ability to carry a variety of bioactive compounds, and the health benefits of natural liposomal ingredients such as phospholipids and sphingolipids for humans [Emami *et al*., 2016]. This is the first study on the sinigrin encapsulation in liposomes, the effect on recovery after *in vitro* digestion process, and its antioxidant potential by prolonging the oxidative stability of olive oil.

Characterization of sinigrin-loaded liposomes

Encapsulation efficiency of 62±3% has been achieved *via* encapsulation of sinigrin in liposomes by the proliposome method using a commercially available mixture of Phospolipon 90G. In addition to the reports showing that proliposome method provides better encapsulation efficacy in comparison

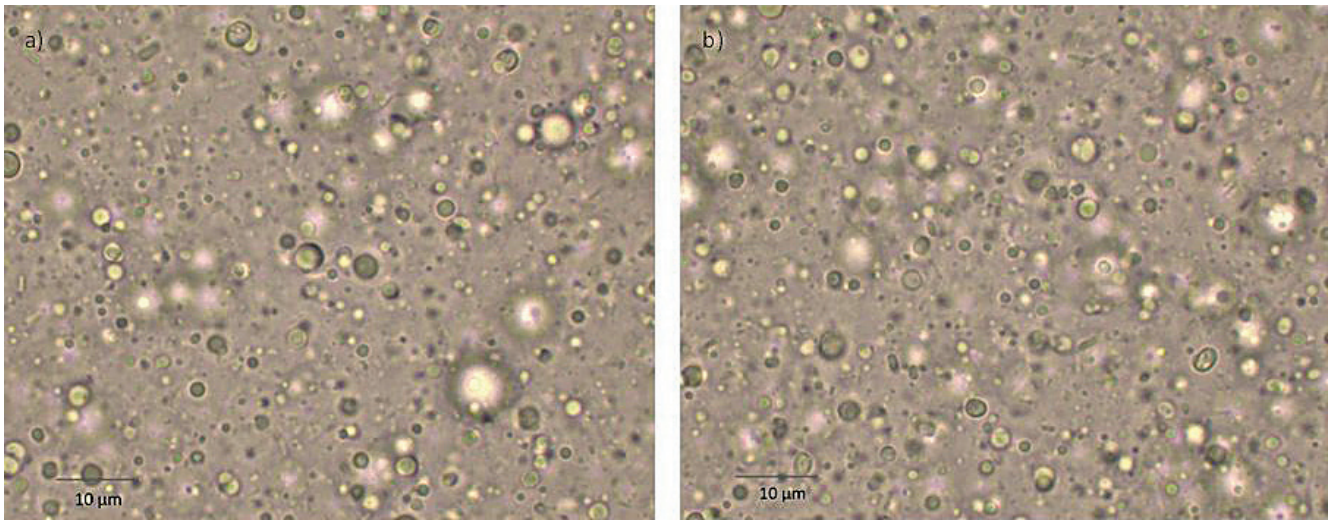

FIGURE 2. Micrographs of a) empty liposomes and b) liposomes with ensapuslated sinigrin obtained by a light microscope (1,000×magnification).

to some other methods for liposomes preparation, *e.g.* ethanol injection method [Chen *et al*., 2012] or thin-film method [Isailović *et al*., 2013], it was chosen in this study as a method that is easily applicable on the industrial scale [Đorđević *et al*., 2015]. It has been reported that in the case of polyphenols, the efficiency of encapsulation in liposomes varied between 10 and 70% depending on the molecular weight of the encapsulated compound (and consequently the ability to leak out from liposomes) and its molecular structure and the affinity to phospholipidic membranes [Đorđević *et al*., 2015]. For the lipophilic molecules, such as resveratrol, encapsulation efficiency up to 97% was achieved using the proliposome method [Isailović *et al*., 2013]. Similar results to those demonstrated in this study for encapsulation of sinigrin, as a water-soluble compound, were obtained in the case of (+)-catechin encapsulation in liposomes (approximately 70%). Furthermore, the entrapment efficiency of phenolic compounds of algal extract in soy lecithin liposomes was shown to be 50.2% by Savaghebi *et al*. [2020], while an entrapment efficiency of 47.5% was obtained for encapsulation of garlic extract in liposomes [Pinilla *et al*., 2017]. The slight variation may be associated with a difference in the encapsulation method or lecithin concentration applied [Rashinidejad *et al*., 2014; Savaghebi *et al*., 2020]. Although obtained encapsulation efficacy in this study is in accordance with the results of other reports and could be accepted as satisfying, further studies should investigate the effects of the addition of different components in liposomes preparation, since they have been recognized as important in encapsulation efficiency improvement. For instance, the addition of chitosan coatings on liposomes was found to be beneficial in encapsulation efficiency or slow-release improvement [Akgün *et al*., 2020; Li *et al*., 2015].

Figure 2 (a-b) shows the micrographs obtained by a light microscope of the produced empty liposomes (control) and liposomes loaded with sinigrin. We have noticed the similarity in control and sinigrin-containing liposomes at the first glance, both revealing spherical structures, which have been typically observed for phosphatidylcholine liposomes [Pinilla *et al*., 2017]. Since the used microscopic technique could not provide quantitative data or detailed insight into the morphology, like other more sophisticated techniques – atomic force microscopy or transmission electron microscopy, further characterization of the liposomes prepared in this study relied on dynamic light scattering technique.

Determination of mean diameter, PDI and zeta potential has revealed satisfying size uniformity of liposomes containing sinigrin. Compared with the control, the encapsulation of sinigrin did not lead to a statistically significant change in surface charge, as well as the mean diameter (Table 1). The obtained results can be explained by the incorporation

TABLE 1. Zeta potential, polydispersity index (PDI) and mean diameter of liposomes with and without encapsuled sinigrin during 2-week storage at 4°C.

Sample	Zeta potential (mV)			PDI			Mean diameter (nm)		
	0 days	7 days	14 days	0 days	7 days	14 days	0 days	7 days	14 days
Liposomes without sinigrin (control)	-34.6±0.5	-33.8±0.4	-32.0±0.8	0.454±0.01	0.450±0.01	0.461±0.03	1070±267	1260±432	1365±402
Liposomes with encapsulated sinigrin	-24.0±0.5	-28.4±0.8	-30.1±0.1	0.497±0.07	0.566±0.04	0.509±0.03	1196±267	1227±553	1263±308

All measurements were made in triplicate and results are reported as mean ± standard deviation.

of the bioactive compound within the aqueous core of liposomes, and only slightly between the bilayer membranes of liposomes or their surface. The PDI determines the particle size distribution and system homogeneity. A system whose PDI ranges from 0 to 0.5 is considered homogeneous [Balanč *et al*., 2016]. Zeta potential is a physicochemical parameter that represents the charge on the particle surface. It correlates with the stability of colloidal suspensions: thus, a high absolute value of the zeta potential indicates a more stable system [Mateos *et al*., 2019]. Our results regarding zeta potential of sinigrin-loaded liposomes are comparable with the results from other studies on the encapsulation of different bioactive ingredients in lecithin liposomes [Akgün *et al*., 2020; Pinilla *et al*., 2017; Savaghebi *et al*., 2020]. The obtained negative values of the zeta potential (Table 1), revealed satisfying electrostatic stabilization of the preparation, preventing aggregation of liposomes [Lin *et al*., 2018]. This was confirmed by the results of stability testing, since the mean diameter of liposomes with sinigrin did not change for more than 6% during 2-week storage at 4°C (Table 1). The observed slight changes in zeta potential could be a result of rearrangement of phospholipids, which are responsible for negative zeta potential values, due to the presence of phosphate groups (PO_4^{3-}) in phospholipids.

The physical stability of sinigrin liposomes and prolonged release of sinigrin over 5 h, as shown by the sinigrin release kinetic curves (Figure 3), indicated that the obtained liposomes made of natural phospholipids present potentially adequate carriers for this compound. In the control solution of sinigrin, distribution of sinigrin happened rapidly, reaching maximum content in acceptor cell after 180 min. As expected, sinigrin release from liposomes was slower, achieving the maximum content in the acceptor compartment after more than 300 min. In the release profile of sinigrin from liposomes in an aqueous medium there was the initial burst, which was probably associated with the small amount of surface-bound sinigrin. The initial burst (which lasted 15 min) was followed by a slow lag phase (which lasted another 15 min) and then a second burst release phase. It is generally believed that the molecules entrapped within liposomes are released primarily by three mechanisms [Pothakamury & Barbosa-C'anovas, 1995]. These are 1) diffusion of molecules through the intact liposomal membrane into the surrounding environment, 2) erosion of liposomal membrane caused by phospholipid degradation, and 3) swelling of pores in the liposomal membrane allowing the leakage of entrapped molecules [Liu *et al*., 2020]. The existence of lag-phase in the release pattern of sinigrin-loaded liposomes in this study may indicate that, apart from diffusion, some changes of the liposomal membranes, like erosion or swelling, were involved, too.

In vitro digestion and antioxidant potential of sinigrin loaded liposomes

The digestion of food *in vivo* is a complex process and includes mouth, stomach, and small intestine, as compartments where the digestion can be done. Liquid food stays in the mouth for a very short time because it does not need to undergo chewing. Thus, the digestion of sinigrin solution and liposomes with sinigrin as samples that are in the liquid

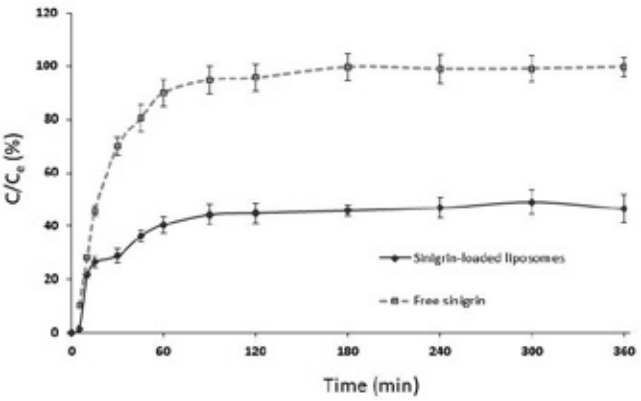

FIGURE 3. Kinetic curve of release of sinigrin from liposomes and prolife of free sinigrin in aqueous solution against time (control). C: sinigrin concentration at time t; C_e: sinigrin equilibrium concentration. Measurements were made in triplicate and results are shown as mean and standard division.

state would start in the gastric compartment and then be continued in the intestinal section. However, in this study, it was only possible to perform digestion discontinuously, starting from gastric or intestinal conditions simulation, and the percentage of unbroken molecules of sinigrin was monitored. We are aware of the limitation of such kind of analysis, so the establishment of reliable *in vitro-in vivo* correlation could not be expected. However, we believe that even preliminary data obtained from the two-phase digestion could contribute to further optimization in the development of sinigrin-loaded liposomes and their incorporation in real food matrices. The results of the *in vitro* recovery of free sinigrin and sinigrin released from liposomes after simulated gastric and duodenal digestion phases are given in Table 2 and Table 3, respectively. The recovery of free sinigrin was high after simulated gastric (87.39%) and duodenal digestion (83.31%) (Table 2). The recovery of free sinigrin in simulated acidic medium without human digestive enzymes was lower (71.23%), while in simulated slightly basic medium free sinigrin was almost completely stable (98.15%) (Table 2). High gastrointestinal stability of sinigrin was also reported by other authors who investigated its stability after a simulated digestion process with commercial digestive enzymes [Kuljarachanan *et al*., 2020]. Hwang *et al*. [2019] reported high stability of sinigrin in kale after gastric digestion with commercial digestive enzymes, but in contrast, the authors reported a low stability rate of sinigrin in kale after simulated duodenal digestive phase. This discrepancy can be explained by the effect of plant matrix on the duodenal stability of sinigrin and/or the differences between *in vitro* studies based on human and commercial digestive enzymes. Discrepancies between *in vitro* digestion studies with human and commercial digestive enzymes have already been reported [Aarak *et al*., 2013; Zorić *et al*., 2016]. Table 3 shows results of the recovery of sinigrin released from liposomes. Sinigrin loaded in liposomes was protected from the influence of pH and digestive enzymes. Namely, starting from 38% of available sinigrin in the case of liposomes, after the digestion process, the percentage of free sinigrin increased to 52.50% in the gastric medium and 52.71% in the duodenal medium. A similar portion of available sinigrin after digestion

TABLE 2. Concentration and recovery of sinigrin after its two-phase *in vitro* digestion.

Digestion phase	Concentration (μM)	Recovery (%)
Befor digestion (control)	61.03±1.55	
After gastric digestion	53.34±2.26	87.39
After duodenal digestion	50.85±0.23	83.31
pH 2.5 (without digestive enzymes)	43.48±0.41	71.23
pH 7.5 (without digestive enzymes)	59.91±0.15	98.15

The quantification of sinegrin was performed by HPLC-UV. Results are expressed as mean ± standard deviation (n=3).

TABLE 3. Concentration and recovery of sinigrin after a two-phase *in vitro* digestion of sinigrin-loaded liposomes.

Digestion phase	Concentration (μM)	Recovery (%)
Befor digestion (control)	1.08±0.12	38.00
After gastric digestion	1.49±0.32	52.50
After duodenal digestivom	1.50±0.47	52.71
pH 2.5 (without digestive enzymes)	1.43±0.41	50.16
pH 7.5 (without digestive enzymes)	1.24±0.22	43.74

The quantification of sinigrin was performed by HPLC-UV. Results are expressed as mean ± standard deviation (n=3).

of sinigrin-loaded liposomes in the gastric and duodenal medium was somewise unexpected result. Namely, it is generally accepted that liposomal structural integrity remains practically unchanged under gastric conditions, while the lipid digestion and consequent liposomes destruction occur primarily in the duodenum [Liu *et al*., 2020]. Since gastric juice in this study was obtained from human volunteers, it may be speculated that the samples were rich in gastric lipases. On the other hand, it is known that apart from the disruption of liposomal structure by pancreatic enzymes, bile salts contribute crucially to the digestion of lipids in duodenal medium, since the activity of phospholipase A_2 and lipase requires the presence of bile salts [Liu *et al*., 2020]. The low level of bile salts in the intestinal juices collected from healthy human donors could be a possible explanation for the obtained results on liposomes digestion. Furthermore, since the bile salts are very potent surface-active compounds, their content in the human juices used may not be sufficient for the complete lipid digestion and liposomes degradation, but adequate for rearrangement of the liposomes to smaller ones still encapsulating sinigrin. Although it is considered that without digestive enzymes, the change of pH through gastrointestinal system does not influence the liposomes' structure [Liu *et al*., 2019], the results on the available amount of sinigrin after incubation in a medium with pH 2.5 and 7.5 indicate that not just diffusion, but also swelling of liposomes in acidic/basic media and their transformation to the gelled state could contribute to sinigrin release. Overall, the obtained results proved the protective effect of liposomes on sinigrin digestion under various conditions, since a high portion of sinigrin remains encapsulated and thus is available for further release and transformation to highly bioactive isothiocyanates. This indicates real potential for liposomes application as a prolonged delivery system of sinigrin in food matrices. For that sake, besides the use of free sinigrin, in this study we have tested its potential after encapsulation in liposomes for the preservation of oxidative stability of edible oil.

Results presented in Table 4 show the effect of free sinigrin (at the concentration of 0.2%) on the prolongation of the oxidative stability of olive oil (the percentage of the prolongation was 23.5%). This effect was higher with sinigrin loaded in liposomes (the percentage of the prolongation of the oxidative stability was 38.68%, at the concentration of 0.2%). Weil *et al*. [2004] reported that sinigrin inhibited lipid peroxidation

TABLE 4. Induction time of oxidation of olive oil with the addition of sinigrin, singrin loaded in liposomes and pure liposomes in Rancimat test. The quantity of olive oil was 2.5 g. Concentrations of samples (sinigrin, sinigrin-liposomes complex, and pure liposomes in olive oil) were 0.2 and 0.1% (*w/w*).

Sample	Induction time (h)	
	0.2%	0.1%
Sinigrin	8.10±0.11	7.60±0.28
Sinigrin-liposomes	10.11±0.55	9.24±0.40
Liposomes	3.22±0.48	4.15± 0.31

The induction time of pure olive oil oxidation (control) was 6.20±0.31 h. All measurements were made in triplicate and results are reported as mean ± standard divisoin.

by 71% *in vitro*. The effectiveness of liposome systems in prolonging the induction period was reported by Gortzi *et al*. [2008]. The low oxidative stability of pure liposomes (without bioactive compound) (Table 4) can be explained by the lipophilic components present in lipid bilayers, which stabilized the liposome membranes but also underwent to oxidation firstly due to the presence of double bonds prone to oxidative degradation [Huang *et al*., 2019]. It is already known that encapsulated antioxidants (for instance, essential oils and polyphenols) protect lipid bilayers from oxidation to some extent [Balanč *et al*., 2016; Detoni *et al*., 2012]. In our case, encapsulated sinigrin in liposomes partially stabilized the liposomal membrane, protecting itself from degradation, so it could prevent lipid peroxidation of olive oil.

The application of the sinigrin-loaded liposomes as a protective agent against lipid peroxidation might be of great interest in lipid-based food systems.

CONCLUSION

The present study demonstrated the high stability of sinigrin after simulated digestion with human gastric and duodenal medium, and the influence of a slightly basic medium on the stability of sinigrin. The use of liposomes enabled the protection of sinigrin under the conditions of the simulated digestive process (stomach and duodenum) and prolonged its release in the gastric and duodenal medium. Moreover,

the liposomal form enhanced the effect of sinigrin on prolonging the induction time of edible oil compared to the free form of sinigrin. The innovative potential of the sinigrin-loaded liposomes in real functional food systems or their use as dietary supplements deserves further investigation.

RESEARCH FUNDING

The research was funded by the Croatian Science Foundation within the project "Plants as a source of bioactive sulphur compounds and their ability to hyperracumulate metals" (IP-06–2016–1316).

CONFLICT OF INTEREST

The authors declare no conflict of interest.

COMPLICANCE WITH ETHICAL STANDARDS

This article contains a study with human digestive juices. The approval for the collection of digestive juices was obtained from the Ethics Committee of the University Hospital Centre Split.

ORCID IDs

T. Bilušić https://orcid.org/0000-0001-8834-9562
I. Blažević https://orcid.org/0000-0002-0715-3216
A. Bratanić https://orcid.org/0000-0002-3261-183X
B. Bugarski https://orcid.org/0000-0002-1846-8555
I. Drvenica https://orcid.org/0000-0003-4985-1642

REFERENCES

1. Aarak, K.E., Kirkhus, B., Holm, H., Vogt, G., Jacobsen, M., Vegarud, G.E. (2013). Release of EPA and DHA from salmon oil – a comparison of *in vitro* digestion with human and porcine gastrointestinal enzymes. *British Journal of Nutrition*, *110*(8), 1402–1410. https://doi.org/10.1017/S0007114513000664
2. Akgün, D., Gültekin-Özgüven, M., Yücetepe, A., Altin, G., Gibis, M., Weiss, J., Özçelik, B. (2020). Stirred-type yoghurt incorporated with sour cherry extract in chitosan-coated liposomes. *Food Hydrocolloids, 101*, art. no. 105532. https://doi.org/10.1016/j.foodhyd.2019.105532
3. Almaas, H., Cases, A.L., Devold, T.G., Holm, H., Langsrud, T., Aabakken, L., Aadnoey, T., Vegarud, G.E. (2006). *In vitro* digestion of bovine and caprine milk by human gastric and duodenal enzymes. *International Dairy Journal*, *16*(9), 961–968. https://doi.org/10.1016/j.idairyj.2005.10.029
4. Balanč, B., Trifković, K., Đorđević, V., Marković, S., Pjanović, R., Nedović, V., Bugarski, B. (2016). Novel resveratrol delivery systems based on alginate-sucrose and alginate-chitosan microbeads containing liposomes. *Food Hydrocolloids*, *61*, 832–842. https://doi.org/10.1016/j.foodhyd.2016.07.005
5. Blažević, I., Đulović, A., Maravić, A., Čikeš Čulić, V., Montaut, S., Rollin, P. (2019). Antimicrobial and cytotoxic activities of *Lepidium latifolium* L. hydrodistillate, extract and its major sulfur volatile allyl isothiocyanate. *Chemistry & Biodiversity*, *16*(4), art. no. e1800661. https://doi.org/10.1002/cbdv.201800661
6. Blažević, I., Montaut, S., Burčul, F., Olsen, C.E., Burow, M., Rollin, P., Agerbirk, N. (2020). Glucosinolate structural diversity, identification, chemical synthesis and metabolism in plants. *Phytochemistry*, *169*, art. no. 112100. https://doi.org/10.1016/j.phytochem.2019.112100
7. Chen, Y., Wu, Q., Zhang, Z., Yuan, L., Liu, X., Zhou, L. (2012). Preparation of curcumin-loaded liposomes and evaluation of their skin permeation and pharmacodynamics. *Molecules*, *17*(5), 5972–5987. https://doi.org/10.3390/molecules17055972
8. Cheng, D.L., Hasimoto, K., Uda, Y. (2004). *In vitro* digestion of sinigrin and glucotropaeolin by single strains of Bifidobacterium and identification of the digestive products. *Food Chemistry and Toxicology*, *42*(3), 351–357. https://doi.org/10.1016/j.fct.2003.09.008
9. Corrales, M., Fernandez, A., Han, J.H. (2014). Antimicrobial packaging systems. Chapter 7, in J.H. Han (Ed.), *Innovation in Food Packaging*, Elsevier, pp. 133–170. https://doi.org/10.1016/B978-0-12-394601-0.00007-2
10. Detoni, C.B., de Oliveira, D.M., Santo, I.E., Pedro, A.S., El-Bacha, R., da Silva Velozo, E., Ferreira, D., Sarmento, B., de Magalhães Cabral-Albuquerque, E.C. (2012). Evaluation of thermal-oxidative stability and antiglioma activity of zanthoxylum tingoassuiba essential oil entrapped into multi- and unilamellar liposomes. *Journal of Liposome Research*, *22*(1), 1–7. https://doi.org/10.3109/08982104.2011.573793
11. Đorđević, V., Balanč, B., Belščak-Cvitanović, A., Lević, S., Trifković, K., Kalušević, A., Kostić, I., Komes, D., Bugarski, B., Nedović, V. (2015). Trends in encapsulation technologies for delivery of food bioactive compounds. *Food Engineering Review*, *7*, 452–490. https://doi.org/10.1007/s12393-014-9106-7
12. Emami, S., Azadmard-Damirchi, S., Peighambardoust, S.H., Valizadeh, H., Hesari, J. (2016). Liposomes as carrier vehicles for functional compounds in food sector. *Journal of Experimental Nanoscience*, *11*(9), 737–759. https://doi.org/10.1080/17458080.2016.1148273
13. Ettlinger, M.G., Lundeen, A.J. (1956). The mustard oil of *Limnanthes douglasii* seed, *m*-methoxybenzyl isothiocyanate. *Journal of American Chemical Society*, *78*(9), 1952–1954. https://doi.org/10.1021/ja01590a052
14. Furlund, C.B., Ulleberg, E.K., Devold, T.G., Flengsrud, R., Jacobson, M., Sekse, C., Holm, H., Vegarud, G.E. (2013). Identification of lactoferrin peptides generated by digestion with human gastrointestinal enzymes. *Journal of Dairy Sciences*, *96*(1), 75–88. https://doi.org/10.3168/jds.2012-5946
15. Gaede, H.C., Gawrisch, K. (2003). Lateral diffusion rates of lipid, water, and a hydrophobic drug in a multilamellar liposome. *Biophysical Journal*, *85*(3), 1734–1740. https://doi.org/10.1016/S0006-3495(03)74603-7
16. Girgin, N., Nehir El, S. (2015). Effects of cooking on *in vitro* sinigrin bioaccessibility, total phenols, antioxidant and antimutagenic activity of cauliflower. *Journal of Food Composition and Analysis*, *37*, 119–127. https://doi.org/10.1016/j.jfca.2014.04.013

17. Gortzi, O., Lalas, S., Tsaknis, J., Chinou, I. (2007). Enhanced bioactivity of *Citrus limon* (Lemon Greek cultivar) extracts, essential oil and isolated compounds before and after encapsulation in liposomes. *Planta Medica*, *73*, 184. https://doi.org/10.1055/s-2007-986965
18. Gortzi, O., Lalas, S., Chinou, I., Tsaknis, J. (2008). Reevaluation of bioactivity and antioxidant activity of *Myrtus communis* extract before and after encapsulation in liposomes. *European Food Research and Technology*, *226*, 583–590. https://doi.org/10.1007/s00217-007-0592-1
19. Huang, M., Liang, C., Tan, C, Huang, S., Ying, R., Wang, Y., Zhang, Y. (2019). Liposome co-encapsulation as a strategy for the delivery of curcumin and resveratrol. *Food & Function, 10*, 6447–6458. https://doi.org/10.1039/C9FO01338E
20. Hwang, E.S., Bornhorst, G.M., Oteiza, P.I., Mitchell, A.E. (2019). Assessing the fate and bioavailability of glucosinolates in kale (*Brassica oleracea*) using simulated human digestion and Caco-2 cell uptake models. *Journal of Agricultural and Food Chemistry*, *67*(34), 9492–9500. https://doi.org/10.1021/acs.jafc.9b03329
21. Isailović, B.D., Kostić, I.T., Zvonar, A., Đorđević, V.B., Gašperlin, M., Nedović, V.A., Bugarski, B.M. (2013). Resveratrol loaded liposomes produced by different techniques. *Innovative Food Science and Emerging Technologies*, *19*, 181–189. https://doi.org/10.1016/j.ifset.2013.03.006
22. ISO 6886:1996. Animal and vegetable fats and oil – Determination of oxidation stability (Accelerated oxidation test).
23. Jie, M., Cheung, W.M., Yu, V., Zhou, Y., Tong, P.H., Ho, J.W.S. (2014). Anti-proliferative activities of sinigrin on carcinogen-induced hepatotoxicity in rats. *PLoS ONE*, *9*(10), art. no. e110145. https://doi.org/10.1371/journal.pone.0110145
24. Kuljarachanan, T., Fu, N., Chiewchan, N., Devahastin, S., Chen, X.D. (2020). Evolution of important glucosinolates in three common *Brassica* vegetables during their processing into vegetable powder and *in vitro* gastric digestion. *Food & Function*, *11*(1), 211–220. https://doi.org/10.1039/C9FO00811J
25. Li, Z., Paulson, A.T., Gil, T.A. (2015). Encapsulation of bioactive salmon protein hydrolysates with chitosan-coated lipsomes. *Journal of Functional Foods*, *19*, Part A, 733–743. https://doi.org/10.1016/j.jff.2015.09.058
26. Lin, L., Zhu, Y., Thangaraj, B., Abdel-Samie, M.A.S., Cui, H. (2018). Improving the stability of thyme essential oil solid liposome by using β-cyclodextrin as a cryoprotectant. *Carbohydrate Polymers*, *188*, 243–251. https://doi.org/10.1016/j.carbpol.2018.02.010
27. Liović, N., Bošković, P., Drvenica, I., Režek Jambrak, A., Dropulić, A.M., Krešić, G., Nedović, V., Zorić, Z., Pedisić, S., Bilušić, T. (2019). Phenolic extracts from *Vaccinium corymbosum* L. loaded in microemulsions and liposomes as enhancers of olive oil oxidative stability. *Polish Journal of Food Nutrition and Sciences*, *69*(1), 23–33. https://doi.org/10.31883/pjfns-2019-0003
28. Liu, W., Ye, Y., Han, F., Han, J. (2019). Advances and challenges in liposome digestion: Surface interaction, biological fate, and GIT modeling. *Advances in Colloid and Interface Science*, *263*, 52–67. https://doi.org/10.1016/j.cis.2018.11.007.
29. Liu, W., Hou, Y., Jin, Y., Wang, Y., Xu, X., Han, J. (2020). Research progress on liposomes: Application in food, digestion behavior and absorption mechanism. *Trends in Food Science & Technology*, *104*, 177–189. https://doi.org/10.1016/j.tifs.2020.08.012
30. Malheiros, P.S., Daroit, D.J., Brandelli, A. (2010). Food applications of liposome encapsulated antimicrobial peptides. *Trends in Food Science & Technology*, *21*(6), 284–292. https://doi.org/10.1016/j.tifs.2010.03.003
31. Maruthupandy, M., Seo, J. (2019). Allyl isothiocyanate encapsulated halloysite covered with polyacrylate as a potential antibacterial agent against food spoilage bacteria. *Materials Science and Enginerring: C, Material for Biological Application*, *105*, art. no. 110016. https://doi.org/10.1016/j.msec.2019.110016
32. Mateos, H., Valentini, A., Robles, E., Brooker, A., Cioffi, N., Palazzo, G. (2019). Measurement of the zeta-potential of solid surfaces through Laser Doppler Electrophoresis of colloid tracer in a dip-cell: survey of the effect of ionic strength, pH, tracer chemical nature and size. *Colloids and Surfaces A: Physicochemical and Engineering Aspects*, *576*, 82–90. https://doi.org/10.1016/j.colsurfa.2019.05.006
33. Mazumder, A., Dwivedi, A., Fox, L.T., Brümer, A., du Preez, J., Gerber, M., du Plessis, J. (2016). *In vitro* skin permeation of sinigrin from its phytosome complex. *Journal of Pharmacy and Pharmacology*, *68*(12), 1577–1583. https://doi.org/10.1111/jphp.12594
34. Melrose, J. (2019). The glucosinolates: A sulphur glucoside family of mustard anti-tumor and antimicrobial phytochemicals of potential therapeutic application. *Biomedicines*, *7*(3), art. no. 62. https://doi.org/10.3390/biomedicines7030062
35. Mithen, R., Bennet, R., Marquez, J. (2010). Glucosinolate biochemical diversity and innovation in the Brassicales. *Phytochemistry*, *71*(17–18), 2074–2086. https://doi.org/10.1016/j.phytochem.2010.09.017
36. Mitsiogianni, M., Koutsidis, G., Mavroudis, N., Trafalis, D.T., Botaitis, S., Franco, R., Zoumpourlis, V., Amery, T., Galanis, A., Pappa, A., Panayiotidis, M.I. (2019). The role of isothiocyanates as cancer chemo-preventive, chemo-therapeutic and anti-melanoma agents. *Antioxidants*, *8*(4), art. no. 106. https://doi.org/10.3390/antiox8040106
37. Moghimipour, E., Aghel, N., Mahmoudabadi, A.Z., Ramezani, Z., Handali, S. (2012), Preparation and characterization of liposomes containing essential oil of *Eucalyptus camaldulensis* leaf. *Junidshapur Journal of Natural Pharmaceutical Products*, *7*(3), 117–122. https://doi.org/10.17795/jjnpp-5261
38. Park, S.Y., Barton, M., Pendleton, P. (2012). Controlled release of allyl isothiocyanate for bacteria growth management. *Food Control*, *23*(2), 478–484. https://doi.org/10.1016/j.foodcont.2011.08.017
39. Pinilla, C.M.B., Noreña, C.P.Z., Brandelli, A. (2017). Development and characterization of phosphatidylcholine nanovesicles, containing garlic extract, with antilisterial activity in milk. *Food Chemistry*, *220*, 470–76. https://doi.org/10.1016/j.foodchem.2016.10.027
40. Pothakamury, U.R., Barbosa-C'anovas, G.V. (1995). Fundamental aspects of controlled release in foods. *Trends in Food Science & Technology, 6*(12), 397–406. https://doi.org/10.1016/S0924-2244(00)89218-3

41. Pulliero, A., Wu, Y., Fenoglio, D., Parodi, A., Romani, M., Soares, C.P., Filaci, G., Lee, J.L., Sinkam, P.N., Izzotti, A. (2015). Nanoparticles increase the efficacy of cancer chemopreventive agents in cells exposed to cigarette smoke condensate. *Carcinogenesis*, *36*(3), 368–377. https://doi.org/10.1093/carcin/bgv008
42. Radünz, M., Dos Santos Hackbart, H.C., Pontes Bona, N., Stark Pedra, N., Hoffman, J.F., Moro Stefanello, F., Da Rosa Zavareze, E. (2020). Glucosinolates and phenolic compounds rich broccoli extract: Encapsulation by electrospraying and antitumor activity against glial tumor cells. *Colloids and Surfaces B: Biointerfaces*, *192*, art. no. 111020. https://doi.org/10.1016/j.colsurfb.2020.111020
43. Rashidinejad, A., Birch, E.J., Sun-Waterhouse, D., Everett, D.W. (2014). Delivery of green tea catechin and epigallocatechin gallate in liposomes incorporated into low-fat hard cheese. *Food Chemistry*, *156*, 176–183. https://doi.org/10.1016/j.foodchem.2014.01.115
44. Romeo, L., Iori, R., Rollin, P., Bramanti, P., Mazzon, E. (2018). Isothiocyanates: An overview of their antimicrobial activity against human infections. *Molecules*, *23*(3), art. no. 624. https://doi.org/10.3390/molecules23030624
45. Savaghebi, D., Barzegar, M., Mozafari, M.R. (2020). Manufacturing of nanoliposomal extract from *Sargassum boveanum* algae and investigating its release behavior and antioxidant activity. *Food Science & Nutrition*, *8*(1), 299–310. https://doi.org/10.1002/fsn3.1306
46. Sun, M., Dang, U.J., Di Pasqua, A.J. (2019). Phenethyl isothiocyanate and cisplatin co-encapsulated in a liposomal nanoparticle for treatment of non-small cell lung cancer. *Molecules*, *24*(4), art. no. 801. https://doi.org/10.3390/molecules24040801
47. Takahashi, M., Uechi, S., Takara, K., Asikin, Y., Wada, K. (2009). Evaluation of an oral carrier system in rats: bioavailability and antioxidant properties of liposome-encapsulated curcumin. *Journal of Agricultural and Food Chemistry*, *57*(19), 9141–9146. https://doi.org/10.1021/jf9013923
48. Tsao, R., Yu, Q., Friesen, I., Potter, J., Chiba, M. (2000). Factors affecting the dissolution and degradation of oriental mustard-derived sinigrin and allyl isothiocyanate in aqueous media. *Journal of Agricultural Food Chemistry*, *48*(5), 1898–1902. https://doi.org/10.1021/jf9906578
49. Waser, L.R., Watson, W.H. (1963). Crystal structure of sinigrin. *Nature*, *198*, 1297–1298. https://doi.org/10.1038/1981297b0
50. Wechtersbach, L., Poklar Ulrih, N., Cigic, B. (2012). Liposomal stabilization of ascorbic acid in model systems and in food matrices. *LWT – Food Science and Technology*, *45*(1), 43–49. https://doi.org/10.1016/j.lwt.2011.07.025
51. Weil, M.J., Zhang, Y., Nair, M.G. (2004). Colon cancer proliferating desulfosinigrin in wasabi (*Wasabia japonica*). *Nutrition and Cancer*, *48*(2), 207–213. https://doi.org/10.1207/s15327914nc4802_11
52. Wu, X., Zhou, Q., Xu, K. (2009). Are isothiocyanates potential anti-cancer drugs? *Acta Pharmacologica Sinica, 30*, 501–512. https://doi.org/10.1038/aps.2009.50
53. Zorić, Z., Markić, J., Pedisić, S., Bučević-Popović, V., Generalić-Mekinić, I., Grebenar, K., Bilušić, T. (2016). Stability of rosmarinic acid in aqueous extracts from different Lamiaceae species after *in vitro* digestion with human gastrointestinal enzymes. *Food Technology and Biotechnology*, *54*(1), 97–102. https://doi.org/10.17113/ftb.54.01.16.4033
54. Yang, S., Liu, W., Liu, C., Liu, W., Tong, G., Zheng, H., Zhou, W. (2012). Characterization and bioavailability of vitamin C nanoliposomes prepared by film evaporation-dynamic high pressure microfluidization. *Journal of Dispersion Science and Technology*, *33*(11), 1608–1614. https://doi.org/10.1080/01932691.2011.629511
55. Yuan, Y.G., Zhang, S., Hwang, J.Y., Kong, I.K. (2018). Nanoparticles potentiates cytotoxicity and apoptotic potential of camptothecin in human cervical cancer cells. *Oxidative Medicine and Cellular Longevity*, *2018*, art. no. 6121328. https://doi.org/10.1155/2018/6121328

Pol. J. Food Nutr. Sci., 2021, Vol. 71, No. 4, pp. 451–461
On-line ISSN: 2083-6007
Print ISSN: 1230-0322
DOI: 10.31883/pjfns/143584
http://journal.pan.olsztyn.pl

Original article
Section: Food Quality and Functionality

Impact of Sodium Alginate and Dried Apple Pomace Powder as a Carrier Agent on the Properties of Freeze-Dried Vegetable Snacks

Magdalena Karwacka, Martyna Gumkowska, Katarzyna Rybak, Agnieszka Ciurzyńska, Monika Janowicz*

Department of Food Engineering and Process Management, Institute of Food Science, Warsaw University of Life Sciences, 159c Nowoursynowska St., 02–776, Warsaw, Poland

Key words: freeze-drying, vegetable snacks, sodium alginate, apple pomace, carrier agent, physicochemical properties

The food industry is committed to supplying nutritious products that are attractive and convenient for consumers. Freeze-dried fruit and vegetable snacks that exemplify such products are difficult to obtain since it is necessary to use a carrier agent (usually a hydrocolloid ingredient) which meets the requirements of a sustainable development conceptual framework. Therefore, research has been undertaken to replace such a carrier agent with food waste fruit pomace. This study compared selected physicochemical properties of freeze-dried vegetable snacks obtained through the addition of sodium alginate and dried apple pomace powder in terms of the viability of replacing hydrocolloid carrier agents in freeze-dried products with fruit pomace. Three vegetable sets containing: yellow bean, carrot and potato were prepared and modified by adding diverse carrier agents. Snacks with the addition of dried apple pomace powder featured higher dry matter content and true and apparent density, but sodium alginate-structured products were harder and more porous. Dried apple pomace powder improved the health-promoting properties of the snacks, such as total phenolic content and antioxidant capacity. The type of additive also affected the internal structure of the products. The results indicate that the application of both dried apple pomace powder and sodium alginate as carrier agents can result in snacks characterised by repeatable quality, but it is unclear whether the total replacement of hydrocolloid is sustainably efficient.

INTRODUCTION

Consumers are becoming increasingly aware of the importance of nutrition and a balanced diet as far as their health and quality of life is concerned. Although the popularity of a plant-based diet preventing civilisation diseases and environmental crisis is constantly increasing, the consumption of large amounts of highly-processed and nutrient-poor food products is regarded as an outstanding issue to be addressed for various age groups [Ciurzyńska *et al.*, 2019a]. Because of the fast pace of life, consumers are often forced to reach for convenient and easy-to-eat products, such as healthy and unhealthy snacks that are abundant on store shelves. Although the healthy snack market is abundant with dried fruits, vegetables, nuts and cereal bars, they compete with candies and other high-energy products. It has been proven that consumer choices depend on the accessibility and visibility of products [van Kleef *et al.*, 2012]. A major impact on the attractiveness of dried snacks is shown by their textural and sensory properties. Consumers seek a pleasurable eating experience that may be ensured by rich flavour and aroma as well as crunchiness and crispness, although many consumers also declare an interest in the nutritional values of food [Silva-Espinoza *et al.*, 2021].

Freeze-drying is a method that preserves the structure of the products because of its mechanism (water is removed in a gas state instead of a liquid state). This phenomenon is caused by low pressure in the freeze-dryer chamber, which accounts for the process to be run at a low temperature. The pre-set parameters of food dehydration by means of freeze-drying influence both the physical and nutritional properties of products [Nowak & Jakubczyk, 2020]. The properties of dried (especially freeze-dried) food products may be modulated by both the process parameters and by adding structure-forming agents such as hydrocolloids. This combination of hydrocolloid carrier agents and the freeze-drying method ensures structure preservation and avoids undesirable changes that may occur during thermal treatment, such as air-drying [Cassanelli *et al.*, 2018]. There have been several studies on the use of hydrocolloids as carrier agents in the production of freeze-dried snacks, *e.g.* gellan gum [Cassanelli *et al.*, 2018], pectin, xanthan gum and locust bean gum [Ciurzyńska *et al.*, 2019b], sodium alginate [Ciurzyńska *et al.*,

* Corresponding Author:
E-mail: magdalena_karwacka@sggw.edu.pl (M.Sc. M. Karwacka)

Submitted: 31 August 2021
Accepted: 4 November 2021
Published on-line: 1 December 2021

© Copyright by Institute of Animal Reproduction and Food Research of the Polish Academy of Sciences
© 2021 Author(s). This is an open access article licensed under the Creative Commons Attribution-NonCommercial-NoDerivs License (http://creativecommons.org/licenses/by-nc-nd/4.0/).

2020; Kuo *et al.*, 2021], gum arabic and bamboo fibre [Silva-Espinoza *et al.*, 2021] and many others.

It has been shown that hydrocolloids can produce innovative and attractive food products, but processes of obtaining hydrocolloids are usually complex and require significant chemical reagents, time and equipment, which cause high energy consumption [Liew *et al.*, 2019]. According to sustainable development goals, a major challenge for agriculture and the food industry is a reduction of carbon and energy footprints, which have an adverse impact on the natural environment. Food processing optimisation and solid waste management constitute one of the ways to follow this conceptual framework [Karwacka *et al.*, 2020]. Therefore, all over the world, scientists are conducting research into reusing food waste and by-products as innovative food products. The addition of fruit pomace as a structure and texture-forming carrier agent in dairy, meat, bakery and pastry products is becoming a major topic [Kruczek *et al.*, 2016], but there is no research available on using pomace as a carrier agent in freeze-dried products. Fruit pomace has high nutritional and functional potential. For example, apple pomace is a rich source of polysaccharides, dietary fibre, micro- and macro-elements, as well as bioactive compounds, such as antioxidants [Skinner *et al*., 2018], and it displays gelation capacity and the ability to retain water [Masiarz *et al.*, 2019].

This study compared selected physicochemical properties of freeze-dried vegetable snacks (obtained through the addition of sodium alginate and dried apple pomace powder) to investigate replacing hydrocolloid carrier agents in freeze-dried products with fruit pomace powders.

MATERIAL AND METHODS

Material

Frozen vegetables (yellow been, carrot and potato) provided by Unifreeze sp. z o.o. (Poland), dried apple pomace powder (AP) (Greenherb, Łańcut, Poland), sodium alginate (SA) (Agnex, Białystok, Poland) and calcium lactate (Agnex, Białystok, Poland) were used to prepare freeze-dried snacks.

Snack preparation

Before deploying technological processes, all products used for snack preparation were weighed in the proportions shown in Table 1. A 600-g portion of vegetables was used in one technological cycle.

Yellow bean (YB) was blanched at 85°C for 4 min and potato (P) cubes (1×1×1 cm) were cooked at 100°C for 15 min using Thermomix TM5 (Vorkwerk, Wuppertal, Germany). Thermal treatment was launched when the water with vegetables reached the pre-set temperature. Carrot (C) cubes (1×1×1 cm) were thawed at ambient temperature for about 30 min. The vegetables, after having undergone the aforementioned treatment, were ground to varying degrees. The YB was cut in a laboratory knife mill GRINDOMIX GM 200 (Retsch, Haan, Germany) for 1 min, applying the continuous mode and a knife speed of 4,500 rpm. The P cubes were blended into smooth puree using a hand blender (Bosch, Gerlingen, Germany). The C cubes were milled in a meat grinder (Zelmer, Rzeszów, Poland), using a mesh of 4 mm in diameter.

To produce snacks with apple pomace powder (Table 1), the pre-processed vegetables and AP were mixed with a whisk, placed into 3.5×2.0×10.5 cm silicone moulds and frozen at -40°C in a shock freezer (Irinox Shock Freezer HCM 51.20, Treviso, Italy). The addition of AP to the vegetables in the amount of 2 g/100 g maintained an appropriate structure and did not change the organoleptic features of the snacks developed in preliminary studies. To produce snacks with sodium alginate, SA was added to the pre-processed vegetables and whisked using a manual blender. After measuring the specific volume of water containing calcium lactate, it was heated up to 40°C until the salt dissolved. This solution was then poured into the vegetables and whisked again to be put into 3.5×2.0×10.5 cm silicone moulds and frozen at -40°C. After freezing the snacks, they were put into a Gamma 1–16 LSCplus freeze-dryer (Martin Christ Gefriertrocknungsanlagen GmbH, Osterode, Harz, Germany) and dried for about 48 h at a shelf temperature of 30°C and a pressure of 63 Pa. Freeze-dried snacks were packed into polyethylene zip-up bags and stored in darkness.

Out of 600 g of the vegetable input, five freeze-dried vegetable snacks (5 g in average weight) were obtained. The properties of freeze-dried vegetable snacks were determined using 15 randomly selected snacks as the output of five technological cycles.

Monitoring drying kinetics

During the freeze-drying process, changes in the weight of the snacks were recorded with special software (SWL0125, Mensor, Ząbki, Poland) every 5 min for the first 120 min of the drying process and subsequently every 15 min until the end of the freeze-drying process. The samples were dried

TABLE 1. Composition of the freeze-dried vegetable snacks with sodium alginate and dried apple pomace powder (g/100 g).

Ingredient	YB-SA	YB/C-SA	YB/P/C-SA	YB-AP	YB/C-AP	YB/P/C-AP
Yellow bean (YB)	50	35	35	100	70	70
Carrot (C)	–	15	7.5	–	30	15
Potato (P)	–	–	7.5	–	–	15
Water		48.4			–	
Sodium alginate (SA)		1.5			–	
Calcium lactate		0.1			–	
Apple pomace (AP)		–			+2	

to a constant weight and the process was carried out two times for each type of vegetable snack.

Based on the recorded weight changes and dry matter contents, the drying kinetics of the freeze-dried vegetable snacks was determined and expressed in terms of the moisture content throughout the duration of the freeze-drying process. The moisture content was calculated according to the equation formula:

$$u = \frac{m_t - m_e}{m_e \times dm_e}$$

where: u is moisture content (g H_2O/g dry matter (d.m.)), m_t is product weight while being dried (g), m_e is dried product residual weight (g) and dm_e is the dry matter content of a dried product (g/100 g).

Dry matter content determination

Water content was determined by hot air drying of 0.5 to 1 g of vegetable snacks before and after freeze-drying in a convective dryer SUP 65 W/G (WAMED, Warsaw, Poland) at 70°C for 24 h, according to Association of Official Analytical Chemists (AOAC) procedure [AOAC, 2002]. After drying, the samples were chilled in a desiccator and weighed again. The water content of the samples was calculated in terms of the difference in weight before and after drying divided by the weight of the sample before drying. Measurements were taken three times for each sample.

Water activity measurement

The water activity of freeze-dried vegetable snacks was measured using HygroLab C1 meter (Rotronic AG, Bassersdorf, Switzerland) at 25±1°C. Measurements of each sample were performed in triplicate according to the manufacturer's instructions.

True density determination

The volume of the dried solid matter was measured using a helium pycnometer (Quantachrome Instruments, Boynton Beach, FL, USA) according to the method described by Tsami *et al.* [1998]. The sample was placed into a large measurement cell and cleaned with helium three times before measurement. A pycnometer software (version 2.7) was used for converting the results into true density. The procedure was performed three times for each sample.

Apparent density determination

The apparent density of the freeze-dried vegetable snacks was determined using the modified method presented by Tsami *et al.* [1998] using chia seed displacement. The weighed cuboidal samples were put in a glass cylinder that was then filled up with chia seeds to reach a volume of 25 mL. The measurement was performed ten times for each freeze-dried snack. The apparent density was calculated in terms of the ratio of the weight to the geometric sample volume.

Analysis of textural properties

The textural properties of the freeze-dried vegetable snacks were determined by the modified method described by Meullenet & Gross [1999]. A compression test was conducted in a TA.HD plus texture analyser (Stable Micro Systems, Surrey, UK) using a 20 mm diameter platen probe, applying a test speed of 0.5 mm/s. The measurement was performed on twenty cuboid samples of the freeze-dried vegetable snacks (1×1×1 cm) until 50% deformation of their initial height was obtained. The compression force was recorded by the Texture Export software to determine compression curves and maximum force.

X-Ray tomography imaging

The microstructure of the freeze-dried vegetable snacks was analysed using the X-ray micro-CT SkyScan 1272 system (Bruker microCT, Kontich, Belgium). Cuboidal samples of the freeze-dried vegetable snacks (1×1×1 cm) were attached to the rotation stage using double-sided adhesive tape. Measurements were performed based on the following parameters: a pixel size of 13.4 μm, accelerating voltage of 40 kV and 193 μA of supply current. To obtain a radiographic image size of 2016 by 2016 pixels, the samples were rotated every 0.2° step until the full rotation of 360°. The output images were loaded into the NRecon1.6.3.2 computer program (Bruker microCT) and converted into a 3D reconstruction of the sample. The greyscale images were binarised by using the lower intensity pixels as the background (air, pores) and higher intensity pixels as the freeze-dried snack input. The porosity and mean pore distribution were calculated based on the 3D data using CTAn v.1.10.1.0 software (Bruker microCT) [Gondek *et al.*, 2013].

Colour analysis

The colour of freeze-dried vegetable snacks was determined using a Konica-Minolta CM-5 colorimeter (Osaka, Japan). The CIE L*a*b* system (CIE standard Illuminate D65, an angle of 0°, the diameter of the measurement hole equalled 8 mm) and the reflectance mode were used. Before the measurement, the colorimeter was calibrated with black and white reference tiles. The lightness (L^*), redness (a^*) and yellowness (b^*) were measured within 20 repetitions. To evaluate the colour changes, the total colour difference (ΔE) was calculated according to the following equation formula [Methakhup *et al.*, 2005]:

$$\Delta E = \sqrt{(\Delta L^*)^2 + (\Delta a^*)^2 + (\Delta b^*)^2}$$

where: ΔL^*, Δa^*, Δb^* are the differences in lightness (L^*), redness (a^*) and yellowness (b^*) between the vegetable snacks before and after freeze-drying.

Extract preparation

The extract of the freeze-dried vegetable snacks was prepared using 25 mL of an 80% (*v/v*) aqueous ethanol solution (Avantor Performance Materials, Gliwice, Poland) and 2 g of the freeze-dried snack ground in an analytical mill (IKA A11 basic, IKA Werke GmbH & Co. KG, Staufen, Germany). The mixture was warmed to 80°C and then filtered. The filtrate was transferred into a volumetric flask and filled with an 80% (*v/v*) ethanol solution up to 50 mL. This procedure was performed three times for each sample. The extracts were used to determine the total phenolic contents (TPC) and the antioxidant capacity of the snacks.

Total phenolic content determination

The TPC was determined according to Singleton *et al.* [1999] method. The volumes of 0.18 mL of the extract of the vegetable snacks and 0.3 mL of Folin-Ciocalteau's reagent (Merck, Darmstadt, Germany) were put into a glass tube filled in with 4.82 mL of distilled water. The tube was stirred and left in the ambient temperature for 3 min. Next, 0.6 mL of saturated sodium carbonate (Avantor Performance Materials) was added, the mixture was stirred again and left in darkness for 1 h. The absorbance of mixtures was measured using a spectrophotometer (Helios Gamma, Thermo Fisher Scientific, Waltham, MA, USA) at a 750 nm wavelength *versus* a blank sample of distilled water with Folin-Ciocalteau's reagent and without any extract. The TPC was expressed in terms of gallic acid equivalents (GAE) per 100 g of snack d.m. The analysis was performed twice for each extract.

Antioxidant capacity determination using DPPH assay

To determine antioxidant capacity of the freeze-dried vegetable snacks using the DPPH assay [Brand-Williams *et al.,* 1995], 16 h before the analysis, 2,2-diphenyl-1-picrylhydrazyl radical (DPPH$^{\bullet}$) solution was prepared by dissolving DPPH$^{\bullet}$ (Sigma-Aldrich, Steinheim, Germany) in methanol and stored at 4°C in darkness. Directly before the analysis, the DPPH$^{\bullet}$ solution was diluted by mixing with an 80% (*v/v*) aqueous ethanol solution to a final solution absorbance within the range of 0.680–0.720 at 515 nm. Various volumes (0.1, 0.2, 0.3, 0.4 mL) of the extract of snacks were put into separate glass tubes and filled with 80% ethanol up to 2 mL. These mixtures were supplemented with 2 mL of a DPPH$^{\bullet}$ solution. After stirring for 30 min in darkness at room temperature, the absorbance was measured at 515 nm using a Helios Gamma spectrophotometer (Thermo Fisher Scientific) *versus* an 80% (*v/v*) aqueous ethanol solution as a blank sample. The assay was carried out twice for each extract. The results were expressed in terms of the EC_{50}, proving that the extract concentration had the ability to scavenge 50% of DPPH$^{\bullet}$. The results were expressed in mg of snack d.m. per mL of the extract.

Antioxidant capacity determination using ABTS assay

To determine the antioxidant capacity of the freeze-dried vegetable snacks using the ABTS assay [Re *et al.,* 1999], an ABTS radical cation solution was prepared by dissolving persulfate (Sigma-Aldrich) and ABTS (Sigma-Aldrich) in the distilled water and storing it for 16 h in darkness to obtain 7 mM solutions. Before the analysis, the ABTS$^{\bullet+}$ solution was mixed with an 80% (*v/v*) aqueous ethanol solution to obtain the reagent proving the absorbance ranging from 0.680 to 0.720 at 734 nm. Varied volumes (0.025, 0.05, 0.075, 0.1 mL) of freeze-dried vegetable snack extracts were put into glass tubes, and 3 mL of the ABTS$^{\bullet+}$ solution was added. The tubes were then stirred and kept for 6 min in darkness at the ambient temperature. The 80% (*v/v*) aqueous ethanol solution served as a blank sample. The absorbance of mixtures was measured at 734 nm using a Helios Gamma spectrophotometer (Thermo Fisher Scientific). The assay was carried out twice for each extract. The results were expressed in terms of the EC_{50} (mg d.m./mL).

Statistical analysis

To identify significant differences between the values for tested snacks, the ANOVA with Tukey's post-hoc test (at $p<0.05$) were performed. Moreover, in order to recognise the relationship between the parameters, Pearson's correlation analysis was carried out and correlation coefficient (r) was determined. The statistical analysis was carried out using STATISTICA 13 software (TIBCO Software, Palo Alto, CA, USA).

RESULTS AND DISCUSSION

The dry matter contents of vegetable snacks before and after drying are shown in Table 2. The dry matter content of fresh vegetable pulps with dried apple pomace powder was 10.36 g/100 g to 10.70 g/100 g. The addition of the sodium alginate as a structure-forming component caused the need for water. Therefore, the initial dry matter content was significantly lower (6.29 g/100 g to 6.76 g/100 g) in the output obtained using a hydrocolloid. There were no significant ($p\geq0.05$) differences between the dry matter content of the samples with homogenous additive components and varied vegetable ingredients. Water removal during the freeze-drying reduced the weight of the snacks with SA and AP by 94.20% and 89.11%, respectively. The dried

TABLE 2. Dry matter content of vegetable snacks with sodium alginate (SA) and dried apple pomace powder (AP) before and after freeze-drying process, and water activity of the freeze-dried products.

Snack	Dry matter content before drying (g/100 g)	Dry matter content after drying (g/100 g)	Water activity
YB-SA	6.29±0.21^{b}	97.19±0.19^{b}	0.012±0.003^{a}
YB/C-SA	6.39±0.16^{b}	97.31±0.20^{b}	0.013±0.002^{a}
YB/P/C-SA	6.76±0.13^{b}	97.31±0.29^{b}	0.010±0.002^{ab}
YB-AP	10.52±0.18^{a}	98.35±0.02^{a}	0.009±0.003^{ab}
YB/C-AP	10.36±0.16^{a}	98.27±0.11^{a}	0.010±0.002^{ab}
YB/P/C-AP	10.70±0.29^{a}	98.20±0.15^{a}	0.006±0.002^{b}

Results are expressed as mean±standard deviation. Different letters (^{a,b}) in columns indicate significant differences at $p<0.05$. Vegetable ingredients: yellow bean (YB), carrot (C) and potato (P).

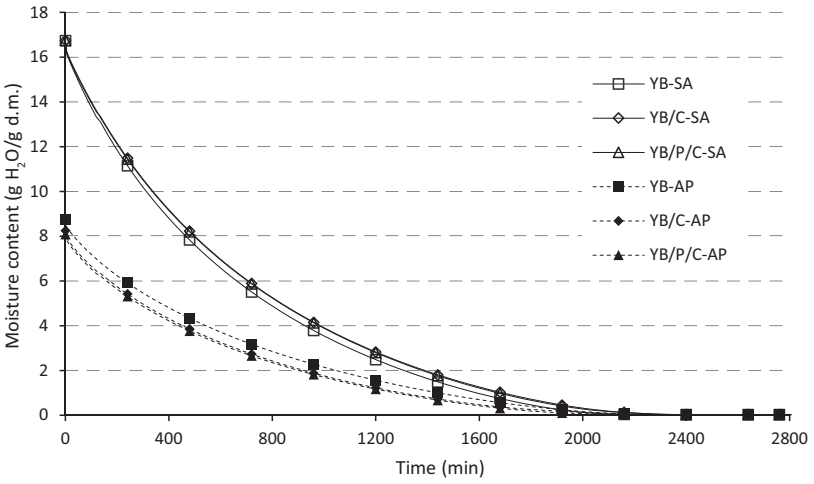

FIGURE 1. Drying kinetic curves obtained for freeze-drying of vegetable snacks with sodium alginate (SA) and dried apple pomace powder (AP) at 30°C. Vegetable ingredients: yellow bean (YB), carrot (C) and potato (P).

materials were characterised by a very high dry matter content and a corresponding low water content, which indicated very low water activity (0.006–0.013). Although the type of additive significantly affected the water content of the samples, the corresponding differences were not evidently reflected by water activity. Similar results of the low water activity and high dry matter content of freeze-dried vegetable snacks with hydrocolloids were obtained by Ciurzyńska *et al.* [2020]. Low water content and activity are factors that restrain chemical and biochemical reactions in food products. They also inhibit the development of microorganisms, thus affecting the safety and stability of products and prolonging their shelf life [Rahman & Labuza, 2020].

Freeze-drying kinetic curves are presented in Figure 1. They show changes in the moisture content in the dried output in terms of the dehydration process duration. The type of used additive determined the drying course. The initial moisture content of the samples with an addition of SA was about two times higher than in the case of the samples with AP. Such a phenomenon was caused by the addition of water to snacks with SA, as mentioned above. The equilibrium moisture content achieved by the end of the freeze-drying process was 0.028 g H_2O/g d.m. for the input supplemented with SA and 0.018 g H_2O/g d.m. for the samples with the AP addition. The type of the additive also influenced the duration of drying, which was about 2,800 min for each snack containing the SA and 2,760 min for the AP samples. The drying time of vegetable snacks was determined by the parameters of the freeze-drying process (temperature and pressure) selected in the preliminary tests. The preliminary experiments were conducted for about two days at a shelf temperature of 30°C and at a pressure of 63 Pa, which allowed obtaining a product with an appropriate structure and texture that accounted for the features that matter to a possible snack consumer. At the same time, the process duration was determined by measuring the temperature in the thermal centre of the freeze-dried vegetable snacks until the pre-set temperature of the shelf in the device was reached to be consistent with the procedure relevant to the freeze-drying porous amorphous products [Ciurzyńska & Lenart, 2011]. The course of the drying curves indicates that, in this study, the freeze-drying process depended on the moisture content of the experimental input. A lower rate of water removal at the same temperature and pressure resulted from a lower moisture content. The freeze-drying process course is affected by the sample thickness, while the size of ice crystals depends on the moisture content in the fresh sample and the composition of the matrix, as well as the process conditions such as temperature and pressure [Oyinloye & Yoon, 2020]. Due to the processing parameters and the very low moisture content, freeze-dried products are usually in an amorphous state, which ensures their textural and structural properties. However, since they are also very prone to adsorb water, and hydrocolloids are also characterised by a high ability to retain water, the drying process needs to be carried out until the moisture content is low in order to prevent glass transition and structure collapse [Cassanelli *et al.*, 2018; Silva-Espinoza *et al.*, 2020].

The true density of the freeze-dried vegetable snacks in terms of the density of the solid material is shown in Table 3. The snacks obtained by adding the apple pomace powder were characterised by 7% higher true density than the input supplemented with sodium alginate. The true density of the products was also dependent on vegetable ingredients. Irrespective of any carrier agent, the lowest values of the true density were obtained for the snacks containing only blanched yellow bean (YB-SA and YB-AP), whereas cooked potato puree caused an increase in the true density, and the highest values were noted for the YB/P/C-SA and YB/P/C-AP. Oikonomopoulou *et al.* [2011] demonstrated that the true density of freeze-dried agricultural products and mushrooms significantly differed from one another and depended on the type of pre-treatment used (*e.g.* boiling duration). Such results were probably caused by differences in the molecular weight of the skeletal compounds of the snacks and the presence of small, closed pores. However, according to Marques *et al.* [2006] using helium allows penetrating all small and closed pores during measurement. Koua *et al.* [2019] also noted the relationship between the moisture content and the true density of the dried input,

TABLE 3. True and apparent density, porosity and hardness of freeze-dried vegetable snacks with sodium alginate (SA) and dried apple pomace powder (AP).

Snack	True density (g/cm^3)	Apparent density (g/cm^3)	Porosity (%)	Hardness (N)
YB-SA	1.460±0.002^{f}	0.073±0.003^{c}	69.46±2.51^{ab}	20.29±2.93^{b}
YB/C-SA	1.469±0.000^{e}	0.065±0.004^{d}	73.90±3.73^{a}	18.94±2.79^{cb}
YB/P/C-SA	1.478±0.001^{d}	0.075±0.004^{c}	65.65±1.10^{abc}	27.36±1.64^{a}
YB-AP	1.578±0.001^{c}	0.135±0.009^{b}	59.39±2.34^{c}	12.71±1.95^{e}
YB/C-AP	1.583±0.001^{b}	0.130±0.005^{b}	64.11±0.32^{bc}	15.29±2.52^{d}
YB/P/C-AP	1.596±0.001^{a}	0.143±0.006^{a}	61.43±1.68^{bc}	16.83±2.56^{cd}

Results are expressed as mean±standard deviation. Different letters (^{a,b,c,d,e,f}) in columns indicate significant differences at $p<0.05$. Vegetable ingredients: yellow bean (YB), carrot (C) and potato (P).

but in the current study, the samples containing less water were characterised by a higher true density and in the aforementioned study it was reverse.

The capacity of the hydrocolloids to create a porous structure also influenced the apparent density of the freeze-dried snacks (Table 3), which was 46% to 50% lower for the samples supplemented with sodium alginate (SA) than it was for the AP variants. The apparent density was strongly correlated with the true density of the input (r=0.99). Since using a hydrocolloid compound allowed for the preservation of the structure during freeze-drying, a smaller weight of the substance occupied a similar volume as the AP samples. Hydrocolloids are prone to creating a porous structure by using mixing and aerating devices such as blenders [Ciurzyńska *et al.*, 2017], and in such cases, replacement of the sodium alginate with apple pomace powder led to the formation of a structure with a smaller amount of closed pores and caused a higher content of the solid mass inside the sample. The differences in the internal structure of the snacks are presented in Figure 2. According to the displayed cross-section scans and 3D visualisations, the skeletal elements were much more condensed in the case of the snacks with the addition of AP than in the case of the products with SA. As shown in Figure 3, for the snacks supplemented with SA, the more frequent appearance of pores with a mean diameter larger than 0.16 mm was observed, while in the AP snacks, a larger number of smaller pores with a mean diameter lower than 0.10 mm was noted. The hydrophilic nature of sodium alginate reduces the mobility of water [Rhim, 2004; Borchard *et al.*, 2005], which induces the formation of large ice crystals and, consequently, a larger size of pores compared to the addition of dried apple pomace powder. The type of carrier agent also affected the total porosity of the freeze-dried snacks (Table 3). Porosity ranged from 59.39% to 73.90% and lower results were received for snacks with the addition of dried apple pomace powder. There was a strong negative correlation between the porosity and density results ($r_{true\ density}$=-0.83, $r_{apparent\ density}$=-0.87). During freeze-drying, since pores are created where ice crystals are removed [Voda *et al.*, 2012], the presented outcomes could also be caused by the amount of water removed from the sample. The water content was higher in the products supplemented with sodium alginate. Differences in the apparent density, porosity and pore distribution arise from the type of additive and technological process that was consistent with the specific nature of the carrier agent used. Mixing ingredients of the snacks with a whisk initiated aeration of the hydrocolloid, which resulted in a very porous structure. For a dried apple pomace powder addition, since aeration was absent and the cellular composition of ingredients was destroyed by grinding, the pores were smaller and porosity was lower in these snacks. The porosity and apparent density of freeze-dried agricultural products depended on the duration of thermal pre-treatment and drying conditions. Since the pressure in a drying chamber influenced those features, higher porosity

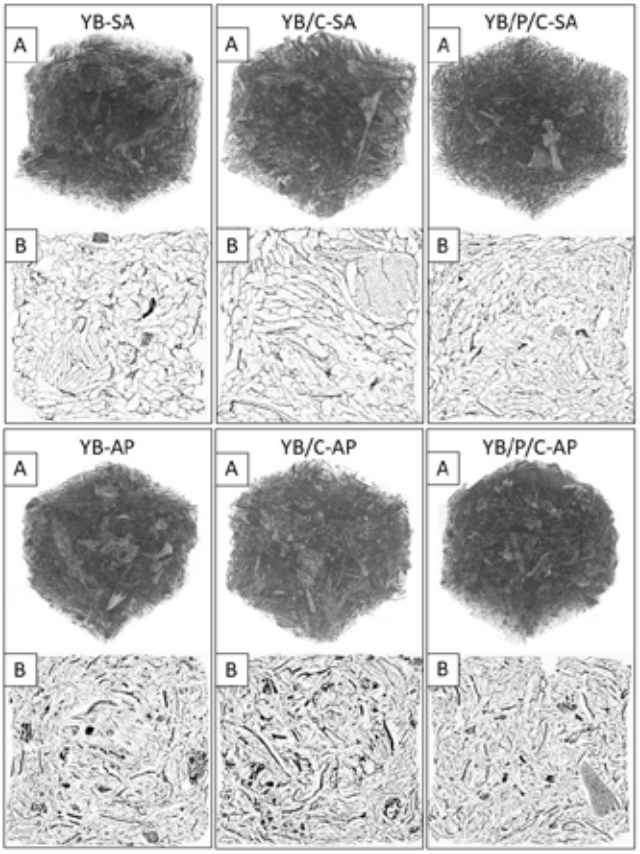

FIGURE 2. 3D images (A) and the cross-section (B) of freeze-dried vegetable snacks with sodium alginate (SA) and dried apple pomace powder (AP). Vegetable ingredients: yellow bean (YB), carrot (C) and potato (P).

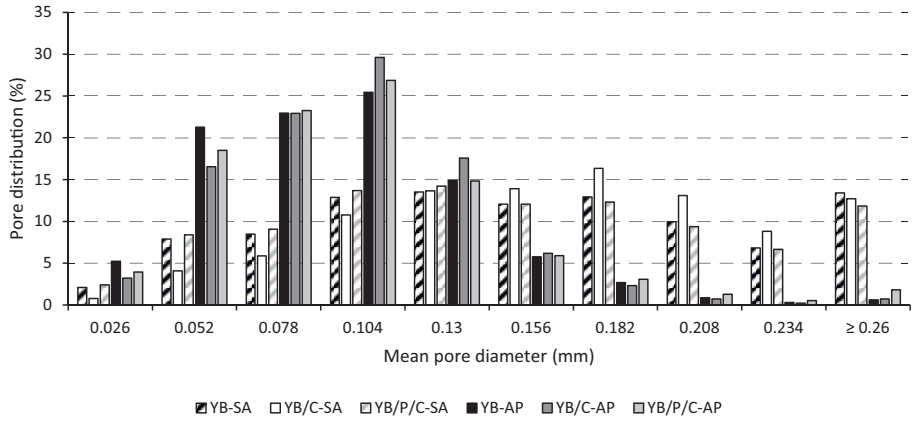

FIGURE 3. Percentage distribution of pore sizes in freeze-dried vegetable snacks with sodium alginate (SA) and dried apple pomace powder (AP). Vegetable ingredients: yellow bean (YB), carrot (C) and potato (P).

and a lower apparent density were caused by the low pressure in the drying chamber [Oikonomopoulou *et al.*, 2011].

The type of additive also affected the textural properties of the freeze-dried vegetable snacks, which happens to be almost as important as sensory properties for both consumers and manufacturers. In general, products obtained after adding dried apple pomace powder were characterised by lower hardness (12.71–16.83 N) than the snacks supplemented with sodium alginate (18.94–27.36 N), as expressed in terms of the maximum force recorded during a compression test (Table 3). However, there were similarities between YB/P/C-AP and YB/C-SA variants. A higher hardness was correlated with a more stable internal structure of the tested sample. For both the AP and SA additives, the YB/P/C snacks were characterised by the highest hardness value, which was induced by the structure and texture-forming properties of the starch contained in the cooked potato puree [Pieniazek & Messina, 2017]. The type of the carrier agent determined not only the hardness of the freeze-dried snacks, but also the course of the compression curves presented in Figure 4. The SA sample curves were full of periodic drops of compression force, while for snacks with the AP addition they were much smoother, and some drops appeared only on the YB/P/C-AP curve. The occurrence of these drops indicated the cracking of the internal structure of the sample as a result of the applied force. For snacks with added AP, the course of the curves was softer because they were compressed without breaking

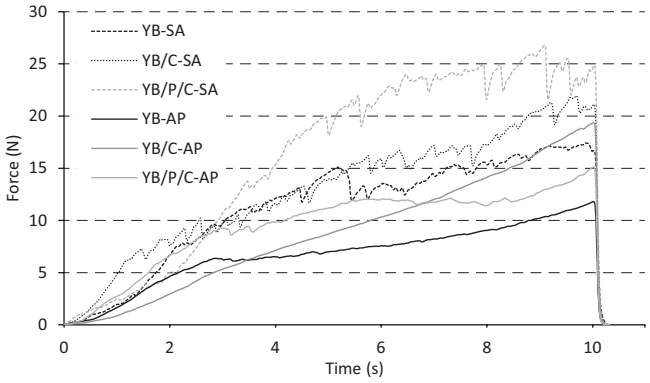

FIGURE 4. Example compression curves of freeze-dried vegetable snacks with sodium alginate (SA) and dried apple pomace powder (AP). Vegetable ingredients: yellow bean (YB), carrot (C) and potato (P).

and cracking, except for the YB/P/C-AP variant, which was harder. Internal cracks were characteristic of fragile and dry input, especially in samples obtained with the freeze-drying method [Rowicka *et al.*, 2002].

The colour parameters of the freeze-dried vegetable snacks are presented in Table 4. The L^* values of snacks before drying ranged from 53.69 to 57.39. There were no significant ($p \geq 0.05$) differences between the YB samples with the addition of sodium alginate and apple pomace powder, but for other recipes L^* was lower for the AP samples than for

TABLE 4. Colour parameters of freeze-dried vegetable snacks with sodium alginate (SA) and dried apple pomace powder (AP).

Snack	L^* before drying	a^* before drying	b^* before drying	L^* after drying	a^* after drying	b^* after drying	ΔE
YB-SA	57.35±0.20^{a}	-5.35±0.11^{e}	31.51±0.20^{e}	76.45±1.43^{a}	-10.62±0.41^{e}	34.56±0.91^{a}	17.09±1.02^{c}
YB/C-SA	54.33±0.24^{d}	8.93±0.66^{b}	35.16±0.19^{b}	71.49±1.69^{bc}	4.76±2.17^{b}	25.29±2.13^{c}	18.27±2.94^{bc}
YB/P/C-SA	57.13±0.14^{b}	1.75±0.15^{d}	31.91±0.16^{d}	74.11±1.1^{ab}	-2.94±0.47^{d}	23.69±2.92^{c}	19.42±3.45^{ab}
YB-AP	57.39±0.04^{a}	1.48±0.04^{d}	31.94±0.07^{d}	75.32±2.77^{ab}	-3.14±0.48^{d}	30.67±1.33^{b}	19.71±1.45^{ab}
YB/C-AP	53.69±0.05^{d}	13.32±0.22^{a}	36.35±0.11^{a}	69.12±2.87^{c}	6.62±1.91^{a}	34.23±2.76^{a}	19.38±1.98^{ab}
YB/P/C-AP	54.49±0.07^{c}	7.42±0.19^{c}	32.38±0.14^{c}	68.54±1.41^{c}	0.89±0.95^{c}	32.08±1.53^{b}	20.75±1.14^{a}

Results are expressed as means±standard deviation. Different letters (^{a,b,c,d,e}) in columns indicate significant differences at $p<0.05$. Vegetable ingredients: yellow bean (YB), carrot (C) and potato (P). Colour parameters: lightness (L^*), redness (a^*), yellowness (b^*) and total colour difference (ΔE).

the SA samples, which means that the snacks with apple pomace powder were darker. After freeze-drying, the L^* parameter of each sample increased. The aforementioned trends were also relevant to the dried products, and the snacks with SA were characterised by higher lightness than the AP samples.

Chroma parameter a^*, which accounts for greenness and redness, was the lowest for the YB snacks and was the highest for the YB/C, regardless of the carrier agent used (Table 4). This trend occurred both before drying and for freeze-dried snacks and was related to the quantity of carrot contained in vegetable mixes, which caused the insertion of orange colorants such as carotenoids. The type of additive caused a^* parameter of each vegetable variant to be significantly higher for the input with AP than for the samples supplemented with AS. If a^* parameter went up, those samples were redder, which was caused by the colour of dried pomace powder that could contain enzymatic and thermal browning products [Krokida *et al.*, 1998], which resulted from pressing the juice and drying the pomace.

The values of chroma parameter b^* were positive for every tested sample (Table 4). Such results meant that each snack, regardless of the vegetable composition or the type of additive used, was yellow, and no blue shades were noted. Fresh vegetable pulps with an addition of SA were characterised by significantly ($p<0.05$) lower yellowness, but after freeze-drying, b^* parameters of the SA products increased while b^* of snacks with AP decreased. The AP freeze-dried vegetable snacks were also characterised by higher yellowness than the SA products.

The influence of an apple pomace addition on the colour parameters in various food products was compiled by Antonic *et al.* [2020] and, in most cases, the products were darker and characterised by higher a^* and b^* parameters. Although the colour changes were usually regarded as a quality-decreasing factor, an increase in nutritive value and sensory features was also observed.

The total colour change that occurred during the freeze-drying process, expressed as ΔE, ranged from 17.09 to 20.75 (Table 4), as noted for the YB-SA and YB/P/C-AP, respectively. Neither the addition of the sodium alginate nor the dried apple pomace powder caused a significantly higher or lower change in the colour of every vegetable mix. The total colour change involved the increase in lightness and greenness, decrease in redness, as well as changes in yellowness, which appeared to have been caused by the freeze-drying process. Freeze-drying is known as the dehydration method that causes the lowest colour change compared to other drying methods [Krokida *et al.*, 2001; Zalewska *et al.*, 2016].

The total phenolic content (TPC) of freeze-dried vegetable snacks is presented in Figure 5. The products obtained using dried apple pomace powder, *i.e.* the YB-AP, YB/C-AP and YB/P/C-AP, contained 281.6, 303.4 and 281.0 mg GAE/100 g d.m., while the snacks supplemented with sodium alginate contained 103.9, 127.7 and 88.7 mg GAE/100 g d.m., respectively. According to Suárez *et al.* [2010] and Tarko *et al.* [2012], apple pomace is a rich source of phenolic compounds and may be used as an enriching additive in food products. As expected, using AP increased total phenolic contents, but it was surprising that the increases would be so much higher (63%, 58% and 68% for YB, YB/C and YB/P/C variants, respectively).

The antioxidant capacity of snacks determined using DPPH and ABTS assays is shown in Figure 6, as EC_{50} values, which express the capacity of the snack dry matter to scavenge 50% of the DPPH$^{\bullet}$ and ABTS$^{\bullet+}$, respectively. To this end, the lower value indicates a higher antioxidant activity. The DPPH$^{\bullet}$ scavenging capacity of YB, YB/C and YB/P/C snacks supplemented with SA was equivalent to 10.44, 14.51, 16.52 mg d.m./mL, and for the sample supplemented with AP it was 5.03, 5.70, 6.90 mg d.m./mL. The presented data shows that in comparison to sodium alginate samples, the snacks with apple pomace powder had higher antioxidant capacity by 52%, 61% and 58%, respectively. The results obtained with the ABTS assay were 2.85, 2.04, 2.42 and 1.90, 1.92, 1.97 mg d.m./mL, according to the aforementioned sequence. In the cases of the YB and YB/P/C variants, the antioxidant capacity was higher by 33% and 19% for the AP samples, but the EC_{50} values of YB/C snacks were similar ($p\geq0.05$), irrespective of the type of carrier agent used. The antioxidant capacity was correlated with the total phenolic content (r_{ABTS}=-0.76 and r_{DPPH}=-0.91), which means that the more

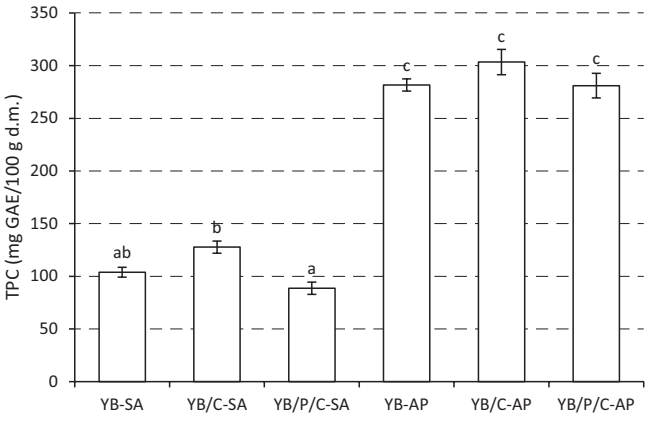

FIGURE 5. Total phenolic content (TPC) of freeze-dried vegetable snacks with sodium alginate (SA) and dried apple pomace powder (AP). Vegetable ingredients: yellow bean (YB), carrot (C) and potato (P) The different letters above bars indicate that the values differ significantly ($p<0.05$).

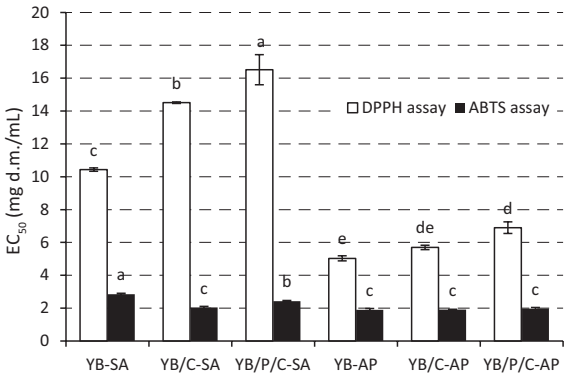

FIGURE 6. Antioxidant capacity of freeze-dried vegetable snacks with sodium alginate (SA) and dried apple pomace powder (AP) determined as EC_{50} using DPPH and ABTS assays. Vegetable ingredients: yellow bean (YB), carrot (C) and potato (P). The different letters above bars indicate that the values differ significantly ($p<0.05$): a-e for results of DPPH assay; a-c for results of ABTS assay.

phenolic compounds are contained in the input, the more radicals it is possible to scavenge. Phenolic compounds are characterised by strong antioxidant activity and, as it has been reported in the literature, during apple juice production, about 90% of them were left in the apple pomace [Wichrowska & Żary-Sikorska 2015]. Freeze-drying is the best method in terms of retention of bioactive compounds such as phenolics, vitamins and colorants in plant products [Bhatta *et al.*, 2020], so it is a desirable method for the production of functional food products. Nevertheless, due to the porous structure of the freeze-dried input, air with oxygen has full access to penetrate it. For this reason, since all bioactive compounds are in danger of degradation and the oxidative stability of such products is lower, appropriate packaging is necessary [Duan *et al.*, 2016].

CONCLUSIONS

In summary, based on the presented results, using dried apple pomace powder and sodium alginate as a carrier agent to produce freeze-dried vegetable snacks produced stable products characterised by repeatable quality. The snacks supplemented with dried apple pomace powder featured higher dry matter content and density, but the sodium alginate-derived products were harder. Dried apple pomace powder improved the health-promoting properties of the snacks, such as the total phenolic content and antioxidant activity. The type of additive also affected textural properties and the internal structure of the products.

Although it is incorrect to state that food waste (particularly apple pomace) is a perfect substitute for a hydrocolloid carrier agent in the case of freeze-dried products, it is worth conducting further research on its nutritive value, sensory and storage properties and to replace only a part of the hydrocolloid with dried pomace powder to improve quality of the product and sustain its texture. Moreover, due to the high content of active ingredients, the addition of fruit pomace may increase the health attractiveness of snack products. At the same time, from an economic point of view, the addition of apple pomace may reduce the cost of producing a unit of the finished product and lower its price on store shelves.

RESEARCH FUNDING

This work was funded by the National Centre for Research and Development, as part of the III BIOSTRATEG. "The development of an innovative carbon footprint calculation method for the basic basket of food products" – task in the project "Development of healthy food production technologies taking into consideration nutritious food waste management and carbon footprint calculation methodology" BIOSTRATEG3/343817/17/NCBR/2018.

CONFLICT OF INTERESTS

Authors declare no conflict of interests.

ORCID IDs

A. Ciurzyńska https://orcid.org/0000-0001-7263-0851
M. Janowicz https://orcid.org/0000-0002-3790-3479
M. Karwacka https://orcid.org/0000-0002-5511-3251
K. Rybak https://orcid.org/0000-0003-3595-0818

REFERENCES

1. Antonic, B., Jancikova, S., Dordevic, D., Tremlova, B. (2020). Apple pomace as food fortification ingredient: A systematic review and meta-analysis. *Journal of Food Science*, *85*(10), 2977–2985. https://doi.org/10.1111/1750-3841.15449
2. AOAC International. Official Methods of Analysis of AOAC International, 17th ed.; AOAC International: Rockville, MD, USA, 2002.
3. Bhatta, S., Stevanovic Janezic, T., Ratti, C. (2020). Freeze-drying of plant-based foods. *Foods*, *9*(1), art. no. 87. https://doi.org/10.3390/foods9010087
4. Borchard, W., Kenning, A., Kapp, A., Mayer, C. (2005). Phase diagram of the system sodium alginate/water: A model for biofilms. *International Journal of Biological Macromolecules*, *35*(5), 247–256. https://doi.org/10.1016/j.ijbiomac.2005.02.006
5. Brand-Williams, W., Cuvelier, M.E., Berset, C. (1995). Use of a free radical method to evaluate antioxidant activity. *LWT – Food Science and Technology, 28*(1), 25–30. https://doi.org/10.1016/S0023-6438(95)80008-5
6. Cassanelli, M., Norton, I., Mills, T. (2018). Role of gellan gum microstructure in freeze drying and rehydration mechanisms. *Food Hydrocolloids*, *75*, 51–61. https://doi.org/10.1016/j.foodhyd.2017.09.013
7. Ciurzyńska, A., Cieśluk, P., Barwińska, M., Marczak, W., Ordyniak, A., Lenart, A., Janowicz, M. (2019a). Eating habits and sustainable food production in the development of innovative "healthy" snacks. *Sustainability*, *11*(10), art. no. 2800. https://doi.org/10.3390/su11102800
8. Ciurzyńska, A., Jasiorowska, A., Ostrowska-Ligęza, E., Lenart, A. (2019b). The influence of the structure on the sorption properties and phase transition temperatures of freeze-dried gels. *Journal of Food Engineering*, *252*, 18–27. https://doi.org/10.1016/j.jfoodeng.2019.02.008
9. Ciurzyńska, A., Marczak, W., Lenart, A., Janowicz, M. (2020). Production of innovative freeze-dried vegetable snack with hydrocolloids in terms of technological process and carbon footprint calculation. *Food Hydrocolloids*, *108*, art. no. 105993. https://doi.org/10.1016/j.foodhyd.2020.105993
10. Ciurzyńska, A., Mieszkowska, A., Olsiński, I., Lenart, A. (2017). The effect of composition and aeration on selected physical and sensory properties of freeze-dried hydrocolloid gels. *Food Hydrocolloids*, *67*, 94–103. https://doi.org/10.1016/j.foodhyd.2016.12.042
11. Ciurzyńska, A., Lenart, A. (2011). Freeze-drying-application in food processing and biotechnology – a review. *Polish Journal of Food and Nutrition Sciences*, *61*(3), 165–171. https://doi.org/10.2478/v10222-011-0017-5

12. Duan, X., Yang, X., Ren, G., Pang, Y., Liu, L., Liu, Y. (2016). Technical aspects in freeze-drying of foods. *Drying Technology*, *34*(11), 1271–1285. https://doi.org/10.1080/07373937.2015.1099545
13. Gondek, E., Jakubczyk, E., Herremans, E., Verlinden, B., Hertog, M., Vandendriessche, T., Verboven, P., Antoniuk, A., Bongaers, E., Estrade, P., Nicolaï, B.M. (2013). Acoustic, mechanical and microstructural properties of extruded crisp bread. *Journal of Cereal Science*, *58*(1), 132–139. https://doi.org/10.1016/j.jcs.2013.03.010
14. Karwacka, M., Ciurzyńska, A., Lenart, A., Janowicz, M. (2020). Sustainable development in the agri-food sector in terms of the carbon footprint: A Review. *Sustainability*, *12*(16), art. no. 6463. https://doi.org/10.3390/su12166463
15. Koua, B.K., Koffi, P.M.E., Gbaha, P. (2019). Evolution of shrinkage, true density, porosity, heat and mass transfer coefficients during indirect solar drying of cocoa beans. *Journal of the Saudi Society of Agricultural Sciences*, *18*(1), 72–82. https://doi.org/10.1016/j.jssas.2017.01.002
16. Krokida, M.K., Maroulis, Z.B., Saravacos, G.D. (2001). The effect of the method of drying on the colour of dehydrated products. *International Journal of Food Science & Technology*, *36*(1), 53–59. https://doi.org/10.1046/j.1365-2621.2001.00426.x
17. Krokida, M.K., Tsami, E., Maroulis, Z.B. (1998). Kinetics of color changes during drying of some fruits and vegetables. *Drying Technology*, *16*(3–5), 667–685. https://doi.org/10.1080/07373939808917429
18. Kruczek, M., Drygaś, B., Habryka, C. (2016). Pomace in fruit industry and their contemporary potential application. *World Scientific News*, *48*, 259–265.
19. Kuo, C.C., Qin, H., Cheng, Y., Jiang, X., Shi, X. (2021). An integrated manufacturing strategy to fabricate delivery system using gelatin/alginate hybrid hydrogels: 3D printing and freeze-drying. *Food Hydrocolloids*, *111*, art. no. 106262. https://doi.org/10.1016/j.foodhyd.2020.106262
20. Liew, S.Q., Teoh, W.H., Yusoff, R., Ngoh, G.C. (2019). Comparisons of process intensifying methods in the extraction of pectin from pomelo peel. *Chemical Engineering and Processing – Process Intensification*, *143*, art. no. 107586. https://doi.org/10.1016/j.cep.2019.107586
21. Marques, L.G., Silveira, A.M., Freire, J.T. (2006). Freeze-drying characteristics of tropical fruits. *Drying Technology*, *24*(4), 457–463. https://doi.org/10.1080/07373930600611919
22. Masiarz, E., Kowalska, H., Bednarska, M. (2019). The application of plant pomace as a source of dietary fiber and other bio-ingredients in the creation of pro-healthy, sensory and technological properties of baking products®. *Postępy Techniki Przetwórstwa Spożywczego, 1*, 103–107.
23. Methakhup, S., Chiewchan, N., Devahastin, S. (2005). Effects of drying methods and conditions on drying kinetics and quality of Indian gooseberry flake. *LWT – Food Science and Technology, 38*(6), 579–587. https://doi.org/10.1016/j.lwt.2004.08.012
24. Meullenet, J.F., Gross, J. (1999). Instrumental single and double compression tests to predict sensory texture characteristics of foods. *Journal of Texture Studies*, *30*(2), 167–180. https://doi.org/10.1111/j.1745-4603.1999.tb00209.x
25. Nowak, D., Jakubczyk, E. (2020). The freeze-drying of foods – The characteristic of the process course and the effect of its parameters on the physical properties of food materials. *Foods*, *9*(10), art. no. 1488. https://doi.org/10.3390/foods9101488
26. Oikonomopoulou, V.P., Krokida, M.K., Karathanos, V.T. (2011). The influence of freeze drying conditions on microstructural changes of food products. *Procedia Food Science*, *1*, 647–654. https://doi.org/10.1016/j.profoo.2011.09.097
27. Oyinloye, T.M., Yoon, W.B. (2020). Effect of freeze-drying on quality and grinding process of food produce: A review. *Processes*, *8*(3), art. no. 354. https://doi.org/10.3390/pr8030354
28. Pieniazek, F., Messina, V. (2017). Texture and color analysis of freeze-dried potato (cv. Spunta) using instrumental and image analysis techniques. *International Journal of Food Properties*, *20*(6), 1422–1431. https://doi.org/10.1080/10942912.2016.1211143
29. Rahman, M.S., Labuza, T.P. (2020). Water activity and food preservation. In M.S. Rahman (Ed.) *Handbook of Food Preservation*. 3rd edition, CRC Press, Boca Raton, pp. 487–506. https://doi.org/10.1201/9780429091483
30. Re, R., Pellegrini, N., Proteggente, A., Pannala, A., Yang, M., Rice-Evans, C. (1999). Antioxidant activity applying an improved ABTS radical cation decolorization assay. *Free Radical Biology and Medicine*, *26*(9–10), 1231–1237. https://doi.org/10.1016/S0891-5849(98)00315-3
31. Rhim, J.W. (2004). Physical and mechanical properties of water resistant sodium alginate films. *LWT – Food Science and Technology*, *37*(3), 323–330. https://doi.org/10.1016/j.lwt.2003.09.008
32. Rowicka, R., Nowak, D., Lewicki, P.P. (2002). Effect of water activity on mechanical properties of freeze-dried apple cubes. *Żywność. Nauka. Technologia. Jakość*, *1*(30), 66–78 (in Polish; English abstract).
33. Silva-Espinoza, M.A., del Mar Camacho, M., Martínez-Navarrete, N. (2020). Use of different biopolymers as carriers for purposes of obtaining a freeze-dried orange snack. *LWT – Food Science and Technology*, *127*, art. no. 109415. https://doi.org/10.1016/j.lwt.2020.109415
34. Silva-Espinoza, M.A., Salvador, A., Camacho, M.D.M., Martínez-Navarrete, N. (2021). Impact of freeze-drying conditions on the sensory perception of a freeze-dried orange snack. *Journal of the Science of Food and Agriculture*, *101*(11), 4585–4590. https://doi.org/10.1002/jsfa.11101
35. Singleton, V.L., Orthofer, R., Lamuela-Raventós, R.M. (1999). Analysis of total phenols and other oxidation substrates and antioxidants by means of Folin-Ciocalteu reagent. *Methods in Enzymology*, *299*, 152–178. https://doi.org/10.1016/S0076-6879(99)99017-1
36. Skinner, R.C., Gigliotti, J.C., Ku, K.M., Tou, J.C. (2018). A comprehensive analysis of the composition, health benefits, and safety of apple pomace. *Nutrition Reviews*, *76*(12), 893–909. https://doi.org/10.1093/nutrit/nuy033
37. Suárez, B., Álvarez, Á.L., García, Y.D., del Barrio, G., Lobo, A.P., Parra, F. (2010). Phenolic profiles, antioxidant activity and *in vitro* antiviral properties of apple pomace. *Food Chemistry*, *120*(1), 339–342. https://doi.org/10.1016/j.foodchem.2009.09.073

38. Tarko, T., Duda-Chodak, A., Bebak, A. (2012). Biological activity of selected fruit and vegetable pomaces. *Żywność. Nauka. Technologia. Jakość*, *19*(4), 55–65 (in Polish; English abstract).
39. Tsami, E., Krokida, M.K., Drouzas, A.E. (1998). Effect of drying method on the sorption characteristics of model fruit powders. *Journal of Food Engineering*, *38*(4), 381–392. https://doi.org/10.1016/S0260-8774(98)00130-7
40. van Kleef, E., Otten, K., van Trijp, H.C. (2012). Healthy snacks at the checkout counter: A lab and field study on the impact of shelf arrangement and assortment structure on consumer choices. *BMC Public Health*, *12*(1), art. no. 1072. https://doi.org/10.1186/1471-2458-12-1072
41. Voda, A., Homan, N., Witek, M., Duijster, A., van Dalen, G., van der Sman, R., Nijsse, J., van Vliet, L., Van As, H., van Duynhoven, J. (2012). The impact of freeze-drying on microstructure and rehydration properties of carrot. *Food Research International*, *49*(2), 687–693. https://doi.org/10.1016/j.foodres.2012.08.019
42. Wichrowska, D., Żary-Sikorska, E. (2015). Health-promoting properties of apple press pomace. *Inżynieria i Aparatura Chemiczna*, *54*(5), 286–287 (in Polish).
43. Zalewska, M., Otreszko-Arski, A., Zalewski, M. (2016). The influence of convective drying and freeze drying on the colour of selected fruits. *Aparatura Badawcza i Dydaktyczna*, *21*, 141–145 (in Polish).

Pol. J. Food Nutr. Sci., 2021, Vol. 71, No. 4, pp. 463–480
On-line ISSN: 2083-6007
Print ISSN: 1230-0322
DOI: 10.31883/pjfns/144044
http://journal.pan.olsztyn.pl

Original article
Section: Nutritional Research

Nutritional Properties, Antioxidant and Antihaemolytic Activities of the Dry Fruiting Bodies of Wild Edible Mushrooms Consumed by Ethnic Communities of Northeast India

Merilin Kakoti[1,2], *Dibya Jyoti Hazarika*[1,3], *Assma Parveen*[1], *Samim Dullah*[1], *Alokesh Ghosh*[1], *Dipankar Saha*[1], *Madhumita Barooah*[1], *Robin Chandra Boro*[1]*

[1]*Department of Agricultural Biotechnology, Assam Agricultural University, Jorhat – 785013, Assam, India*
[2]*Department of Bioengineering and Technology, Gauhati University Institute of Science and Technology, Gauhati University, Guwahati – 781014, Assam, India*
[3]*DBT-North East Centre for Agricultural Biotechnology, Assam Agricultural University, Jorhat – 785013, Assam, India*

Key words: antihaemolytic activity, basidiomycota, radical scavenging activity, nutrients, organic acids, phenolic acids

A variety of cultivated mushrooms in Northeast India are well known for their taste, nutritional and medicinal benefits. Many wild-growing mushrooms are also consumed due to their exotic flavours and tastes; however, the scientific exploration of their nutritional and bioactive properties is still negligible. In the present study, the 32 wild edible mushroom samples of 11 species collected from different parts of Northeast India were evaluated for their proximate composition, mineral and vitamin (ascorbic acid and riboflavin) contents, antioxidant and antihaemolytic activity, and profiles of organic and phenolic acids. *Lentinus sajor-caju* and *Lentinus squarrosulus* had the highest carbohydrate content (49.80 g/100 g dry weight (d.w.) and 46.36 g/100 g d.w., respectively), crude protein content (20.72 g/100 g d.w. and 20.54 g/100 g d.w., respectively) and a considerable content of minerals. The highest fat content was determined in *Lentinus velutinus* (7.17 g/100 g d.w.). Among the minerals, potassium was found as the most abundant in all the samples. The extracts of *L. sajor-caju, L. squarrosulus,* and *Pleurotus pulmonarius* were characterized by the highest antioxidant activity, while these of *L. sajor-caju*, *Pleurotus ostreatus*, *P. pulmonarius* and *Agaricus bisporus* showed the highest antihaemolytic potential. The HPLC analysis allowed determining the high contents of ascorbic acid and a few organic and phenolic acids such as lactic acid, gallic acid, 3,4-dihydroxybenzoic acid and *trans*-cinnamic acid in the tested mushrooms. Other compounds *viz.* citric acid, caffeic acid, riboflavin, vanillic acid, pyruvic acid, and *p*-coumaric acid were detected with variations. This study established the nutritional and health benefits of wild edible mushrooms of Northeast India region for consumption as functional foods in the human diet.

INTRODUCTION

Mushrooms (including the members of Basidiomycota and the fruiting body forming Ascomycota) are considered to be one of the important components of the forest ecosystem. They have been gaining in importance since ancient times due to their edibility, psychotropic properties, poisonous nature, and mycorrhizal or parasitic associations with the forest trees. With an estimation of around 1.5 million fungal species on earth [Hawksworth, 2001], more than 31,000 species of Basidiomycota (which form the fruiting bodies) and more than 66,000 species of Ascomycota (a small fraction of which forms the fruiting bodies) are well-characterized [Martins, 2017; Taylor *et al*., 2015]. Among the discovered mushroom species, there are abundant numbers of wild edible mushrooms which are consumed world-wide. These mushrooms need to be evaluated for their nutritional composition and bioactive metabolites.

Many mushrooms are rich in nutrients, medicinal, and plant growth-promoting compounds [Ghate & Sridhar, 2016], whereas, many others contain toxic metabolites. Edible mushrooms contain considerable amount of nutritional compounds including carbohydrates (especially non-reducing sugars), proteins, minerals and vitamins. Presence of phenolics, tocopherols, carotenoids and ascorbic acid in mushroom fruiting bodies make them a good source of natural antioxidants [Sánchez, 2017]. These antioxidant molecules provide biochemical support to the growth of fruiting bodies by neutralizing the oxidative stresses provided by reactive oxygen species and free radicals. Likewise, consumption of foods that are rich in natural antioxidants provide excellent health benefits and protects our body against oxidative stresses and aging signs [Chang, 1996; Lindequist *et al*., 2005]. Recent studies have demonstrated the antihaemolytic potential of a few mushroom species [Madhanraj *et al*., 2019; Sharif *et al*., 2017]. Antihaemolytic compounds are antioxidants that

* Corresponding Author:
E-mail: robin.boro@aau.ac.in (R.Ch. Boro)

Submitted: 2 April 2021
Accepted: 17 November 2021
Published on-line: 13 December 2021

© Copyright by Institute of Animal Reproduction and Food Research of the Polish Academy of Sciences
© 2021 Author(s). This is an open access article licensed under the Creative Commons Attribution-NonCommercial-NoDerivs License (http://creativecommons.org/licenses/by-nc-nd/4.0/).

inhibit the lysis of red blood cells caused by oxidative agents [Shabbir *et al*., 2013].

The Northeast (NE) India possesses a richness in forests, with an abundance of many tree species and other woody plants. The biodiversity of woody plants can be correlated with an equally diverse mycoflora. Ethnic communities inhabiting different regions of Northeast India regularly consume edible mushrooms collecting from the wild based on their traditional knowledge on mushroom identities and their nutritional benefits. However, the diversity of wild mushrooms from this region is not well documented in terms of nutritional properties and bioactive properties. Earlier studies have identified some of the wild edible mushrooms from the states of NE India including Assam, Arunachal Pradesh, Meghalaya, and Nagaland [Khaund & Joshi, 2013; Parveen *et al*., 2017; Sarma *et al*., 2010]. However, nutritional profiling of majority of these wild edible mushrooms are not well investigated. In our recent study, a molecular genetic analysis was conducted to identify 50 wild mushrooms collected from different regions of five Northeastern states of India, out of which 32 edible samples belonging to 11 different species were detected based on their morphological characters as well as genetic information of the internal transcribed spacer (ITS) region [Kakoti *et al*., 2021]. Most of these edible mushrooms are part of the regular diet of various tribal and non-tribal communities. Therefore, the present investigation was conducted to evaluate the species-wise nutritional profiling including proximate composition, mineral and vitamin (ascorbic acid and riboflavin) contents, bioactivity (antioxidant and antihaemolytic activities) and contents of organic and phenolic acids of those 32 wild edible mushrooms to establish their edibility as functional food.

MATERIALS AND METHODS

Collection of the fruiting bodies of mushrooms

The fruiting bodies of different mushrooms were collected from different locations of five North-Eastern states of India (Assam, Arunachal Pradesh, Manipur, Meghalaya, and Nagaland). The fruiting bodies were cleaned at the site of collection with distilled water and immediately taken to the laboratory by packing inside the collection bags. A total of 32 wild-edible mushroom samples were used in this study and their fundamental sampling information are described in Table 1. These information are also available online at Barcode of Life Data (BOLD) system (http://www.boldsystems.org/). Morphological description of molecular identities (ITS barcode details) of the samples was provided previously [Kakoti *et al*., 2021]. BOLD submission IDs and GenBank Accession numbers are provided in Table 1.

Preparation of dry powder

The mushroom fruiting bodies were initially shade-dried with dry air to remove the excessive moisture from the samples and placed in a hot air oven at 45°C until the residual moisture was removed. This process took 16–24 h depending on the sample characteristics. Dry mushrooms were then powdered using a grinder and sieved through 0.5 mm net.

Determination of moisture content

Moisture content of the fresh mushrooms was determined using the Association of Official Analytical Chemists (AOAC) standard protocol [AOAC, 1996]. Briefly, about 20 g of freshly collected samples were weighed, shade-dried at room temperature for 2 h inside a laminar air flow hood (to remove the excessive moisture), and placed in a hot-air oven at 105°C for 5 h. The dishes were later cooled in a desiccator and weighed with the lid on. The moisture content of the mushrooms was estimated using the formula:

$$\text{Moisture content of fresh sample (g/100 g)} = \left(\frac{\text{Fresh weight (g)} - \text{Dry weight (g)}}{\text{Fresh weight (g)}}\right) \times 100$$

The residual moisture content in the dry fruiting powders was determined from 1 g dry powder by placing in a hot-air oven at 105°C for 5 h.

$$\text{Moisture content of dry powder (g/100 g)} = \left(\frac{\text{Initial dry weight (g)} - \text{final dry weight (g)}}{\text{Initial dry weight (g)}}\right) \times 100$$

Moisture content of the dry powder was used to calculate the actual dry weight of the samples.

Determination of ash content

The ash content of mushrooms was determined from the dried, fine powders of the mushroom fruiting bodies. One gram of powder was weighed into a crucible, which was placed in a muffle furnace initially at 130°C for 1 h, and finally the temperature was increased to 600°C for about 6 h. The powder was cooled in a desiccator and weighed. The ash content was calculated using the following equation:

$$\text{Ash content (g/100 g)} = \left(\frac{\text{Weight of ash (g)}}{\text{Weight of dry mushroom (g)}}\right) \times 100$$

Finally, ash content of dried mushrooms was expressed as g per 100 g of powder dry weight (d.w.).

Determination of crude protein content

The crude protein in the dried and powdered mushroom tissue was determined using the macro-Kjeldhal method [method 984.13; AOAC, 1990] with necessary modifications. Briefly, 100 mg of the mushroom powder was subjected to acid digestion in a KelPlus digestion apparatus (Pelican equipment, Channai, Tamil Nadu, India). The digested sample was distilled following the alkali treatment and the released ammonia was extracted in 2.5% boric acid using the KelPlus automatic distiller (Pelican equipment). The resultant solution was then titrated manually against 0.02 N sulfuric acid to determine the nitrogen content. The crude protein content was calculated from the nitrogen content by multiplying with a factor of 4.38 [Reis *et al*., 2012]. The results were expressed as g per 100 g of d.w. of mushroom powders.

Determination of total carbohydrate content

Dried mushroom powder (100 mg) was mixed with 2.5 N HCl and boiled in a water bath for 3 h. The hydrolysate was neutralized with sodium carbonate. The volume was made up

to 100 mL and supernatant was collected by centrifugation. Carbohydrate content in the supernatant was determined using the anthrone method [Sadasivam & Manickam, 1996]. Total carbohydrate content of mushroom powders was expressed as g per 100 g of d.w.

Determination of fat content

The total fat content of dried mushroom fruiting bodies was determined using the gravimetric method [AOAC, 2007]. Fat was extracted with ethanol : diethyl ether : petroleum ether (5:12:12, *v/v/v*) after hydrolysis of the dry mushroom powder with concentrated HCl. The petroleum ether layer was separated after proper mixing and dried to obtain the fat, which was further weighed. Total fat content in dried mushrooms was calculated as follows:

$$\text{Fat content (g/100 g)} = \left(\frac{\text{Weight of the extracted fat (g)}}{\text{Sample weight (g)}}\right) \times 100$$

The results were expressed as g per 100 g of d.w. of mushroom powders.

Determination of mineral content

The contents of minerals *viz*. calcium, magnesium, potassium, sodium, zinc, iron, copper and manganese, in the dried mushroom fruiting bodies were determined using an iCE3000 atomic absorption spectrometer (Thermo Scientific, Waltham, MA, USA). Extracts were prepared by digesting the powdered mushroom samples in nitric acid and hydrogen peroxide as described earlier [Soylak *et al*., 2005]. The phosphorus content was estimated using the molybdovanadate method [method 965.17; AOAC, 1990]. The content of each element was determined using a calibration curve plotted with known concentrations of the respective standards. Results were expressed based on d.w. of mushroom powders.

Extract preparation from the fruiting bodies

Dry powdered fruiting bodies (1 g) were extracted overnight using 100 mL of methanol and the supernatant was carefully filtered through Whatman No. 42 filter paper (GE Healthcare, Chicago, IL, USA) taking the care that minimal residue was transferred to the filter paper. Supernatant was collected and the residue was extracted with another 100 mL of methanol as described above. For the determination of total phenolic content, the filtered supernatant was directly used in the assay. For antioxidant and antihaemolytic activities analysis, the extracts were evaporated to dryness using a rotary evaporator and re-dissolved in a required volume (to prepare the working solutions) of methanol or phosphate buffered saline (PBS; 10 mM Na_2HPO_4, 1.8 mM KH_2PO_4, 137 mM NaCl and 2.7 mM KCl, pH 7.4), respectively, as per the requirements for further experiments.

Determination of total phenolic content

Total phenolic content in the methanol extracts of mushroom samples was estimated spectrophotometrically, based on the procedure described by Singleton & Rossi [1965] with some modifications. First, 1 mL of the extract was mixed with 1 mL of a Folin-Ciocalteu's phenol reagent. After 3 min, 1 mL of a saturated sodium carbonate solution was added to the mixture and adjusted to the total volume to 10 mL with distilled water. The reaction mixture was kept in dark for 90 min, after that the absorbance was recorded at 725 nm. Known concentrations of gallic acid were used to prepare the standard curve. The total phenolic content of the samples was calculated based on the graph and expressed as mg gallic acid equivalents (GAE) per 100 g of d.w. of mushroom powders.

DPPH radical scavenging activity

The 2,2-diphenyl-1-picrylhydrazyl (DPPH, Sigma, Saint Louis, MO, USA) radical scavenging activity was determined by the Blois's method [Blois, 1958] with minor modifications. The extract and reference standard solutions in methanol (1 mL) were prepared in different concentrations and mixed individually with 0.5 mL of 0.15 mM DPPH$^{\bullet}$ solution. α-Tocopherol was used as the reference standard [Boonsong *et al*., 2016]. The percentage of inhibition of DPPH$^{\bullet}$ was obtained by measuring the absorbance at 517 nm using an Evolution 202 UV–Vis double beam spectrophotometer (Thermo Scientific) and calculation using the following formula:

$$\text{\% Inhibition of DPPH radical} = \left(\frac{\text{Absorbance of control} - \text{Absorbance of sample}}{\text{Absorbance of control}}\right) \times 100$$

The % inhibition data was used to calculate the IC_{50} value – concentration of extract that could scavenge 50% of DPPH radicals. Additionally, the results were expressed as the tocopherol equivalent antioxidant activity (TEAA) in mg tocopherol equivalent per 100 g of d.w. of mushroom powder.

Determination of antihaemolytic activity

The antihaemolytic activity of the dried mushrooms was evaluated using the spectrophotometric method described previously by Shabbir *et al*. [2013] with minor modifications. Briefly, the reaction mixture consisted 0.5 mL of mushroom extract with varying concentrations *viz*., 100, 250, 500, 750 and 1000 μg/mL in PBS and 0.5 mL of a red blood cell (RBC) suspension, and the mixture was incubated at room temperature for 20 min. After incubation, 0.5 mL of hydrogen peroxide (H_2O_2) was supplemented to the mixture for induction of the oxidative degradation of membrane lipids. A control was prepared with a similar volume of the reaction mixture without adding the extract. The reaction mixture was then centrifuged at 500×*g*, 4°C for 5 min and the antihaemolytic activity was assessed spectrophotometrically at 540 nm. The percent of haemolysis was calculated using the following formula:

$$\text{\% Inhibition of haemolysis} = \left(\frac{\text{Absorbance of control} - \text{Absorbance of sample}}{\text{Absorbance of control}}\right) \times 100$$

The % inhibition data was used to calculate the IC_{50} value – concentration of extract that could inhibit the haemolysis of RBC by 50%.

Detection of major organic acids and antioxidant compounds

The organic and phenolic acids and some other metabolites were initially extracted from powdered mushroom

TABLE 1. Sampling details of the wild edible mushrooms collected in Northeast India.

No.	Species name	Sample ID	Habitat	Sampling location	Date of collection	Collected by	GenBank Accession No.	BOLD submission ID
1	*Agaricus bisporus* (J.E. Lange) Imbach 1946	MLS2	Soil containing plant litter	East Khasi Hill, Shillong, Meghalaya	11.04.2018	M. Kakoti, D. J. Hazarika	MK855508	ITSA051–20
2	*Auricularia auricula-judae* (Bull.) Quél. 1886	DIM1	Living tree	Dimapur, Nagaland	30.04.2018	M. Kakoti	MK855509	ITSA040–20
3	*Lentinus sajor-caju* (Fr.) Fr. 1838	APK5	Wood surface	Koronu, Lower Dibang Valley, Arunachal Pradesh	26.03.2018	M. Kakoti, D. J. Hazarika	MK851527	ITSA014–19
		DIM3	Decaying wood	Dimapur, Nagaland	30.04.2018	M. Kakoti	MK851526	ITSA016–19
		DH3	Decaying wood	Haflong, Dima Hasao, Assam	03.07.2017	M. Kakoti	MK851528	ITSA015–19
		MIS2	Decaying wood	Missamara, Golaghat, Assam	25.06.2018	M. Kakoti, D. J. Hazarika	MK851531	ITSA017–19
		MIS7	Fully decayed wood	Missamara, Golaghat, Assam	03.07.2018	M. Kakoti, D. J. Hazarika	MK851530	ITSA018–19
		MP3	Decaying wood	Kohima, Manipur	01.02.2018	M. Kakoti	MK851529	ITSA019–19
4	*Lentinus squarrosulus* Mont. 1842	AAU1	Decaying wood	Assam Agricultural University Campus Barbheta, Jorhat, Assam	15.06.2017	M. Kakoti	MK851539	ITSA020–19
		AAU2	Decaying wood	Assam Agricultural University Campus Barbheta, Jorhat, Assam	15.06.2017	M. Kakoti	MK851538	ITSA021–19
		AAU3	Decaying wood	Assam Agricultural University Campus Barbheta, Jorhat, Assam	15.06.2017	M. Kakoti	MK851536	ITSA022–19
		AAU4	Decaying wood	Assam Agricultural University Campus Barbheta, Jorhat, Assam	15.06.2017	M. Kakoti	MK851535	ITSA023–19
		AAU5	Soil	Assam Agricultural University Campus Barbheta, Jorhat, Assam	15.06.2017	M. Kakoti	MK851534	ITSA024–19
		AAU6	Soil	Assam Agricultural University Campus Barbheta, Jorhat, Assam	15.06.2017	M. Kakoti	MK851533	ITSA025–19
		AAU7	Soil	Assam Agricultural University Campus Barbheta, Jorhat, Assam	15.06.2017	M. Kakoti	MK851532	ITSA026–19
		DH1	Decaying wood	Haflong, Dima Hasao, Assam	03.07.2017	M. Kakoti	MK851537	ITSA027–19
		DIM2	Decaying wood	Dimapur, Nagaland	30.04.2018	M. Kakoti	MK855509	ITSA041–20
		KB2	Dead tree	Bokajan, Karbi Anglong, Assam		M. Kakoti, D. J. Hazarika	MK851540	ITSA028–19
5	*Lentinus velutinus* Fr. 1830	KM5	Soil	Kanubari Tea Estate, Sivasagar, Assam	03.05.2017	M. Kakoti, S. Dullah, A. Parveen	MK855514	ITSA045–20
6	*Lycoperdon scabrum*	BP9	Soil	Barpeta, Assam	31.08.2018	M. Kakoti, A. Ghosh	MK851544	ITSA003–19
		DIM8	Soil	Dimapur, Nagaland	17.06.2018	M. Kakoti	MK851545	ITSA004–19
		KM7	Grassland soil	Kanubari Tea Estate, Sivasagar, Assam	03.05.2017	M. Kakoti, S. Dullah, A. Parveen	MK851546	ITSA005–19
		RB6	Soil	Rongbong, Golaghat, Assam	18.06.2018	M. Kakoti, D. J. Hazarika	MK851547	ITSA006–19

TABLE 1. Continued

No.	Species name	Sample ID	Habitat	Sampling location	Date of collection	Collected by	GenBank Accession No.	BOLD submission ID
7	*Panus lecomtei* (Fr.) Corner 1981	APBN3	Wood surface	Bhismaknagar, Roing, Arunachal Pradesh	26.03.2018	M. Kakoti, D. J. Hazarika	MK851549	ITSA036–19
8	*Pleurotus giganteus* (Berk.) Karun. & K.D. Hyde 2011	KM1	Soil with plant litter	Kanubari Tea Estate, Sivasagar, Assam	03.05.2017	M. Kakoti, S. Dullah, A. Parveen	MK851552	ITSA007–19
		KM2	Soil with plant litter	Kanubari Tea Estate, Sivasagar, Assam	03.05.2017	M. Kakoti, S. Dullah, A. Parveen	MK855519	ITSA044–20
9	*Pleurotus ostreatus* (Jacq.) P. Kumm. 1871	MP1	Decaying wood	Kohima, Manipur	01.02.2018	M. Kakoti	MK855520	ITSA046–20
10	*Pleurotus pulmonarius* (Fr.) Quél. 1872 [synonym. *Pleurotus ostreatus* var. *pulmonarius* (Fr.) Iordanov, Vanev & Fakirova 1979]	MLS1	Decaying wood	East Khasi Hill, Shillong, Meghalaya	11.04.2018	M. Kakoti, D. J. Hazarika	MK851551	ITSA008–19
		MP2	Dead tree surface	Kohima, Manipur	01.02.2018	M. Kakoti	MK855521	ITSA047–20
11	*Polyporus arcularius* (Batsch) Fr. 1821 [synonym. *Lentinus arcularius* (Batsch) Zmitr. 2010]	APBN4	Decaying wood	Bhismaknagar, Lower Dibang Valley, Arunachal Pradesh	26.03.2018	M. Kakoti, D. J. Hazarika	MK851553	ITSA030–19
		DH2	Decaying wood	Haflong, Dima Hasao, Assam	03.07.2017	M. Kakoti	MK851555	ITSA031–19
		MLS6	Decaying wood	East Khasi Hill, Shillong, Meghalaya	23.08.2018	M. Kakoti, D. J. Hazarika	MK851554	ITSA032–19

BOLD: Barcode of Life Data.

fruiting body (1 g) with 25 mL of 80% (*v/v*) acetone in water [Barros *et al*., 2009] for 6 h and filtered through Whatman No. 42 filter paper (GE Healthcare) taking the care that minimal residue was transferred to the filter paper. The precipitate was re-extracted with another 25 mL of 80% (*v/v*) acetone as described above. The crude extracts were concentrated under vacuum and re-dissolved in 20 mL of 50% (*v/v*) methanol. The extracts were then filtered using a membrane syringe filter and a 20 μL of sample was separated through a Cosmosil C-18 column (300×4.6 mm, pore size 5 μm; Nacalai Tesque Inc., Kyoto, Japan) installed in a Hitachi Chromaster 3000 series HPLC system with a diode array detector (Hitachi, Tokyo, Japan). The mobile phase used consisted of acetonitrile (A) and 0.1% (*v/v*) phosphoric acid (H_3PO_4) in water in a gradient mode: 5% of A at 0–2 min, 15% of A at 2–5 min, 40% of A at 5–10 min, 60% of A at 10–15 min, 90% of A at 15––18 min, reverting to 5% of A at 20 min and equilibration with 5% of A till 25 min. Detection of compounds was performed in the range of 200–400 nm. The peaks were compared with individual standards of 11 organic acids and antioxidants *viz.*: ascorbic acid (Sigma-Aldrich, Saint Louis, MO, USA), caffeic acid (Sigma-Aldrich), citric acid (Himedia, Mumbai, Maharastra, India), 3,4-dihydroxybenzoic acid (Sigma-Aldrich), gallic acid (Sigma-Aldrich), lactic acid (Sigma-Aldrich), pyruvic acid (Himedia), *p*-coumaric acid (Sigma-Aldrich), riboflavin (Sigma-Aldrich), *trans*-cinnamic acid (Sigma-Aldrich) and vanillic acid (Sigma-Aldrich). The contents of compounds in mushrooms were calculated from the linear portion of the regression curve prepared from the peak areas of individual reference standards.

Statistical analysis

All the statistical analyses were performed using IBM SPSS software, version 25 (Armonk, NY, USA). To test the significant differences among the samples, one-way analysis of variance (ANOVA) with Duncan's multiple range test was used, while non-parametric Kruskal-Wallis test was used for species-wise comparison. Results were considered to be significant with 95% confidence level and $p<0.05$. Pearson's correlation analysis was performed to calculate the correlation coefficient among total phenolic content, antioxidant activity and antihaemolytic activity. All the experiments, including the preparation of extracts, determination of proximate compositions and bioactivities were performed with three independent replicates for each sample. Three data points were generated from three independent replications for statistical analysis.

RESULTS AND DISCUSSION

Nutritional properties of the wild edible mushrooms

In this study, 32 wild edible mushroom samples collected from different locations of Northeast India were assessed for their nutritional properties. Sample-wise as well as species--wise comparisons of the moisture content among different edible samples are represented in Table 2. The highest moisture content (90.35 g/100 g) was recorded in *Auricularia auricula-judae,* while *Polyporus arcularius* (synonym. *Lentinus arcularius*) was recorded with the lowest moisture content

TABLE 2. Sample-wise and species-wise comparison of proximate compositions of the mushroom fruiting bodies.

No.	Species name & sample code	Moisture content of the fresh fruiting bodies (g/100 g)		Moisture content of the dried powder (g/100 g)		Ash (g/100 g dry weight)		Carbohydrate (g/100 g dry weight)		Crude protein (g/100 g dry weight)		Fat (g/100 g dry weight)	
		Average of samples	Average of species	Average of samples	Average of species	Average of samples	Average of species	Average of samples	Average of species	Average of samples	Average of species	Average of samples	Average of species
1.	*Agaricus bisporus*		**84.50±0.44**^{c}		**2.60±0.10**^{d}		**9.23±0.38**^{a}		**36.52±2.22**^{f}		**18.65±0.80**^{ab}		**2.46±0.18**^{bc}
	MLS2	84.50±0.44^{f}		2.60±0.10^{lmn}		9.23±0.38^{a}		36.52±2.22^{p}		18.65±0.80^{klm}		2.46±0.18^{ef}	
2.	*Auricularia auricula-judae*		**90.35±0.41**^{a}		**2.83±0.06**^{bc}		**5.68±0.39**^{cd}		**42.75±2.42**^{bc}		**19.70±0.94**^{ab}		**1.44±0.00**^{e}
	DIM1	90.35±0.41^{a}		2.83±0.06^{hijkl}		5.68±0.39^{n}		42.75±2.42^{ghi}		19.70±0.94^{hij}		1.44±0.00^{hi}	
3.	*Lentinus sajor-caju*		**81.12±1.17**^{e}		**2.63±0.15**^{d}		**7.19±0.50**^{c}		**49.80±3.34**^{a}		**20.72±1.97**^{a}		**0.62±0.55**^{g}
	APK5	82.20±0.66^{gh}		2.53±0.15^{mn}		7.61±0.31^{defgh}		47.76±2.39^{de}		19.93±0.20^{ghi}		0.24±0.06^{m}	
	DH3	80.22±0.33^{klm}		2.73±0.06^{ijklm}		7.05±0.12^{ijk}		52.09±2.32^{ab}		19.05±0.33^{ijkl}		0.24±0.06^{m}	
	DIM3	82.72±0.46^{g}		2.77±0.15^{ijklm}		7.36±0.37^{fghi}		51.63±1.12^{ab}		22.04±0.42^{cde}		0.75±0.22^{jk}	
	MIS2	81.36±0.48^{hij}		2.67±0.12^{jklm}		6.64±0.32^{kl}		49.88±1.29^{bcd}		23.11±0.32^{ab}		0.31±0.10^{lm}	
	MIS7	80.49±0.48^{jkl}		2.43±0.06^{n}		7.74±0.41^{bcdef}		44.39±1.04^{gh}		17.86±0.45^{mn}		1.71±0.21^{gh}	
	MP3	79.72±0.21^{lm}		2.63±0.12^{klmn}		6.73±0.21^{kl}		53.05±0.85^{a}		22.31±0.32^{bcd}		0.48±0.06^{klm}	
4.	*Lentinus squarrosulus*		**80.48±1.40**^{e}		**2.92±0.36**^{bc}		**7.07±0.41**^{c}		**46.36±3.71**^{b}		**20.54±1.72**^{a}		**2.69±0.69**^{b}
	AAU1	82.17±0.72^{gh}		2.83±0.12^{hijkl}		7.57±0.30^{efgh}		50.53±1.08^{abc}		19.49±0.42^{ijk}		2.57±0.00^{ef}	
	AAU2	80.89±0.65^{ijk}		2.53±0.12^{mn}		6.74±0.23^{jkl}		49.69±0.56^{bcd}		22.87±0.27^{abc}		2.36±0.00^{f}	
	AAU3	78.25±1.06^{n}		2.90±0.10^{fghi}		6.53±0.24^{lm}		48.05±0.59^{cd}		21.15±0.25^{ef}		3.26±0.06^{c}	
	AAU4	79.32±0.79^{m}		2.83±0.06^{hijkl}		7.30±0.13^{fghi}		43.06±1.17^{ghi}		20.67±0.25^{fg}		3.95±0.26^{b}	
	AAU5	81.62±0.42^{hi}		2.73±0.06^{ijklm}		7.02±0.16^{ijk}		45.29±1.99^{efg}		23.30±0.45^{a}		3.19±0.10^{c}	
	AAU6	80.82±0.45^{ijk}		2.43±0.49^{n}		6.75±0.14^{jkl}		39.96±0.36^{jklmn}		21.55±0.12^{def}		2.29±0.06^{f}	
	AAU7	82.11±0.71^{gh}		3.53±0.06^{a}		6.67±0.23^{kl}		43.29±1.88^{ghi}		20.61±0.32^{fgh}		2.49±0.27^{ef}	
	DH1	80.93±0.60^{ijk}		3.33±0.06^{abc}		7.28±0.17^{fghi}		45.00±2.48^{fgh}		19.04±0.33^{ijkl}		3.03±0.06^{cd}	
	DIM2	79.44±0.52^{m}		3.13±0.06^{cde}		7.66±0.10^{cdefg}		51.00±1.10^{ab}		18.70±0.26^{jklm}		2.37±0.27^{f}	
	KB2	79.25±0.34^{m}		2.93±0.06^{efgh}		7.21±0.09^{ghij}		47.76±1.68^{de}		17.99±0.65^{mn}		1.41±0.46^{hi}	
5.	*Lentinus velutinus*		**80.59±0.48**^{e}		**3.37±0.06**^{ab}		**8.16±0.20**^{ab}		**41.22±1.20**^{cde}		**15.36±0.13**^{d}		**7.17±0.15**^{a}
	KM5	80.59±0.48^{ijkl}		3.37±0.06^{ab}		8.16±0.20^{b}		41.22±1.20^{ijkl}		15.36±0.13^{q}		7.17±0.15^{a}	

TABLE 2. Continued

No.	Species name & sample code	Moisture content of the fresh fruiting bodies (g/100 g)		Moisture content of the dried powder (g/100 g)		Ash (g/100 g dry weight)		Carbohydrate (g/100 g dry weight)		Crude protein (g/100 g dry weight)		Fat (g/100 g dry weight)	
		Average of samples	Average of species	Average of samples	Average of species	Average of samples	Average of species	Average of samples	Average of species	Average of samples	Average of species	Average of samples	Average of species
6.	*Lycoperdon scabrum*		**87.42±1.10^{b}**		**2.85±0.13^{c}**		**5.62±0.37^{d}**		**38.55±1.17^{ef}**		**17.31±0.74^{c}**		**0.57±0.16^{g}**
	BP9	86.13±0.24^{de}		2.77±0.06^{ijklm}		5.47±0.21^{n}		38.43±1.08^{nop}		16.41±0.26^{p}		0.62±0.18^{jkl}	
	DIM8	88.71±0.48^{b}		2.87±0.06^{hijk}		5.44±0.17^{n}		37.70±1.55^{op}		17.14±0.25^{nop}		0.41±0.10^{klm}	
	KM7	87.58±1.10^{c}		2.73±0.06^{ijklm}		6.16±0.08^{m}		39.44±0.77^{klmn}		18.08±0.64^{lmn}		0.51±0.10^{jklm}	
	RB6	87.27±0.39^{c}		3.03±0.06^{efg}		5.42±0.30^{n}		38.61±1.01^{mnop}		17.63±0.39^{no}		0.72±0.10^{jk}	
7.	*Panus lecomtei*		**81.39±0.77^{de}**		**3.47±0.12^{a}**		**7.21±0.29^{c}**		**41.44±1.42^{cd}**		**16.52±0.90^{cd}**		**0.86±0.06^{f}**
	APBN3	81.39±0.77^{hij}		3.47±0.12^{ab}		7.21±0.29^{ghij}		41.44±1.42^{ijk}		16.52±0.90^{p}		0.86±0.06^{j}	
8.	*Pleurotus giganteus*		**82.93±1.10^{d}**		**3.42±0.08^{a}**		**8.49±0.46^{ab}**		**38.62±1.76^{def}**		**16.07±1.31^{cd}**		**3.43±0.83^{b}**
	KM1	83.87±0.56^{f}		3.37±0.06^{ab}		8.88±0.17^{a}		39.52±1.34^{klmn}		17.18±0.39^{nop}		4.07±0.26^{b}	
	KM2	81.98±0.28^{gh}		3.47±0.06^{ab}		8.10±0.20^{bc}		37.72±1.89^{op}		14.96±0.62^{q}		2.80±0.65^{de}	
9.	*Pleurotus ostreatus*		**87.58±0.42^{b}**		**3.27±0.06^{abc}**		**7.13±0.13^{c}**		**39.28±1.04^{cdef}**		**19.28±1.09^{ab}**		**1.79±0.12^{d}**
	MP1	87.58±0.42^{c}		3.27±0.06^{bcd}		7.13±0.13^{hijk}		39.28±1.04^{klmn}		19.28±1.09^{ijk}		1.79±0.12^{gh}	
10.	*Pleurotus pulmonarius*		**86.44±0.84^{b}**		**2.98±0.16^{bc}**		**7.18±0.43^{c}**		**41.48±1.32^{c}**		**18.42±1.13^{b}**		**2.15±0.30^{cd}**
	MLS1	87.06±0.55^{cd}		3.10±0.10^{def}		7.37±0.35^{fghi}		40.58±0.94^{ijklm}		19.29±0.83^{ijk}		1.93±0.06^{g}	
	MP2	85.81±0.53^{e}		2.87±0.12^{hijk}		6.98±0.47^{ijkl}		42.39±1.03^{hij}		17.56±0.51^{no}		2.37±0.27^{f}	
11.	*Polyporus arcularius*		**60.36±1.46^{f}**		**3.17±0.33^{abc}**		**8.04±0.21^{b}**		**46.64±2.84^{b}**		**16.41±1.14^{cd}**		**1.34±0.10^{e}**
	APBN4	58.67±0.89^{q}		2.73±0.06^{ijklm}		8.05±0.19^{bcd}		49.42±0.93^{bcd}		17.37±1.01^{nop}		1.41±0.06^{hi}	
	DH2	61.70±0.63^{o}		3.33±0.06^{abc}		8.13±0.26^{bc}		43.16±0.44^{ghi}		15.23±0.37^{q}		1.34±0.10^{hi}	
	MLS6	60.73±0.40^{p}		3.43±0.06^{ab}		7.95±0.21^{bcde}		47.34±0.75^{def}		16.65±0.72^{op}		1.28±0.12^{i}	

All the sample-wise data are represented as average ± standard deviations (SD) of three independent replications, while species-wise data are represented as average ± SD of all the triplicate data belonging to a single species. The different lowercase letters (a, b, c, d, and so on) after each data in columns indicate the significant difference among the samples/species ($p<0.05$).

(60.36 g/100 g). Moisture contents vary among species to species depending on their types of fruiting bodies. Although, differences in moisture content among the members of the same species may vary depending upon the environmental factors such as relative humidity, temperature, and relative amount of metabolic water [Crisan & Sands, 1978; Singdevsachan *et al*., 2014]. Dry fruiting body powders of the mushrooms also retained the minimal amount of moisture ranging from 2.43 g/100 g to 3.53 g/100 g (Table 2). The highest ash content was determined in *Agaricus bisporus* (9.23 g/100 g d.w.), while the lowest one in *Lycoperdon scabrum* (5.62 g/100 g d.w.) and *A. auricula-judae* (5.68 g/100 g d.w.).

Total crude protein content of the edible dried mushrooms showed variations among different species (Table 2). Species-wise comparisons showed that the crude protein content was the highest in *Lentinus sajor-caju* (20.72 g/100 g d.w.), and *Lentinus squarrosulus* (20.54 g/100 g d.w.). Although, there were no significant differences ($p<0.05$) observed in the crude protein content of these two species with that of *A. auricula-judae* (19.70 g/100 g d.w.), *Pleurotus ostreatus* (19.28 g/100 g d.w.) and *A. bisporus* (18.65 g/100 g d.w.). Our results were comparable to the previous findings on the protein contents of edible mushroom species [Kalač, 2013; Phan *et al*., 2012; Reis *et al*., 2012]. However, different researchers found differences in the protein contents based on the external growing parameters. For instance, the protein content in *Pleurotus pulmonarius* was reported to vary from ~14 g/100 g d.w. to 26 g/100 d.w. depending on different carbon sources supplemented during their cultivation process [Smiderle *et al*., 2012]. Therefore, it can be concluded that protein content in wild mushrooms may vary depending upon the substrates on which they grow.

Among the edible mushroom species, *L. sajor-caju* showed the highest carbohydrate contents (49.80 g/100 g d.w.), which was followed by *P. arcularius* (46.64 g/100 g d.w.), *L. squarrosulus* (46.36 g/100 g d.w.) and *A. auricula-judae* (42.75 g/100 g d.w.) (Table 2). Our results could be compared with the carbohydrate content of edible mushrooms as reported earlier [Johnsy *et al*., 2011; Nwanze *et al*., 2005]. Carbohydrates are the most abundant constituents of mushrooms, which include sugars (monosaccharides, their derivatives and oligosaccharides) as well as both reserved and construction polysaccharides [Kalač, 2013]. Compared to the small amount of reducing sugars present in mushrooms, chitin and starch constitute the major fraction of total carbohydrates [Manzi *et al*., 2001]. Mushrooms contain digestible carbohydratess (such as glucose, glycogen, mannitol, and trehalose) as well as non-digestible carbohydrate (such as β-glucan, chitin and mannans). Both of these carbohydrate forms constitute the total carbohydrates in mushroom fruiting bodies [Ho *et al*., 2020].

Species-wise comparison showed the highest total fat content in *Lentinus velutinus* (7.17 g/100 g d.w.), which was followed by *Pleurotus giganteus* (3.43 g/100 g d.w.) and *L. squarrosulus* (2.69 g/100 g d.w.). The lowest total fat content was determined in the samples of *L. scabrum* (0.57 g/ 100 g d.w.) and *L. sajor-caju* (0.62 g/100 g d.w.) (Table 2). Typically, mushrooms have been reported to have a low fat content compared to the carbohydrate and protein contents. Fruiting bodies of edible mushrooms mostly contain *cis*-linoleic acid as a major fatty acid which varies from 22–65% in abundance of total fat. The other major fatty acids in mushrooms include *cis*-oleic acid, palmitic acid, and stearic acids [Günç Ergönül *et al*., 2013].

The mineral content analysis of the edible dried mushrooms revealed that there were significant differences among the tested samples. Table 3 and Table 4 show the species-wise average contents of macro- and microelements, respectively, of the mushroom samples. Among all the minerals, potassium (K) content was the highest in all the samples. Species-wise comparison showed that potassium content varied among different species and the highest content was in *P. ostreatus* (2074.0 mg/100 g d.w.), along with *A. bisporus*, *P. pulmonarius*, *L. squarrosulus*, *L. sajor-caju*, *A. auricula-judae* and *Panus lecomtei* (Table 3). Previous studies also reported potassium as the predominant macroelement among different mushroom species [Dursun *et al.*, 2006; Gençcelep *et al.*, 2009]. The phosphorus content was the highest in *L. velutinus* (318.8 mg/100 g d.w.), which was followed by that in *P. pulmonarius* (294.3 mg/100 g d.w.) and *P. ostreatus* (285.2 mg/100 g d.w.). The highest calcium (Ca) content was found in *L. sajor-caju* (232.0 mg/100 g of d.w.), which was non-significantly higher ($p\geq0.05$) than in *A. auricula-judae* (222.3 mg/100 g of d.w.), and few other species (Table 3). There were very little differences in the magnesium (Mg) content among different species. The average sodium (Na) content of *A. bisporus* was the highest among the analysed mushroom species (Table 3). On the other hand, the lowest sodium content was found in *P. lecomtei*. Four microelements, namely iron (Fe), zinc (Zn), copper (Cu), and manganese (Mn), were also determined using atomic absorption spectroscopy (Table 4). The findings revealed exceptionally high iron content in *A. auricula-judae* (97.30 mg/100 g d.w.) compared to the samples of other species. Iron contents of *L. squarrosulus*, *L. sajor-caju*, *P. pulmonarius* and *A. bisporus* were also found high. Compared to iron contents, other three elements (Zn, Cu and Mn) were determined at lower levels, which was consistent with findings of other authors [Dursun *et al*., 2006; Gençcelep *et al*., 2009]. As suggested by previous findings, the mineral contents of mushrooms are greatly affected by geographical locations, growing substrates and several other internal and external factors including growth conditions and genetic factors [Gençcelep *et al.*, 2009; Mallikarjuna *et al.*, 2013; Uzun *et al.*, 2017]. It was also reported that bioavailability of some elements in mushrooms, especially copper, is low for human due to limited absorption from the small intestine [Schellmann *et al*., 1980].

Total phenolic content (TPC) in the dry mushrooms

Phenolic compounds are a major class of secondary plant metabolites with an important role in the protection against oxidation processes [Croft, 1999]. Numerous studies have proved that mushrooms also contain many phenolics equivalent to plant phenolics with potent radical scavenging ability [Elmastas *et al*., 2007; Turkoglu *et al*., 2007]. Here, total phenolic contents of the wild edible mushrooms were determined spectrophotometrically using the Folin-Ciocalteu reagent after extraction with methanol. Methanol can be considered

as the most suitable solvent for the extraction of organic compounds including phenolics. Previously, it was reported that extraction of phenolics with methanol resulted in the highest TPC compared to ethanol, acetone and water [Do *et al*., 2020]. In the present study, the total phenolic content ranged from 59.2 to 1051.5 mg GAE/100 g d.w. for the dried mushrooms (Table 5). Species-wise comparisons showed that the highest TPC was found in the samples of *L. sajor-caju* (831.3 mg GAE/100 g of d.w.), which was followed by *P. lecomtei* (780.9 mg GAE/100 g of d.w.) and *P. pulmonarius*. Samples belonging to the species *P. arcularius* had the lowest TPC (109.1 mg GAE/100 g of d.w.) compared to those of other species (Table 5). There are extensive reports concerning the phenolic contents of mushrooms; however, comparison of findings is difficult due to diversity in research materials, environmental conditions, habitats, analytical methods or ways of expressing the findings [Nowacka *et al*., 2014]. Our study demonstrated higher total phenolic contents in wild mushrooms (such as *L. sajor-caju, P. ostreatus,* and *P. pulmonarius*) compared to the cultivated strains of those species described earlier [Jeena *et al*., 2014]; however, total phenolic contents as high as 2.17–36.19 mg/g d.w. have been described earlier for a few edible mushrooms [Boonsong *et al*., 2016].

Antioxidant activity

DPPH radical scavenging activity of the mushroom samples was evaluated and the species-wise results were compared based on the IC_{50} of the methanolic extracts, as well as the tocopherol equivalent antioxidant activity (TEAA). The results suggested that the samples of the species *L. sajor-caju, L. squarrosulus,* and *P. pulmonarius* exhibited higher antioxidant activity indicated by the lower IC_{50} and higher TEAA as compared to other species (Table 5). IC_{50} signifies the ability of the extract to scavenge the DPPH radical in a concentration-dependent manner. Based on the IC_{50}, our results were comparable with those of earlier reports, which suggested that 40–60% inhibition of DPPH radical occurred in the presence of ~500 μg/mL mushroom extracts [Boonsong *et al*., 2016]; although, concentrations as high as 5–20 mg/mL for scavenging 40–60% of DPPH radical were also reported for few edible mushroom extracts [Cheung *et al*., 2003; Jeena *et al*., 2014; Wong & Chye, 2009]. Extraction solvents play a crucial role in the determination of antioxidant activity of biological samples. Previous studies reported a high extraction yield of antioxidants from mushrooms with high antioxidant properties using methanol and ethyl acetate [Akata *et al.*, 2019; Lakshmi *et al.*, 2004]. In our study, there was a positive correlation between total phenolic content and TEAA, with a correlation coefficient of 0.544 ($p<0.01$), suggesting the major role of phenolic compounds in antioxidant activity of mushroom powders. It was earlier reported that the antioxidant properties of button mushrooms varied between 5.49 and 10.48 nmol Trolox equivalent/mg d.w. based on their growing stages, and the antioxidant activity of those samples correlated with the ergosterol content [Shao *et al.*, 2010].

Antihaemolytic activity

Antihaemolytic activity of the extracts was tested in goat RBC cells in the presence of the haemolytic agent H_2O_2. Extracts from the mushroom powders showed inhibition of haemolytic activity, which was found to be increased with increasing concentrations of the extracts (data not shown). Table 4 shows sample-wise and species-wise comparisons of the antihaemolytic activities of the dried fruiting body extracts. The samples belonging to the species *L. sajor-caju*, *P. ostreatus*, *P. pulmonarius* and *A. bisporus* showed the highest antihaemolytic activity compared to the samples of other species. Few extracts of *L. squarrosulus* indicated low IC_{50} values, suggesting to have prominent antihaemolytic activity. The antihaemolytic activity of the mushroom extracts can be correlated to their antioxidative potential, or total plenolic content [Afsar *et al.*, 2016]. Haemolytic agents, like H_2O_2, oxidize the lipids in the plasma membrane of RBC cells, due to which haemoglobins release to the extracellular matrix. Phenolic compounds in the mushroom extracts inhibit the oxidation of lipids by H_2O_2 due to their antioxidant potential. There are plenty of reports demonstrating the antihaemolytic activity of phytoconstituents from different plant species [Alinezhad *et al*., 2013; Besbas *et al*., 2020; Chansiw *et al*., 2018]; however, only few studies have described the antihaemolytic potential of the extracts from the fruiting bodies of mushrooms. In an earlier study [Sharif *et al*., 2017], haemolytic inhibitory activity was evaluated in five different extracts (obtained using methanol, ethanol, ethyl acetate, *n*-hexane and water) of *Ganoderma lucidum* against human erythrocytes. The results suggested that two extracts (water and *n*-hexane) showed the antihaemolytic activity but, the other two extracts (ethyl acetate and ethanol) were detected as toxic. The decrease in toxicity of the five extracts was found to be in the order of ethyl acetate>ethanol>methanol>*n*-hexane>water [Sharif *et al*., 2017].

Content of organic acids, phenolic acids and vitamins (ascorbic acid and riboflavin) in mushrooms

The presence of organic and phenolic acids and other metabolites in the mushroom extracts was determined using the HPLC analysis by comparing the retention times (t_R) and the absorption maxima of the separated peaks with these of reference standards (supplementary Table S1). The chromatograms of selected mushroom extract (DIM1) and 11 commercially available reference substances used for the identification of mushroom powder compounds are shown in Figure 1. Few phenolic acids, including 3,4-dihydroxybenzoic acid (t_R: 10.2 min), gallic acid (t_R: 8.5 min), and *trans*-cinnamic acid (t_R: 15.4 min), were identified in most of the tested samples (Table 6). Other non-phenolic acids, including ascorbic acids (t_R: 3.8 min) and lactic acid (t_R: 4.8 min), were also detected abundantly in most of the samples. Few other organic and phenolic acids, like citric acid (t_R: 6.0 min), caffeic acid (t_R: 9.7 min), vanillic acid (t_R: 10.6 min), pyruvic acid (t_R: 14.4 min), and *p*-coumaric acid (t_R: 14.6 min), showed species-specific variation in their presence and contents (Table 6). Riboflavin was detected with moderate to low content (9–65 mg/100 g d.w.) in few species only. The presence of compounds with antioxidant activities has supported the earlier findings of this study. Previous studies also reported some major non-phenolic and phenolic acids, such as ascorbic acids, citric acid, caffeic acid, vanillic acid, gallic acid, and *trans*-cinnamic acid, in edible mushroom

TABLE 3. Macroelement contents (mg/100 g dry weight) of the dried mushroom fruiting bodies.

No.	Species name & sample code	Ca		K		Mg		Na		P	
		Average of samples	Average of species	Average of samples	Average of species	Average of samples	Average of species	Average of samples	Average of species	Average of samples	Average of species
1.	*Agaricus bisporus*		**158.6±10.2**^{ab}		**1882.8±23.8**^{a}		**35.86±0.2**^{a}		**99.3±1.0**^{a}		**247.4±5.3**^{c}
	MLS2	158.6±10.2^{g}		1882.8±23.8^{e}		35.9±0.2^{bcd}		99.3±1.0^{a}		247.4±5.3^{e}	
2.	*Auricularia auricula-judae*		**222.3±9.2**^{a}		**1625.2±17.5**^{a}		**36.43±0.1**^{a}		**97.6±0.1**^{b}		**199.9±7.5**^{d}
	DIM1	222.3±9.2^{cd}		1625.2±17.5^{i}		36.4±0.1^{a}		97.6±0.1^{b}		199.9±7.5^{k}	
3.	*Lentinus sajor-caju*		**232.0±142.1**^{ab}		**1702.1±269.4**^{a}		**34.82±0.7**^{b}		**47.9±8.0**^{de}		**201.3±17.7**^{d}
	APK5	155.8±4.0^{fg}		1853.2±19.7^{e}		35.5±0.0^{e}		49.8±1.3^{l}		177.1±6.6^{n}	
	DH3	83.2±0.9^{jkl}		2008.8±11.7^{d}		34.4±0.1^{ijk}		45.7±0.3^{mn}		211.6±5.8^{ij}	
	DIM3	61.7±0.8^{lm}		2003.4±49.0^{d}		33.9±0.2^{l}		49.3±0.4^{l}		228.9±6.4^{fg}	
	MIS2	348.7±1.9^{b}		1508.8±8.6^{j}		34.4±0.0^{ijk}		62.8±0.3^{hi}		188.5±5.6^{lm}	
	MIS7	421.4±0.3^{a}		1461.1±28.1^{k}		34.9±0.1^{fgh}		39.1±0.2^{q}		197.8±6.42^{kl}	
	MP3	321.0±0.3^{b}		1377.5±17.3^{l}		35.8±0.1^{cde}		40.6±0.5^{pq}		203.9±3.2^{jk}	
4.	*Lentinus squarrosulus*		**135.9±93.5**^{a}		**1795.9±262.8**^{a}		**35.8±0.6**^{a}		**68.4±24.1**^{c}		**227.4±31.2**^{c}
	AAU1	157.3±1.7^{fg}		1731.8±21.4^{fgh}		36.7±0.1^{a}		87.6±0.6^{d}		230.2±6.1^{fg}	
	AAU2	60.3±3.7 ^{lm}		2371.8±12.4^{a}		35.8±0.1^{cde}		73.4±1.8^{e}		198.2±3.45^{kl}	
	AAU3	47.7±1.1^{mn}		2188.7±23.3^{b}		35.5±0.1^{e}		52.2±1.1^{k}		235.3±6.7^{fg}	
	AAU4	114.8±1.3^{hij}		1745.7±38.2^{fg}		35.8±0.1^{cde}		93.9±0.18^{c}		287.7±6.1^{c}	
	AAU5	118.8±7.1^{hi}		1703.7±27.1^{gh}		35.7±0.0^{cde}		56.6±2.2^{j}		265.3±2.4^{d}	
	AAU6	240.3±8.4^{c}		1517.7±8.6^{j}		35.8±0.3^{bcde}		71.7±0.7^{f}		235.6±7.5^{f}	
	AAU7	58.8±2.2^{lm}		1758.2±12.3^{f}		36.0±0.1^{bc}		99.4±1.4^{a}		207.9±4.4^{ijk}	
	DH1	119.3±0.9^{hi}		1599.1±29.2^{i}		35.0±0.1^{fg}		39.7±0.4^{q}		182.7±4.0^{mn}	
	DIM2	94.9±2.8^{ijk}		1756.0±20.8^{f}		34.7±0.1^{hij}		23.1±0.2^{s}		199.2±3.0^{k}	
	KB2	346.8±98.7^{b}		1586.3±24.7^{i}		36.6±0.1^{a}		86.2±1.2^{d}		232.0±4.3^{fg}	
5.	*Lentinus velutinus*		**42.7±1.7**^{c}		**1337.3±17.3**^{b}		**35.6±0.1**^{ab}		**95.9±0.6**^{c}		**318.8±7.6**^{a}
	KM5	42.7±1.7^{mn}		1337.3±17.3^{l}		35.6±0.1^{de}		95.9±0.6^{b}		318.8±7.6^{a}	

TABLE 3. Continued

No.	Species name & sample code	Ca		K		Mg		Na		P	
		Average of samples	Average of species	Average of samples	Average of species	Average of samples	Average of species	Average of samples	Average of species	Average of samples	Average of species
6.	*Lycoperdon scabrum*		**103.5±29.6**^{b}		**1003.0±110.4**^{c}		**34.5±0.5**^{bc}		**47.3±10.8**^{ef}		**232.5±16.4**^{c}
	BP9	135.7±0.18^{gh}		862.6±22.4^{pq}		33.9±0.1^{l}		35.5±0.6^{r}		256.5±6.3^{de}	
	DIM8	116.0±0.1^{hij}		1154.6±43.8^{m}		34.5±0.1^{ijk}		42.6±0.4^{o}		224.6±1.7^{gh}	
	KM7	58.6±0.1^{lm}		990.0±16.1^{n}		35.0±0.1^{fg}		63.6±0.0^{h}		215.9±6.7^{hi}	
	RB6	103.7±2.4^{hij}		1004.9±8.6^{n}		34.5±0.7^{ij}		47.3±0.6^{m}		232.9±3.9^{fg}	
7.	*Panus lecomtei*		**156.1±4.3**^{ab}		**1538.8±17.1**^{a}		**34.2±0.0**^{c}		**35.3±0.2**^{f}		**197.8±5.0**^{d}
	APBN3	156.1±4.3^{fg}		1538.2±17.1^{j}		34.2±0.0^{k}		35.3±0.2^{r}		197.8±5.0^{kl}	
8.	*Pleurotus giganteus*		**22.6±2.3**^{d}		**968.3±51.7**^{c}		**33.3±2.0**^{bc}		**57.2±4.8**^{cde}		**242.2±13.9**^{c}
	KM1	20.7±0.6^{n}		1014.7±11.2^{n}		31.6±0.1^{m}		52.9±0.9^{k}		254.2±4.0^{e}	
	KM2	24.4±1.8^{n}		921.9±10.0^{o}		35.1±0.1^{f}		61.5±0.3^{i}		230.1±5.8^{fg}	
9.	*Pleurotus ostreatus*		**187.2±0.2**^{a}		**2074.0±72.6**^{a}		**34.6±0.0**^{bc}		**58.2±0.4**^{cde}		**285.2±9.2**^{b}
	MP1	187.215±0.2^{ef}		2074.0±72.6^{c}		34.6±0.0^{hij}		58.2±0.4^{j}		285.2±9.2^{c}	
10.	*Pleurotus pulmonarius*		**116.6±54.1**^{ab}		**1774.5±97.7**^{a}		**35.3±0.9**^{abc}		**64.8±24.7**^{cde}		**294.3±12.5**^{b}
	MLS1	67.3±3.1^{klm}		1688.9±23.3^{h}		36.1±0.1^{b}		87.4±0.7^{d}		284.6±9.9^{c}	
	MP2	165.9±0.8^{fg}		1860.2±35.9^{e}		34.6±0.0^{ij}		42.2±0.9^{op}		304.0±3.6^{b}	
11.	*Polyporus arcularius*		**207.6±98.0**^{ab}		**820.2±56.9**^{d}		**34.6±0.2**^{bc}		**66.1±18.6**^{cd}		**227.2±18.9**^{c}
	APBN4	94.5±2.7^{ijk}		882.3±13.5^{op}		34.5±0.0^{ijk}		87.3±1.1^{d}		205.6±4.2^{jk}	
	DH2	320.3±7.4^{b}		755.7±26.6^{r}		34.66±0.06^{hij}		44.7±0.2^{n}		248.2±6.7^{c}	
	MLS6	207.9±9.5^{de}		822.6±2.4^{q}		34.73±0.42^{ghi}		66.4±3.6^{g}		227.8±1.9^{fg}	

All the sample-wise data are represented as average ± standard deviations (SD) of three independent replications, while species-wise data are represented as average ± SD of all the triplicate data belonging to a single species. The different lowercase letters (a, b, c, d, and so on) after each data in columns indicate the significant difference among the samples/species ($p<0.05$).

TABLE 4. Microelement contents (mg/100 g dry weight) of the dried mushroom fruiting bodies.

No.	Species name & sample code	Cu		Fe		Mn		Zn	
		Average of samples	Average of species	Average of samples	Average of species	Average of samples	Average of species	Average of samples	Average of species
1.	*Agaricus bisporus*		**3.46±0.03**^{a}		**24.73±1.15**^{bc}		**3.48±0.02**^{b}		**8.34±0.19**^{a}
	MLS2	3.46±0.03^{a}		24.73±1.15^{kl}		3.48±0.02^{fg}		8.34±0.19^{c}	
2.	*Auricularia auricula-judae*		**1.98±0.03**^{b}		**97.30±4.52**^{a}		**15.15±0.61**^{a}		**7.15±0.39**^{ab}
	DIM1	1.98±0.03^{d}		97.30±4.52^{a}		15.15±0.61^{a}		7.15±0.39^{e}	
3.	*Lentinus sajor-caju*		**1.12±0.56**^{c}		**19.01±7.52**^{c}		**2.54±0.64**^{c}		**4.60±0.51**^{bc}
	APK5	1.57±0.01^{h}		32.36±0.85^{gh}		3.50±0.16^{fg}		5.45±0.07^{fg}	
	DH3	0.32±0.01^{q}		7.67±0.16^{rs}		2.54±0.18^{l}		4.28±0.07^{klm}	
	DIM3	0.53±0.00^{o}		15.55±0.50^{o}		2.79±0.04^{jk}		4.95±0.07^{hi}	
	MIS2	1.69±0.02^{g}		19.49±0.14^{n}		1.58±0.04^{o}		4.01±0.05^{mnop}	
	MIS7	1.00±0.04^{k}		19.85±0.53^{n}		2.81±0.02^{jk}		4.45±0.33^{k}	
	MP3	1.60±0.04^{h}		19.17±0.04^{n}		1.99±0.01^{n}		4.49±0.24^{jk}	
4.	*Lentinus squarrosulus*		**1.33±0.51**^{c}		**35.64±16.98**^{b}		**3.75±0.94**^{b}		**5.47±1.94**^{abc}
	AAU1	1.62±0.03^{h}		57.75±1.55^{c}		4.70±0.04^{c}		8.76±0.17^{b}	
	AAU2	1.09±0.01^{j}		40.77±1.31^{f}		2.58±0.05^{l}		4.99±0.07^{h}	
	AAU3	0.70±0.01^{n}		9.18±0.28^{qr}		5.00±0.04^{b}		3.67±0.12^{q}	
	AAU4	1.33±0.02^{i}		19.87±0.92^{n}		4.51±0.06^{cd}		4.34±0.11^{kl}	
	AAU5	0.72±0.02^{n}		22.74±1.05^{m}		4.40±0.08^{d}		3.96±0.28^{nop}	
	AAU6	1.87±0.04^{f}		49.77±0.18^{d}		2.22±0.01^{m}		5.52±0.17^{fg}	
	AAU7	1.93±0.05^{e}		26.58±0.85^{ij}		2.99±0.04^{ij}		5.54±0.13^{fg}	
	DH1	0.58±0.00^{o}		46.76±0.57^{e}		3.22±0.09^{hi}		4.35±0.11^{kl}	
	DIM2	1.58±0.01^{h}		23.13±0.20^{lm}		4.43±0.03^{d}		4.14±0.09^{lmno}	
	KB2	1. 87±0.04^{f}		59.88±1.34^{b}		3.41±0.05^{gh}		9.38±0.08^{a}	
5.	*Lentinus velutinus*		**0.74±0.02**^{cd}		**7.05±0.40**^{e}		**4.08±0.20**^{b}		**2.31±0.02**^{d}
	KM5	0.74±0.02^{mn}		7.05±0.40^{s}		4.08±0.20^{e}		2.31±0.02^{r}	
6.	*Lycoperdon scabrum*		**0.88±0.07**^{c}		**11.26±0.66**^{d}		**0.72±0.04**^{d}		**4.35±0.38**^{c}
	BP9	0.97±0.02^{k}		10.97±0.40^{p}		0.76±0.02^{qr}		4.22±0.09^{klmn}	
	DIM8	0.88±0.02^{l}		12.13±0.59^{p}		0.75±0.01^{qr}		3.90±0.08^{opq}	
	KM7	0.78±0.03^{m}		10.65±0.12^{pq}		0.67±0.03^{rs}		4.91±0.09^{hi}	
	RB6	0.88±0.02^{l}		11.28±0.07^{p}		0.72±0.01^{qr}		4.35±0.01^{kl}	
7.	*Panus lecomtei*		**0.25±0.02**^{d}		**7.12±0.30**^{e}		**0.75±0.02**^{d}		**5.35±0.06**^{abc}
	APBN3	0.25±0.02^{r}		7.12±0.30^{s}		0.75±0.02^{qr}		5.35±0.06^{g}	
8.	*Pleurotus giganteus*		**0.86±0.48**^{cd}		**5.95±2.84**^{e}		**0.92±0.70**^{d}		**2.54±1.64**^{d}
	KM1	0.42±0.02^{p}		3.37±0.21^{t}		0.29±0.06^{t}		1.04±0.06^{s}	
	KM2	1.30±0.03^{i}		8.53±0.39^{rs}		1.55±0.06^{op}		4.03±0.12^{mnop}	
9.	*Pleurotus ostreatus*		**0.78±0.03**^{cd}		**33.12±0.09**^{b}		**0.47±0.04**^{d}		**3.82±0.03**^{d}
	MP1	0.78±0.03^{m}		33.12±0.09^{g}		0.47±0.04st		3.82±0.03^{pq}	
10.	*Pleurotus pulmonarius*		**1.43±0.64**^{bc}		**30.82±0.66**^{b}		**3.31±0.48**^{b}		**6.25±1.67**^{abc}
	MLS1	2.02±0.02^{d}		30.65±0.96^{h}		3.69±0.38^{f}		7.77±0.12^{d}	
	MP2	0.85±0.01^{l}		30.99±0.27^{h}		2.94±0.04^{j}		4.72±0.01^{ij}	
11.	*Polyporus arcularius*		**2.10±0.45**^{b}		**25.68±2.31**^{b}		**0.96±0.32**^{d}		**5.65±1.32**^{abc}
	APBN4	1.58±0.01^{h}		23.03±0.22^{lm}		1.33±0.03^{p}		4.13±0.09^{lmno}	
	DH2	2.61±0.02^{b}		28.25±0.16^{i}		0.59±0.03^{rs}		7.15±0.07^{e}	
	MLS6	2.10±0.11^{c}		25.74±0.87^{jk}		0.97±0.06^{q}		5.66±0.28^{f}	

All the sample-wise data are represented as average ± standard deviations (SD) of three independent replications, while species-wise data are represented as average ± SD of all the triplicate data belonging to a single species. The different lowercase letters (a, b, c, d, and so on) after each data in columns indicate the significant difference among the samples/species ($p<0.05$).

TABLE 5. Total phenolic content, DPPH radical scavenging activity and antihaemolytic activity of the mushroom samples.

No.	Species name & sample code	Total phenolic content (mg GAE/100 g dry weight)		DPPH radical scavenging activity				Antihaemolytic activity; IC_{50} (μg/mL of extract)	
				IC50 (μg/mL of extract)		TEAA (mg/100 g dry weight)			
		Average of samples	Average of species	Average of samples	Average of species	Average of samples	Average of species	Average of samples	Average of species
1.	*Agaricus bisporus*		**299.2±21.0**^{c}		**979.3±51.9**^{a}		**120.2±6.5**^{de}		**462.9±2.6**^{cd}
	MLS2	299.2±21.0^{pq}		979.3±51.9^{a}		120.2±6.5^{op}		462.9±2.6^{j}	
2.	*Auricularia auricula-judae*		**172.5±3.6**^{d}		**828.7±39.8**^{b}		**93.9±4.6**^{e}		Not determined
	DIM1	172.5±3.6^{rs}		828.7±39.8^{c}		93.9±4.6^{q}		Not determined	
3.	*Lentinus sajor-caju*		**831.3±156.9**^{a}		**330.6±52.4**^{f}		**345.9±38.0**^{a}		**340.9±58.5**^{d}
	APK5	622.5±60.7^{gh}		277.5±3.3^{m}		396.1±4.7^{a}		283.8±36.1^{lmn}	
	DH3	677.1±45.8^{fg}		322.0±7.6^{ijkl}		341.4±8.1^{c}		299.3±20.9^{m}	
	DIM3	923.7±67.7^{b}		434.8±8.6^{h}		296.4±5.9^{gh}		316.8±24.1^{lm}	
	MIS2	836.1±26.4^{cd}		292.0±11.7^{lm}		389.7±15.8^{a}		342.2±22.6^{l}	
	MIS7	876.6±82.4^{bc}		333.8±10.9^{ijk}		318.0±10.4^{e}		438.9±28.1^{jk}	
	MP3	1051.5±41.4^{a}		323.7±3.1^{ijk}		333.6±3.2^{cd}		364.1±43.3^{kl}	
4.	*Lentinus squarrosulus*		**418.6±158.6**^{c}		**361.8±73.9**^{def}		**328.5±46.7**^{a}		**481.1±142.3**^{c}
	AAU1	254.8±7.3^{qr}		249.6±4.5^{n}		394.9±7.1^{a}		325.0±59.0 ^{klm}	
	AAU2	175.4±49.8^{rs}		339.0±15.3^{ij}		324.6±15.0^{de}		409.4±5.5^{k}	
	AAU3	247.7±30.3^{qr}		352.7±6.6^{i}		317.1±5.9^{e}		281.8±1.2^{n}	
	AAU4	561.6±45.6^{hi}		466.4±35.2^{g}		269.1±20.2^{jk}		671.2±1.9^{cd}	
	AAU5	297.4±6.3^{pq}		431.5±14.0^{h}		294.4±9.4^{gh}		663.2±5.00^{cd}	
	AAU6	398.7±30.9^{lmno}		317.8±15.2^{jkl}		394.0±19.0^{a}		589.15±4.9^{e}	
	AAU7	520.8±17.5^{ijk}		328.8±9.4^{ijk}		357.4±10.3^{b}		557.7±3.9^{g}	
	DH1	568.0±14.5^{hi}		339.7±8.7^{ij}		312.5±7.9^{ef}		457.3±7.2^{j}	
	DIM2	612.5±15.0^{gh}		486.7±8.7^{g}		260.9±4.6^{k}		552.8±2.4^{g}	
	KB2	549.4±15.8^{hij}		305.5±4.8^{klm}		359.7±5.6^{b}		303.9±1.2^{m}	
5.	*Lentinus velutinus*		**248.0±31.6**^{c}		**833.1±12.9**^{b}		**120.5±1.9**^{de}		**579.3±1.3**^{bc}
	KM5	248.0±31.6^{qr}		833.1±12.9^{c}		120.5±1.9^{op}		579.3±1.3^{f}	
6.	*Lentinus scabrum*		**396.6±57.5**^{c}		**711.4±32.3**^{c}		**141.5±14.9**^{c}		**630.7±64.9**^{b}
	BP9	382.5±12.3^{mnop}		731.4±17.0^{d}		139.3±3.2^{n}		727.2±17.3^{c}	
	DIM8	321.1±2.9^{opq}		677.8±8.3^{e}		164.9±2.0^{m}		639.7±15.0^{d}	
	KM7	411.2±13.9^{lmn}		688.7±14.2^{e}		129.3±2.7^{nop}		579.3±1.3^{f}	
	RB6	471.4±16.2^{jkl}		747.7±10.7^{d}		131.8±1. 9no		576.7±13.7^{f}	
7.	*Panus lecomtei*		**780.9±14.6**^{ab}		**417.6±6.0**^{def}		**276.8±4.0**^{b}		**550.9±2.2**^{c}
	APBN3	780.9±14.6^{de}		417.6±6.0^{h}		276.8±4.0^{ij}		550.9±2.2^{g}	
8.	*Pleurotus giganteus*		**330.6±18.7**^{c}		**444.1±109.2**^{de}		**266.3±39.9**^{b}		**1037.5±114.1**^{a}
	KM1	330.2±18.8^{nopq}		344.6±6.0^{ij}		302.5±5.24^{fg}		937.7±10.3^{b}	
	KM2	331.0±22.8^{nopq}		543.6±7.0^{f}		230.1±3.0^{l}		1137.2±50.8^{a}	
9.	*Pleurotus ostreatus*		**461.3±38.0**^{bc}		**426.9±13.5**^{d}		**284.3±9.2**^{ab}		**350.4±7.6**^{cd}
	MP1	461.3±38.0^{klm}		426.9±13.5^{h}		284.3±9.2^{hi}		350.4±7.6^{l}	
10.	*Pleurotus pulmonarius*		**662.1±139.6**^{ab}		**332.4±10.0**^{ef}		**342.4±21.3**^{a}		**357.5±154.6**^{cd}
	MLS1	608.9±199.4^{gh}		339.0±6.2^{ij}		324.2±5.9^{de}		498.4±1.6^{h}	
	MP2	715.3±22.6^{ef}		325.8±9.0^{ijk}		360.7±10.01		216.6±13.8^{o}	
11.	*Polyporus arcularius*		**109.1±46.9**^{e}		**914.6±17.7**^{a}		**124.4±7.3**^{d}		**487.7±7.3**^{c}
	APBN4	156.7±5.9^{s}		921.8±13.6^{b}		115.1±1.7^{p}		485.9±1.5^{i}	
	DH2	59.2±27.7^{t}		917.6±18.6^{b}		130.1±2.6^{nop}		496.9±0.8^{h}	
	MLS6	111.4±29.4st		904.5±21.8^{b}		127.8±3.1^{nop}		480.4±1.5^{i}	
12.	Reference standard (Tocopherol)			18.9±2.3^{o}				286.5±2.1^{n}	

All the sample-wise data are represented as average ± standard deviations (SD) of three independent replications, while species-wise data are represented as average ± SD of all the triplicate data belonging to a single species. The different lowercase letters (a, b, c, d, and so on) after each data in columns indicate the significant difference among the samples/species ($p<0.05$). GAE: gallic acid equivalents; TEAA: tocopherol equivalent antioxidant activity.

TABLE 6. Contents of the organic acids, phenolic acids riboflavin and ascorbic acid in dried mushroom fruiting bodies (mg/100 g d.w.) determined using HPLC.

Sample ID	Ascorbic acid (t_R=3.8 min)	Lactic acid (t_R=4.8 min)	Citric acid (t_R=6.0 min)	Gallic acid (t_R=8.5 min)	Caffeic acid (t_R=9.7 min)	3,4-Dihydroxybenzoic acid (t_R=10.2 min)	Riboflavin (t_R=10.6 min)	Vanillic acid (t_R=10.8 min)	Pyruvic acid (t_R=14.4 min)	*p*-Coumaric acid (t_R=14.6 min)	*trans*-Cinnamic acid (t_R=15.4 min)
MLS2	114.2±5.6^{g}	109.5±9.2^{i}	116.5±14.2^{d}	13.6±0.3^{g}	ND	19.6±1.9^{m}	9.2±2.7^{e}	26.7±2.6^{a}	2.4±1.0^{g}	ND	30.4±1.3^{e}
DIM1	63.5±4.2^{ij}	52.4±5.0^{k}	ND	2.3±0.0^{k}	2.7±0.9^{g}	36.6±0.3^{k}	42.7±3.1^{b}	13.2±3.7^{bc}	2.3±0.7^{g}	1.1±0.3^{e}	14.5±4.1^{hij}
APK5	31.2±0.8^{l}	140.5±2.9^{gh}	73.7±7.4^{e}	2.6±0.7^{k}	8.0±0.3^{d}	14.5±0.7^{n}	ND	4.2±4.2^{def}	ND	1.4±0.0^{e}	9.2±1.0^{j}
DIM3	79.2±1.3^{hi}	120.9±11.2^{h}	18.6±2.0^{h}	104.3±7.6^{cd}	ND	61.1±1.3^{i}	65.1±7.6^{a}	4.9±2.3^{ef}	21.7±1.0^{e}	2.1±0.1^{d}	13.4±1.5^{hi}
DH3	55.2±2.1^{j}	192.7±8.9^{f}	ND	6.9±0.7^{i}	ND	9.3±0.1^{o}	ND	ND	2.3±0.3^{g}	ND	11.3±1.3^{ij}
MIS2	18.3±2.7^{mn}	74.4±7.2^{j}	ND	10.4±1.5^{h}	4.4±0.0^{f}	17.1±0.9^{m}	ND	ND	ND	ND	14.5±2.1^{hi}
MIS7	86.5±6.7^{h}	150.3±12.1^{g}	25.1±3.9^{f}	ND	6.0±0.7^{e}	11.0±1.2^{no}	ND	ND	ND	ND	12.3±0.7^{i}
MP3	77.3±4.3^{hi}	89.9±9.8^{ij}	ND	7.0±0.9^{i}	ND	21.4±2.1^{lm}	11.5±1.3^{e}	ND	10.8±1.0^{f}	ND	39.0±1.6^{c}
AAU1	36.8±2.1^{k}	68.7±10.1^{j}	3.7±1.9^{j}	2.3±0.3^{k}	ND	30.4±2.7^{kl}	ND	ND	ND	ND	12.3±0.7^{i}
AAU2	170.6±2.3^{e}	150.9±2.1^{g}	ND	2.3±0.3^{k}	ND	25.2±2.9^{l}	ND	ND	ND	ND	10.2±0.3
AAU3	398.1±31.2^{a}	643.2±4.7^{a}	ND	99.91^{d}	ND	282.3±2.3^{c}	ND	ND	ND	ND	19.8±1.2^{g}
AAU4	85.4±8.4hi^{hi}	145.1±12.5^{g}	3.00±0.7^{j}	17.6±3.1^{fg}	ND	51.4±2.6^{j}	ND	ND	ND	ND	11.5±2.1^{i}
AAU5	125.2±3.8^{f}	148.6±23.8^{fg}	ND	18.5±2.6^{fg}	ND	36.6±6.3^{k}	ND	ND	1.5±0.7^{gh}	ND	11.7±0.3^{i}
AAU6	347.9±3.9^{b}	469.8±28.5^{e}	ND	14.5±0.5^{g}	ND	73.6±4.6^{h}	ND	ND	ND	ND	12.1±0.7^{i}
AAU7	6.9±4.1^{op}	62.04±8.7^{jk}	8.6±1.3^{i}	4.7±2.3^{jk}	ND	17.7±0.6^{m}	ND	ND	ND	ND	11.8±0.3
DH1	19.8±0.9^{m}	32.8±8.2^{l}	20.18±1.8^{gh}	5.2±0.5^{j}	ND	20.1±0.3^{lm}	ND	ND	ND	ND	35.8±1.8^{cd}
DIM2	167.6±10.5^{e}	174.8±7.3^{f}	45.6±7.2^{f}	9.6±0.7^{h}	ND	61.1±4.5^{i}	29.1±1.7^{c}	9.4±0.7^{d}	2.0±0.3^{gh}	ND	15.1±0.7^{h}
KB2	9.12±3.7^{o}	95.3±11.8^{i}	ND	9.8±0.5^{h}	ND	34.0±1.7^{k}	ND	ND	ND	ND	14.3±0.3^{h}
KM5	17.42±2.8^{mn}	38.5±13.8^{l}	ND	13.6±0.3^{g}	2.8±0.3^{g}	1.5±0.8^{p}	12.5±2.3^{de}	ND	ND	ND	14.5±1.3^{h}
BP9	165.81±3.7^{e}	269.4±14.6^{e}	141.0±3.1^{c}	66.7±1.3^{e}	25.6±2.7^{c}	351.5±10.3^{a}	ND	7.9±1.6^{d}	31.6±3.5^{d}	1.4±0.0^{e}	41.1±2.3^{c}
DIM8	36.77±4.3^{k}	123.9±12.1	18.7±3.3^{h}	15.4±1.0^{g}	25.6±0.3^{c}	140.6±6.1^{f}	ND	3.8±0.7^{f}	80.8±2.7^{a}	50.8±2.1^{b}	77.3±1.4^{a}
KM7	55.2±2.1^{j}	155.2±8.2^{fg}	18.7±4.1^{h}	18.0±5.7^{fg}	25.9±1.6^{c}	164.8±5.9^{e}	ND	3.8±1.0^{f}	80.8±4.6^{a}	53.8±4.6^{b}	66.7±3.2^{b}
RB6	92.1±4.7^{h}	202.2±11.4^{f}	141.0±12.1^{c}	24.2±3.0^{f}	25.6±0.7^{c}	199.4±13.6^{d}	ND	3.8±1.3^{f}	36.51±2.0^{c}	39.2±0.7^{c}	20.7±1.7^{g}
APBN3	81.0±10.5^{hi}	184.6±16.1^{f}	165.5±10.0^{b}	26.9±0.8^{f}	25.6±0.0^{c}	178.6±4.8^{d}	ND	3.8±1.3^{f}	41.43±2.7^{c}	45.1±3.9^{b}	30.4±1.3^{e}
KM1	20.18±4.1^{m}	166.6±14.2^{fg}	ND	64.5±0.6^{e}	12.5±2.8^{d}	49.0±1.9^{j}	16.3±0.7^{d}	1.9±0.3^{g}	1.0±0.3^{hi}	ND	14.5±1.6^{h}
KM2	283.78±21.3^{c}	178.1±7.8^{f}	ND	164.1±2.7^{b}	38.7±1.3^{b}	175.2±3.5^{d}	38.9±4.5^{b}	12.1±0.0^{c}	2.0±0.3^{g}	ND	15.6±1.7^{h}
MP1	352.0±5.8^{b}	463.6±12.4^{c}	190.0±8.6^{a}	197.3±3.5^{a}	48.5±1.3^{a}	322.1±4.9^{b}	ND	16.3±1.4^{b}	64.83^{b}	71.2±3.1^{a}	68.8±2.1^{b}
MLS1	407.3±9.2^{a}	537.1±21.6^{b}	ND	119.8±10.7^{c}	ND	88.7±2.1^{h}	71.5±3.1^{a}	16.3±0.7^{b}	3.3±1.0^{g}	ND	26.1±0.3^{f}
MP2	213.7±8.5^{d}	351.0±18.4^{d}	92.1±4.8^{e}	146.3±13.6^{bc}	ND	109.5±2.8^{g}	ND	7.9±1.3^{d}	2.0±0.2^{g}	ND	32.6±3.2^{de}
APBN4	13.73±3.1^{no}	39.6±5.6^{l}	ND	2.4±0.5^{k}	ND	11.8±1.4^{no}	ND	ND	1.8±0.0^{h}	1.4±0.6^{e}	35.8±3.8^{cd}
DH2	52.44±5.7^{j}	59.76±5.7^{jk}	86.0±7.1^{e}	11.4±2.5^{gh}	2.8±0.3^{g}	67.1±6.9^{i}	70.3±2.3^{a}	ND	1.3±0.4^{h}	1.1±0.3^{e}	32.6±1.3^{de}
MLS6	11.75±3.4^{o}	91.58±2.1^{i}	3.0±0.7^{j}	2.6±3.8^{k}	2.6±0.0^{g}	9.3±2.3^{no}	11.3±1.9^{e}	ND	1.3±0.3^{h}	1.1±0.0^{e}	12.3±0.7^{ij}

All the sample-wise data are represented as average ± standard deviations (SD) of three independent replications. The different lowercase letters (a, b, c, d, and so on) after each data in columns indicate the significant difference among the samples/species (p<0.05). ND: not detected; t_R: retention time.

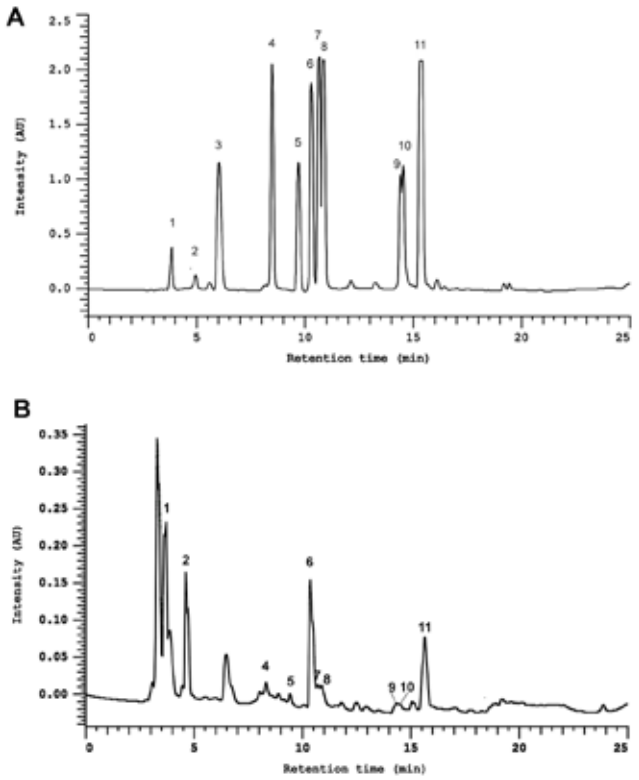

FIGURE 1. High performance liquid chromatography (HPLC) separation of the reference standards (A) and mushroom extract of DIM1 sample (B). Peaks for different compounds are designated with numbers: 1. ascorbic acid, 2. lactic acid, 3. citric acid, 4. gallic acid, 5. caffeic acid, 6. 3,4-dihydroxybenzoic acid, 7. riboflavin, 8. vanillic acid, 9. pyruvic acid, 10. *p*-coumaric acid, and 11. *trans*-cinnamic acid.

samples [Gąsecka *et al*., 2018; Valentão *et al*., 2005; Yahia *et al*., 2017]. It is noteworthy that apart from the selected peaks, there were other peaks in the HPLC chromatograms which were not identified using standards. Therefore, we do not deny the presence of other compounds in the mushroom extracts as they were not targeted for evaluation in this study. It was previously reported that the organic acid profile varied among different wild growing species of *Agaricus*, where lactic acid and succinic acid were found most abundantly in the tested mushrooms [Gąsecka *et al*., 2018]. In the present study, similar findings were recorded with heterogeneous distribution of organic acids among different mushroom species with intra-specific variations in the relative abundance of few organic acids. The presence of important phenolic acids in the fruiting bodies of edible mushrooms make them functional foods as they can protect human body from different diseases due to their strong antioxidant properties [Ribeiro *et al*., 2015; Valentão *et al*., 2005].

CONCLUSIONS

Based on the findings of our study, the dried edible mushrooms, especially *L. sajor-caju* and *L. squarrosulus* had a high nutritive value and a potent antioxidant activity. The samples of other mushroom species including, *P. ostreatus*, *P. pulmonarius*, *A. bisporus* and *A. auricle-judae*, also featured considerable nutritional and antioxidant properties. The high nutritional value of these wild edible mushrooms may enlighten their scope for domestication and cultivation, thereby contributing towards the complementation of food security and nutritional demands among the indigenous communities of Northeast India, especially, the people preferring the vegetarian diet. Moreover, mushroom extracts could be an emerging source of natural antioxidants, like phenolic acids (3,4-dihydroxybenzoic and *trans*-cinnamic acids) and ascorbic acid. Our study has demonstrated the antihaemolytic activity of several wild edible mushrooms from Northeast India, which contained several important organic acids and mentioned antioxidant metabolites. Consumption of such wild edible mushrooms with radical scavenging activity and antihaemolytic potential might be beneficial to combat oxidative damages in the human body.

ACKNOWLEDGEMENTS

The authors are grateful to the Department of Agricultural Biotechnology, Assam Agricultural University, Jorhat, Assam for providing laboratory space and facilities for conducting the present work. The authors are also thankful to DBT – North East Centre for Agricultural Biotechnology, Assam Agricultural University, Jorhat, Assam for providing necessary facilities and publication support.

RESEARCH FUNDING

This work was funded by the Science and Engineering Research Board (SERB), Department of Science and Technology, New Delhi, India, vide project sanction no. EEQ/2016/000631 without any influence over experimental design, findings and data interpretation. Article Processing Fee was received from DBT-North East Centre for Agricultural Biotechnology, Assam Agricultural University, Jorhat, Assam.

CONFLICT OF INTEREST

The authors declare that they have no conflict of interest.

ORCID IDs

M. Barooah https://orcid.org/0000-0002-3768-5336
R.C. Boro https://orcid.org/0000-0002-0866-3357
S. Dullah https://orcid.org/0000-0002-6433-2149
A. Ghosh https://orcid.org/0000-0001-8576-105X
D.J. Hazarika https://orcid.org/0000-0001-6370-4230
M. Kakoti https://orcid.org/0000-0002-5021-7692
A. Parveen https://orcid.org/0000-0002-9745-4118
D. Saha https://orcid.org/0000-0001-7258-9801

SUPPLEMENTARY MATERIALS

The following are available online at http://journal.pan.olsztyn.pl/Nutritional-Properties-Antioxidant-and-Antihaemolytic-Activities-of-the-Dry-Fruiting,144044,0,2.html

Supplementary Table S1: Retention times and absorption maxima of the 11 standards used for the identification of the compounds in the mushrooms.

REFERENCES

1. Afsar, T., Razak, S., Khan, M.R., Mawash, S., Almajwal, A., Shabir, M., Haq, I.U. (2016). Evaluation of antioxidant, antihemolytic and anticancer activity of various solvent extracts of *Acacia hydaspica* R. Parker aerial parts. *BMC Complementary and Alternative Medicine*, *16*(1), art. no. 258. https://doi.org/10.1186/s12906-016-1240-8
2. Akata, I., Zengin, G., Picot, C.M.N., Mahomoodally, M.F. (2019). Enzyme inhibitory and antioxidant properties of six mushroom species from the Agaricaceae family. *South African Journal of Botany*, *120*, 95–99. https://doi.org/10.1016/j.sajb.2018.01.008
3. Alinezhad, H., Azimi, R., Zare, M., Ebrahimzadeh, M.A., Eslami, S., Nabavi, S.F., Nabavi, S.M. (2013). Antioxidant and antihemolytic activities of ethanolic extract of flowers, leaves, and stems of *Hyssopus officinalis* L. var. *angustifolius*. *International Journal of Food Properties*, *16*(5), 1169–1178. https://doi.org/10.1080/10942912.2011.578319
4. AOAC. (1990). *Official methods of analysis of the association of official analytical chemists* (15th ed.). Association of Official Analytical Chemists International.
5. AOAC. (1996). Moisture in animal feed, Method 930.15. In *Official Method of Analysis* (16th ed.). Association of Official Analytical Chemists International.
6. AOAC. (2007). Fat by acid hydrolysis. In *Official Methods of Analysis* (18th Edith). Association of Official Analytical Chemists International.
7. Barros, L., Dueñas, M., Ferreira, I.C.F.R., Baptista, P., Santos-Buelga, C. (2009). Phenolic acids determination by HPLC–DAD–ESI/MS in sixteen different Portuguese wild mushrooms species. *Food and Chemical Toxicology*, *47*(6), 1076–1079. https://doi.org/https://doi.org/10.1016/j.fct.2009.01.039
8. Besbas, S., Mouffouk, S., Haba, H., Marcourt, L., Wolfender, J.-L., Benkhaled, M. (2020). Chemical composition, antioxidant, antihemolytic and anti-inflammatory activities of *Ononis mitissima* L. *Phytochemistry Letters*, *37*, 63–69. https://doi.org/https://doi.org/10.1016/j.phytol.2020.04.002
9. Blois, M.S. (1958). Antioxidant determinations by the use of a stable free radical. *Nature*, *181*(4617), 1199–1200. https://doi.org/10.1038/1811199a0
10. Boonsong, S., Klaypradit, W., Wilaipun, P. (2016). Antioxidant activities of extracts from five edible mushrooms using different extractants. *Agriculture and Natural Resources*, *50*(2), 89–97. https://doi.org/10.1016/J.ANRES.2015.07.002
11. Chang, R. (1996). Functional properties of edible mushrooms. *Nutrition Reviews*, *54*(11), S91–S93. https://doi.org/https://doi.org/10.1111/j.1753-4887.1996.tb03825.x
12. Chansiw, N., Paradee, N., Chotinantakul, K., Srichairattanakool, S. (2018). Anti-hemolytic, antibacterial and anti-cancer activities of methanolic extracts from leaves and stems of *Polygonum odoratum*. *Asian Pacific Journal of Tropical Biomedicine*, *8*(12), 580–585. https://doi.org/10.4103/2221-1691.248094
13. Cheung, L.M., Cheung, P.C.K., Ooi, V.E.C. (2003). Antioxidant activity and total phenolics of edible mushroom extracts. *Food Chemistry*, *81*(2), 249–255. https://doi.org/10.1016/S0308-8146(02)00419-3
14. Crisan, E.V., Sands, A. (1978). *Nutritional value*. In S.T. Chang, W.A. Hayes (Eds.) *The Biology and Cultivation of Edible Mushrooms*, Chapter 6, Academic Press, pp. 137–168. https://doi.org/10.1016/B978-0-12-168050-3.50012-8
15. Croft, K.D. (1999). Antioxidant effects of plant phenolic compounds. In *Antioxidants in Human Health and Disease*, CABI Publishing, pp. 109–121. http://www.academia.edu/download/6745089/Antioxidants_in_Human_Health_and_Disease.pdf#page=129
16. Do, T.H., Truong, H.B., Nguyen, H.C. (2020). Optimization of extraction of phenolic compounds from *Ocimum basilicum* leaves and evaluation of their antioxidant activity. *Pharmaceutical Chemistry Journal*, *54*(2), 162–169. https://doi.org/10.1007/s11094-020-02181-3
17. Dursun, N., Özcan, M.M., Kaşık, G., Öztürk, C. (2006). Mineral contents of 34 species of edible mushrooms growing wild in Turkey. *Journal of the Science of Food and Agriculture*, *86*, 1087–1094. https://doi.org/10.1002/jsfa.2462
18. Elmastas, M., Isildak, O., Turkekul, I., Temur, N. (2007). Determination of antioxidant activity and antioxidant compounds in wild edible mushrooms. *Journal of Food Composition and Analysis*, *20*(3–4), 337–345. https://doi.org/10.1016/J.JFCA.2006.07.003
19. Gąsecka, M., Magdziak, Z., Siwulski, M., Mleczek, M. (2018). Profile of phenolic and organic acids, antioxidant properties and ergosterol content in cultivated and wild growing species of Agaricus. *European Food Research and Technology*, *244*(2), 259–268. https://doi.org/10.1007/s00217-017-2952-9
20. Gençcelep, H., Uzun, Y., Tunçtürk, Y., Demirel, K. (2009). Determination of mineral contents of wild-grown edible mushrooms. *Food Chemistry*, *113*(4), 1033–1036. https://doi.org/10.1016/J.FOODCHEM.2008.08.058
21. Ghate, S.D., Sridhar, K.R. (2016). Contribution to the knowledge on macrofungi in mangroves of the southwest India. *Plant Biosystems – An International Journal Dealing with All Aspects of Plant Biology*, *150*(5), 977–986. https://doi.org/10.1080/11263504.2014.994578
22. Günç Ergönül, P., Akata, I., Kalyoncu, F., Ergönül, B. (2013). Fatty acid compositions of six wild edible mushroom species. *The Scientific World Journal*, *2013*, art. no. 163964. https://doi.org/10.1155/2013/163964
23. Hawksworth, D.L. (2001). Mushrooms: The extent of the unexplored potential. *International Journal of Medicinal Mushrooms*, *3*(4), art. no. 5. https://doi.org/10.1615/IntJMedMushr.v3.i4.50
24. Ho, L.-H., Zulkifli, N.A., Tan, T.-C. (2020). Edible mushroom: nutritional properties, potential nutraceutical values, and its utilisation in food product development. In A.K. Passari, S. Sánchez (Eds.), *An Introduction to Mushroom*. IntechOpen. https://doi.org/10.5772/intechopen.91827
25. Jeena, G.S., Punatha, H., Prakash, O., Chandra, M., Kushwaha, K.P.S. (2014). Study on *in vitro* antioxidant potential of some cultivated *Pleurotus* species (oyster mushroom). *Indian Journal of Natural Products and Resources (IJNPR) [Formerly Natural Product Radiance (NPR)]*, *5*(1), 56–61. http://14.139.47.23/index.php/IJNPR/article/view/12457
26. Johnsy, G., Sargunam, S.D., Dinesh M.G., Kaviyarasan, V. (2011). Nutritive value of edible wild mushrooms collected from

the western ghats of Kanyakumari district. *Botany Research International*, *4*(4), 69–74. https://www.researchgate.net/publication/268270094

27. Kakoti, M., Hazarika, D.J., Kumar, A., Barooah, M., Modi, M.K., Bhattacharyya, A., Boro, R.C. (2021). Genetic diversity and dna barcoding of wild mushrooms from Northeast India. *Iranian Journal of Science and Technology, Transactions A: Science*, *45*(2), 469–479. https://doi.org/10.1007/s40995-021-01067-7
28. Kalač, P. (2013). A review of chemical composition and nutritional value of wild-growing and cultivated mushrooms. *Journal of the Science of Food and Agriculture*, *93*(2), 209–218. https://doi.org/10.1002/jsfa.5960
29. Khaund, P., Joshi, S.R. (2013). Wild edible macrofungal species consumed by the Khasi tribe of Meghalaya, India. *Indian Journal of Natural Products and Resources*, *4*(2), 197–204.
30. Lakshmi, B., Tilak, J.C., Adhikari, S., Devasagayam, T.P.A., Janardhanan, K.K. (2004). Evaluation of antioxidant activity of selected Indian mushrooms. *Pharmaceutical Biology*, *42*(3), 179–185. https://doi.org/10.1080/13880200490514023
31. Lindequist, U., Niedermeyer, T.H.J., Jülich, W.-D. (2005). The pharmacological potential of mushrooms. *Evidence-Based Complementary and Alternative Medicine: ECAM*, *2*(3), 285–299. https://doi.org/10.1093/ecam/neh107
32. Madhanraj, R., Ravikumar, K., Maya, M.R., Ramanaiah, I., Venkatakrishna, K., Remeshkumar, K., Veeramanikandan, V., Eyini, M., Balaji, P. (2019). Evaluation of anti-microbial and anti-haemolytic activity of edible basidiomycetes mushroom fungi. *Journal of Drug Delivery and Therapeutics*, *9*(1), 132–135. https://doi.org/10.22270/jddt.v9i1.2277
33. Mallikarjuna, S.E., Ranjini, A., Haware, D.J., Vijayalakshmi, M.R., Shashirekha, M.N., Rajarathnam, S. (2013). Mineral composition of four edible mushrooms. *Journal of Chemistry*, *2013*, art. no. 805284. https://doi.org/10.1155/2013/805284
34. Manzi, P., Aguzzi, A., Pizzoferrato, L. (2001). Nutritional value of mushrooms widely consumed in Italy. *Food Chemistry*, *73*(3), 321–325. https://doi.org/10.1016/S0308-8146(00)00304-6
35. Martins, A. (2017). The numbers behind mushroom biodiversity. In I.C.F.. Ferreira, P. Morales, L. Barros (Eds.), *Wild Plants, Mushrooms and Nuts: Functional Food Properties and Applications,* John Wiley Sons Ltd., pp. 15–50. https://doi.org/10.1002/9781118944653.ch2
36. Nowacka, N., Nowak, R., Drozd, M., Olech, M., Los, R., Malm, A. (2014). Analysis of phenolic constituents, antiradical and antimicrobial activity of edible mushrooms growing wild in Poland. *LWT – Food Science and Technology*, *59*(2), 689–694. https://doi.org/10.1016/j.lwt.2014.05.041
37. Nwanze, P.I., Khan, A.U., Ameh, J.B., Umoh, V.J. (2005). The effect of the interaction of various pond grains with different culture medium on carpophore dry weights and stipe and pilus diameters of *Lentinus squarrosulus* (Mont.) Singer. *African Journal of Biotechnology*, *4*(7), 615–619. https://doi.org/10.5897/AJB2005.000-3112
38. Parveen, A., Khataniar, L., Goswami, G., Hazarika, D.J., Das, P., Gautom, T., Barooah, M., Boro, R.C. (2017). A Study on the diversity and habitat specificity of macrofungi of Assam, India. *International Journal of Current Microbiology and Applied Sciences*, *6*(12), 275–297. https://doi.org/10.20546/ijcmas.2017.612.034
39. Phan, C., Wong, W., David, P., Naidu, M., Sabaratnam, V. (2012). *Pleurotus giganteus* (Berk.) Karunarathna K.D. Hyde: Nutritional value and *in vitro* neurite outgrowth activity in rat pheochromocytoma cells. *BMC Complementary Alternative Medicine*, *2012*, art. no. 102. https://doi.org/10.1186/1472-6882-12-102
40. Reis, F., Barros, L., Martins, A., Ferreira, I. (2012). Chemical composition and nutritional value of the most widely appreciated cultivated mushrooms: an inter-species comparative study. *Food and Chemical Toxicology*, *50*(2), 191–197. https://doi.org/10.1016/j.fct.2011.10.056
41. Ribeiro, A., Ruphuy, G., Lopes, J.C., Dias, M.M., Barros, L., Barreiro, F., Ferreira, I.C.F.R. (2015). Spray-drying microencapsulation of synergistic antioxidant mushroom extracts and their use as functional food ingredients. *Food Chemistry*, *188*, 612–618. https://doi.org/https://doi.org/10.1016/j.foodchem.2015.05.061
42. Sadasivam, S., Manickam, A. (1996). *Biochemical Methods*. New Age International. https://books.google.co.in/books?hl=en&lr=&id=JuuwBg_D1mIC&oi=fnd&pg=PR7&ots=T4w6WVBltF&sig=f03iwoOZEBxNKdhlYPhyaf8_SBo&redir_esc=y#v=onepage&q&f=false
43. Sánchez, C. (2017). Reactive oxygen species and antioxidant properties from mushrooms. *Synthetic and Systems Biotechnology*, *2*(1), 13–22. https://doi.org/https://doi.org/10.1016/j.synbio.2016.12.001
44. Sarma, T.C., Sarma, I., Patiri, B.N. (2010). Edible mushroom used by some ethnic tribes of western Assam. *The Bioscan*, *3*(Special issue), 613–625. https://doi.org/10.13140/RG.2.1.3531.1842
45. Schellmann, B., Hilz, M.-J., Opitz, O. (1980). Cadmium- und Kupferausscheidung nach Aufnahme von Champignon-Mahlzeiten (Fecal excretion of cadmium and copper after mushroom (*Agaricus*) diet). *Zeitschrift Fur Lebensmittel-Untersuchung Und -Forschung*, *171*(3), 189–192 (in German; English abstract). https://doi.org/10.1007/BF01042648
46. Shabbir, M., Khan, M.R., Saeed, N. (2013). Assessment of phytochemicals, antioxidant, anti-lipid peroxidation and anti-hemolytic activity of extract and various fractions of *Maytenus royleanus* leaves. *BMC Complementary and Alternative Medicine*, *13*(1), art. no. 143. https://doi.org/10.1186/1472-6882-13-143
47. Shao, S., Hernandez, M., Kramer, J. K. G., Rinker, D.L., Tsao, R. (2010). Ergosterol profiles, fatty acid composition, and antioxidant activities of button mushrooms as affected by tissue part and developmental stage. *Journal of Agricultural and Food Chemistry*, *58*(22), 11616–11625. https://doi.org/10.1021/jf102285b
48. Sharif, S., Shahid, M., Mushtaq, M., Akram, S., Rashid, A. (2017). Wild mushrooms: A potential source of nutritional and antioxidant attributes with acceptable toxicity. *Preventive Nutrition and Food Science*, *22*(2), 124–130. https://doi.org/10.3746/pnf.2017.22.2.124
49. Singdevsachan, S.K., Patra, J.K., Tayung, K., Sarangi, K., Thatoi, H. (2014). Evaluation of nutritional and nutraceutical poten-

tials of three wild edible mushrooms from Similipal Biosphere Reserve, Odisha, India. *Journal of Consumer Protection and Food Safety*, *9*(2), 111–120. https://doi.org/10.1007/s00003-014-0861-4

50. Singleton, V.L., Rossi, J.A. (1965). Colorimetry of total phenolics with phosphomolybdic-phosphotungstic acid reagents. *American Journal of Enology and Viticulture*, *16*(3), 144–158. https://www.ajevonline.org/content/16/3/144.short
51. Smiderle, F.R., Olsen, L.M., Ruthes, A.C., Czelusniak, P.A., Santana-Filho, A.P., Sassaki, G.L., Gorin, P.A.J., Iacomini, M. (2012). Exopolysaccharides, proteins and lipids in *Pleurotus pulmonarius* submerged culture using different carbon sources. *Carbohydrate Polymers*, *87*(1), 368–376. https://doi.org/10.1016/J.CARBPOL.2011.07.063
52. Soylak, M., Saraçoğlu, S., Tüzen, M., Mendil, D. (2005). Determination of trace metals in mushroom samples from Kayseri, Turkey. *Food Chemistry*, *92*(4), 649–652. https://doi.org/10.1016/J.FOODCHEM.2004.08.032
53. Taylor, T.N., Krings, M., Taylor, E.L. (2015). Basidiomycota. In T.N. Taylor, M. Krings, E.L. Taylor (Eds.), *Fossil Fungi*, Academic Press, pp. 173–199. https://doi.org/https://doi.org/10.1016/B978-0-12-387731-4.00009-8
54. Turkoglu, A., Duru, E., Mercan, N., Kivrak, I., Gezer, K. (2007). Antioxidant and antimicrobial activities of *Laetiporus sulphureus* (Bull.) Murrill. *Food Chemistry*, *101*, 267–273. https://doi.org/10.1016/j.foodchem.2006.01.025
55. Uzun, Y., Gençcelep, H., Kaya, A., Akçay, M.E. (2017). The mineral contents of some wild edible mushrooms. *Journal of Fungus*, *8*(2), 178–183. https://doi.org/10.15318/Fungus.2017.49
56. Valentão, P., Lopes, G., Valente, M., Barbosa, P., Andrade, P.B., Silva, B.M., Baptista, P., Seabra, R.M. (2005). Quantitation of nine organic acids in wild mushrooms. *Journal of Agricultural and Food Chemistry*, *53*(9), 3626–3630. https://doi.org/10.1021/jf040465z
57. Wong, J.Y., Chye, F.Y. (2009). Antioxidant properties of selected tropical wild edible mushrooms. *Journal of Food Composition and Analysis*, *22*(4), 269–277. https://doi.org/10.1016/J.JFCA.2008.11.021
58. Yahia, E.M., Gutiérrez-Orozco, F., Moreno-Pérez, M.A. (2017). Identification of phenolic compounds by liquid chromatography-mass spectrometry in seventeen species of wild mushrooms in Central Mexico and determination of their antioxidant activity and bioactive compounds. *Food Chemistry*, *226*, 14–22. https://doi.org/https://doi.org/10.1016/j.foodchem.2017.01.044

Pol. J. Food Nutr. Sci., 2021, Vol. 71, No. 4, pp. 481–483
http://journal.pan.olsztyn.pl

Instruction for Authors
Section: Editorial News

INSTRUCTIONS FOR AUTHORS

SUBMISSION. Original contributions relevant to food and nutrition sciences are accepted on the understanding that the material has not been, nor is being, considered for publication elsewhere. **All papers should be submitted and will be processed electronically via Editorial Manager system (available from PJFNS web site: http://journal.pan.olsztyn.pl). On submission, a corresponding author will be asked to provide: Cover letter; Files with Manuscripts, Tables, Figures/Photos; and Names of two potential reviewers (one from the author's homeland – but outside author's Institution, and the other from abroad).** All papers which have been qualified as relevant with the scope of our Journal are reviewed. All contributions, except the invited reviews are charged. Proofs will be sent to the corresponding author or to the first author and should be returned within one week since receipt. No new material may be inserted in the text at proof stage. It is the author's duty to proofread proofs for errors.

Authors should very carefully consider the preparation of papers to ensure that they communicate efficiently, because it permits the reader to gain the greatest return for the time invested in reading. Thus, we are more likely to accept those that are carefully designed and conform the instruction. Otherwise, papers will be rejected and removed from the on-line submission system.

SCOPE. The Polish Journal of Food and Nutrition Sciences publishes original, basic and applied papers, and reviews on fundamental and applied food research, preferably these based on a research hypothesis, in the following Sections:

Food Technology:
– Innovative technology of food development including biotechnological and microbiological aspects
– Effects of processing on food composition and nutritional value

Food Chemistry:
– Bioactive constituents of foods
– Chemistry relating to major and minor components of food
– Analytical methods

Food Quality and Functionality:
– Sensory methodologies
– Functional properties of food
– Food physics
– Quality, storage and safety of food

Nutritional Research Section:
– Nutritional studies relating to major and minor components of food (excluding works related to questionnaire surveys)

"News" section:
– Announcements of congresses
– Miscellanea

OUT OF THE SCOPE OF THE JOURNAL ARE:
– Works which do not have a substantial impact on food and nutrition sciences
– Works which are of only local significance i.e. concern indigenous foods, without wider applicability or exceptional nutritional or health related properties
– Works which comprise merely data collections, based on the use of routine analytical or bacteriological methods (i.e. standard methods, determination of mineral content or proximate analysis)
– Works concerning biological activities of foods but do not provide the chemical characteristics of compounds responsible for these properties
– Nutritional questionnaire surveys
– Works related to the characteristics of foods purchased at local markets
– Works related to food law
– Works emphasizing effects of farming / agricultural conditions / weather conditions on the quality of food constituents
– Works which address plants for non-food uses (i.e. plants exhibiting therapeutic and/or medicinal effects)

TYPES OF CONTRIBUTIONS. *Reviews:* (at least: 30 pages and 70 references) these are critical and conclusive accounts on trends in food and nutrition sciences; *Original papers:* (maximally: 30 pages and 40 references) these are reports of substantial research; *Reports on post and forthcoming scientific events, and letters to the Editor* (all up to three pages) are also invited (free of charge).

REVIEW PROCESS. All scientific contributions will be peer-reviewed on the criteria of originality and quality. Submitted manuscripts will be pre-evaluated by Editor-in-Chief and Statistical Editor (except for review articles), and when meeting PJFNS' scope and formal requirements, they will be sent to a section Editor who upon positive pre-evaluation will assign at least two reviewers from Advisory Board Members, reviewers suggested by the author or other experts in the field. Based on the reviews achieved, Section Editor and Editor-in-Chief will make a decision on whether a manuscript will be accepted for publication, sent back to the corresponding author for revision, or rejected. Once a manuscript is sent back to the corresponding author for revision, all points of the reviews should be answered or rebuttal should be provided in the Explanation letter. The revised manuscripts will be checked by Section Editor and by the original reviewers (if necessary), and a final decision will be made on acceptance or rejection by both Section Editor and Editor-in-Chief.

© Copyright by Institute of Animal Reproduction and Food Research of the Polish Academy of Sciences
© 2021 Author(s). This is an open access article licensed under the Creative Commons Attribution-NonCommercial-NoDerivs License (http://creativecommons.org/licenses/by-nc-nd/4.0/).

Polish Journal of Food and Nutrition Sciences uses CrossCheck's iThenticate software to detect instances of similarity in submitted manuscripts. In publishing only original research, PJFNS is committed to deterring plagiarism, including self-plagiarism. Your manuscript may be screened for similarity to published materials.

COPYRIGHT LICENSE AGREEMENT referring to Authorship Responsibility and Acknowledgement, Conflict of Interest and Financial Disclosure, Copyright Transfer, are required for all authors, i.e. *Authorship Responsibility and Acknowledgement*: Everyone who has made substantial intellectual contributions to the study on which the article is based (for example, to the research question, design, analysis, interpretation, and written description) should be an author. It is dishonest to omit mention of someone who has participated in writing the manuscript ("ghost authorship") and unfair to omit investigator who have had important engagement with other aspects of the work. All contributors who do not meet the criteria for authorship should be listed in an Acknowledgments section. Examples of those who might be acknowledged include a person who provided purely technical help, writing assistance, or a department chairperson who provided only general support. Any financial and material support should also be acknowledged. *Conflict of Interest and Financial Disclosure*: Authors are responsible for disclosing financial support from the industry or other conflicts of interest that might bias the interpretation of results. *Copyright License Agreement*: Authors agree that papers accepted become the copyright of the Institute of Animal Reproduction and Food Research of the Polish Academy of Sciences in Olsztyn, Poland, and may not be published elsewhere without the Editor's permission in writing.

A manuscript will not be published once the signed form has not been submitted to the Editor with the manuscript revised after positive reviews.

ETHICAL APPROVAL OF STUDIES AND INFORMED CONSENT. For all manuscripts reporting data from studies involving human participants or animals, formal approval by an appropriate institutional review board or ethics committee is required and should be described in the Methods section. For those investigators who do not have formal ethics review committees, the principles outlined in the Declaration of Helsinki should be followed. For investigations of humans, state in the Methods section the manner in which informed consent was obtained from the study participants (i.e., oral or written). Editors may request that authors provide documentation of the formal review and recommendation from the institutional review board or ethics committee responsible for oversight of the study.

UNAUTHORIZED USE AND COPYRIGHT AGREEMENT. Published manuscripts become the property of the Institute of Animal Reproduction and Food Research of the Polish Academy of Sciences (IAR&FR PAS) and may not be published elsewhere without written permission. Unauthorized use of the PJFNS name, logo, or any content for commercial purposes or to promote commercial goods and services (in any format, including print, video, audio, and digital) is not permitted by IAR&FR PAS.

MANUSCRIPTS. A manuscript in English must be single-sided, preferably in Times New Roman (12) with 1.5-point spacing, without numbers of lines. The Editor reserves the right to make literary corrections and to make suggestions to improve brevity. English is the official language. The English version of the paper will be checked by Language Editor. Unclear and unintelligible version will be sent to the author(s) for correction.

Every paper should be divided under the following headings in this order: a **Title** (possibly below 150 spaces), **Running title** (up to 50 spaces, submitted under the Title); the Names(s) of the author(s) in full. In paper with more than one author, the asterisk indicates the name of the author to whom correspondence and inquiries should be addressed, otherwise the first author is considered for the correspondence. Current full postal address of the indicated corresponding author or the first author must be given in a footnote on the title page; the Place(s) where the work was done including the institution name, city, country if not Poland. In papers originated from several institutions the names of the authors should be marked with respective superscripts; the **Key words** (up to 6 words or phrases) for the main topics of the paper; an **Abstract** (up to 250 words for regular papers and reviews and 100 words for Short Reports) summarizing briefly main results of the paper, no literature references; an **Introduction** giving essential background by saying why the research is important, how it relates to previous works and stating clearly the objectives at the end; **Materials and Methods** with sufficient experimental details permitting to repeat or extend the experiments. Literature references to the methods, sources of material, company names and location (city, country) for specific instruments must be given. Describe how the data were evaluated, including selection criteria used; **Results and Discussion** presented together (in one chapter). Results should be presented concisely and organized to supplement, but not repeat, data in tables and figures. Do not display the data in both tabular and graphic form. Use narrative form to present the data for which tables or figures are unnecessary. Discussion should cover the implications and consequences, not merely recapitulating the results, and it must be accomplished with concise **Conclusions**; **Acknowledgements** should be made to persons who do not fill the authorship criteria (see: Authorship forms); **Research funding** should include financial and material support; and **References** as shown below.

REFERENCES each must be listed alphabetically at the end of the paper (each should have an Arabic number in the list) in the form as follows: **Periodicals** – names and initials of all the authors, year of publication, title of the paper, journal title as in Chemical Abstracts, year of publication, volume, issue, inclusive page numbers; **Books** – names and initials of all the authors, names of editors, chapter title, year of publication, publishing company, place of publication, inclusive page numbers; **Patents** – the name of the application, the title, the country, patent number or application number, the year of publication.

For papers published in language other than English, manuscript title should be provided in English, whereas a note on the original language and English abstract should be given in parentheses at the end.

The reference list should only include peer-reviewed full-text works that have been published or accepted for publication. Citations of MSc/PhD theses and works unavailable to international Editors, Reviewers, and Readers should be limited as much as possible.

References in the text must be cited by name and year in square parentheses (e.g.: one author – [Tokarz, 1994]; two authors – [Słonimski & Campbell, 1987]; more than two authors – [Amarowicz *et al*., 1994]). If more than one paper is published in the same year by the same author or group of authors use [Tokarz, 1994a, b]. Unpublished work must only be cited where necessary and only in the text by giving the person's name.

Examples:

Article in a journal:

Słonimski, B.A., Campbell, L.D., Batista, E., Howard B. (2008). Gas chromatographic determination of indole glucosinolates. *Journal of Science and Food Agriculture*, *40*(5), 131–143.

Book:

Weber, W., Ashton, L., Milton, C. (2012). *Antioxidants – Friends or Foes?* 2nd edition. PBD Publishing, Birmingham, UK. pp. 218–223.

Chapter in a book:

Uden, C., Gambino, A., Lamar, K. (2016). Gas chromatography. In M. Queresi, W. Bolton (Eds.), *CRC Handbook of Chromatography*, CRC Press Inc., Boca Raton, Florida, USA, pp. 44–46.

ABBREVIATIONS AND UNITS. Abbreviations should only be used when long or unwieldy names occur frequently, and never in the title; they should be given at the first mention of the name. Metric SI units should be used. The capital letter L should be used for liters. Avoid the use of percentages (% g/g,% w/w; Mol-%; vol-%), ppm, ppb. Instead, the expression such as g/kg, g/L, mg/kg, mg/mL should be used. A space must be left between a number and a symbol (e.g. 50 mL not 50mL). A small x must be used as multiplication sign between numeric values (e.g. 5×10^2 g/mL). Statistics and measurements should be given in figures, except when the number begins a sentence. Chemical formulae and solutions must specify the form used. Chemical abbreviations, unless they are internationally known, Greek symbols and unusual symbols for the first time should be defined by name. Common species names should be followed by the Latin at the first mention, with contracting it to a single letter or word for subsequent use.

FIGURES should be submitted in separate files. Each must have an Arabic number and a caption. Captions of all Figures should be provided on a separate page "Figure Captions". Figures should be comprehensible without reference to the text. Self-explanatory legend to all figures should be provided under the heading "Legends to figures"; all abbreviations appearing on figures should be explained in figure footnotes. Three-dimensional graphs should only be used to illustrate real 3-D relationships. Start the scale of axes and bars or columns at zero, do not interrupt them or omit missing data on them. Figures must be cited in Arabic numbers in the text.

TABLES should be submitted in separate files. They should be as few in number and as simple as possible (like figures, they are expensive and space consuming), and include only essential data with appropriate statistical values. Each must have an Arabic number and a caption. Captions of all Tables should be provided on a separate page "Table Captions". Tables should be self-explanatory; all abbreviations appearing in tables should be explained in table footnotes. Tables must be cited in Arabic numbers in the text.

PAGE CHARGES. A standard publication fee has been established at the rate of 450 EUR + tax (if applicable) irrespective of the number of pages and tables/figures. For Polish Authors an equivalent fee was set at 1950 PLN + VAT. Payment instructions will be sent to Authors via e-mail with acceptance letter.

Information on publishing and subscription is available from:

Ms. Joanna Molga
Editorial Office of Pol. J. Food Nutr. Sci.
Institute of Animal Reproduction and Food Research
Tuwima 10 Str., 10–748 Olsztyn 5, Poland
phone (48 89) 523–46–70, fax (48 89) 523–46–70;
e-mail: pjfns@pan.olsztyn.pl; http://journal.pan.olsztyn.pl

Nutrition